An Ecological Study of Gunston Cove

2020

FINAL REPORT

October 2021

by

R. Christian Jones
Professor
Department of Environmental Science and Policy
Director
Potomac Environmental Research and Education Center
George Mason University
Project Director

Kim de Mutsert
Assistant Professor
Department of Environmental Science and Policy
Associate Director
Potomac Environmental Research and Education Center
George Mason University

Amy Fowler
Assistant Professor
Department of Environmental Science and Policy
Faculty Fellow
Potomac Environmental Research and Education Center
George Mason University

to

Department of Public Works and Environmental Services
County of Fairfax, VA

Back of Title Page

Table of Contents

An Ecological Study of Gunston Cove – 2020

Executive Summary

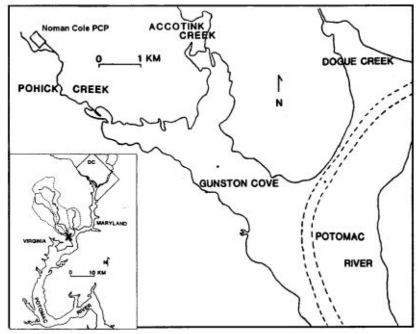

Gunston Cove is an embayment of the tidal freshwater Potomac River located in Fairfax County, Virginia about 12 miles (20 km) downstream of the I-95/I-495 Woodrow Wilson Bridge. The Cove receives treated wastewater from the Noman M. Cole, Jr. Pollution Control Plant and inflow from Pohick and Accotink Creeks which drain much of central and southern Fairfax County. The Cove is bordered on the north by Fort Belvoir and on the south by the Mason Neck. Due to its tidal nature and shallowness, the Cove does not seasonally stratify vertically, and its water mixes gradually with the adjacent tidal Potomac River mainstem. Thermal stratification can make nutrient management more difficult, since it can lead to seasonal oxygen-diminished bottom waters that may result in fish mortality. Since 1984 George Mason University personnel, with funding and assistance from the Wastewater Management Program of Fairfax County, have been monitoring water quality and biological communities in the Gunston Cove area including stations in the Cove itself and the adjacent River mainstem. This document presents study findings from 2019 in the context of the entire data record.

The Chesapeake Bay, of which the tidal Potomac River is a major subestuary, is the largest and most productive coastal system in the United States. The use of the bay as a fisheries and recreational resource has been threatened by overenrichment with nutrients which can cause nuisance algal blooms, hypoxia in stratified areas, and a decline of fisheries. As a major discharger of treated wastewater into the tidal Potomac River, particularly Gunston Cove, Fairfax County has been proactive in decreasing nutrient loading since the late 1970's. Due to the strong management efforts of the County and the robust monitoring program, Gunston Cove has proven an extremely valuable case study in eutrophication recovery for the bay region and even internationally. The onset of larger areas of SAV coverage in Gunston Cove will have further effects on the biological resources and water quality of this part of the tidal Potomac River.

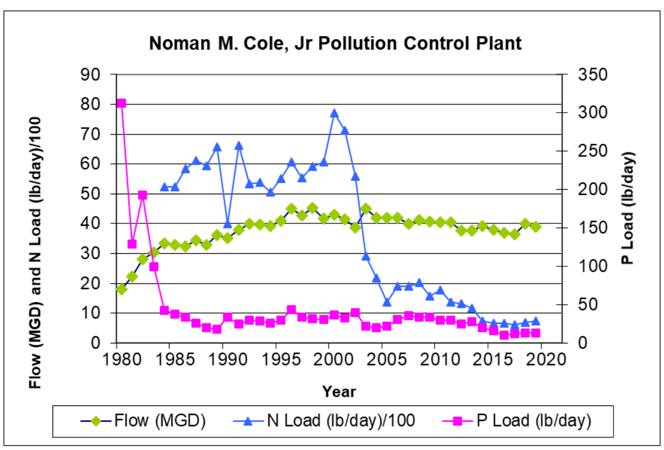

As shown in the figure to the left, phosphorus loadings were dramatically reduced in the early 1980's. In the last several years, nitrogen, and solids loadings as well as effluent chlorine concentrations have also been greatly reduced or eliminated. These reductions have been achieved even as flow through the plant has slowly increased.

The ongoing ecological study reported here provides documentation of major improvements in water quality and biological resources which can be attributed to those efforts. Water quality improvements have been substantial in spite of the increasing population and volume of wastewater produced. The 37 year data record from Gunston Cove and the nearby Potomac River has revealed many important long-term trends that validate the effectiveness of County initiatives to improve treatment and will aid in the continued management and improvement of the watershed and point source inputs.

In 2020 air temperature was below normal in April and May, but well above normal from June through August. Precipitation was well above normal in April, July, August, and September but below normal in May. The only water quality sample date that was preceeded by substantial rainfall was May 5. River flows which could impact the study area in May and August/September.

Mean water temperature was similar at the two stations with a pronounced dip in late May and a peak of about 30° in late. Specific conductance showed a strong decline in the aftermath of the high early May flows, but recovered by late May and varied over a relatively narrow range for the rest of the year. Dissolved oxygen saturation and concentration (DO) were consistently higher in the cove and there was little seasonal pattern at either site. Field pH patterns mirrored those in DO. Total alkalinity was generally higher in the river than in the cove. Values were similar at the two sites early in the year, but then the cove station steadily decreased. Water clarity as measured by Secchi disk transparency and light attenuation coefficient both exhibited a strong decline in the aftermath of the early May high flows, but recovered and remained stready for the rest of the year. Values indicated only moderately good water clarity.

Ammonia nitrogen never exceeded the rather high detection limit of 0.1 mg/L values making analysis of any temporal or spatial trends impossible. After a slight bump upwards in the cove in May, nitrate values declined steadily through July at both stations with river values consistently about 0.5 mg/L than those in the cove. Nitrite was much lower overall (right). Organic nitrogen showed marked decline in late May, then increased through July before dropping back in the fall. It was generally about 0.1 mg/L higher in the cove than in the river. Total phosphorus showed a little seasonal or spatial trend hovering at about 0.05 mg/L. Soluble reactive phosphorus was generally somewhat higher in the river, but showed little consistent seasonal trend. N to P ratio declined at both stations through July and then increased slightly in August and September with most values between 15 and 25, a range which is still indicative of P limitation of phytoplankton and SAV. BOD was generally higher in the cove than in the river. TSS was consistently between 10 and 20 except for one high value in the river in September. VSS did not show strong spatial and temporal patterns.

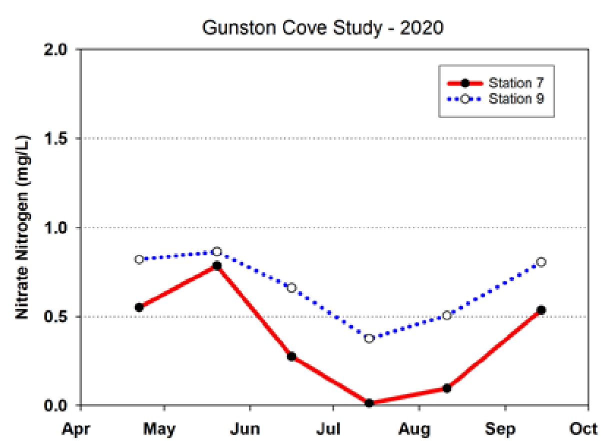

In the cove algal populations as measured by chlorophyll *a* were consistently higher in the cove than in the river through most of the year (left). High values in the cove were found in late May and late June. The late June maximum was composed predominantly of diatoms with *Melosira* being the most important. The cyanobacteria *Oscillatoria* and *Anabaena* were also important. In the river phytoplankton chlorophyll was generally lower than in the cove and *Melosira* was again the important diatom and *Oscillatoria* was the important cyanobacterium.

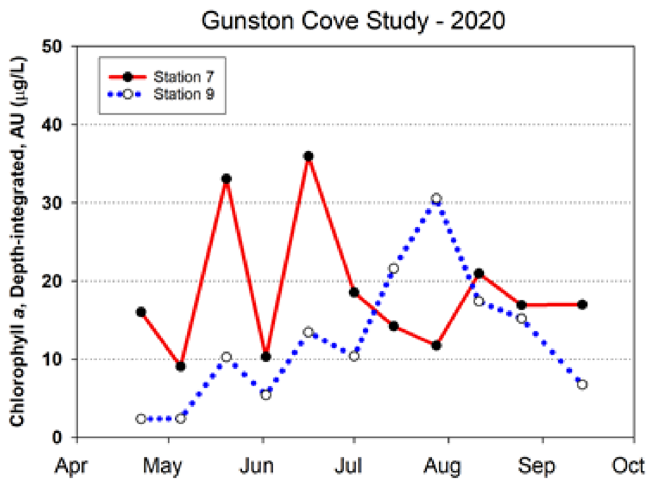

Rotifers continued to be the most numerous microzooplankton in 2020. Rotifer densities were unusually high (over 10,000/L) in early June in the cove due to a *Filinia* bloom. *Keratella* and *Brachionus* dominated for the remainder of the year. Rotifer densities were consistently lower in the river than in the cove with *Brachionus a*s the dominant. *Bosmina*, a small cladoceran was low at both stations except for a peak in early June in the cove. *Diaphanosoma*, a larger cladoceran, was very abundant in the cove in mid-June exceeding 4000/m^3. It had two peaks of about 2000/m^3 in the river. *Daphnia* was only found at low values in 2020. *Sida* was present in the river at the same times as *Diaphanosoma*. *Leptodora* exhibited peaks in mid-June in the cove and June and mid-July in the river at 400-600/m^3. Copepod nauplii had a distinct seasonal pattern in the cove reaching 250/L in mid-June. In the river the peak was somewhat lower. The calanoid copepod *Eurytemora* was very abundant in the cove in late May and June attaining 6500/m^3, but was much lower for the rest of the year. It reached almost 5000/m^3 in the river is mid-June. A second calanoid *Diaptomus* was found at much lower levels. Cyclopoid copepods had a strong maximum in the river of 10,000/m^3 in late July, but otherwise were at low levels in 2020.

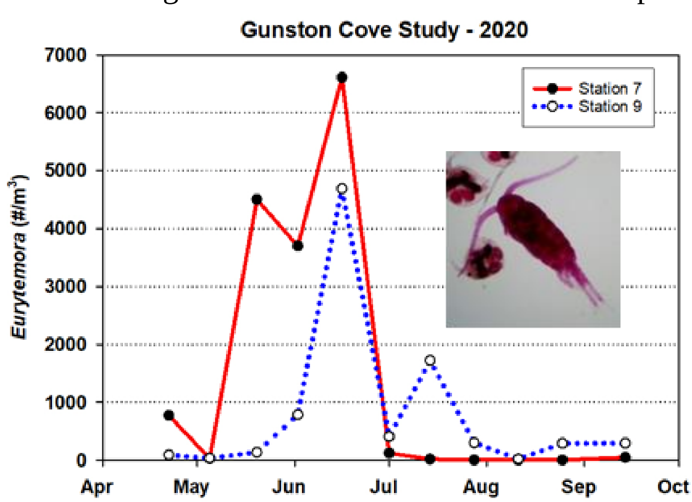

In 2020 ichthyoplankton was dominated by clupeids, most of which were Alewife, Gizzard Shad, and Blueback Herring, and to a lesser extent Hickory Shad, and American Shad. Although clupeids constituted the majority of the catch, there were six other species were identified in the ichthyoplankton samples. Of those, White Perch was found in relatively high densities. White Perch was mostly found in the Potomac mainstem, confirming its affinity for open water. Other taxa were found in very low densities, similar to the previous year. The highest density of fish larvae occurred late May and early June, which was driven by a high density of Clupeid larvae. The non-clupeid larval density was highest in late May, which was driven by White Perch larvae.

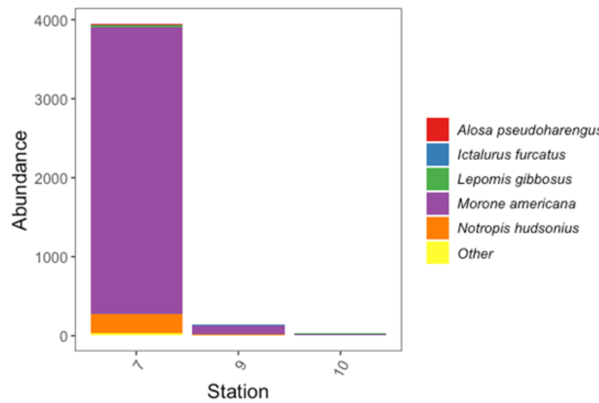

Due to COVID restrictions, fish sampling was confined to July to September. In trawls (right), White Perch dominated, followed by Spottail Shiner. White Perch was by far the most abundant species and was found in all months at all stations, with peak abundance in July in the cove. We collected a lot less Blue Catfish than in 2018, but still 18 in the mainstem and 1 in the cove. Abundances have likely not reduced since last year, large specimens tend to avoid our gear. With the smaller catch in 2020, we still found a disparity between catches of Blue Catfish in the mainstem versus the cove, which supports the theory that Blue Catfish has an affinity for the mainstem, potentially leaving embayments like Gunston Cove to serve as a refuge for native catfishes. We collected two native catfish in 2020.

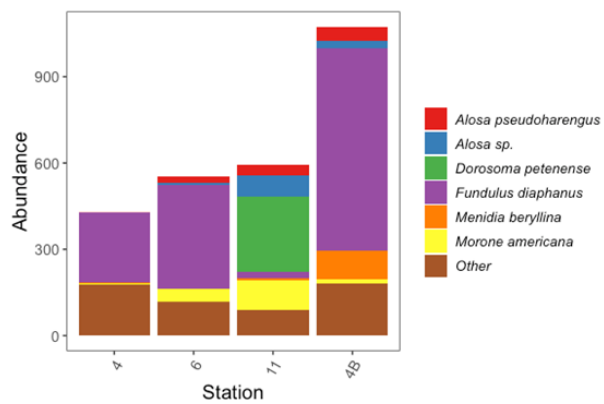

In seines, the most abundant species was Banded Killifish composing about 50% of the catch. Banded Killifish was far more abundant in seines than in trawls, which emphasizes the preference of Banded Killifish for the shallow littoral zone (which is the area sampled with a seine, while trawls sample the open water). The abundance peak of Banded Killifish was in late July. Threadfin shad was the dominant in the seine station nearest the river channel. Other relatively abundant species collected with the seines were White Perch, Inland Silverside, Goldfish, Quillback and Eastern Silvery Minnow (left).

As in most previous years, oligochaetes were the most common invertebrates collected in ponar samples in 2020. Chironomids (midge larvae) were co-dominant in the cove, being almost as common as the oligochaetes. Amphipods, isopods, Asiatic clams, and chironomids were common in the river. Multivariate analysis showed a clear and consistent difference between cove benthic communities and those in the river. Shells and leaves were found in samples from both the cove and river.

Due to COVID restrictions we were unable to conduct the anadromous fish monitoring program in 2020.

Coverage of submersed aquatic vegetation (SAV) in 2020 continued its strong rebound after very limited abundances in 2018 due to high turbidity and subsequent low light levels. *Hydrilla*, minor naiad, and coontail were the most abundant SAV. Standaridized data on SAV coverage from VIMS resumed in 2019 and continues to show a major sustained improvement in water clarity and subsequent recovery of SAV beds. Jones (2020) demonstrated that the cove ecosystem changed from a "turbid water" state dominated by phytoplankton to a "clear water" state dominated by SAV in 2005. As shown in the figure above the data for 2020 indicates that the "clear water" state is continuing with improved water clarity (Secchi depth), lower phytoplankton (chlorophyll a), and greater coverage of SAV as indicated in the graph to the right.

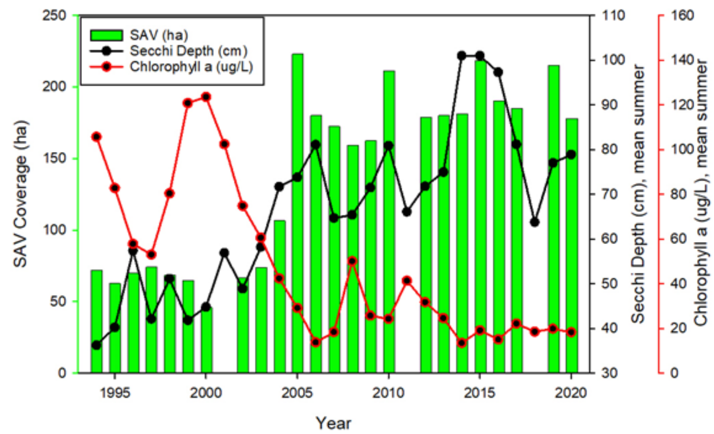

A second significant change in water quality documented by the study has been the removal of chlorine and ammonia from the Noman M. Cole, Jr. Pollution Control Plant effluent. A decline of over an order of magnitude in ammonia nitrogen has been observed in the Cove as compared to earlier years. The declines in ammonia and the elimination of chlorine from the effluent (to values well below those that may result is toxicity problems) have allowed fish to recolonize tidal Pohick Creek which now typically has more spawning activity than tidal Accotink Creek. Monitoring of creek fish allowed us to observe recovery of this habitat which is very important for spawning species such as shad. The decreased ammonia, suspended solids, and phosphorus loading from the plant have contributed to overall Chesapeake Bay cleanup. Unfortunately, we are unable to continue to track further declines in ammonia concentrations since all values are now below the detection limit reported by the County.

Another trend of significance which is indicative of the Cove recovery is the change in the relative abundance of fish species. While it is still the dominant species in trawls, White Perch has gradually been displaced in seines by Banded Killifish. This trend continued in 2017 with Banded Killifish being much more abundant in seines than White Perch. In general this is a positive development as the net result has been a more diverse fish community. Blue Catfish have entered the area recently, were quite abundant in 2018 and maintained a presence in 2019 and 2020. Blue Catfish are regarded as rather voracious predators and may negatively affect the food web. Other catfish are down significantly now that the Blue Catfish is present.

Clearly, recent increases in SAV provide refuge and additional spawning habitat for Banded Killifish and Sunfish. Analysis shows that White Perch dominance was mainly indicative of the community present when there was no SAV; increased abundances of Bay Anchovy indicative for the period with some SAV; and Banded Killifish and Largemouth Bass indicative of the period when SAV beds were expansive. In 2020 seine collections were dominated by Banded Killifish. While the seine does not sample these SAV areas directly, the enhanced growth of SAV provides a large bank of Banded Killifish that spread out into the adjacent unvegetated shoreline areas and are sampled in the seines. The fyke nets that do sample the SAV areas directly documented a dominance of Sunfish and Banded Killifish in the SAV beds. In addition to SAV expansion, the invasive Blue Catfish may also have both direct (predation) and indirect (competition) effects, especially on species that occupy the same niche such as Brown Bullhead and Channel Catfish. Overall, these results indicate that the fish assemblage in Gunston Cove is dynamic and supports a diversity of commercial and recreational fishing activities.

In summary, it is important to continue the data record that has been established to allow assessment of how the continuing increases in volume and improved efforts at wastewater treatment interact with the ecosystem as SAV increases and plankton and fish communities change in response. Furthermore, changes in the fish communities from the standpoint of habitat alteration by SAV and introductions of exotics like snakeheads and blue catfish need to be followed. 2018 was highly instructive in showing how extreme rainfall conditions can alter the ecosystem and at least temporarily impede recovery. However, 2019 and 2020 data indicate that the ecosystem was resilient and resumed the “clear water” state in 2019.

Global climate change is becoming a major concern worldwide. Since 2000 a slight, but consistent increase in summer water temperature has been observed in the Cove which may reflect the higher summer air temperatures documented globally. Other potential effects of directional climate change remain very subtle and not clearly differentiated given seasonal and cyclic variability.

We recommend that:

1. Long term monitoring should continue. The revised schedule initiated in 2004 which focuses sampling in April through September has captured the major trends affecting water quality and the biota. The Gunston Cove study is a model for long term monitoring which is necessary to document the effectiveness of management actions. This process is sometimes called adaptive management and is recognized as the most successful approach to ecosystem management.
2. Two aspects of the program should be reviewed.
    a. In 2016 phytoplankton cell counts frequency was decreased from twice monthly to monthly as a cost-saving step. But it does result in some sampling dates not having phytoplankton data to go along with the other variables. If funds are available, we recommend reinstituting twice monthly phytoplankton counts.
    b. As nutrient concentrations have decreased in the river and cove due to management successes, we are now encountering a substantial number of samples which are below detection limits. This becomes a problem in data analysis. To date we have set “below dection limits” values at ½ the detection limit, but this becomes less defensable the greater the proportion of these values. This is particularly true of ammonia nitrogen. We continue to recommend that this be addressed.
3. The fyke nets have proven to be a successful addition to our sampling routine. Even though a small, non-quantitative sample is collected due to the passive

nature of this gear, it provides us with useful information on the community within the submersed aquatic vegetation beds. Efficient use of time allows us to include these collections in a regular sampling day with little extra time or cost. We recommend continuing with this gear as part of the sampling routine in future years.

4. Anadromous fish sampling is an important part of this monitoring program and has gained interest now that the stock of river herring has collapsed, and a moratorium on these taxa has been established in 2012. We recommend continued monitoring, and we plan to use the collections before and during the moratorium to help determine the effect of the moratorium. Our collections will also form the basis of a population model that can provide information on the status of the stock.
5. We have instituted some improvements to the benthic monitoring program including the quantitative characterization of larger (>5 mm) particles in the samples which we expect to help explain the variations we see in benthic communities between samples and station.

Reference: Jones, R.C. 2020. Recovery of a Tidal Freshwater Embayment from Eutrophication: a Multidecadal Study. *Estuaries and Coasts*. Forthcoming in print. Available online at: https://link.springer.com/article/10.1007/s12237-020-00730-3

List of Abbreviations

BOD	Biochemical oxygen demand
cfs	cubic feet per second
DO	Dissolved oxygen
ha	hectare
l	liter
LOWESS	locally weighted sum of squares trend line
m	meter
mg	milligram
MGD	Million gallons per day
NS	not statistically significant
NTU	Nephelometric turbidity units
SAV	Submersed aquatic vegetation
SRP	Soluble reactive phosphorus
TP	Total phosphorus
TSS	Total suspended solids
um	micrometer
VSS	Volatile suspended solids
#	number

THE ONGOING AQUATIC MONITORING PROGRAM

FOR THE GUNSTON COVE AREA

OF THE TIDAL FRESHWATER POTOMAC RIVER

2020

FINAL REPORT
October 2021

R. Christian Jones
Professor
Department of Environmental Science and Policy
Director
Potomac Environmental Research and Education Center
George Mason University
Project Director

Kim de Mutsert
Assistant Professor
Department of Environmental Science and Policy
Associate Director
Potomac Environmental Research and Education Center
George Mason University
Co-Principal Investigator

Amy Fowler
Assistant Professor
Department of Environmental Science and Policy
Faculty Fellow
Potomac Environmental Research and Education Center
George Mason University
Co-Principal Investigator

to

Department of Public Works and Environmental Services
County of Fairfax, VA

INTRODUCTION

This section reports the results of the on-going aquatic monitoring program for Gunston Cove conducted by the Potomac Environmental Research and Education Center at George Mason University and Fairfax County's Environmental Monitoring Branch. This study is a continuation of work originated in 1984 at the request of the County's Environmental Quality Advisory Committee and the Department of Public Works. The original study design utilized 12 stations in Gunston Cove, the Potomac mainstem, and Dogue Creek. Due to budget limitations and data indicating that spatial heterogeneity was not severe, the study has evolved such that only two stations are sampled, but the sampling frequency has been maintained at semimonthly during the growing season. This sampling regime provides reliable data given the temporal variability of planktonic and other biological communities and is a better match to other biological sampling programs on the tidal Potomac including those conducted by the Maryland Department of Natural Resources and the District of Columbia. The 1984 report entitled "An Ecological Study of Gunston Cove – 1984" (Kelso et al. 1985) contained a thorough discussion of the history and geography of the cove. The reader is referred to that document for further details.

This work's primary objective is to determine the status of biological communities and the physico-chemical environment in the Gunston Cove area of the tidal Potomac River for evaluation of long-term trends. This will facilitate the formulation of well-grounded management strategies for maintenance and improvement of water quality and biotic resources in the tidal Potomac. Important byproducts of this effort are the opportunities for faculty research and student training which are integral to the educational programs at GMU.

The authors wish to thank the numerous individuals and organizations whose cooperation, hard work, and encouragement have made this project successful. We wish to thank the Fairfax County Department of Public Works and Environmental Services, Wastewater Planning and Monitoring Division, Environmental Monitoring Branch, particularly Steve Winesett, Juan Reyes and Shahram Mohsenin for their advice and cooperation during the study. Benny Gaines deserves recognition for field sample collection on days when Fairfax County collected independent samples. The entire analytical staff at the Noman Cole lab is gratefully acknowledged. The Northern Virginia Regional Park Authority facilitated access to the park and boat ramp. Without a dedicated group of field and laboratory workers this project would not have been possible. PEREC field and lab technician Laura Birsa deserves special recognition for day-to-day operations. Dr. Joris van der Ham headed up field fish collecting and Sara Marriott helped with the fish report. Dr. Saiful Islam conducted phytoplankton counts. Thanks also go to Beverly Bachman, Sammie Alexander, Chelsea Gray, Rachel Kelmartin, Sara Marriott, Alex Mott, Sam Mohney, Eran O'Keefe, Daya Stratton-Hall, Christina Seay, and Daria Maslyukova. Claire Buchanan served as a voluntary consultant on plankton identification. Cheryl Skolnick, Francina Osaria, Florencia Gutierrez, and Hillary Hamm were vital in handling budget, personnel and procurement functions.

METHODS

A. Profiles and Plankton: Sampling Day

Sampling was conducted on a semimonthly basis at stations representing both Gunston Cove and the Potomac mainstem (Figures 1a,b). One station was located at the center of Gunston Cove (Station 7) and the second was placed in the mainstem tidal Potomac channel off the Belvoir Peninsula just north of the mouth of Gunston Cove (Station 9). Dates for sampling as well as weather conditions on sampling dates and immediately preceding days are shown in Table 1. Gunston Cove is located in the tidal freshwater section of the Potomac about 20 km (13 miles) downstream from Washington, DC.

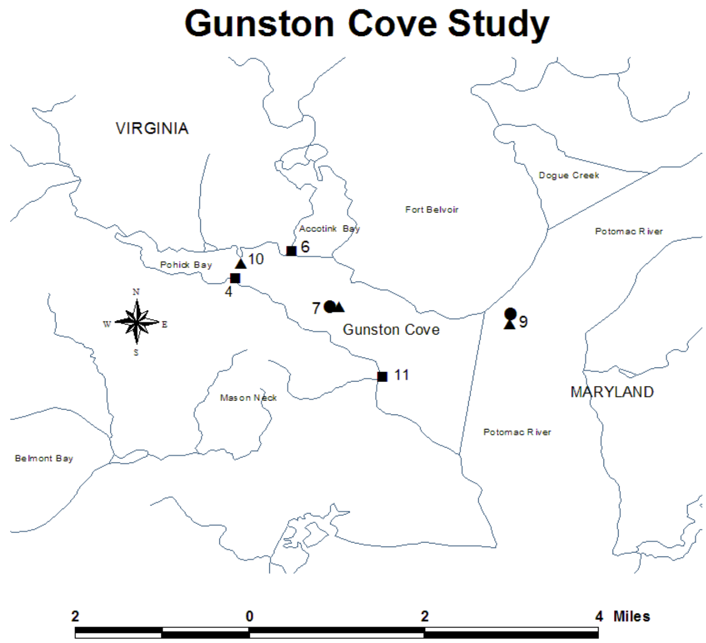

Figure 1a. Gunston Cove area of the Tidal Potomac River showing sampling stations. Circles (●) represent Plankton/Profile stations, triangles (▲) represent Fish Trawl stations, and squares (■) represent Fish Seine stations.

Figure 1b. Fish sampling stations including location and image of the fyke nets.

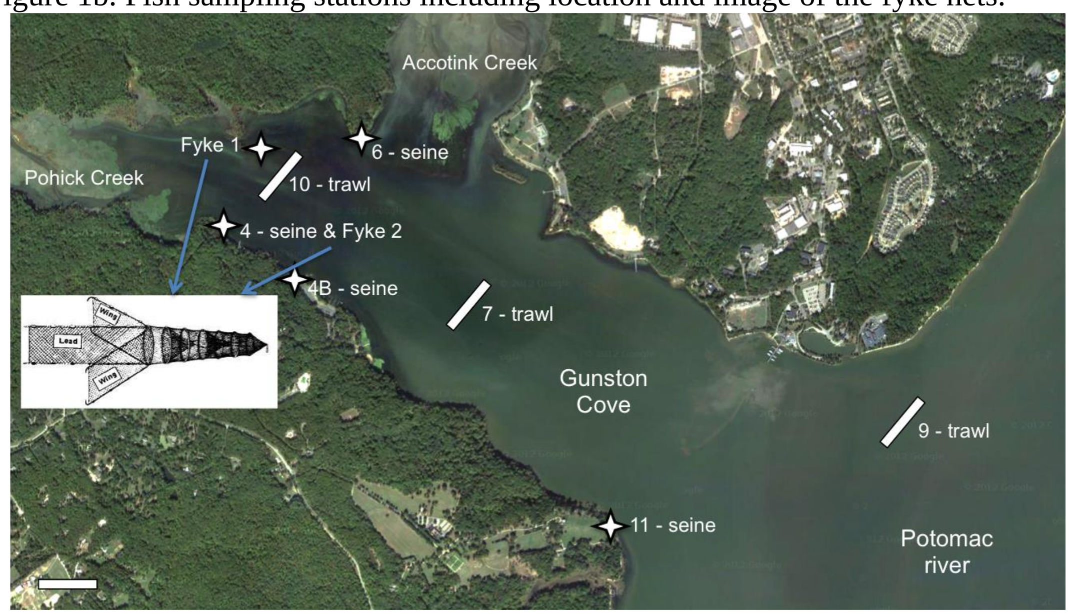

Table 1
Sampling Dates and Weather Data for 2020

Date	Type of Sampling G	F	T	S	Y	Avg Daily Temp (ºC) 1-Day	3-Day	Precipitation (cm) 1-Day	3-Day
Apr 22	G	F				10.0	12.6	0	T
May 5	G					12.2	17.4	0.48	3.07
May 20	G	F				14.4	16.3	T	0.03
Jun 2	G					20.0	19.6	T	T
Jun 16	G					22.2	21.9	0	0
Jul 1	G					22.8	26.7	0.30	0.32
Jul 10			T	S		28.3	28.1	T	T
Jul 14	G	F				27.2	28.1	0	0.38
Jul 24			T	S		27.8	29.1	1.09	7.32
Jul 28	G					31.1	30.2	T	T
Aug 7			T	S		27.2	26.7	0.76	2.34
Aug 11	G	F				28.9	28.3	0	0
Aug 21			T	S		25.0	24.8	T	0.24
Aug 25	G	F				28.3	28.3	T	0.15
Sep 10			T	S		26.1	25.2	7.32	8.94
Sep 14	G	F				22.2	22.0	T	T

Type of Sampling: B: Benthic, G: GMU profiles and plankton, F: nutrient and lab water quality by Fairfax County Laboratory, T: fish collected by trawling, S: fish collected by seining, Y: fish collected by fyke net. All samples collected by GMU personnel.

Sampling was initiated at 10:30 am. Four types of measurements or samples were obtained at each station : (1) depth profiles of temperature, conductivity, dissolved oxygen, pH, and irradiance (photosynthetically active radiation) measured directly in the field; (2) water samples for GMU lab determination of chlorophyll *a* and phytoplankton species composition and abundance; (3) water samples for determination of nutrients, BOD, alkalinity, suspended solids, chloride, and pH by the Environmental Laboratory of the Fairfax County Department of Public Works and Environmental Services; (4) net sampling of zooplankton and ichthyoplankton.

Profiles of temperature, conductivity, dissolved oxygen, and pH were conducted at each station using a YSI 6600 datasonde. Measurements were taken at 0.3 m, 1.0 m, 1.5 m, and 2.0 m in the cove. In the river measurements were made with the sonde at depths of 0.3 m, 2 m, 4 m, 6 m, 8 m, 10 m, and 12 m. Meters were checked for calibration before and after sampling. Profiles of irradiance (photosynthetically active radiation, PAR) were collected with a LI-COR underwater flat scalar PAR probe. Measurements were taken at 10 cm intervals to a depth of 1.0 m. Simultaneous measurements were made with a terrestrial probe in air during each profile to correct for changes in ambient light if needed. Secchi depth was also determined. The readings of at least two crew members were averaged due to variability in eye sensitivity among individuals.

A 1-liter depth-composited sample was constructed from equal volumes of water collected at each of three depths (0.3 m below the surface, middepth, and 0.3 m off of the bottom) using a submersible bilge pump. A 100-mL aliquot of this sample was preserved immediately with acid Lugol's iodine for later identification and enumeration of phytoplankton. The remainder of the sample was placed in an insulated cooler with ice. A separate 1-liter sample was collected from 0.3 m using the submersible bilge pump and placed in the insulated cooler with ice for lab analysis of surface chlorophyll *a*. These samples were analyzed by Mason.

Separate 4-liter samples were collected monthly at each site from just below the surface (0.3 m) and near the bottom (0.3 m off bottom) at each site using the submersible pump. This water was promptly delivered to the nearby Fairfax County Environmental Laboratory for determination of nitrogen, phosphorus, BOD, TSS, VSS, pH, total alkalinity, and chloride.

Microzooplankton was collected by pumping 32 liters from each of three depths (0.3 m, middepth, and 0.3 m off the bottom) through a 44 µm mesh sieve. The sieve consisted of a 12-inch long cylinder of 6-inch diameter PVC pipe with a piece of 44 µm nitex net glued to one end. The 44 µm cloth was backed by a larger mesh cloth to protect it. The pumped water was passed through this sieve from each depth and then the collected microzooplankton was backflushed into the sample bottle. The resulting sample was treated with about 50 mL of club soda and then preserved with formalin containing a small amount of rose bengal to a concentration of 5-10%.

Macrozooplankton was collected by towing a 202 µm net (0.3 m opening, 2 m long) for 1 minute at each of three depths (near surface, middepth, and near bottom). Ichthyoplankton was sampled by towing a 333 µm net (0.5 m opening, 2.5 m long) for 2 minutes at each of the same depths. In the cove, the boat made a large arc during the tow while in the river the net was towed in a more linear fashion along the channel. Macrozooplankton tows were about 300 m and ichthyoplankton tows about 600 m. Actual distance depended on specific wind conditions and tidal current intensity and direction, but an attempt was made to maintain a constant slow forward speed through the water during the tow. The net was not towed directly in the wake of the engine. A General Oceanics flowmeter, fitted into the mouth of each net, was used to establish the exact towing distance. During towing the three depths were attained by playing out rope equivalent to about 1.5-2 times the desired depth. Samples which had obviously scraped bottom were discarded and the tow was repeated. Flowmeter readings taken before and after towing allowed precise determination of the distance towed and when multiplied by the area of the opening produced the total volume of water filtered.

Macrozooplankton and ichthyoplankton were backflushed from the net cup and immediately preserved. Rose bengal formalin with club soda pretreatment was used for macrozooplankton. Ichthyoplankton were preserved in 70% ethanol. Macrozooplankton was collected on each sampling trip; ichthyoplankton collections ended after July because larval fish were normally not found after this time.

Benthic macroinvertebrates were sampled using a petite ponar sampler at Stations 7 and 9. Triplicate samples were collected at each site on dates when water samples for Fairfax County lab analysis were not collected. The protocol in use for the past several years specified that the bottom samples were sieved on site through a 0.5 mm stainless steel sieve. Larger items like SAV, leaves, sticks, and empty shells were rinsed with tap water through the sieve and discarded. The smaller materials remaining on the 0.5 mm sieve were then preserved with rose bengal formalin.

In an effort to understand the role of larger particulate material in structuring the benthic community, a new field protocol was instituted in August 2018. Samples were first sieved through a 5 mm coarse mesh to remove larger items mentioned above. Materials remaining on the 5 mm sieve were thoroughly washed in the field and the material retained on the sieve was transferred to a zip lock bag and placed on ice for further processing in the lab.

Samples were delivered to the Fairfax County Environmental Services Laboratory by 2 pm on sampling day and returned to GMU by 3 pm. At GMU 10-15 mL aliquots of both depth-integrated and surface samples were filtered through 0.45 µm membrane filters (Gelman GN-6 and Millipore MF HAWP) at a vacuum of less than 10 lbs/in^2 for chlorophyll a and pheopigment determination. During the final phases of filtration, 0.1 mL of $MgCO_3$ suspension (1 g/100 mL water) was added to the filter to prevent premature acidification. Filters were stored in 20 mL plastic scintillation vials in the lab freezer for later analysis. Seston dry weight and seston organic weight were measured by filtering 200-400 mL of depth-integrated sample through a pretared glass fiber filter (Whatman 984AH).

Sampling day activities were normally completed by 5:30 pm.

B. Profiles and Plankton: Follow-up Analyses

Chlorophyll *a* samples were extracted in a ground glass tissue grinder to which 4 mL of dimethyl sulfoxide (DMSO) was added. The filter disintegrated in the DMSO and was ground for about 1 minute by rotating the grinder under moderate hand pressure. The ground suspension was transferred back to its scintillation vial by rinsing with 90% acetone. Ground samples were stored in the refrigerator overnight. Samples were removed from the refrigerator and centrifuged for 5 minutes to remove residual particulates.

Chlorophyll *a* concentration in the extracts was determined fluorometrically using a Turner Designs Model 10 field fluorometer configured for chlorophyll analysis as specified by the manufacturer. The instrument was calibrated using standards obtained from Turner Designs. Fluorescence was determined before and after acidification with 2 drops of 10% HCl. Chlorophyll *a* was calculated from the following equation which corrects for pheophytin interference:

$$\text{Chlorophyll } a\ (\mu g/L) = F_s R_s (R_b - R_a)/(R_s - 1)$$

where F_s=concentration per unit fluorescence for pure chlorophyll *a*
R_s=fluorescence before acid / fluorescence after acid for pure chlorophyll *a*
R_b=fluorescence of sample before acid
R_a=fluorescence of sample after acid

All chlorophyll analyses were completed within one month of sample collection.

Phytoplankton species composition and abundance was determined using the inverted microscope-settling chamber technique (Lund et al. 1958). Ten milliters of well-mixed algal sample were added to a settling chamber and allowed to stand for several hours. The chamber was then placed on an inverted microscope and random fields were enumerated. At least two hundred cells were identified to species and enumerated on each slide. Counts were converted to number per mL by dividing number counted by the volume counted. Biovolume of individual cells of each species was determined by measuring dimensions microscopically and applying volume formulae for appropriate solid shapes.

Microzooplankton and macrozooplankton samples were rinsed by sieving a well-mixed subsample of known volume and resuspending it in tap water. This allowed subsample volume to be adjusted to obtain an appropriate number of organisms for counting and for formalin preservative to be purged to avoid fume inhalation during counting. One mL subsamples were placed in a Sedgewick-Rafter counting cell and whole slides were analyzed until at least 200 animals had been identified and enumerated. A minimum of two slides was examined for each sample. References for identification were: Ward and Whipple (1959), Pennak (1978), and Rutner-Kolisko (1974). Zooplankton counts were converted to number per liter (microzooplankton) or per cubic meter (macrozooplankton) with the following formula:

$$\text{Zooplankton } (\#/\text{L or } \#/\text{m}^3) = NV_s/(V_cV_f)$$

where N = number of individuals counted
V_s = volume of reconstituted sample, (mL)
V_c = volume of reconstituted sample counted, (mL)
V_f = volume of water sieved, (L or m^3)

When the large cladoceran *Leptodora* was visible in a sample we used a modified method in which a know subsample was placed in a small petri dish and the entire number of *Leptodora* in this subsample were tallied using a dissecting microscope. These counts were converted to $\#/m^3$ using the above equation.

Ichthyoplankton samples were sieved through a 333 µm sieve to remove formalin and then reconstituted in ethanol. Larval fish were picked from this reconstituted sample with the aid of a stereo dissecting microscope, and the total number of larval fish was counted. Identification of ichthyoplankton was made to family and further to genus and species where possible. The works of Hogue et al. (1976), Jones et al. (1978), Lippson and Moran (1974), and Mansueti and Hardy (1967) were used for identification. The number of ichthyoplankton in each sample was expressed as number per 10 m^3 using the following formula:

$$\text{Ichthyoplankton } (\#/10\text{m}^3) = 10N/V$$

where N = number ichthyoplankton in the sample
V = volume of water filtered, (m^3)

C. Adult and Juvenile Fish

A lockdown in response to the COVID-19 pandemic delayed the start of the adult and juvenile fish sampling season to July 2020. Fishes were sampled by trawling at stations 7, 9, and 10, seining at stations 4, 4B, 6, and 11. Fyke nets were not set in 2020 because we were unable to adhere to the social distance rules for that procedure. For trawling, a try-net bottom trawl with a 15-foot horizontal opening, a ¾ inch square body mesh and a ¼ inch square cod end mesh was used. The otter boards were 12 inches by 24 inches. Towing speed was 2-3 miles per hour and tow length was 5 minutes. In general, the trawl was towed across the axis of the cove at stations 7 and 10 and parallel to the channel at station 9. The direction of tow should not be crucial. Dates of sampling are found in Table 1.

Seining was performed with seine net that was 50 feet long, 4 feet high, and made of knotted nylon with a ¼ inch square mesh. The seining procedure was standardized as much as possible. The net was stretched out perpendicular to the shore with the shore end in water no more than a few inches deep. The net was then pulled parallel to the shore for a distance of 100 feet by a worker at each end moving at a slow walk. Actual distance was recorded if in any circumstance it was lower than 100 feet. At the end of the prescribed distance, the offshore end of the net was swung in an arc to the shore and the net pulled up on the beach to trap the fish. Dates for seine sampling were generally the same as those for trawl sampling. 4B was added to the sampling stations since 2007 because extensive SAV growth interferes with sampling station 4 in late summer.

After collection, the fishes were measured for standard length to the nearest mm. Standard length is the distance from the front tip of the snout to the end of the vertebral column and base of the caudal fin. This is evident in a crease perpendicular to the axis of the body when the caudal fin is pulled to the side.

If the identification of the fish was not certain in the field, the specimen was preserved in 70% ethanol and identified later in the lab. Identification was based on characteristics in dichotomous keys found in several books and articles, including Jenkins and Burkhead (1983), Hildebrand and Schroeder (1928), Loos et al (1972), Dahlberg (1975), Scott and Crossman (1973), Bigelow and Schroeder (1953), Eddy and Underhill (1978), Page and Burr (1998), and Douglass (1999).

D. Submersed Aquatic Vegetation

Data on coverage and composition of submersed aquatic vegetation (SAV) were obtained from the SAV webpage of the Virginia Institute of Marine Science (http://www.vims.edu/bio/sav). Information on this web site was obtained from aerial photographs near the time of peak SAV abundance as well as ground surveys which were used to determine species composition. SAV abundances were also surveyed on August 29. As the research vessel slowly transited the cove, a weighted garden rake was dragged for 10-15 seconds along the bottom and retrieved. Adhering plants were identified and their relative abundance determined. About 40 such measurements were made on that date.

E. Benthic Macroinvertebrates

In the laboratory, materials collected on the 5 mm sieve for each sample were sorted into several groups: SAV, leaves/sticks/wood, shells. Each group was them dried and weighed separately. This was completed within 48 hours of sample collection

In the laboratory materials collected on the 0.5 mm sieve were rinsed with tap water through a 0.5 mm sieve to remove formalin preservative and resuspended in tap water. All organisms were picked, sorted, identified and enumerated. Picked organisms were retained in ethanol/glycerine.

F. Data Analysis

Several data flows were merged for analysis. Water quality data emanating from the Noman Cole laboratory was used for graphs of both current year seasonal and spatial patterns and long-term trends. Water quality, plankton, benthos and fish data were obtained from GMU samples. Data for each parameter were entered into spreadsheets (Excel or SigmaPlot) for graphing of temporal and spatial patterns for the current year. Long term trend analysis was conducted with Systat by plotting data for a given variable by year and then constructing a LOWESS trend line through the data. For water quality parameters the trend analysis was conducted on data from the warmer months (June-September) since this is the time of greatest microbial activity and greatest potential water quality impact. For zooplankton and fish all data for a given year were used. When graphs are shown with a log axis, zero values have been ignored in the trend analysis. JMP v8.0.1was used for fish graphs. Linear regression and standard parametric (Pearson) correlation coefficients were conducted to determine the statistical significance of linear trends over the entire period of record.

RESULTS

A. Climatic and Hydrologic Factors - 2020

In 2020 temperature was below normal in April and May, but well above normal from June through August (Table 2). There were 38 days with maximum temperature above 32.2°C (90°F) in 2020 which is well above the median number over the past decade. Precipitation was closer to normal in 2020 than in the extremely wet year 2018. However, it was again well above normal in 2020. April, July, and August were about double their normal precipitation in 2020. River and stream flows in 2020 were generally near average except in August when flows were substantially above average in Accotink Creek (Table 3). As with precipitation, flows in 2020 were well below the record flows of 2018.

Table 2. Meteorological Data for 2020. National Airport. Monthly Summary.

MONTH	Air Temp (°C)		Precipitation (cm)	
March	11.9	(8.1)	5.9	(9.1)
April	12.9	(13.4)	16.0	(7.0)
May	17.7	(18.7)	6.3	(9.7)
June	24.9	(23.6)	8.9	(8.0)
July	29.1	(26.2)	16.5	(9.3)
August	26.8	(25.2)	22.2	(8.7)
September	21.5	(21.4)	14.0	(9.6)
October	17.2	(14.9)	11.6	(8.2)

Table 3. Monthly mean discharge at USGS Stations representing freshwater flow into the study area. (+) 2020 month > 2x Long Term Avg. (-) 2020 month < ½ Long Term Avg.

	Potomac River at Little Falls (cfs)		**Accotink Creek at Braddock Rd (cfs)**	
	2020	**Long Term Avg.**	**2020**	**Long Term Avg.**
March	9137 (-)	23600	15.7	42
April	16424	20400	45.1	36
May	20824	15000	27.9	34
June	9747	9030	37.9	28
July	3453	4820	29.5	22
August	6109	4550	50.2 (+)	22
September	4558	5040	26.5	27

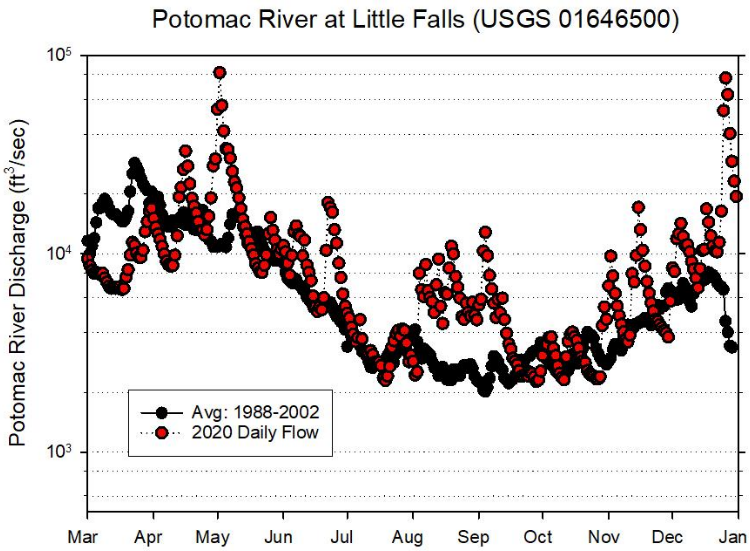

In a tidal freshwater system like the Potomac River, river flow entering from upstream is important in maintaining freshwater conditions and also serves to bring in dissolved and particulate substances from the watershed. High freshwater flows may also flush planktonic organisms downstream and bring in suspended sediments that decrease water clarity. The volume of river flow per unit time is referred to as "river discharge" by hydrologists. Note the long-term seasonal pattern of higher discharges in winter and spring and lower discharges in summer and fall.

Figure 2. Mean Daily Discharge: 2020. Potomac River at Little Falls (USGS Data). Month tick is at the beginning of the month.

These same patterns were seen in the graphs of daily river and stream flow when compared to long-term averages (Figures 2 and 3). River flow in 2020 tracked long term averages fairly closely except in May, June, and especially in August when it was substantially above normal (Figure 2). Local inflow to the cove from Accotink followed the long-term pattern of decreasing base flow through the summer punctuated by storm flows (Figure 3). The high flows were most frequent during August.

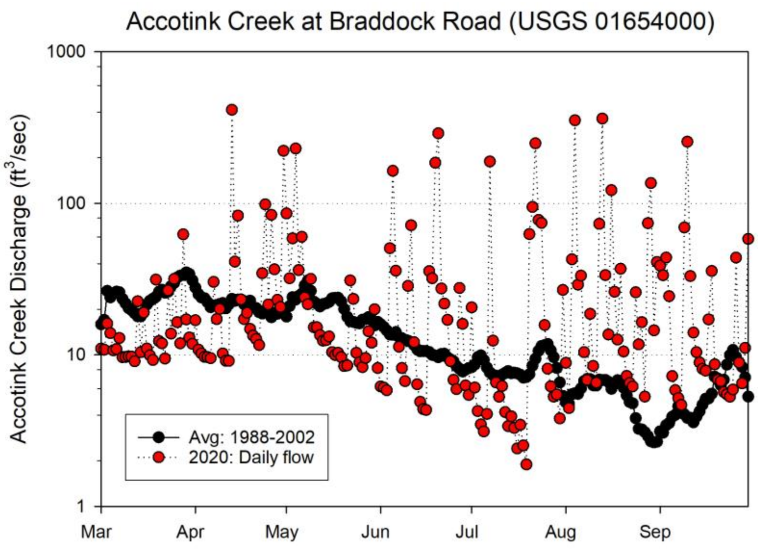

In the Gunston Cove region of the tidal Potomac, freshwater discharge is occurring from both the major Potomac River watershed upstream (measured at Little Falls) and from immediate tributaries. The cove tributary for which stream discharge is available is Accotink Creek. Accotink Creek delivers over half of the stream water which directly enters the cove. While the gauge at Braddock Road only covers the upstream part of the watershed it is probably representative.

.

Figure 3. Mean Daily Discharge: 2020. Accotink Creek at Braddock Road (USGS Data).

B. Physico-chemical Parameters – 2020

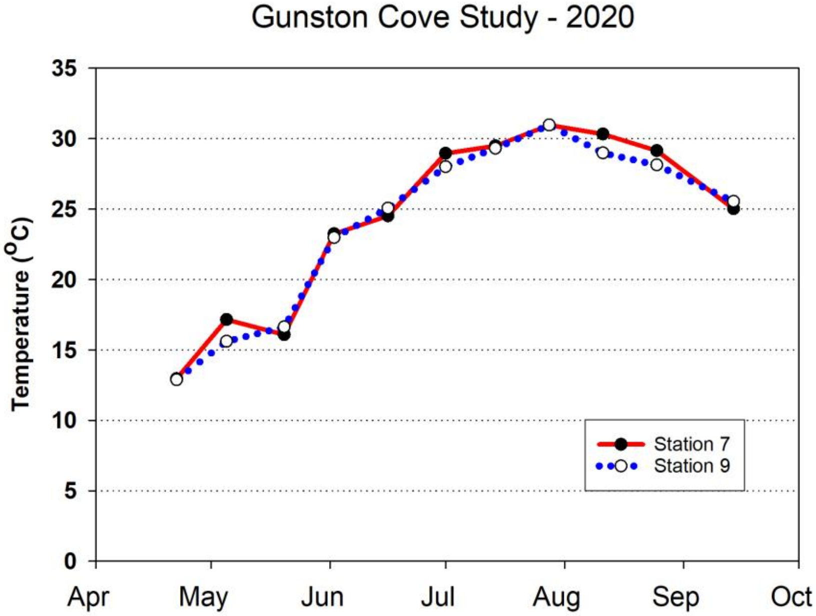

Water temperature is an important factor affecting both water quality and aquatic life. In a well-mixed system like the tidal Potomac, water temperatures are generally fairly uniform with depth.
In a shallow mixed system such as the tidal Potomac, water temperature often closely tracks daily changes in air temperature.

Figure 4. Water Temperature (°C). GMU Field Data. Month tick is at first day of month.

In 2020, water temperature followed the typical seasonal pattern at both sites with the exception of a marked cooling in late May (Figure 4). Both sites were between 25°C and 30°C throughout July and August the perod of highest air trempetatures (Figure 5). For most of the study period, the two stations showed very similar water temperatures.

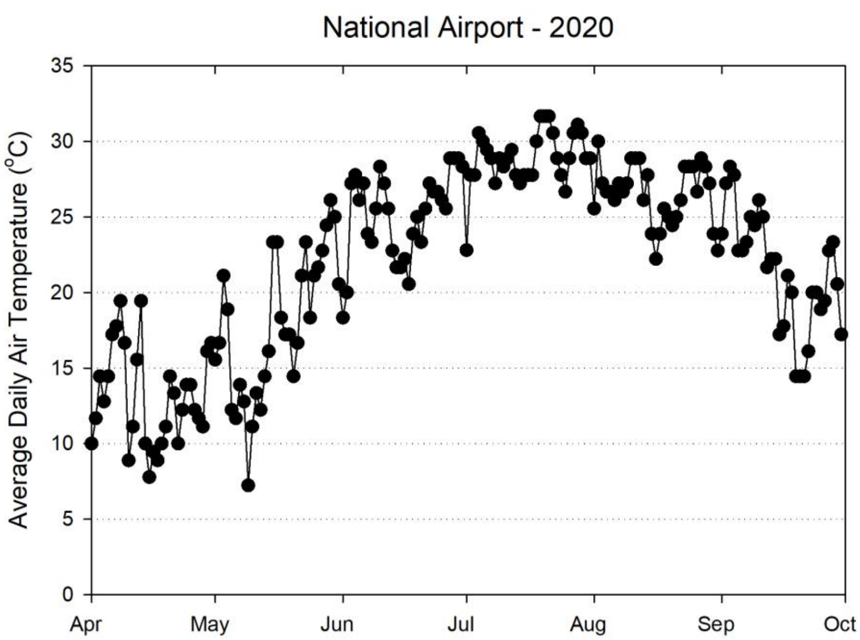

Mean daily air temperature (Figure 5) was a good predictor of water temperature (Figure 4). Variations in daily air temperature were more pronounce in the spring than in the summer.

Figure 5. Average Daily Air Temperature (°C) at Reagan National Airport.

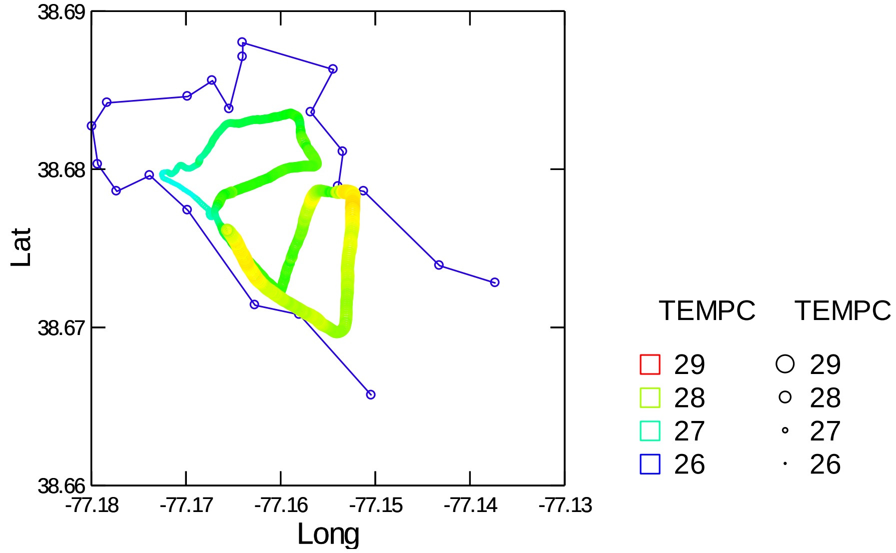

Figure 6. Temperature (ºC) observed in transects across Gunston Cove during data mapping cruise on September 3, 2020.

Temperature and Specific Conductance were measured during data mapping cruise on September 3, 2020 to assess spatial patterns in Gunston Cove. Temperature was slightly higher in the outer part of the cove and slightly lower in Pohick Bay (Figure 6). Specific conductance showed a clear pattern with higher values in Pohick Bay gradually decreasing moving out into the body of Gunston Cove (Figure 7). Accotink Bay was also lower. Pattern suggests an effect of Noman Cole effluent which has higher specific conductance than Gunston Cove. However, higher specific conductance was also seen in the outer part of Gunston Cove which may have seen an influence from the river mainstem..

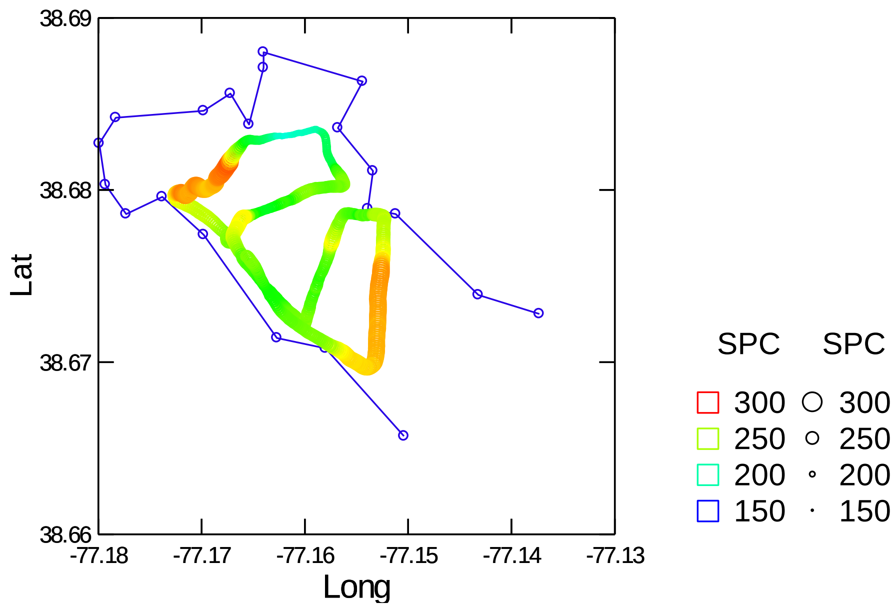

Figure 7. Specific Conductance (uS/cm) observed in transects across Gunston Cove during data mapping cruise on September 3, 2020.

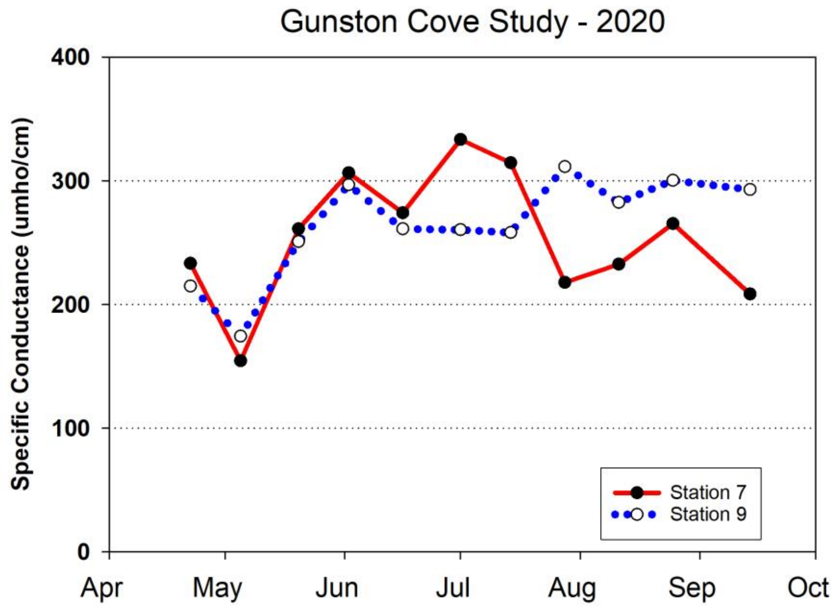

Specific conductance measures the capacity of the water to conduct electricity standardized to 25°C. This is a measure of the concentration of dissolved ions in the water. In freshwater, conductivity is relatively low. Ion concentration generally increases slowly during periods of low freshwater inflow and decreases during periods of high freshwater inflow. In years of low freshwater inflow during the summer and fall, conductance may increase dramatically if brackish water from the estuary reaches the study area.

Figure 8. Specific Conductance (uS/cm). GMU Field Data. Month tick is at first day of month.

Specific conductance was mostly in the 200-300 range except in early May when it dropped below 200 (Figure 8). Values were similar at both stations through mid June. Values were higher in the cove in July, but the river station was hiher in August and September. Chloride ion was consistently higher at Station 7 throughout the year, probably due to the Noman Cole effluent, but values were well within the freshwater range (Figure 9).

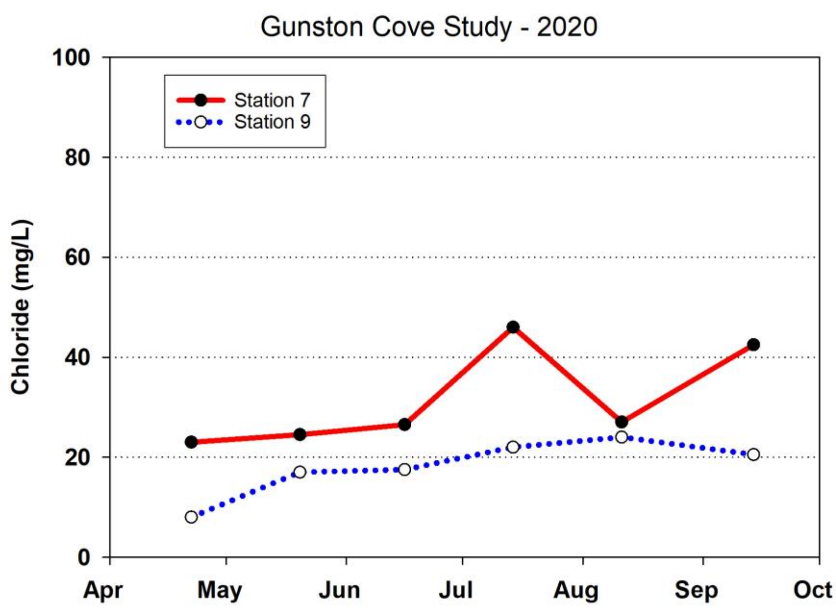

Chloride ion (Cl-) is a principal contributor to conductance. Major sources of chloride in the study area are sewage treatment plant discharges, road salt, and brackish water from the downriver portion of the tidal Potomac. Chloride concentrations observed in the Gunston Cove area are very low relative to those observed in brackish, estuarine, and coastal areas of the Mid-Atlantic region. Chloride often peaks markedly in late summer or fall when brackish water from down estuary may reach the cove as freshwater discharge declines.

Figure 9. Chloride (mg/L). Fairfax County Lab Data. Month tick is at first day of month.

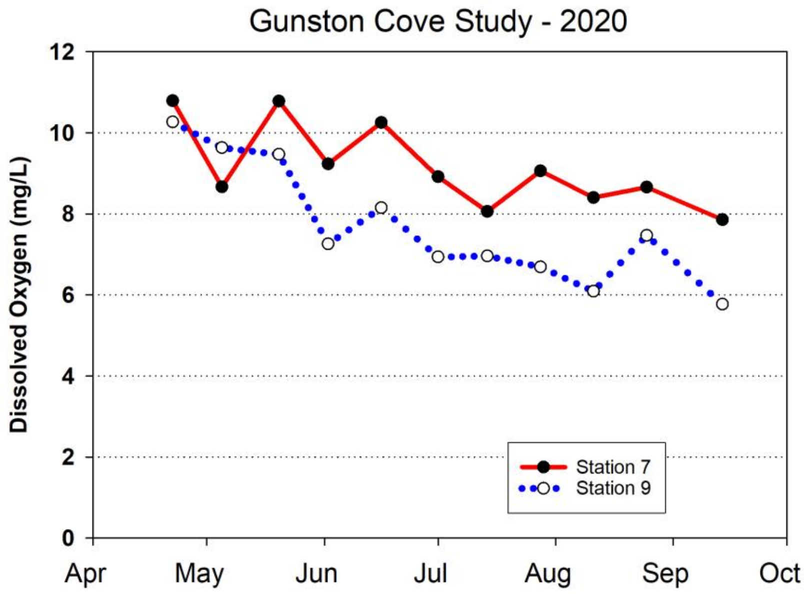

Oxygen dissolved in the water is required by freshwater animals for survival. The standard for dissolved oxygen (DO) in most surface waters is 5 mg/L. Oxygen concentrations in freshwater are in balance with oxygen in the atmosphere, but oxygen is only weakly soluble in water so water contains much less oxygen than air. This solubility is determined by temperature with oxygen more

Figure 10. Dissolved Oxygen (mg/L). GMU Field Data. Month tick is at first day of month.

Dissolved oxygen in mg/L showed a gradual decline through the year at both stations with Station 7 maintaining higher values through most of the year (Figure 10). Figure 11 shows that dissolved oxygen levels in the cove were often substantially above 100% indicating abundant photosynthesis by SAV and phytoplankton. In the river values were generally equal or less than 100% indicating lower photosynthesis and an excess of respiration.

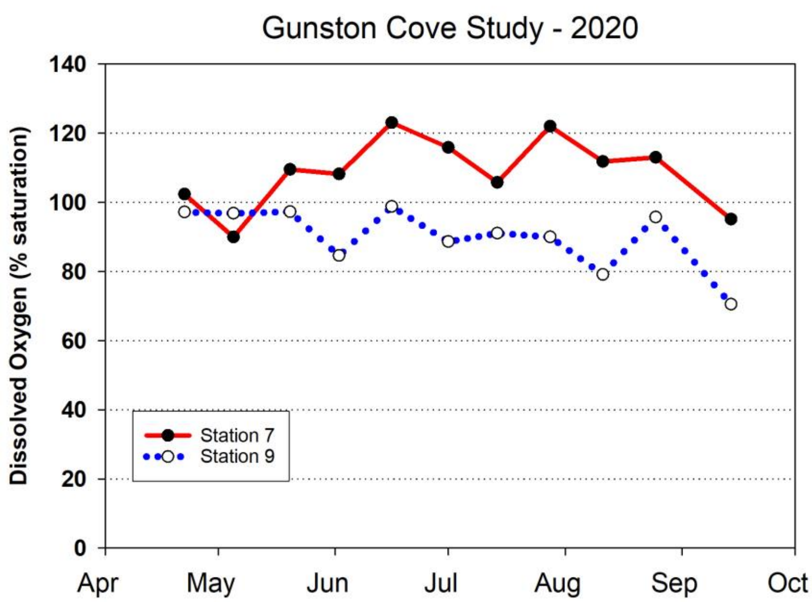

The temperature effect on oxygen concentration can be removed by calculating DO as percent saturation. This allows examination of the balance between photosynthesis and respiration both of which also impact DO. Photosynthesis adds oxygen to the water while respiration removes it. Values above 120% saturation are indicative of intense photosynthesis while values below 80% reflect a preponderance of respiration or decomposition.

Figure 11. Dissolved Oxygen (% saturation). GMU Field Data. Month tick is at first day of month.

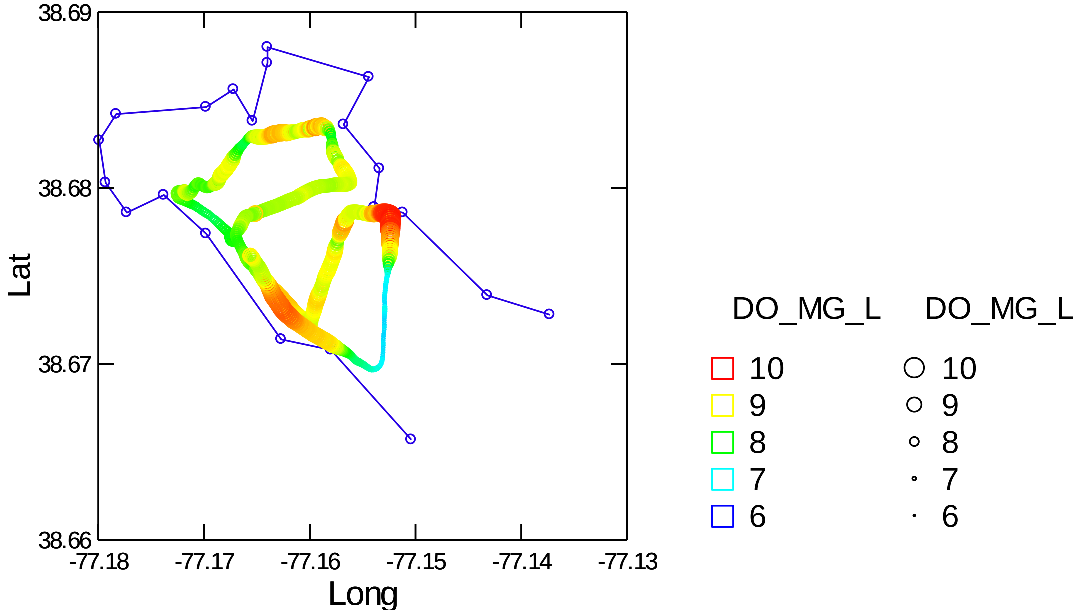

Figure 12. Dissolved Oxygen (mg/L) observed in transects across Gunston Cove during data mapping cruise on September 3, 2020.

Dissolved oxygen levels were highest in the middle part of Gunston Cove, especially along the shoreline (Figures 12&13). The supersaturated DO values indicated strong photosynthetic activity probably due to dense SAV in those two shoreline areas. Values were lowest just riverward of the high values.

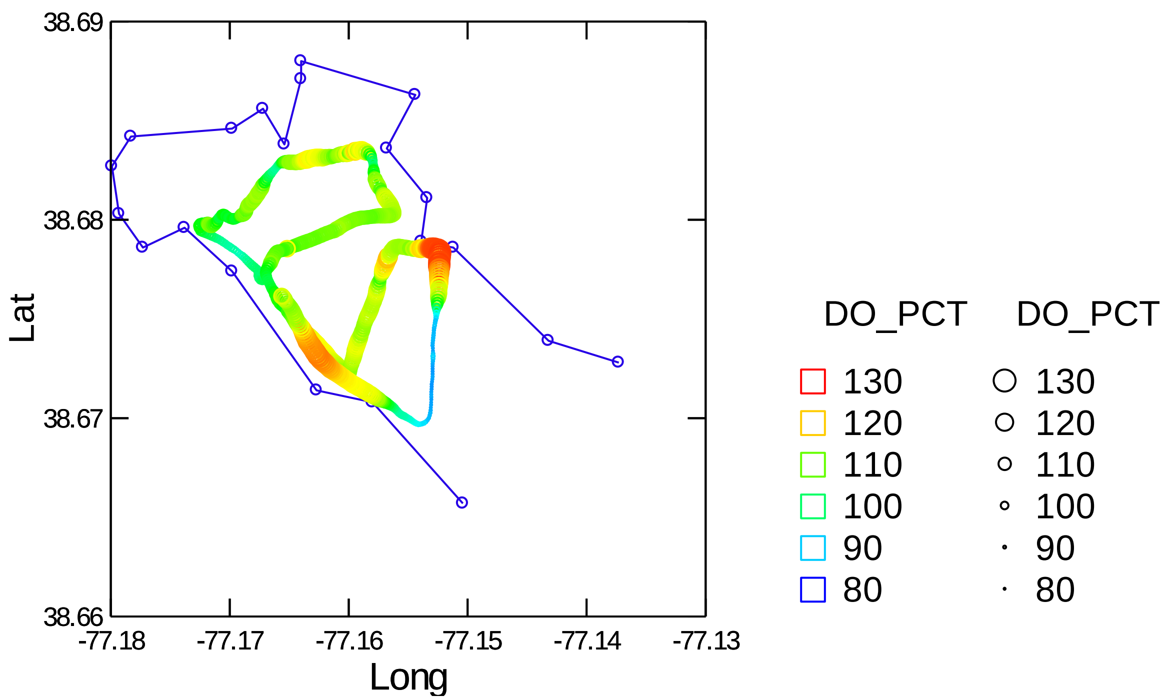

Figure 13. Dissolved Oxygen (% saturation) observed in transects across Gunston Cove during data mapping cruise on September 3, 2020.

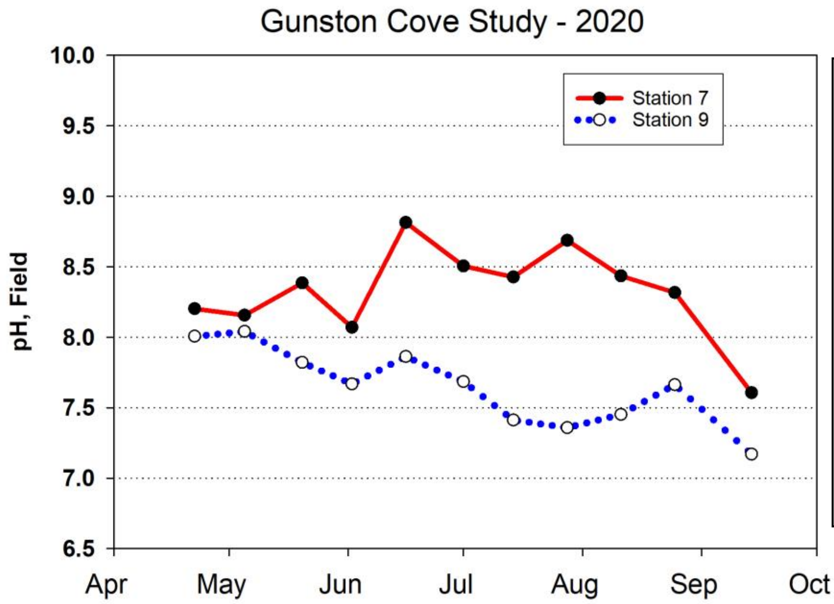

pH is a measure of the concentration of hydrogen ions (H+) in the water. Neutral pH in water is 7. Values between 6 and 8 are often called circumneutral, values below 6 are acidic and values above 8 are termed alkaline. Like DO, pH is affected by photosynthesis and respiration. In the tidal Potomac, pH above 8 indicates active photosynthesis and values above 9 indicate intense

Figure 14. pH. GMU Field Data. Month tick is at first day of month.

Field pH was consistently greater in the cove than in the river again reflecting differences in photosynthetic activity (Figure 14). Times of elevated pH generally corresponded to those in dissolved oxygen. This was also true comparing the spatial pattern of pH (Figure 15) with that of DO (Figure 13) and again is consistent with a photosynthetic activity effect, probably due to SAV since the high values were observed in shallow water near the shoreline where SAV are most abundant..

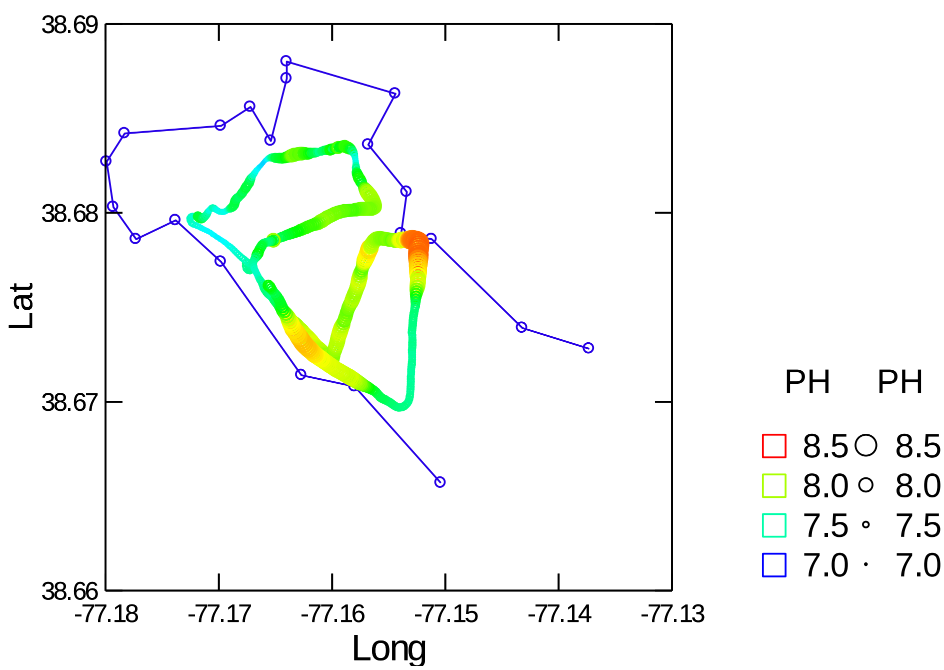

Figure 15. Field pH observed in transects across Gunston Cove during data mapping cruise on September 3, 2020.

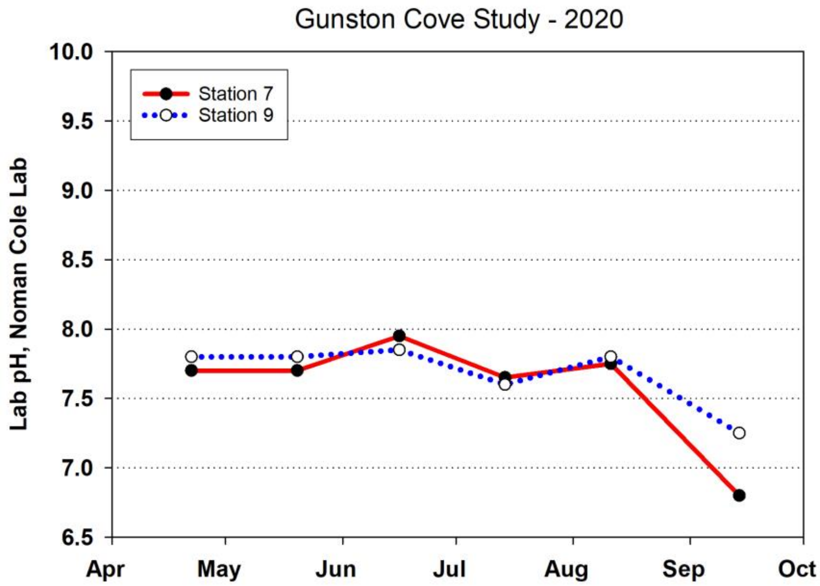

pH may be measured in the field or in the lab. Field pH is more reflective of in situ conditions while lab pH is done under more stable and controlled laboratory conditions and is less subject to error. Newer technologies such as the Hydrolab and YSI sondes used in GMU field data collection are more reliable than previous field pH meters and should give results that are most representative of values actually observed in the river.

Figure 16. pH. Noman Cole Lab Data. Month tick is at first day of month.

Lab pH was collected less frequently, and failed to show enhanced values in the cove (Figure 16). Total alkalinity was consistently higher in the river than in the cove by about 5 units building to almost 50 mg/L difference in September (Figure 17).

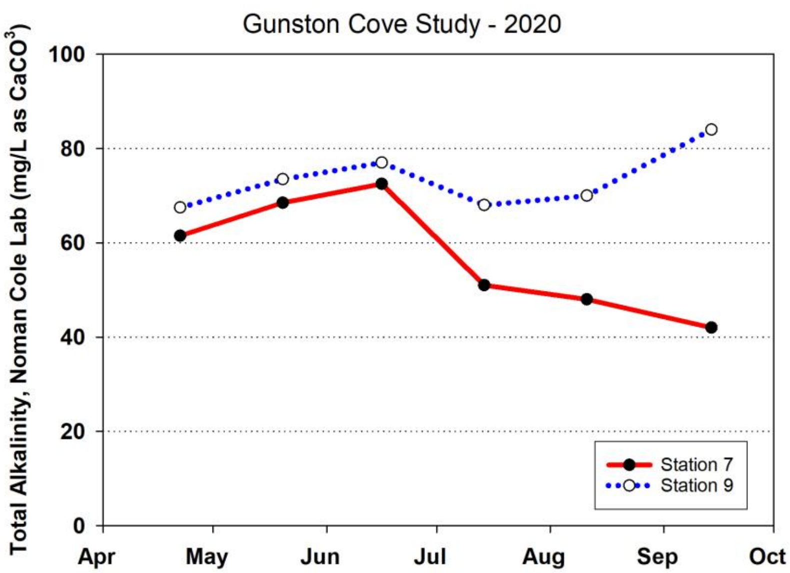

Total alkalinity measures the amount of bicarbonate and carbonate dissolved in the water. In freshwater this corresponds to the ability of the water to absorb hydrogen ions (acid) and still maintain a near neutral pH. Alkalinity in the tidal freshwater Potomac generally falls into the moderate range allowing adequate buffering without carbonate precipitation.

Figure 17. Total Alkalinity (mg/L as $CaCO_3$). Fairfax County Lab data. Month tick is at first day of month.

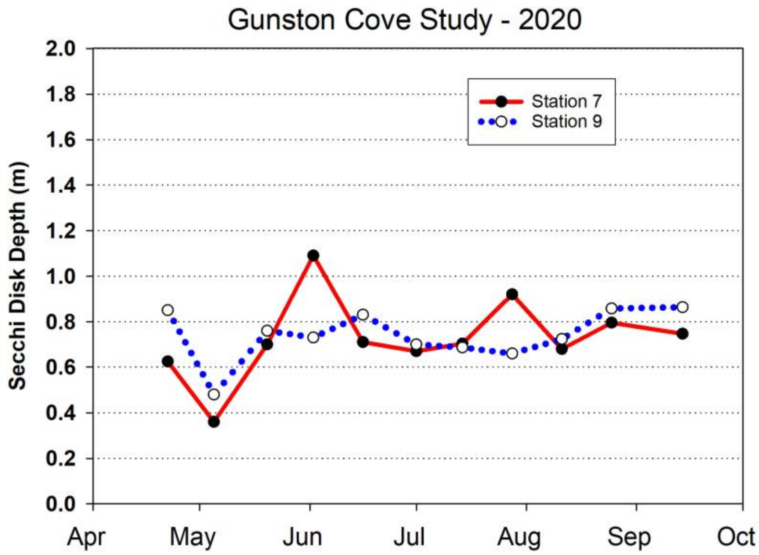

Secchi Depth is a measure of the transparency of the water. The Secchi disk is a flat circle or thick sheet metal or plywood about 6 inches in diameter which is painted into alternate black and white quadrants. It is lowered on a calibrated rope or rod to a depth at which the disk disappears. This depth is termed the Secchi Depth. This is a quick method for determining how far light is penetrating into the water column. Light is necessary for photosynthesis and thereby for growth of aquatic

Figure 18. Secchi Disk Depth (m). GMU Field Data. Month tick is at first day of month.

Water clarity as reflected by Secchi disk transparency was fairly constant at both stations during 2020. Values hovered around 0.7 m for most of the year at both stations. Exceptions were a marked low in early May at both stations and a high of over 1 m in early June in the cove (Figure 18). Light attenuation coefficient exhibited a similar spatial and temporal pattern with a severe decline in early May in the cove (Figure 19).

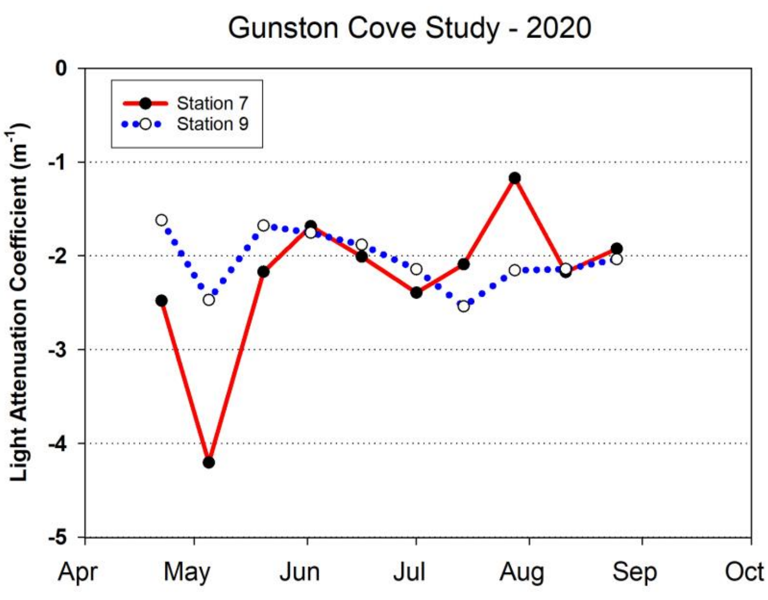

Light Attenuation is another approach to measuring light penetration. This is determined by measuring light levels at a series of depths starting near the surface. The resulting relationship between depth and light is fit to a semi-logarithmic curve and the resulting slope is called the light attenuation coefficient. This relationship is called Beer's Law. It is analogous to absorbance on a spectrophotometer. The greater the light attenuation, the faster light is absorbed with depth. More negative values indicate greater attenuation. Greater attenuation is due to particulate and dissolved material which absorbs and deflects light.

Figure 19. Light Attenuation Coefficient (m^{-1}). GMU Field Data. Month tick is at first day of month.

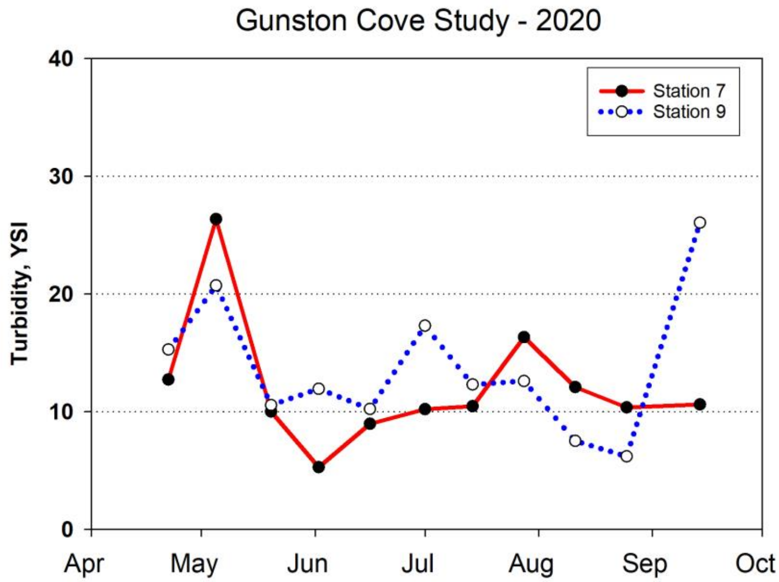

Turbidity is yet a third way of measuring light penetration. Turbidity is a measure of the amount of light scattering by the water column. Light scattering is a function of the concentration and size of particles in the water. Small particles scatter more light than large ones (per unit mass) and more particles result in more light scattering than fewer particles.

Figure 20. Turbidity (NTU). GMU Lab Data. Month tick is at first day of month.

Turbidity exhibited the peak in early May corresponding to low water transparency from Secchi depth (Figure 20). And low turbidity was found in early June when Secchi depth was over 1 m. In the September datamapping cruise, turbidity was generally low except in Pohick Bay where it was somewhat higher, perhaps due to sediment resuspension during the cruise (Figure 21)..

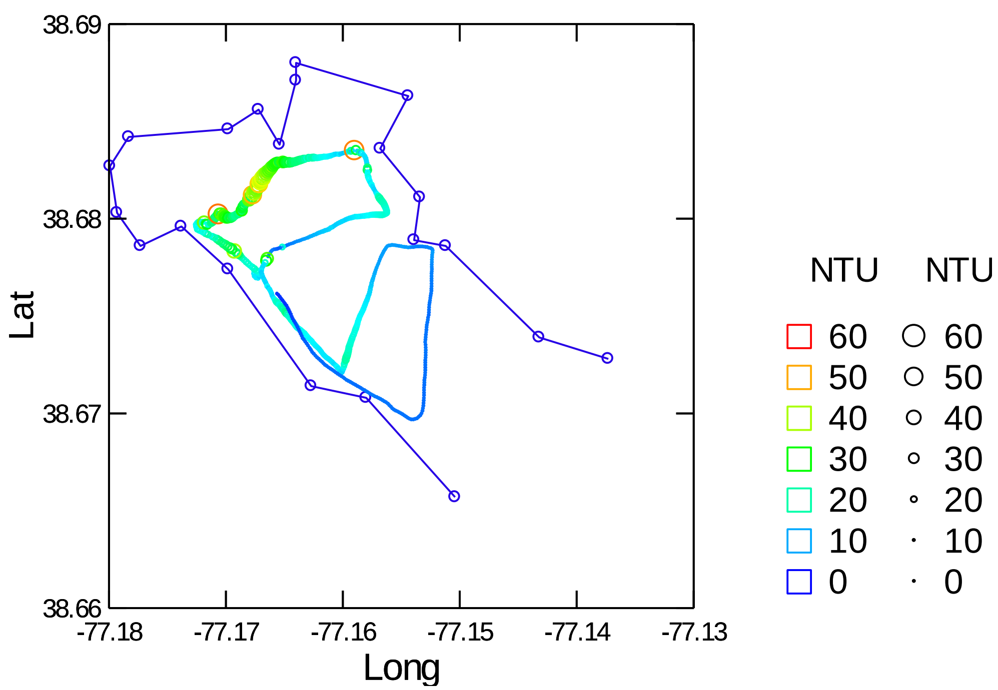

Figure 21. Turbidity (NTU) observed in transects across Gunston Cove during data mapping cruise on September 3, 2020.

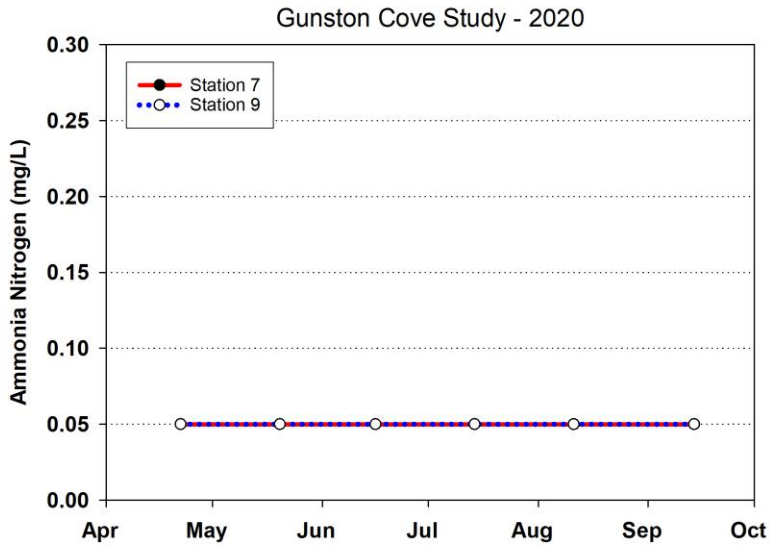

Ammonia nitrogen measures the amount of ammonium ion (NH_4^+) and ammonia gas (NH_3) dissolved in the water. Ammonia nitrogen is readily available to algae and aquatic plants and acts to stimulate their growth. While phosphorus is normally the most limiting nutrient in freshwater, nitrogen is a close second. Ammonia nitrogen is rapidly oxidized to nitrate nitrogen when oxygen is present in the water.

Figure 22. Ammonia Nitrogen (mg/L). Fairfax County Lab Data. Month tick is at first day of month. (Limit of detection: 0.10 mg/L, LD values graphed as 0.05 mg/L)

Ammonia nitrogen was below detection limits in all samples reported in 2020 (Figure 22). Unfortunately, the detection limit at the Fairfax County Lab has increased substantially in the past several years from 0.01 mg/L to 0.1 mg/L. As we pointed out in the 2019 report, this has made it impossible to detect any further improvements in ammonia levels. Nitrate nitrogen levels were consistently higher in the river than in the cove (Figure 23). A clear seasonal decline was observed at both stations, but values remained consistently higher in the river. In cove, nitrate concentrations were near detection limits in July.

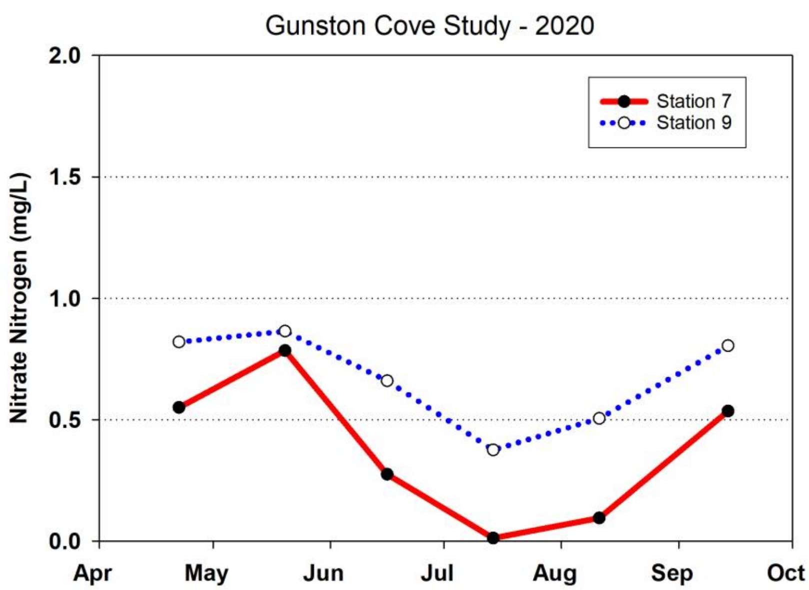

Nitrate Nitrogen refers to the amount of N that is in the form of nitrate ion (NO_3^-). Nitrate ion is the most common form of nitrogen in most well oxidized freshwater systems. Nitrate concentrations are increased by input of wastewater, nonpoint sources, and oxidation of ammonia in the water. Nitrate concentrations decrease when algae and plants are actively growing and removing nitrogen as part of their growth.

Figure 23. Nitrate Nitrogen (mg/L). Fairfax County Lab Data. Month tick is at first day of month. (Limit of detection: 0.01 mg/L; LD values graphed as 0.005 mg/L)

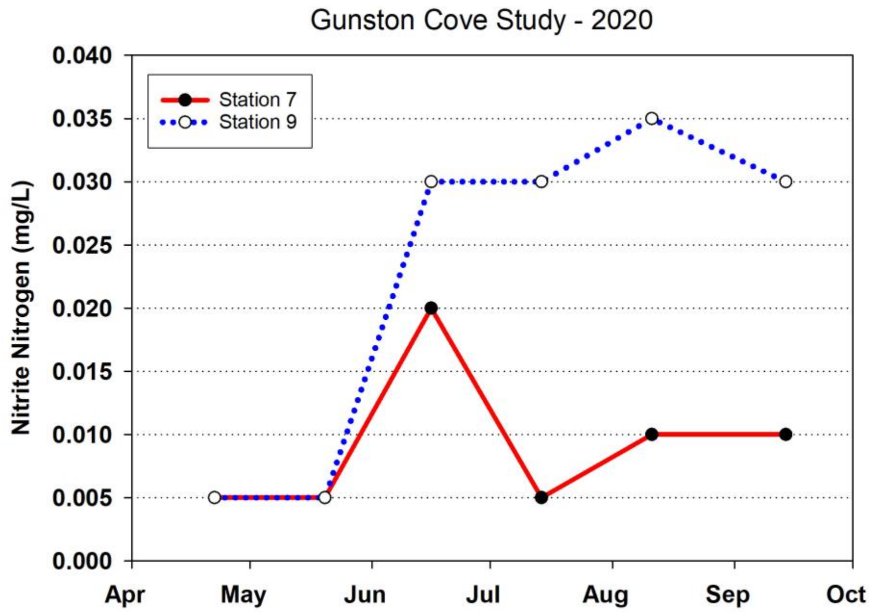

Nitrite nitrogen consists of nitrogen in the form of nitrite ion (NO_2^-). Nitrite is an intermediate in the oxidation of ammonia to nitrate, a process called nitrification. Nitrite is usually in very low concentrations unless there is active nitrification.

Figure 24. Nitrite Nitrogen (mg/L). Fairfax County Lab Data. Month tick is at first day of month. (limit of detection = 0.01 mg/L).

Nitrite nitrogen was low and quite variable, but higher in the summer and fall and consistently higher in the river (Figure 24). Organic nitrogen was quite variable at both stations. Values in the cove were consistently 0.05 to 1.0 mg/L higher in cove was higher than the river (Figure 25). A minimum was observed in late May and a maximum in July.

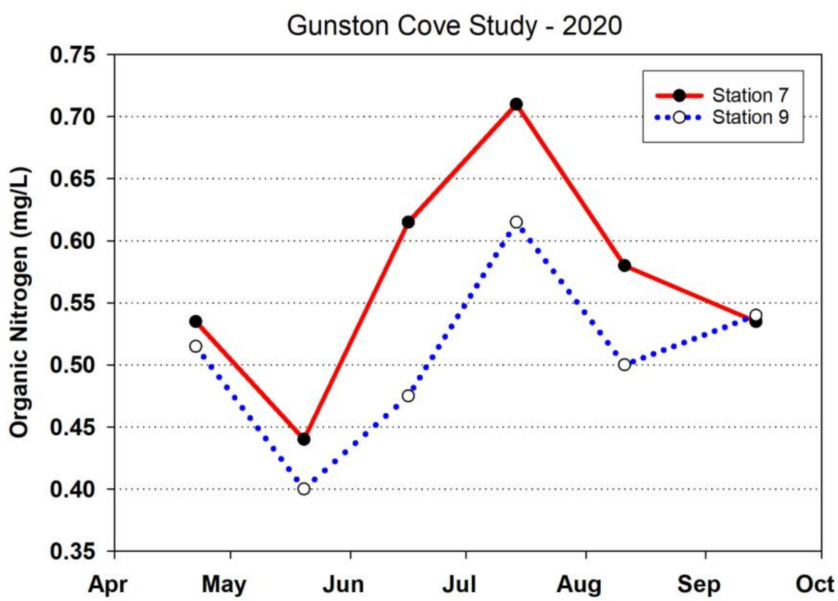

Organic nitrogen measures the nitrogen in dissolved and particulate organic compounds in the water. Organic nitrogen comprises algal and bacterial cells, detritus (particles of decaying plant, microbial, and animal matter), amino acids, urea, and small proteins. When broken down in the environment, organic nitrogen results in ammonia nitrogen. Organic nitrogen is determined as the difference between total Kjeldahl nitrogen and ammonia nitrogen.

Figure 25. Organic Nitrogen (mg/L). Fairfax County Lab Data. Month tick is at first day of month.

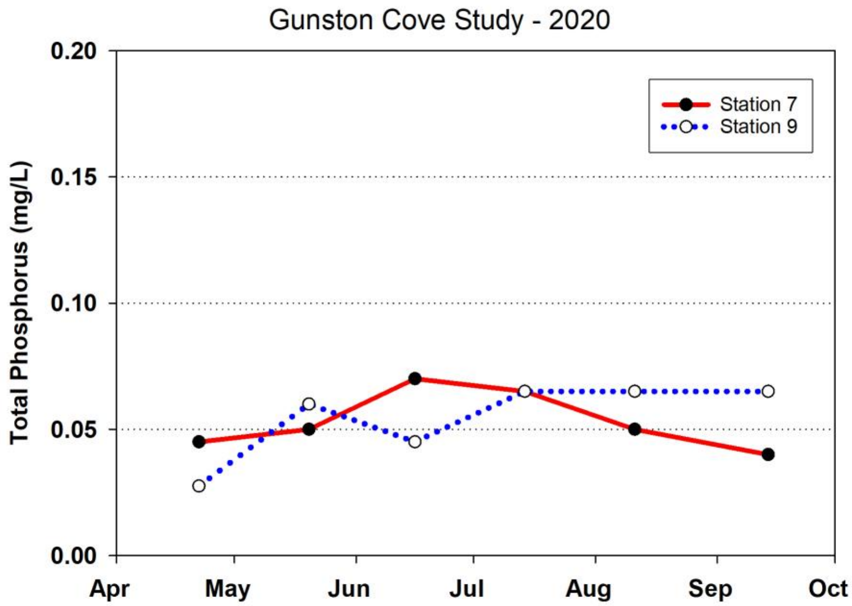

Phosphorus (P) is often the limiting nutrient in freshwater ecosystems. As such the concentration of P can set the upper limit for algal growth. Total phosphorus is the best measure of P availability in freshwater since much of the P is tied up in biological tissue such as algal cells. Total P includes phosphate ion (PO_4^{-3}) as well as phosphate inside cells and phosphate bound to inorganic particles such as clays.

Figure 26. Total Phosphorus (mg/L). Fairfax County Lab Data. Month tick is at first day of month. (Limit of detection: 0.03 mg/L)

Total phosphorus was similar at both stations on almost all dates and showed very little trend over time at either station (Figure 26). Soluble reactive phosphorus was sometimes much higher in the river (Figure 27).

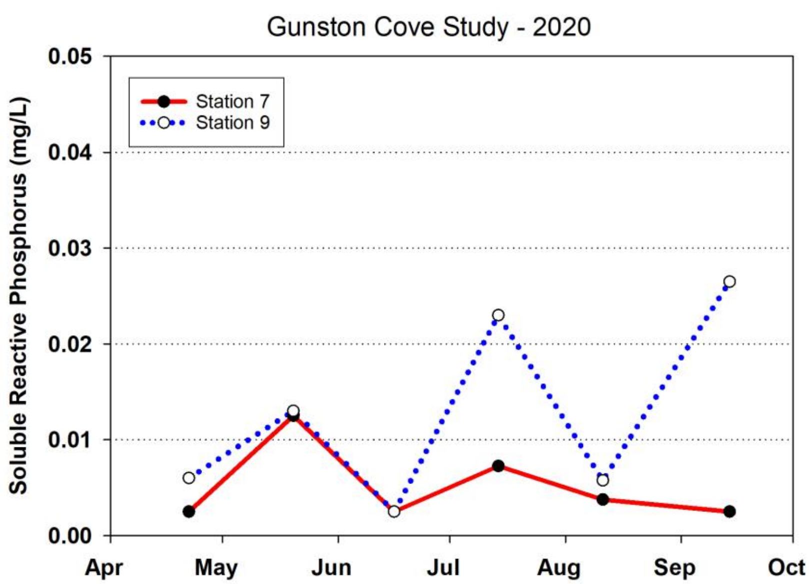

Soluble reactive phosphorus (SRP) is a measure of phosphate ion (PO_4^{-3}). Phosphate ion is the form in which P is most available to primary producers such as algae and aquatic plants in freshwater. However, SRP is often inversely related to the activity of primary producers because they tend to take it up so rapidly. So, higher levels of SRP indicate either a local source of SRP to the waterbody or limitation by a factor other than P.

Figure 27. Soluble Reactive Phosphorus (mg/L). Fairfax County Lab Data. Month tick is at first day of month. (Limit of detection = 0.005 mg/L)

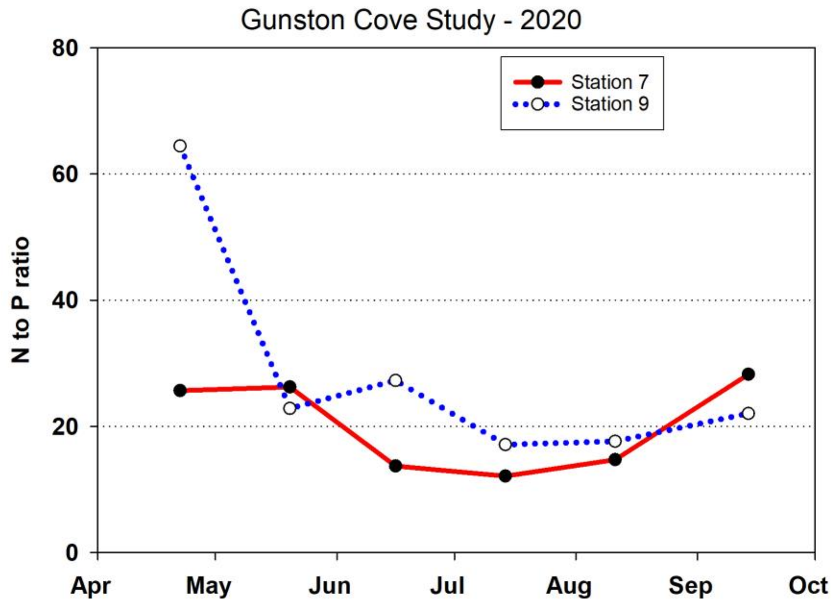

N:P ratio is determined by summing all of the components of N (ammonia, nitrate, nitrite, and organic nitrogen) and dividing by total P. This ratio gives an indication of whether N or P is more likely to be limiting primary production in a given freshwater system. Generally, values above 7.2 are considered indicative of P limitation while values below 7.2 suggest N limitation. N limitation could lead to dominance by cyanobacteria who can fix their own N from the atmosphere.

Figure 28. N/P Ratio (by mass). Fairfax County Lab Data. Month tick is at first day of month.

N/P ratio exhibited little consistent seasonal pattern at either site (Figure 28). Values bottomed out at about 12 in mid-July in the cove approaching N limitation. Values in the river remained consistently above 17 throughout the year, but were also lowest in July. Biochemical oxygen demand (BOD) was consistently higher in the cove than in the river with highest values in June at both stations (Figure 29).

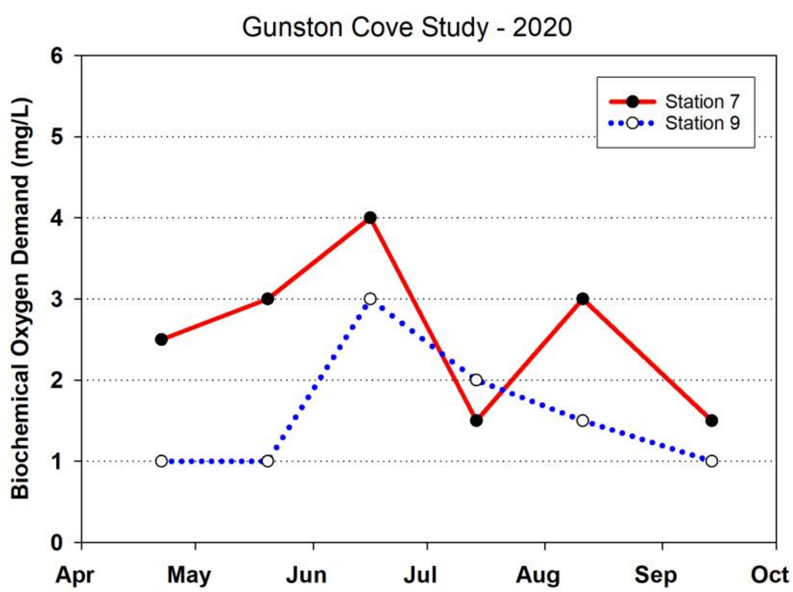

Biochemical oxygen demand (BOD) measures the amount of decomposable organic matter in the water as a function of how much oxygen it consumes as it breaks down over a given numittlber of days. Most commonly the number of days used is 5. BOD is a good indicator of the potential for oxygen depletion in water. BOD is composed both dissolved organic compounds in the water as well as microbes such as bacteria and algae which will respire and consume oxygen during the period of measurement

Figure 29. Biochemical Oxygen Demand (mg/L). Fairfax County Lab Data. Month tick is at first day of month.

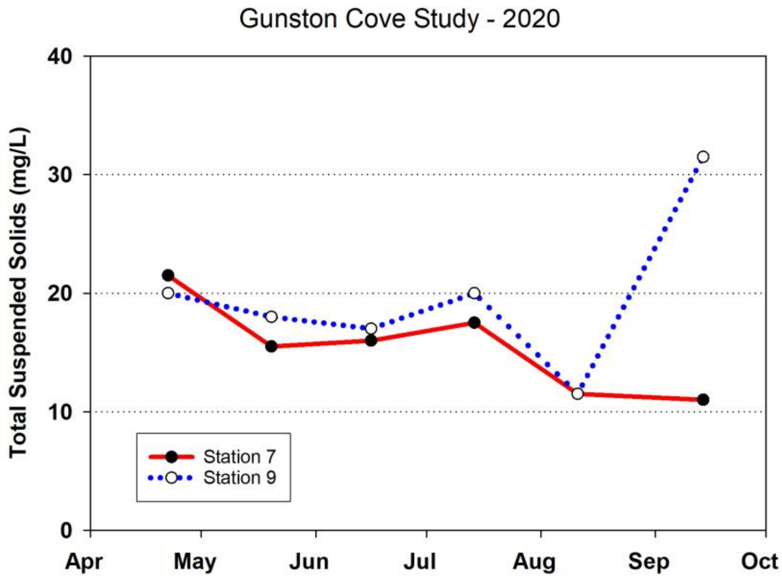

Total suspended solids (TSS) is measured by filtering a known amount of water through a fine filter which retains all or virtually all particles in the water. This filter is then dried and the weight of particles on the filter determined by difference. TSS consists of both organic and inorganic particles. During periods of low river and tributary inflow, organic particles such as algae may dominate. During storm flow periods or heavy winds causing resuspension, inorganic particles may dominate.

Figure 30. Total Suspended Solids (mg/L). Fairfax County Lab Data. Month tick is at first day of month.

Total suspended solids was similar in both cove and river and showed a slight decline at both stations over the year except for a high value in September in the river (Figure 30). Volatile suspended solids was higher in the cove from April through June, but was similar at all stations in July through September (Figure 31). Values did not show much of a seasonal pattern.

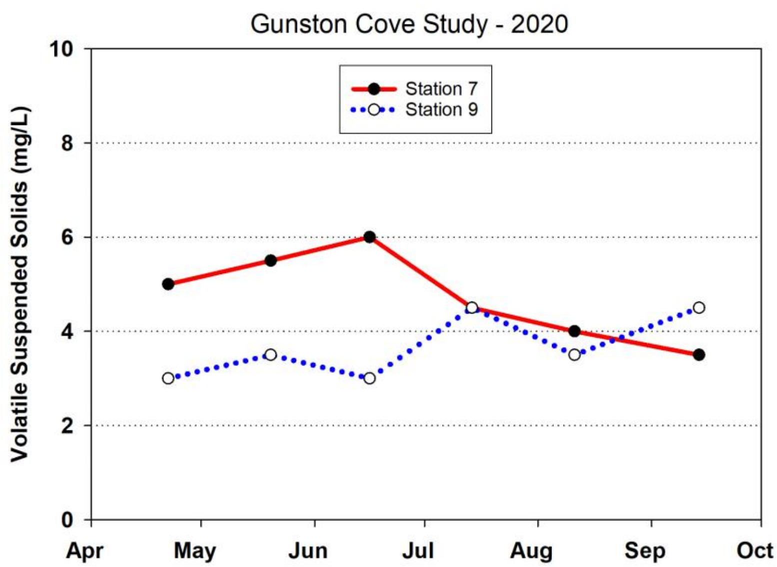

Volatile suspended solids (VSS) is determined by taking the filters used for TSS and then ashing them to combust (volatilize) the organic matter. The organic component is then determined by difference. VSS is a measure of organic solids in a water sample. These organic solids could be bacteria, algae, or detritus. Origins include sewage effluent, algae growth in the water column, or detritus produced within the waterbody or from tributaries. In summer in Gunston Cove a chief source is algal (phytoplankton) growth.

Figure 31. Volatile Suspended Solids (mg/L). Fairfax County Lab Data. Month tick is at first day of month.

C. Phytoplankton -2020

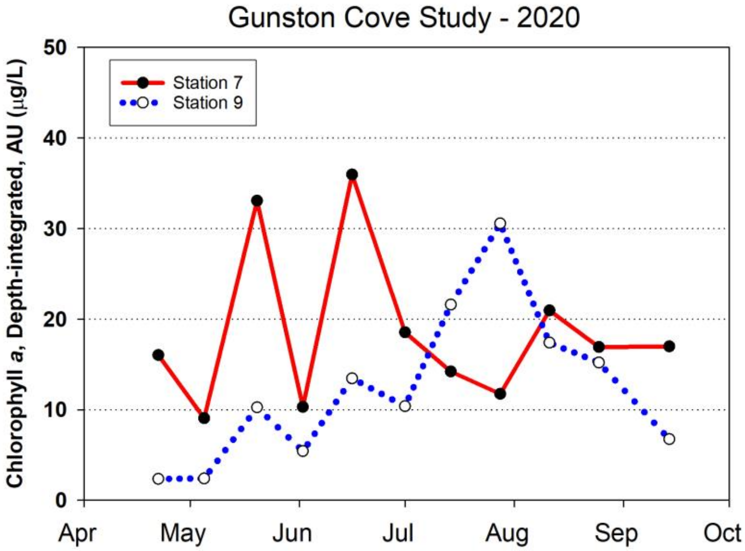

Chlorophyll *a* is a measure of the amount of algae growing in the water column. These suspended algae are called phytoplankton, meaning "plant wanderers". In addition to the true algae (greens, diatoms, cryptophytes, etc.) the term phytoplankton includes cyanobacteria (sometimes known as "blue-green" algae). Both depth-integrated and surface chlorophyll values are measured due to the capacity of phytoplankton to aggregate near the surface under certain conditions.

Figure 32. Chlorophyll *a* (µg/L). Depth-integrated. GMU Lab Data. Month tick is at the first day of month. AU soak procedure.

Chlorophyll *a* at in the cove exhibited two major peaks in mid-May and mid-June each exceeding 30 µg/L (Figures 32&33). During July through September values were between 10 and 20 µg/L. In the river, chlorophyll a exhibited a steady increase to a maximum in late July of about 30 µg/L. Depth-integrated and surface chlorophyll showed similar spatial and temporal patterns.

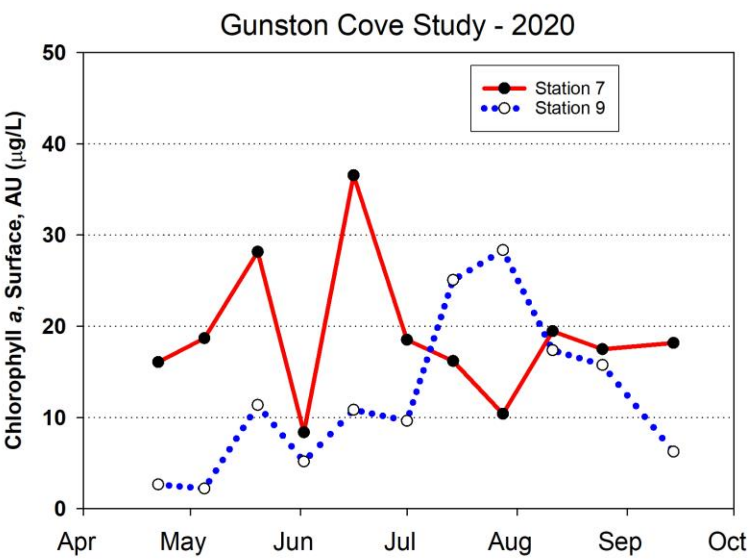

In the Gunston Cove, there is very little difference in surface and depth-integrated chlorophyll levels because tidal action keeps the water well-mixed which overcomes any potential surface aggregation by the phytoplankton. Summer chlorophyll concentrations above 30 ug/L are generally considered characteristic or eutrophic conditions

Figure 33. Chlorophyll *a* (µg/L). Surface. GMU Lab Data. Month tick is at first day of month. AU soak procedure.

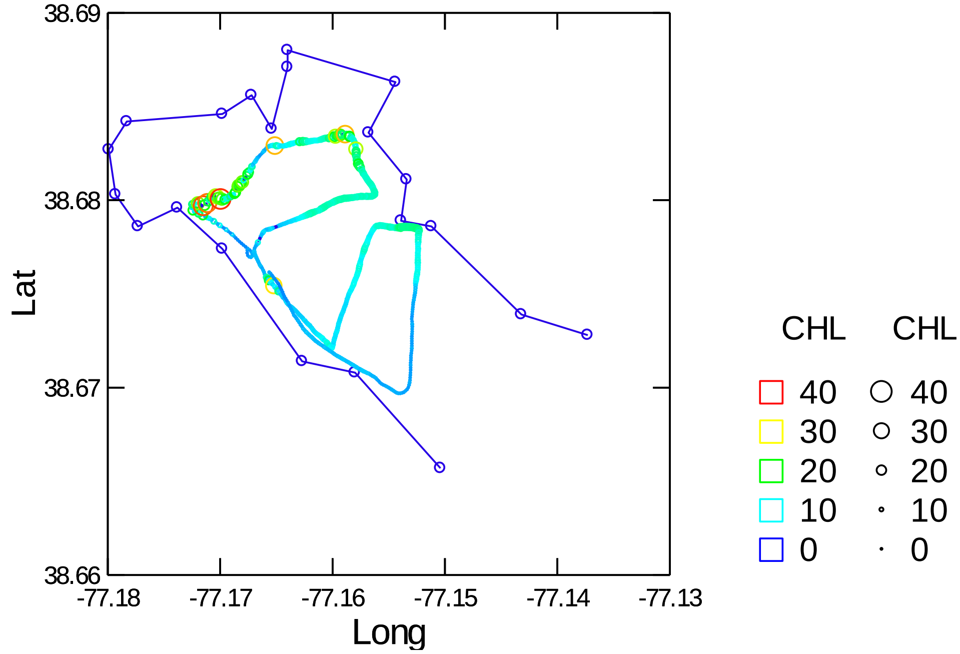

Figure 34. Chlorophyll *a* (µg/L) observed in transects across Gunston Cove during data mapping cruise on September 3, 2020.

Chlorophyll data from the datamapping cruise in 2020 showed a pattern that was different from DO and pH with highest values in Pohick Bay (Figure 34). There was a weak, but statistically significant relationship between DO (%) and Chlorophyll a (Figure 35). The other potential driver of DO, SAV, was highly depressed in 2018, but made a strong comeback in 2019 and 2020. SAV depresses phytoplankton chlorophyll. Thus, the high DO values in 2020 can be attributed to both phytoplankton and SAV photosynthesis.

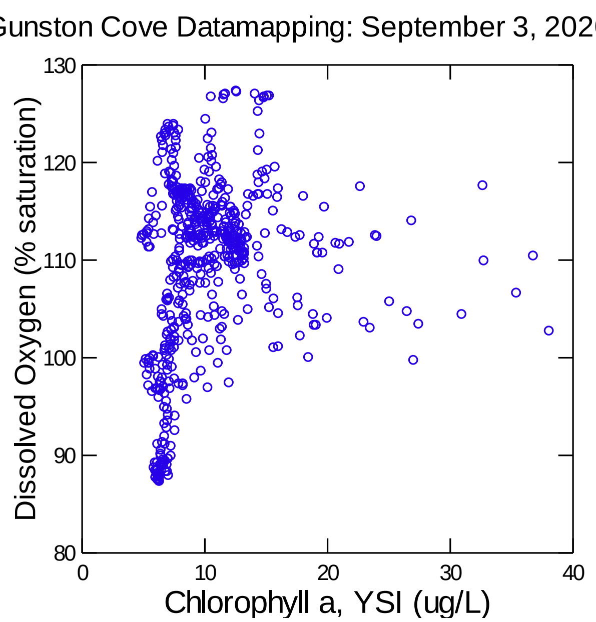

Figure 35. Dissolved Oxygen (% saturation) vs. Chlorophyll a (ug/L) as determined by YSI EXO sonde during datamapping on September 3, 2020.

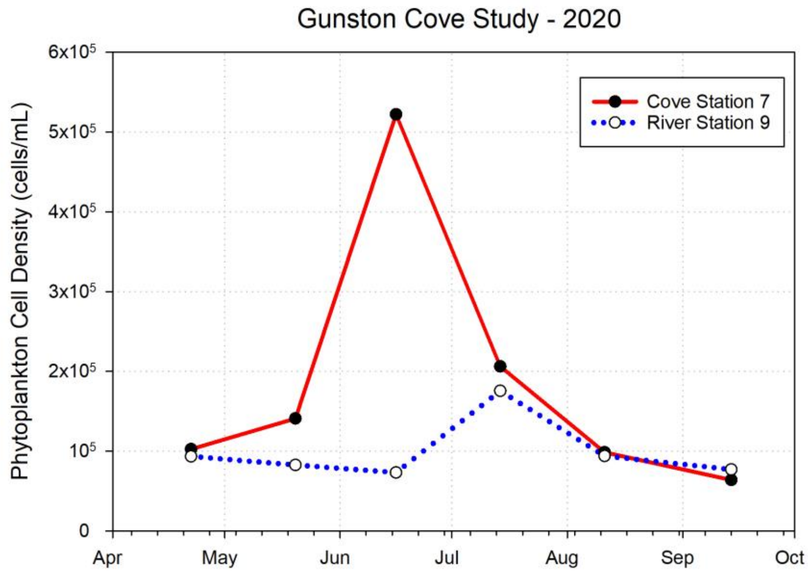

Phytoplankton cell density provides a measure of the number of algal cells per unit volume. This is a rough measure of the abundance of phytoplankton, but does not discriminate between large and small cells. Therefore, a large number of small cells may actually represent less biomass (weight of living tissue) than a smaller number of large cells. However, small cells are typically more active than larger ones so cell density is probably a better indicator of activity than of biomass. The smaller cells are mostly

Figure 36. Phytoplankton Density (cells/mL).

In the cove phytoplankton density was low in April and May, then increased to a strong peak in June (Figure 36), corresponding to the maximum value observed for chlorophyll a (Figure 32 and 33). In the river the highest value for phytoplankton density was observed in July on the same date as the second-highest chlorophyll a value. The river peak for cell biovolume was also found in July, but the biovolume peak for the cove was observed in July when chlorophylls had declined from their June peak (Figure 37).

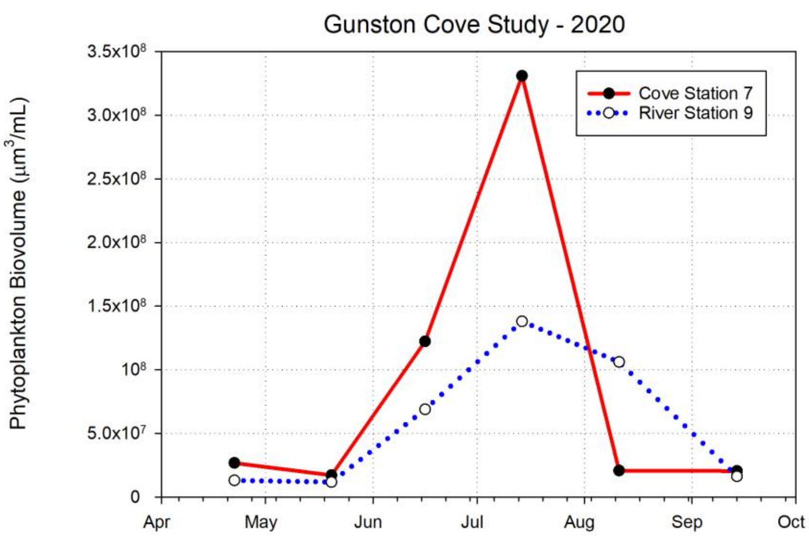

Figure 37. Phytoplankton Biovolume (um^3/mL).

The volume of individual cells of each species is determined by approximating the cells of each species to an appropriate geometric shape (e.g. sphere, cylinder, cone, etc.) and then making the measurements of the appropriate dimensions under the microscope. Total phytoplankton biovolume (shown here) is determined by multiplying the cell density of each species by the biovolume of each cell of that species. Biovolume accounts for the differing size of various phytoplankton cells and is probably a better measure of biomass. However, it does not account for the varying amount of water and other nonliving

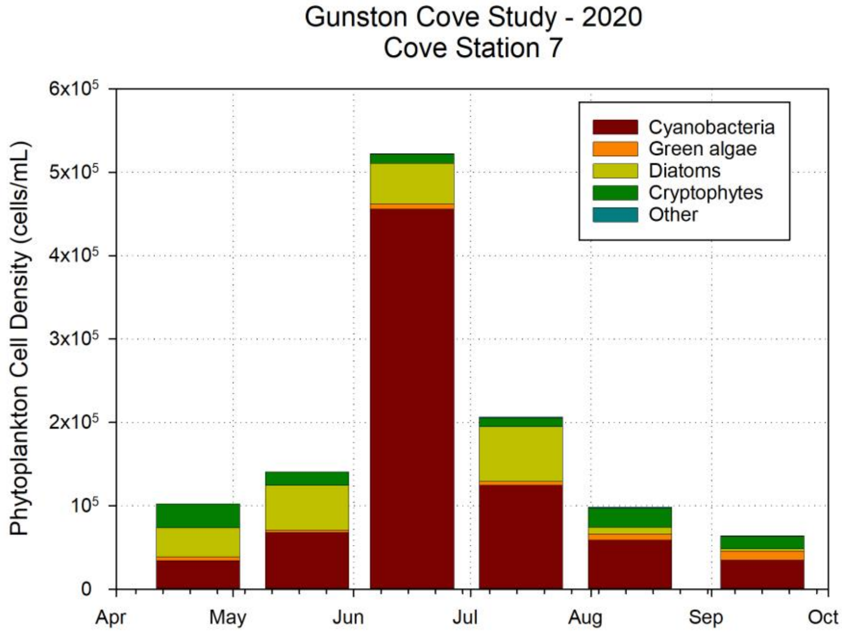

Total phytoplankton cell density can be broken down by major group. The top four groups represent those which are generally most abundant. "Other" includes euglenoids and dinoflagellates. Due to their small size cyanobacteria typically dominate cell density numbers. Their numbers are typically highest in the late summer reflecting an accumulation of cells during favorable summer growing conditions.

Figure 38. Phytoplankton Density by Major Group (cells/mL). Gunston Cove.

In 2020 phytoplankton density in the cove was dominated by cyanobacteria and diatoms for most of the year (Figure 38). In June cyanobacteria were most abundant and dominant. In the river diatoms were co-dominant with cyanobacteria in most months (Figure 39).

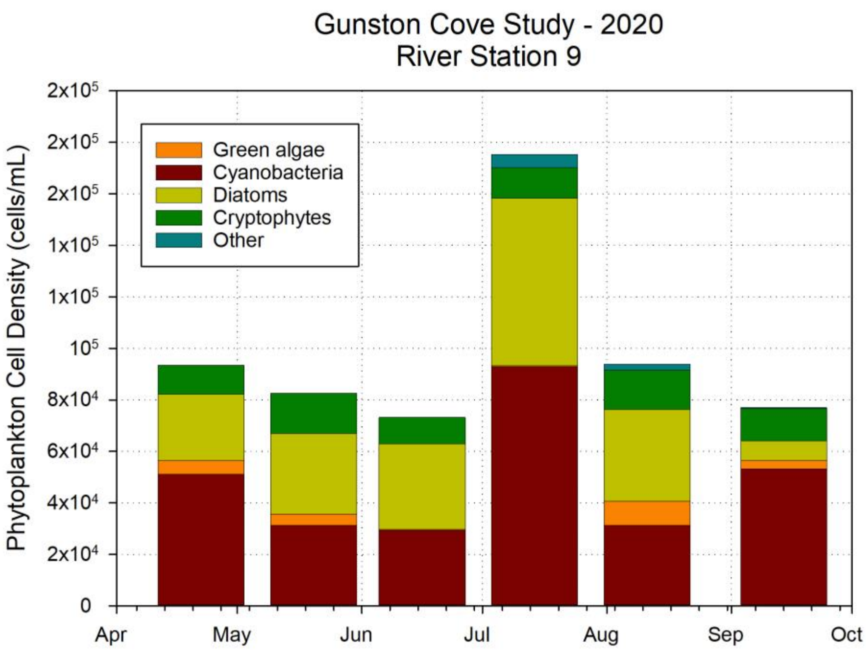

In the river cyanobacteria normally follow similar patterns as in the cove, but attaining lower abundances. This is probably due to the deeper water column which leads to lower effective light levels and greater mixing. Other groups such as diatoms and green algae tend to be more important on a relative basis than in the

Figure 39. Phytoplankton Density by Major Group (cells/mL). River.

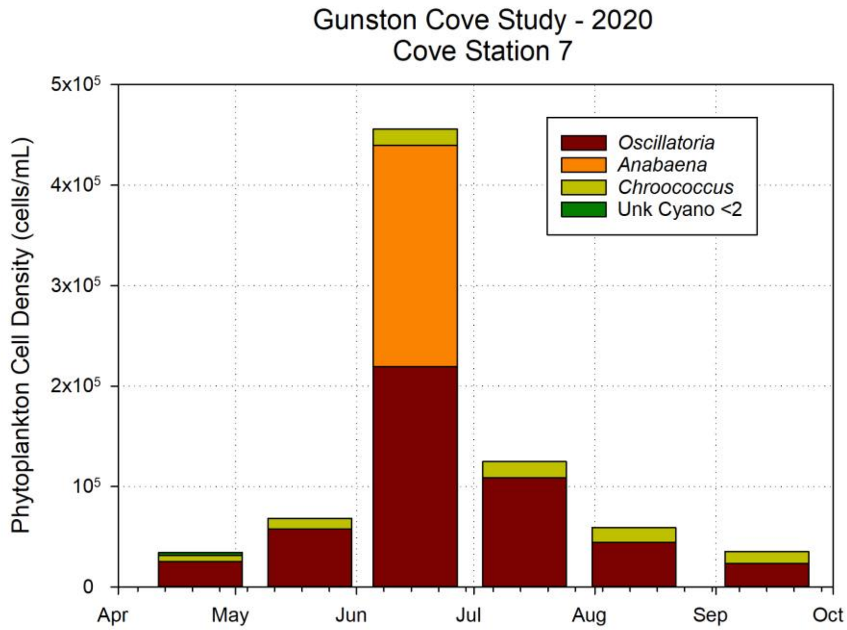

The dominant cyanobacteria on a numerical basis were:
Anabaena – a filament with bead-like cells & heterocysts
Oscillatoria – a filament with cylindrical cells
An unknown unicellular cyanobacterium less than 2 *u*
Chroococcus – individual spherical cells

Figure 40. Phytoplankton Density by Dominant Cyanobacteria (cells/mL). Gunston Cove.

Oscillatoria was the most abundant cyanobacterium in the during most months, sharing dominance with *Anabaena* in June (Figure 40). In the river *Oscillatoria* was dominant from July through September, but *Chroococcus* was dominant in the spring (Figure 41).

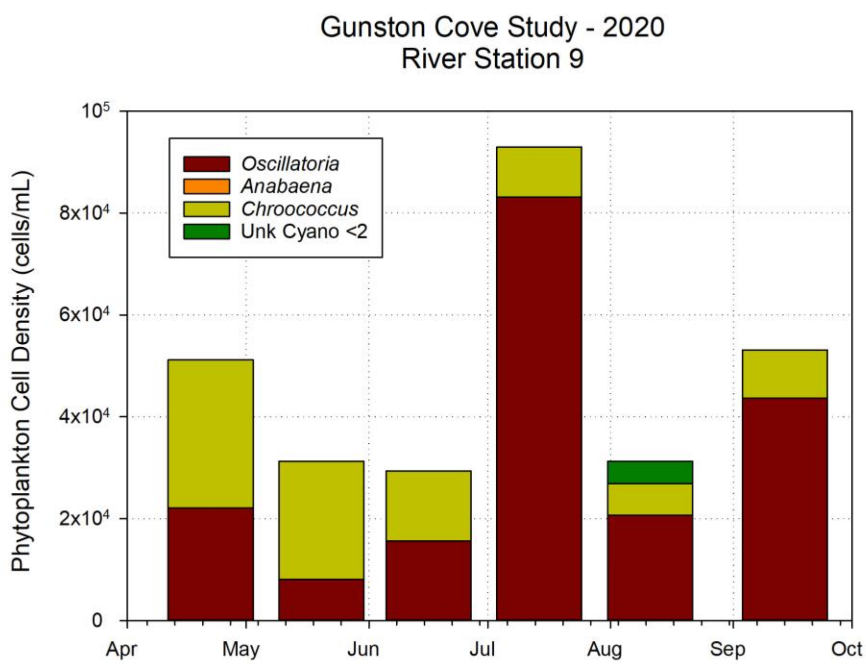

Anabaena

Microcystis

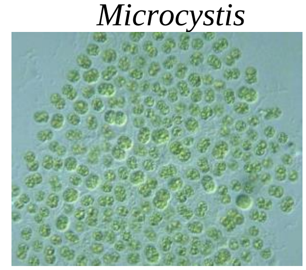

Figure 41. Phytoplankton Density by Dominant Cyanobacteria (cells/mL). River.

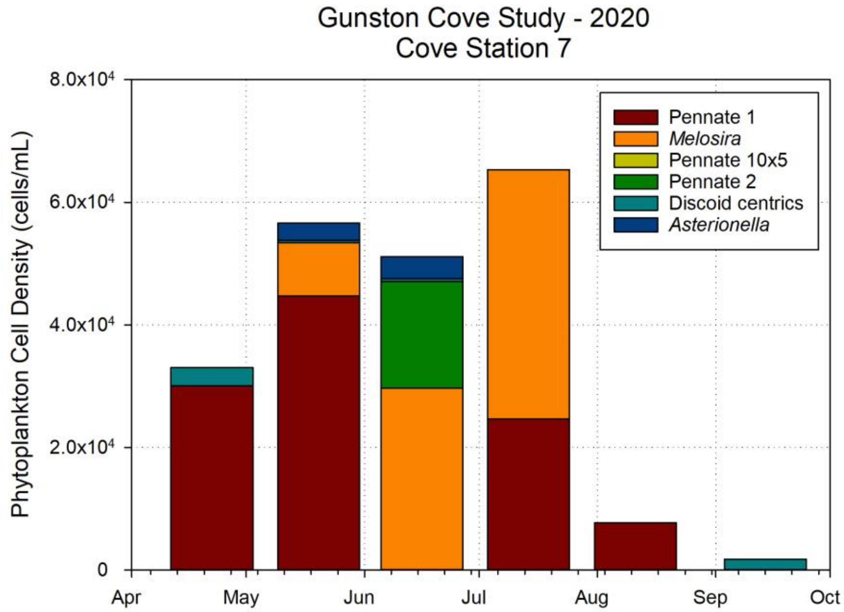

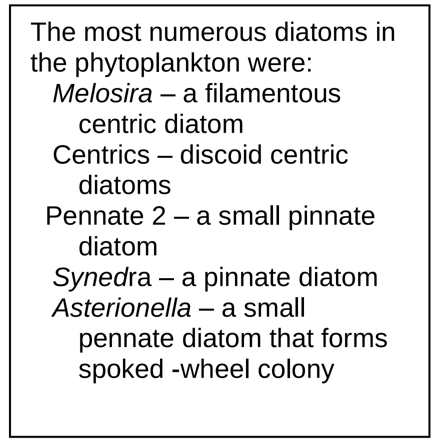

Figure 42. Phytoplankton Density by Dominant Diatoms (cells/mL). Gunston Cove.

Diatom cell density in the cove was composed was dominated by Pennate 1 and *Melosira* (Figure 42). *Melosira* was particularly important in June and July. In the river Pennate 1 was dominant for most of the year with Pennate 10x5 dominant in May and *Melosira* in July (Figure 43).

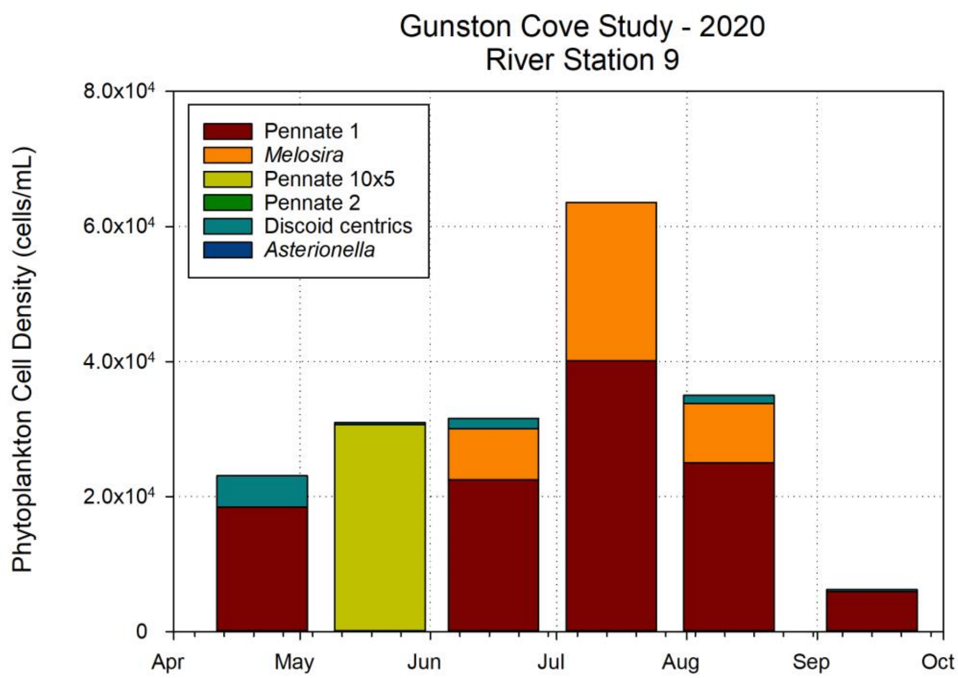

Melosira

Discoid Centrics

Figure 43. Phytoplankton Density by Dominant Diatoms (cells/mL). River.

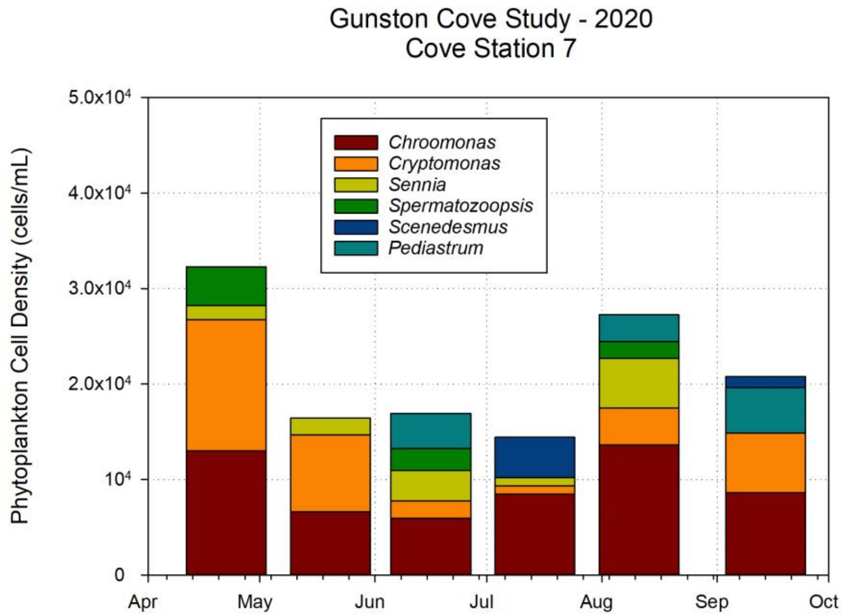

The most numerous phytoplankton among the cryptophytes, green algae and others were:

- *Cryptomonas* – an ellipsoidal, flagellated unicell
- *Chroomonas* – a flagellated cryptomonad unicell
- *Dictyosphaerium* – colony of small green unicells
- *Selenastrum* – single green algal cell as curved rod
- *Pediastrum* – green algal colony
- *Botryococcus* – single green coccoid cell

Figure 44. Phytoplankton Density (#/mL) by Dominant Other Taxa. Gunston Cove.

In the cove a number of other taxa were important, with the combination of *Chroomonas* and *Cryptomonas* being most important (Figure 44). The river station had a similar assemblage with *Chroomonas* dominant in spring and *Cryptomonas* in summer (Figure 45).

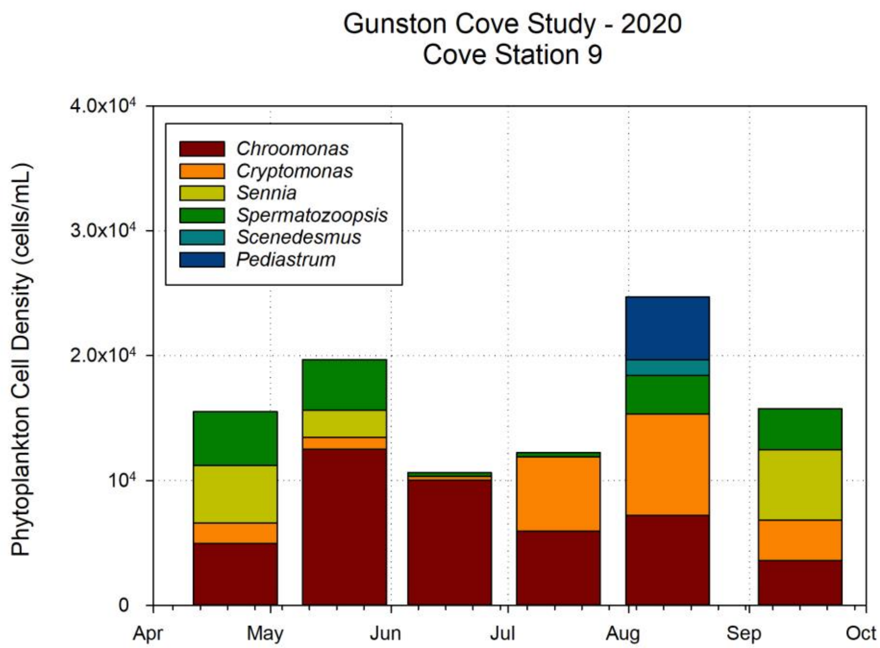

Cryptomonas

Scenedesmus

Figure 45. Phytoplankton Density (#/mL) by Dominant Other Taxa. River.

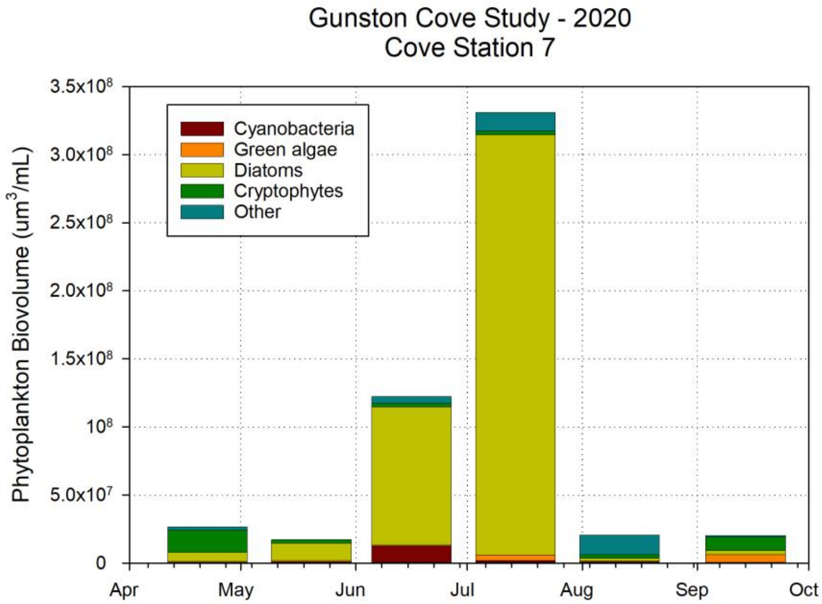

Total phytoplankton biovolume can be broken down into groups:

- **Cyanobacteria** ("blue-green" algae)
- **Green algae**
- **Diatoms** – includes both centric and pinnate
- **Cryptophytes**
- **Other** – includes euglenoids, chrysophytes, and dinoflagellates

Figure 46. Phytoplankton Biovolume (um^3/mL) by Major Groups. Gunston Cove.

In the cove biovolume was strongly dominated by diatoms from April to July (Figure 46). Biovolume in the cove decreased strongly in August and September. In the river, diatoms were dominant in biovolume for the entire year (Figure 47).

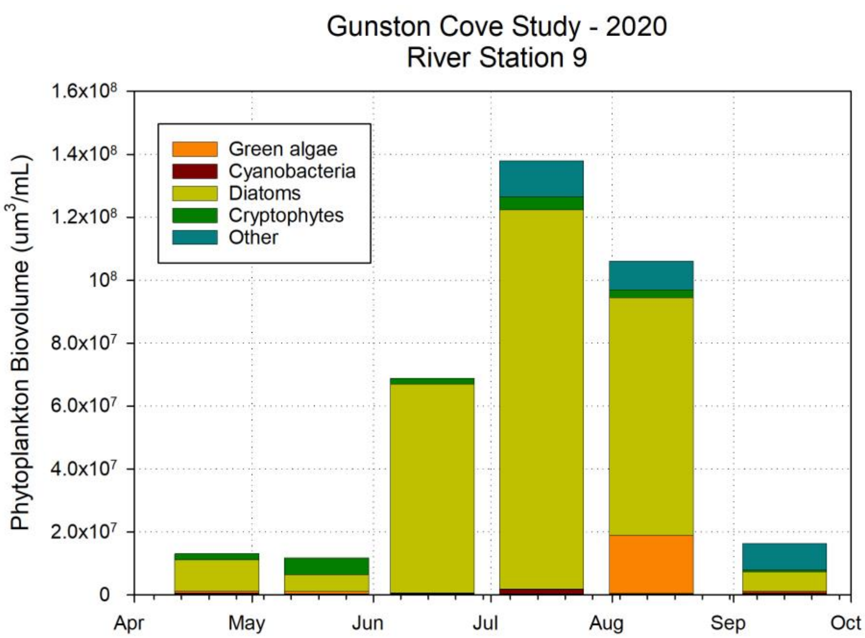

While dominating cell density, cyanobacteria typically make up a much smaller portion of phytoplankton biovolume. As with cell density, biovolume is generally greater in the cove.

Figure 47. Phytoplankton Biovolume (um^3/mL) by Major Groups. River.

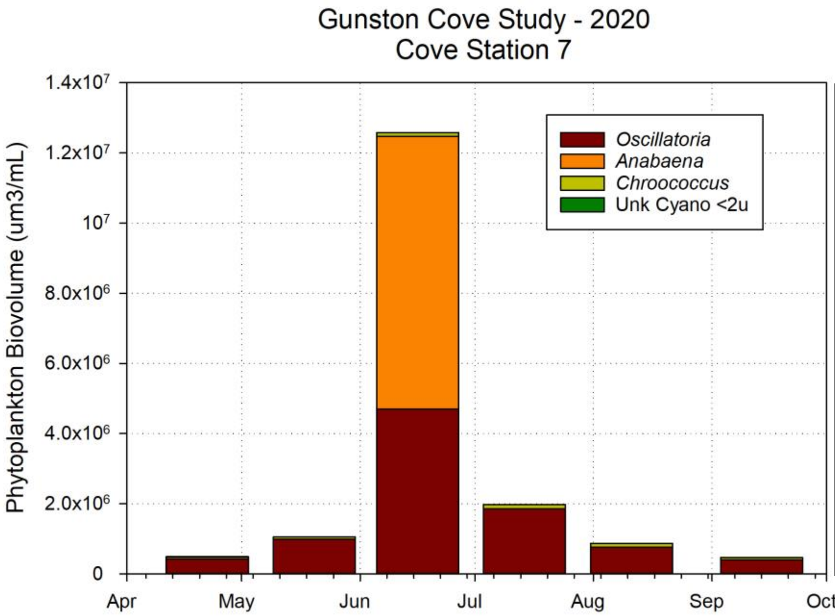

The dominant cyanobacteria on a biovolume basis were:
Anabaena – a filament with bead-like cells & heterocysts
Rhabdoderma – rod-shaped cells in small packets
Oscillatoria – a filament with cylindrical cells
Chroococcus – individual spherical cells
Raphidiopsis – a filament of cylindrical cells

Figure 48. Phytoplankton Biovolume (um^3/mL) by Cyanobacteria Taxa. Gunston Cove.

Oscillatoria accounted for most of the cyanobacterial biovolume in the cove except in June when Anabaena was even more abundant (Figure 48). In the river *Oscillatoria* was usually highly dominant and had a maximum in July (Figure 49).

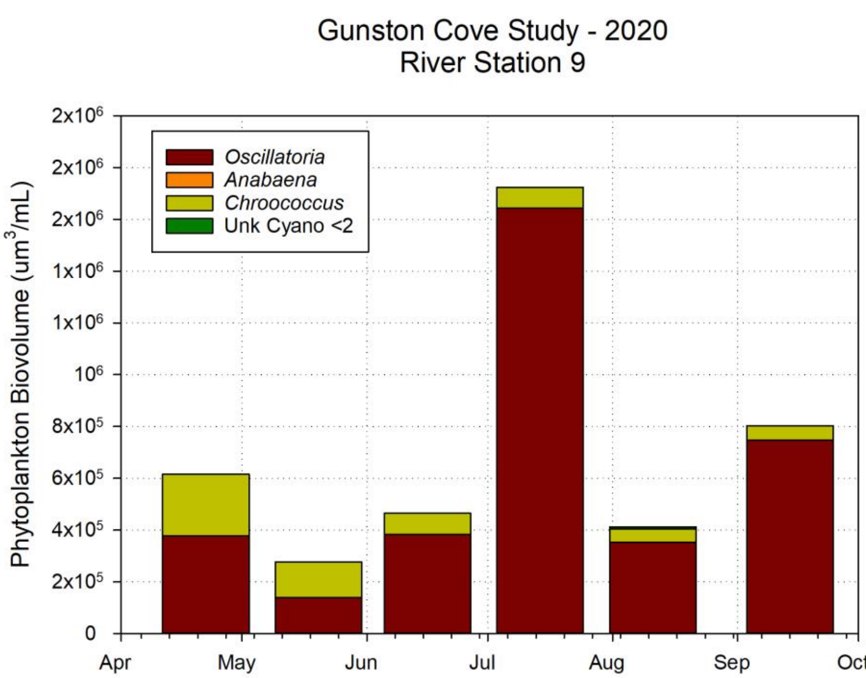

Oscillatoria

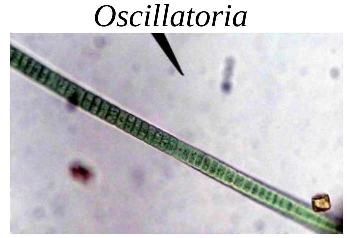

Chroococcus

Figure 49. Phytoplankton Biovolume (um^3/mL) by Cyanobacterial Taxa. River.

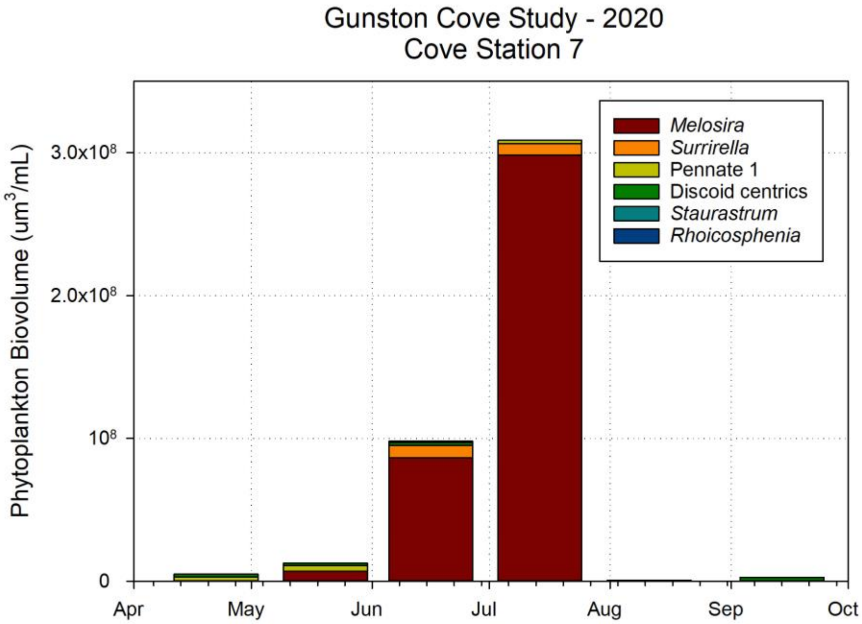

The most numerous diatoms in the phytoplankton were:

- *Melosira* – a filamentous centric diatom
- Centrics – discoid centric diatoms
- *Stauroneis* – larger pennate diatom
- Pennate 2 – a small pinnate diatom
- Pennate 1 – a small pinnate diatom
- *Surirella* – a larger pennate diatom
- *Nitzschia* – a small pennate diatom

Figure 50. Phytoplankton Biovolume (um^3/mL) by Diatom Taxa. Gunston Cove.

In the cove *Melosira* was dominant all year and very abundant in both June and July (Figure 50). In the river the *Melosira* was very abundant in June, July, and August (Figure 51).

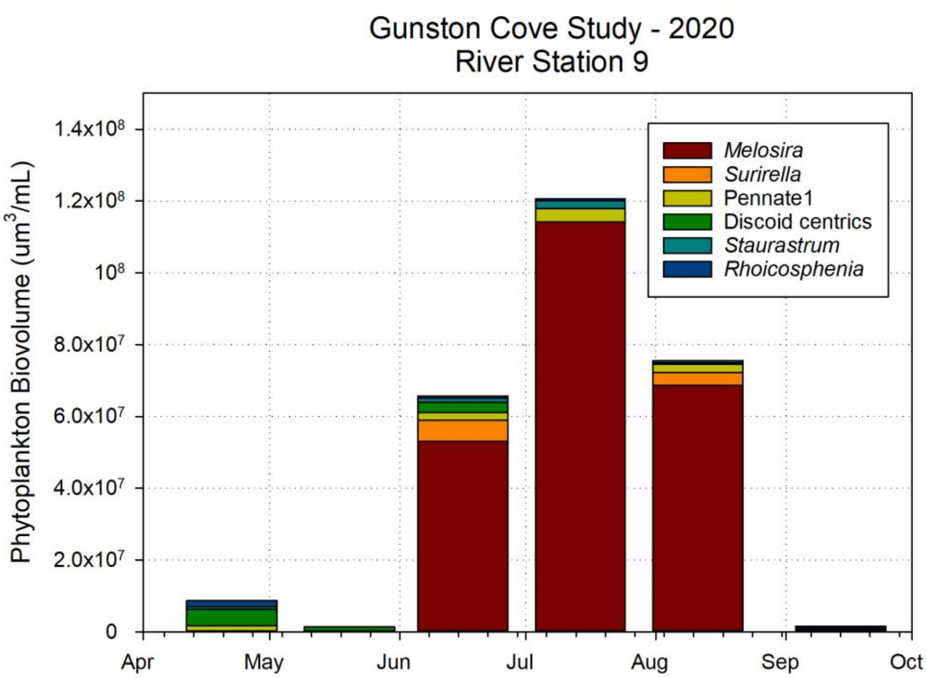

Melosira

Surirella

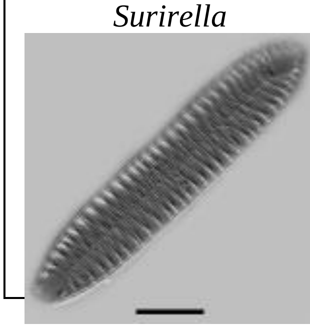

Figure 51. Phytoplankton Biovolume (um^3/mL) by Diatom Taxa. River.

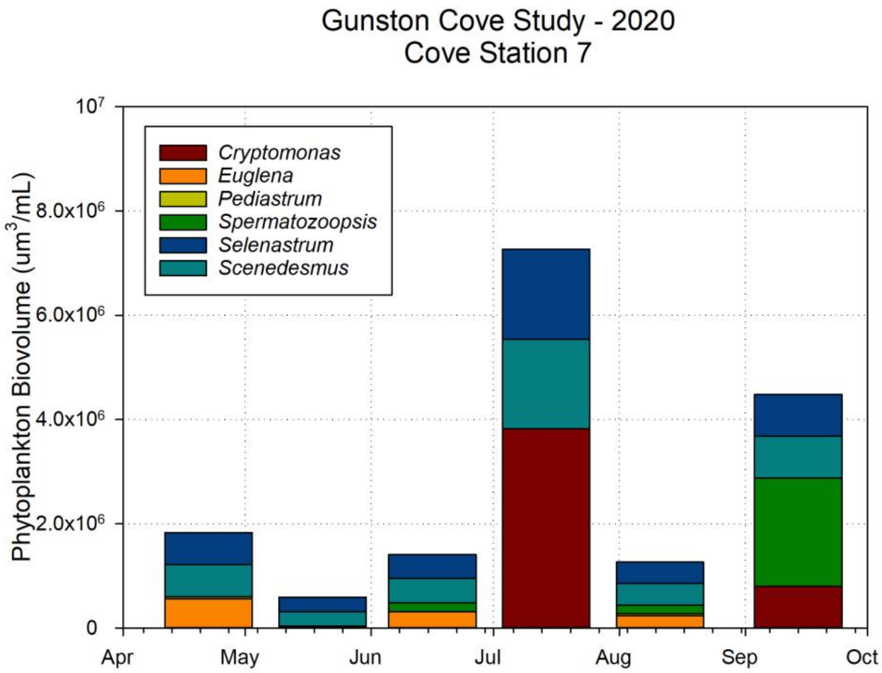

The most numerous phytoplankton among the cryptophytes, green algae and others were:

- *Euglena* – large euglenoid flagellate
- *Cryptomonas* – an ellipsoidal, flagellated unicell
- *Carteria* – flagellated green unicell
- *Mallomonas* – unicellular scaled flagellate
- *Trachelomonas* – spherical, armored euglenoid
- *Ankistrodesmus* – rod-like single celled green alga
- *Oocystis* –green unicells in small packets

Figure 52. Phytoplankton Biovolume (um^3/mL) by Dominant Other Taxa. Gunston Cove.

A number of other taxa contributed to biovolume in the cove in 2020 with *Cryptomonas*, *Selenastrum*, and *Scenedesmus* contributing to the July peak (Figure 52). In the river the *Euglena*, *Cryptomonas*, and *Pediastrum* were most important (Figure 53).

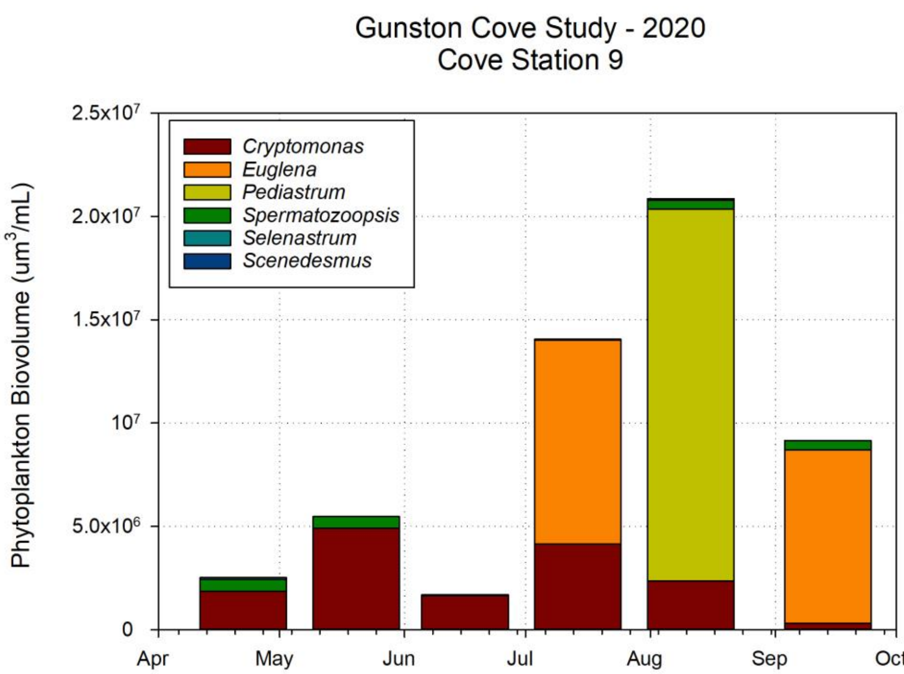

Cryptomonas

Euglena

Figure 53. Phytoplankton Biovolume (um^3/mL) by Dominant Other Taxa. River.

D. Zooplankton – 2020

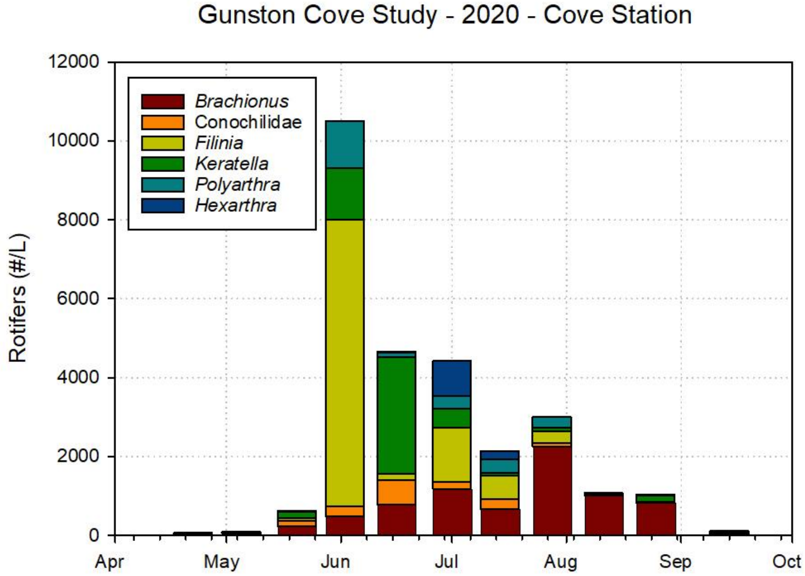

Brachionus (Sta 7, RCJ)

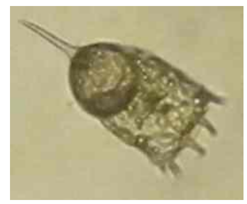

Keratella (Sta 7, RCJ)

Figure 54. Rotifer Density by Dominant Taxa (#/L). Cove.

In the cove, rotifers got off to a rather slow start in 2020, but in early June there was a strong increase in the population led by *Filinia* which attained about 7000/L. Values declined in late June and *Keratella* took over as the dominant. Values remained in the 2000-4000/L range (fairly typical summer levels) through July with *Brachionus* assuming dominance. In the river rotifers were consistently much lower than in the cove with the highest value in late August slightly above 1000/L (Figure 55). *Brachionus* was the dominant in most samples.

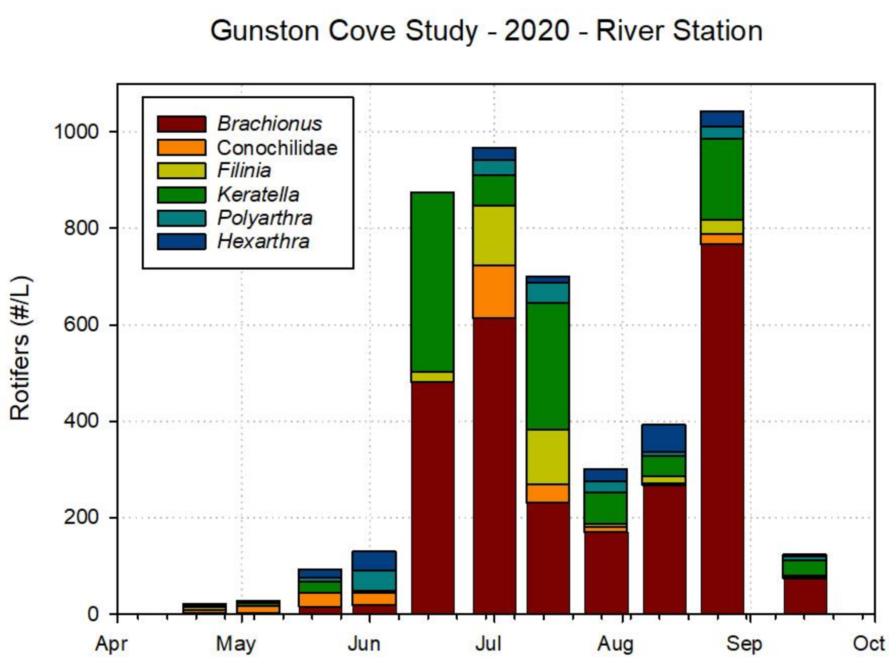

Brachionus (c. 50 um)

Conochilidae

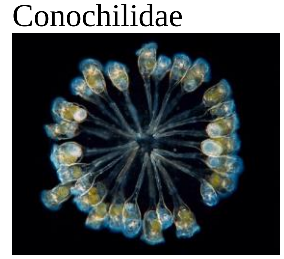

Figure 55. Rotifer Density by Dominant Taxa (#/L). River.

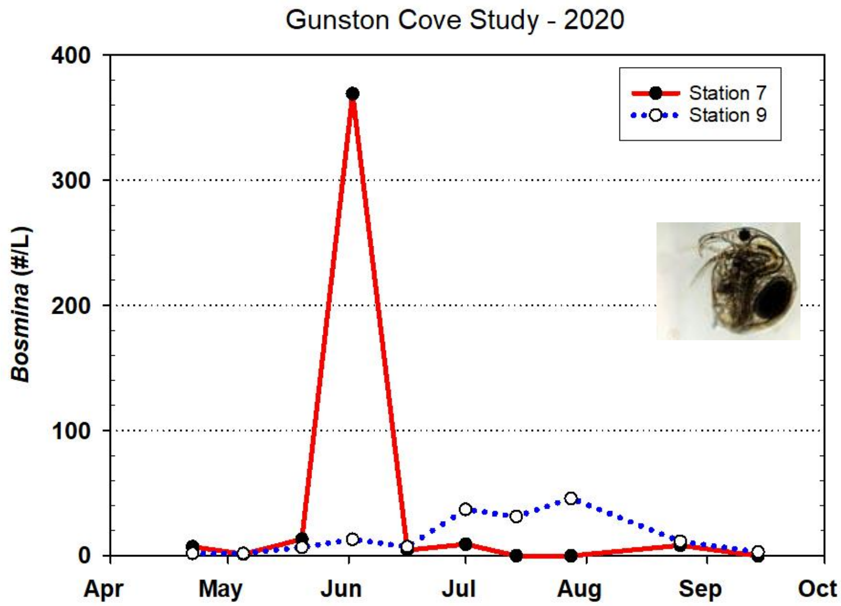

Figure 56. *Bosmina* Density by Station (#/L).

Bosmina is a small-bodied cladoceran, or "waterflea", which is common in lakes and freshwater tidal areas. It is typically the most abundant cladoceran with maximum numbers generally about 100-1000 animals per liter. Due to its small size and relatively high abundances, it is enumerated in the micro-zooplankton samples. *Bosmina* can graze on smaller phytoplankton cells, but can also utilize some cells from colonies by knocking them loose.

In 2020 the small cladoceran *Bosmina* was present at very low levels except in early June when an outbreak was seen in the cove reaching about 370/L (Figure 56). *Diaphanosoma*, typically the most abundant larger cladoceran in the study area, was very abundant in the cove in mid-June reaching nearly 5000/m^3 (Figure 57). Two peaks were observed in the river, mid-June at 1600/m^3 and mid-July at 2200/m^3.

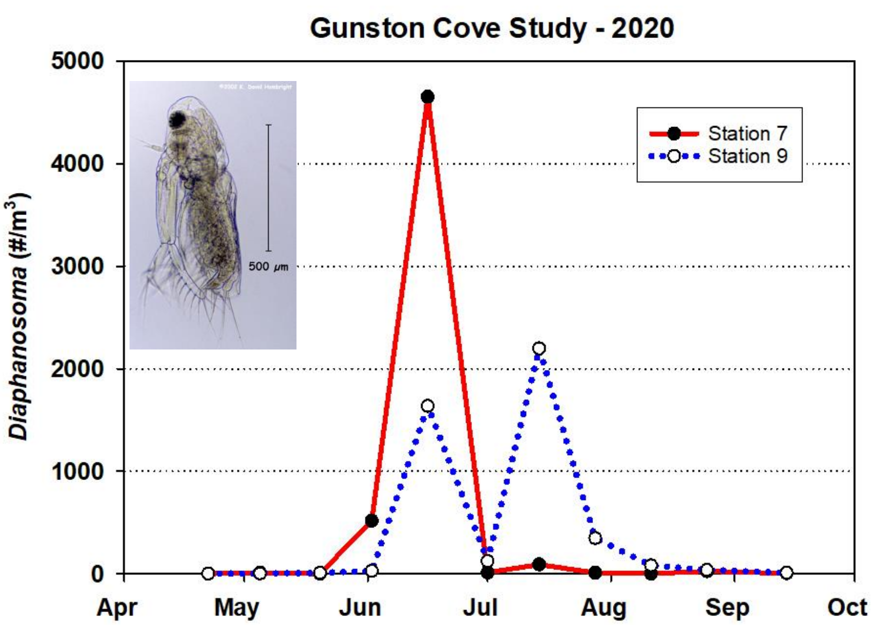

Figure 57. *Diaphanosoma* Density by Station (#/m^3).

Diaphanosoma is the most abundant larger cladoceran found in the tidal Potomac River. It generally reaches numbers of 1,000-10,000 per m^3 (which would be 1-10 per liter). Due to their larger size and lower abundances, *Diaphanosoma* and the other cladocera are enumerated in the macrozooplankton samples. *Diaphanosoma* prefers warmer temperatures than some cladocera and is often common in the summer.

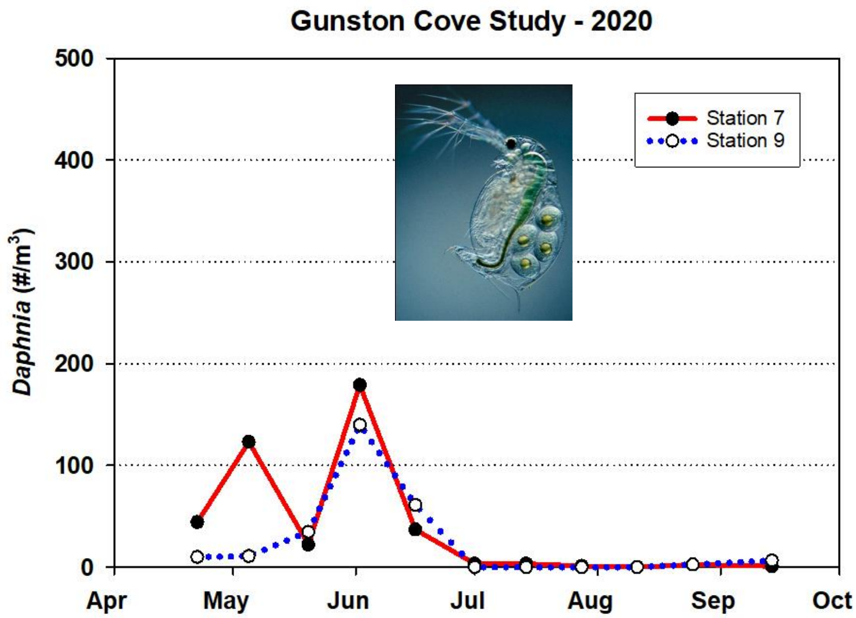

Daphnia, the common waterflea, is one of the most efficient grazers of phytoplankton in freshwater ecosystems. In the tidal Potomac River it is present, but has not generally been as abundant as *Diaphanosoma*. It is typically most common in

Figure 58. *Daphnia* Density by Station (#/m^3).

In 2020 *Daphnia* exhibited very low values at both stations (Figure 58). Highest levels at both stations were in early June at about 150-200/m^3 *Ceriodaphnia* was observed in appreciable numbers on only one date in mid-June in the Cove. (Figure 59).

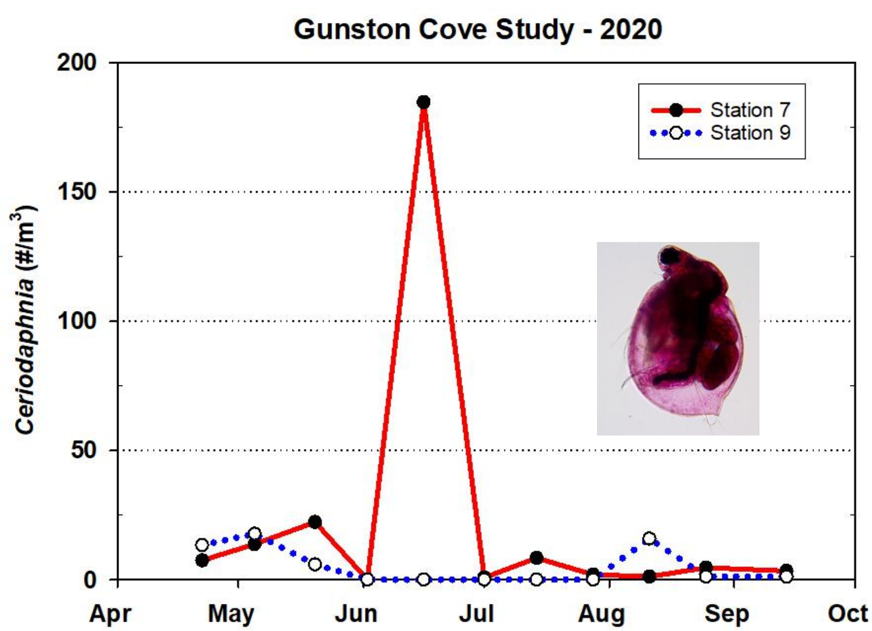

Figure 59. *Ceriodaphnia* Density by Station (#/m^3).

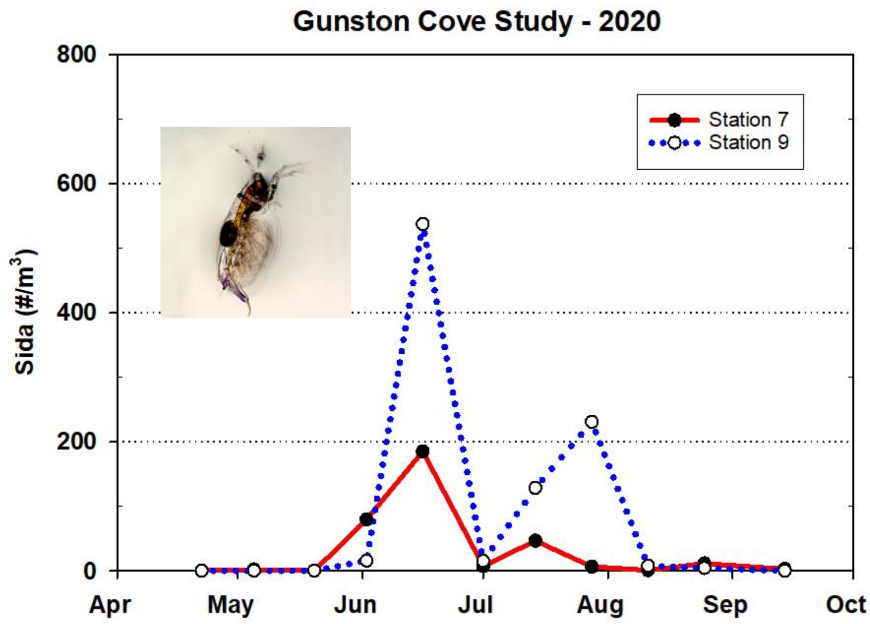

Sida is another waterflea that is often observed in the tidal Potomac River. Like the other cladocera mentioned so far, *Sida* grazes on phytoplankton to obtain its food supply.

Figure 60. *Sida* Density by Station (#/m^3).

Sida, a smallish cladoceran related to *Diaphanosoma*, was present at relatively low levels for most of the year, but reached a peak of over 500/m^3 in June in the river (Figure 60). *Leptodora*, the large cladoceran predator, was quite abundant in 2020 with peaks of nearly 600/m^3 in the river in both June and July and a peak of 400/m^3 in the cove in June (Figure 61).

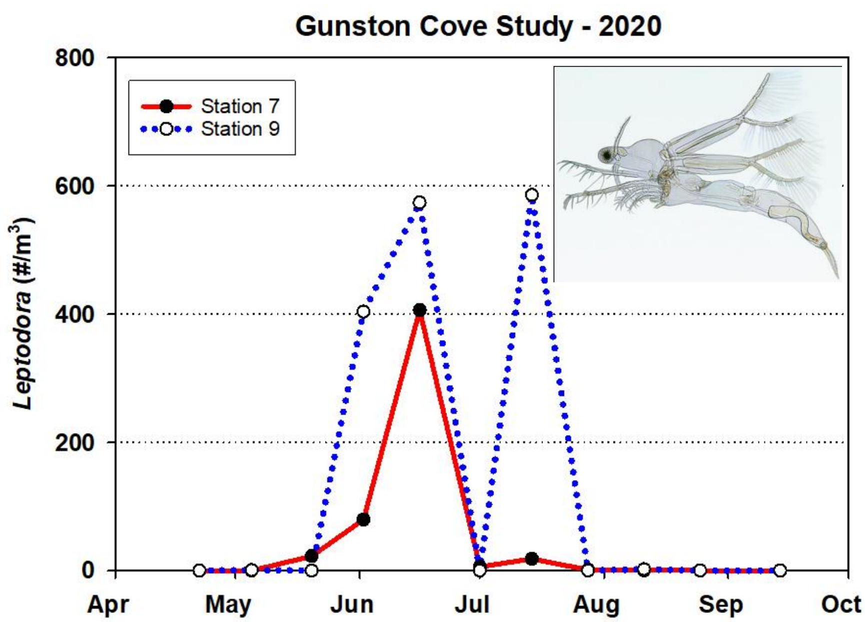

Leptodora is substantially larger than the other cladocera mentioned. Also different is its mode of feeding – it is a predator on other zooplankton. It normally occurs for brief periods in the late spring or early summer.

Figure 61. *Leptodora* Density by Station (#/m^3).

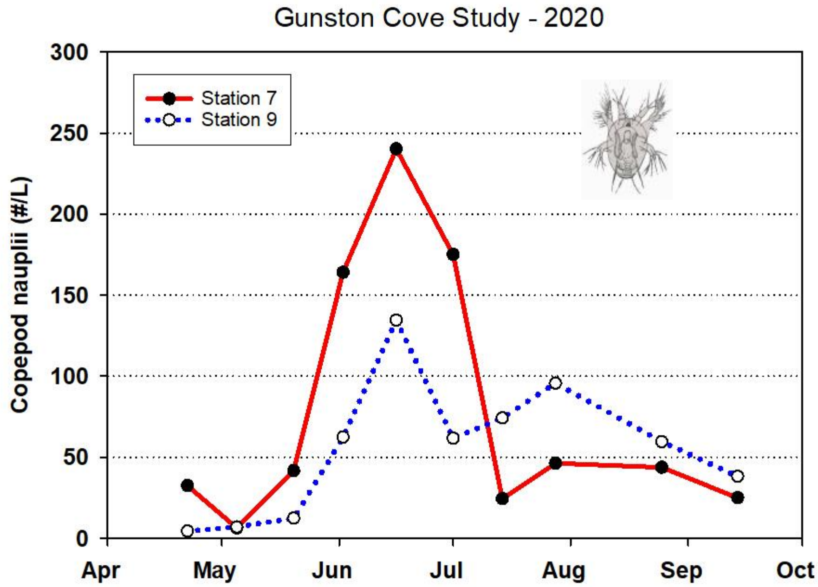

Copepod eggs hatch to form an immature stage called a nauplius. The nauplius is a larval stage that does not closely resemble the adult and the nauplii of different species of copepods are not easily distinguished so they are lumped in this study. Copepods go through 5 naupliar molts before reaching the copepodid stage which is morphologically very similar to the adult. Because of their small size and high abundance, copepod nauplii are enumerated in the micro-zooplankton samples.

Figure 62. Copepod Nauplii Density by Station (#/L).

In the cove copepod nauplii showed a pattern of major increase over the period from May through June at about 250/L followed by an almost equal decline by mid-July (Figure 62). In the river there was a strong increase through mid-June and a gradual decline for the rest of the year. In 2020 *Eurytemora* attained high densities of over 4000/m^3 in May and increased even further in June to over 6500/m^3 in the cove before declining strongly (Figure 63). In the river *Eurytemora* increased later attaining about 4500/m^3 in June.

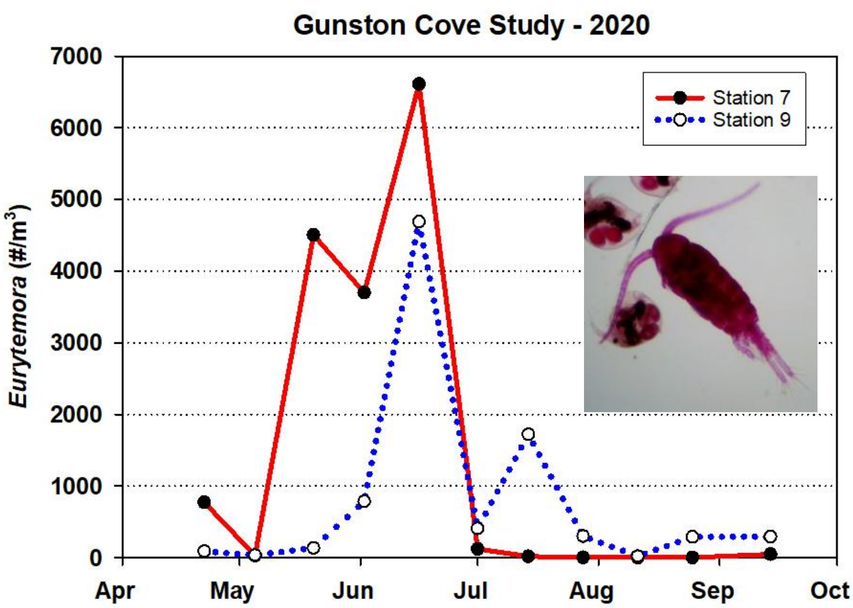

Eurytemora affinis is a large calanoid copepod characteristic of the freshwater and brackish areas of the Chesapeake Bay. *Eurytemora* is a cool water copepod which often reaches maximum abundance in the late winter or early spring. Included in this graph are adults and those copepodids that are recognizable as *Eurytemora*.

Photo credit: Laura Birsa

Figure 63. *Eurytemora* Density by Station (#/m^3).

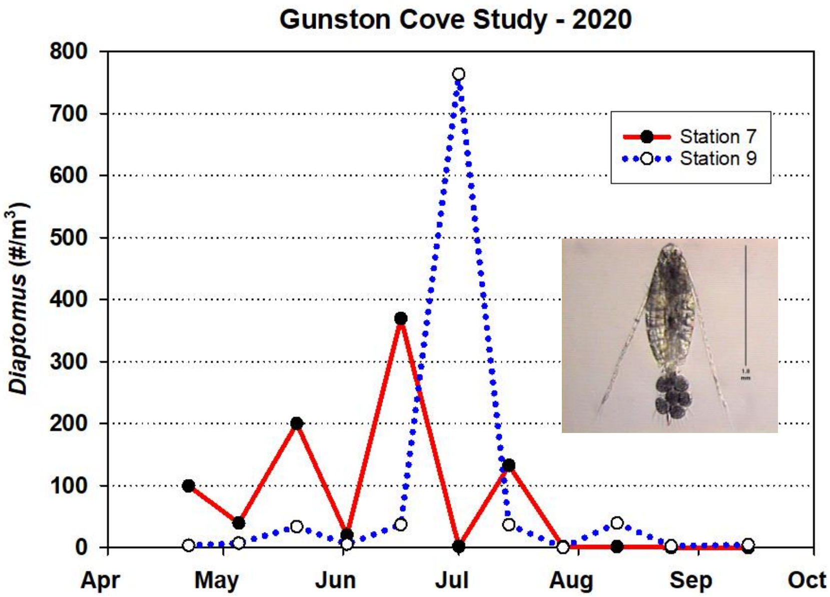

Diaptomus pallidus is a calanoid copepod often found in moderate densities in the Gunston Cove area. *Diaptomus* is an efficient grazer of algae, bacteria, and detrital particles in freshwater ecosystems Included in this graph are adults and those copepodids that are recognizable as *Diaptomus*.

Figure 64. *Diaptomus* Density by Station (#/m^3)

Diaptomus was was restricted to fairly low values in 2020 (Figure 64). Peak in the cove was at 380/m^3 in June and was at 760/m^3 in early July in the river. *Cyclops vernalis* was at low, but increasing values in the cove in spring attaining about 200/m^3 (Figure 65). In the river *C. vernalis* was very low all year.

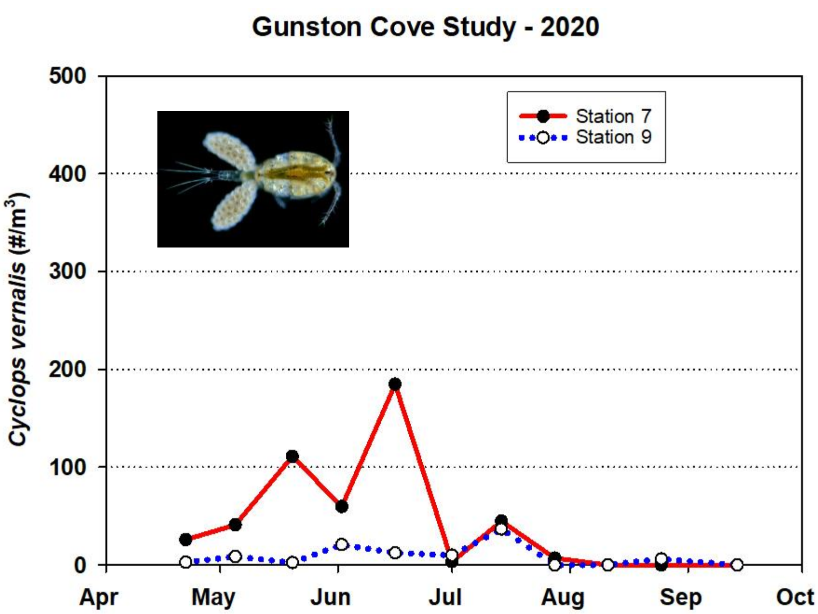

Cyclopoids are the other major group of planktonic copepods. Cyclopoids feed on individual particles suspended in the water including small zooplankton as well as phytoplankton. In this study we have lumped all copepodid and adult cyclopoids together.

Figure 65. *Cyclops vernalis* by Station (#/m^3)..

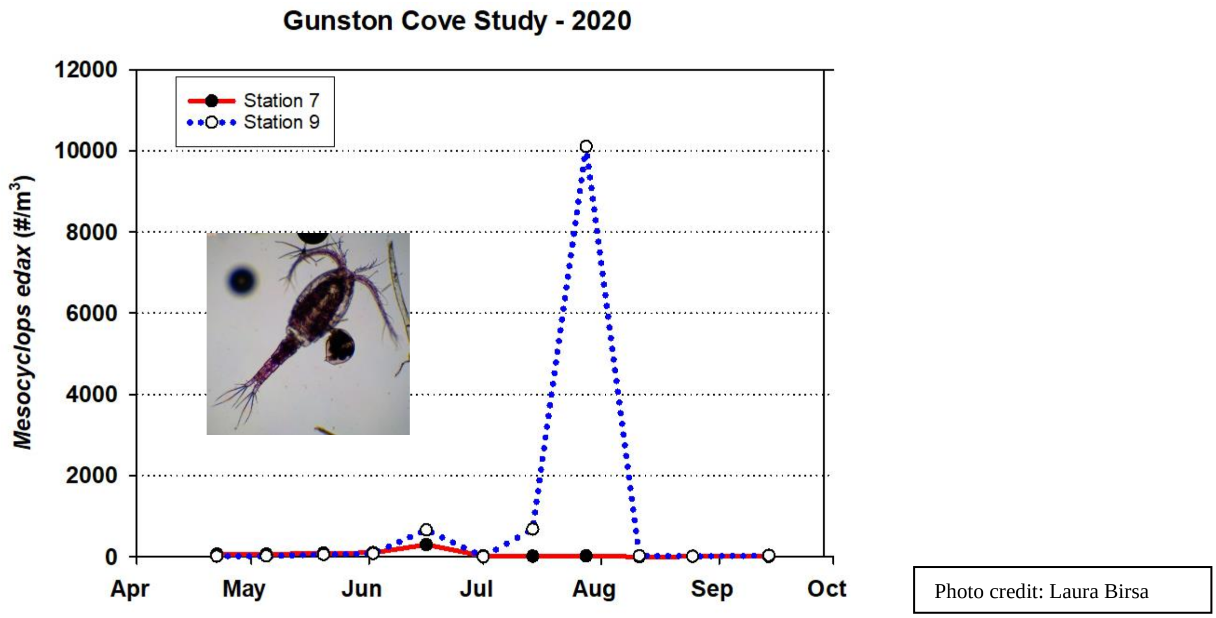

Figure 66. *Mesocyclops edax* by Station (#/m^3).

Mesocyclops edax was found on only a few dates, but attained a very high density of nearly 10,000/m^3 in late July in the river (Figure 66).

E. Ichthyoplankton - 2020

Larval fishes are transitional stages in the development of juvenile fishes. They range in development from newly hatched, embryonic fish to juvenile fish with morphological features similar to those of an adult. Many fishes such as clupeids (herring family), White Perch, Striped Bass, and Yellow Perch disperse their eggs and sperm into the open water. The larvae of these species are carried with the current and termed "ichthyoplankton". Other fish species such as sunfishes and bass lay their eggs in "nests" on the bottom and their larvae are rare in the plankton.

After hatching from the egg, the larva draws nutrition from a yolk sack for a few days time. When the yolk sack diminishes to nothing, the fish begins a life of feeding on other organisms. This post yolk sack larva feeds on small planktonic organisms (mostly small zooplankton) for a period of several days. It continues to be a fragile, almost transparent, larva and suffers high mortality to predatory zooplankton and juvenile and adult fishes of many species, including its own. When it has fed enough, it changes into an opaque juvenile, with greatly enhanced swimming ability. It can no longer be caught with a slow-moving plankton net, but is soon susceptible to capture with the seine or trawl net.

In 2020, we collected 14 samples (7 at Station 7 and 7 at Station 9) during the months April through July and obtained a total of 1798 larvae (Table 4), which is on par with previous years (e.g. 1399 in 2019, 1072 in 2018 and 1751 in 2017). The fish larvae are sometimes too damaged to distinguish at the species level, thus some of the counts are only to the genus level, family level or less (2.2% were unidentified). This year the number identified to the genus level was low like last year; the percent of the catch identified to the Family Clupeidae (but not further) was 9.73 (5.5% last year but 35.4% in 2018). Of the Clupeidae that could be identified to the species level, Gizzard Shad was the dominant species with 30.7% of the catch. All clupeids together constituted 70.1% of the catch. Other abundant clupeids were Alewife at 15.1%, Blueback Herring at 12.5% and Hickory Shad at 1.6%. The dominant non-clupeid species in the catch was White Perch with 18.0% of the catch. Other species somewhat abundant in the ichthyoplankton samples were Inland Silverside at 6.4%. A total of at least 11 species were identified.

Table 4. The number of larval fishes collected in Gunston Cove and the Potomac River in 2020.

Scientific Name	Common Name	7	9	Total	% of Total
Alosa aestivalis	Blueback Herring	52	173	225	12.51
Alosa mediocris	Hickory Shad	20	9	29	1.61
Alosa pseudoharengus	Alewife	96	176	272	15.13
Alosa sapidissima	American Shad	6	1	7	0.39
Alosa sp.	unk. Alosa species	1	0	1	0.06
Carpiodes cyprinus	Quillback	2	0	2	0.11
Clupeidae	unk. clupeid species	33	142	175	9.73
Dorosoma cepedianum	Gizzard Shad	391	161	552	30.70
Eggs	eggs	23	25	48	2.67
Gambusia holbrooki	Mosquitofish	1	0	1	0.06
Lepomis macrochirus	Bluegill	6	0	6	0.33
Menidia beryllina	Inland Silverside	30	85	115	6.40
Morone americana	White Perch	66	258	324	18.02
Perca flavescens	Yellow Perch	1	0	1	0.06
Unidentified	unidentified	16	24	40	2.22
Total		**744**	**1054**	**1798**	**100.00**

The mean density of larvae, which takes the volume of water sampled into account over the time sampled, is shown in Figure 67 and 68. Clupeid larvae in Figure 67 include Blueback Herring, Hickory Shad, Alewife, American Shad, and Gizzard Shad. These have similar spawning patterns, so they are lumped into one group for this analysis. Clupeid larvae peak from mid-May to early June (Figure 67), which is similar to previous years. The abundance of other larvae than Clupeids was lower, and had peak mid-May (Figure 68). Larval density tends to taper off as the summer progresses, as was seen in 2020. The other larvae included all other taxa listed in Table 4.

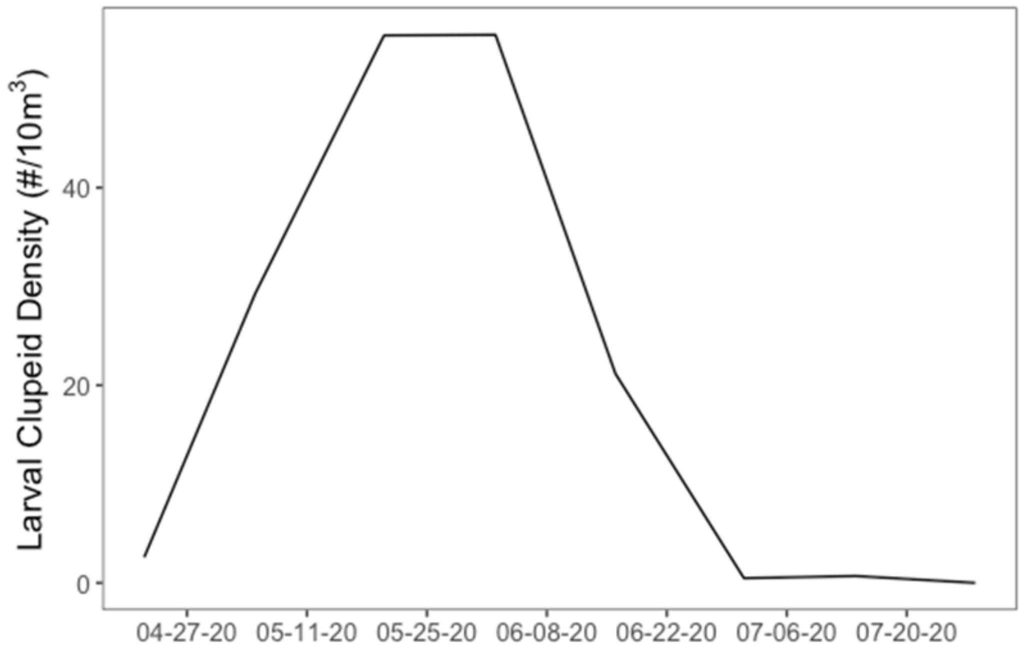

Figure 67. Clupeid larvae, mean density (abundance per $10m^3$).

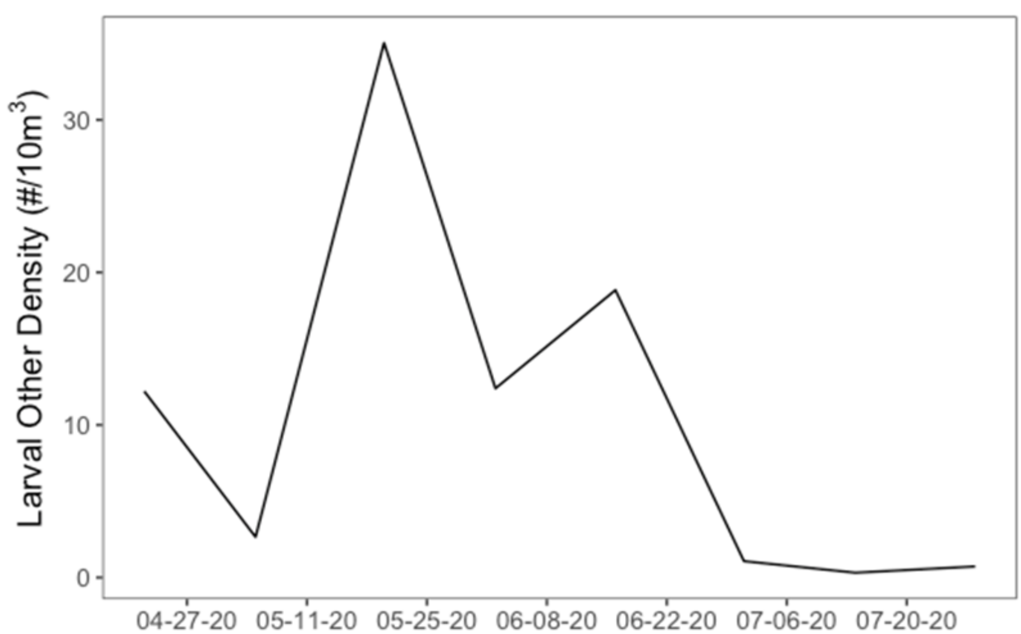

Figure 68. All other larvae, mean density (abundance per $10m^3$)

F. Adult and juvenile fishes – 2020

Trawls

Trawl sampling was conducted between July 10 and September 10 at station 7, 9, and 10. These three fixed stations have been sampled continuously since the inception of the survey. The late start in 2020 (normally mid-April) was due to a lockdown in response to the COVID-19 pandemic. Extensive SAV growth restricted our ability to trawl station 10 to July only. A total of 4127 fishes comprising at least 18 species were collected in all trawl samples combined (Table 5). This is similar to last year, while in 2020 only 12 trawl samples were collected, compared to up to 30 in previous years (total number depending on whether station 10 can be sampled throughout the season, which depends on SAV growth). The most dominant species of the fish collected was White Perch (91.1%, numerically). Dominance of White Perch in the trawls was much higher than previous years (it was 49.8% last year). Spottail Shiner was the second most abundant species (6.2%). Other species were observed sporadically and at low abundances, constituting less than 1% of the total catch per species (Tables 5 and 6).

Table 5. Adult and Juvenile Fish Collected by Trawling. Gunston Cove Study - 2020.

Scientific Name	**Common Name**	**Abundance**	**Percent**
Morone americana	White Perch	3759	91.08
Notropis hudsonius	Spottail Shiner	256	6.20
Lepomis gibbosus	Pumpkinseed	30	0.73
Ictalurus furcatus	Blue Catfish	19	0.46
Alosa pseudoharengus	Alewife	15	0.36
Lepomis macrochirus	Bluegill	10	0.24
Lepomis sp.	unk. sunfish	7	0.17
Etheostoma olmstedi	Tessellated Darter	6	0.15
Dorosoma cepedianum	Gizzard Shad	5	0.12
Hybognathus regius	Eastern Silvery Minnow	5	0.12
Cyprinus carpio	Carp	3	0.07
Alosa aestivalis	Blueback Herring	2	0.05
Alosa sp.	unk. Alosa species	2	0.05
Carassius auratus	Goldfish	2	0.05
Morone saxatilis	Striped Bass	2	0.05
Ameiurus nebulosus	Brown Bullhead	1	0.02
Anguilla rostrata	American Eel	1	0.02
Dorosoma petenense	Threadfin Shad	1	0.02
Ictalurus punctatus	Channel Catfish	1	0.02
Total		**4127**	**100.00**

Table 6. Adult and Juvenile Fish Collected by Trawling. Gunston Cove Study - 2020.

Scientific Name	Common Name	07-10	07-24	08-07	08-21	09-10	Total
Alosa aestivalis	Blueback Herring	0	2	0	0	0	2
Alosa pseudoharengus	Alewife	0	3	7	5	0	15
Alosa sp.	unk. Alosa species	0	0	0	1	1	2
Ameiurus nebulosus	Brown Bullhead	0	1	0	0	0	1
Anguilla rostrata	American Eel	1	0	0	0	0	1
Carassius auratus	Goldfish	1	1	0	0	0	2
Cyprinus carpio	Carp	1	1	1	0	0	3
Dorosoma cepedianum	Gizzard Shad	0	3	0	0	2	5
Dorosoma petenense	Threadfin Shad	0	0	0	1	0	1
Etheostoma olmstedi	Tessellated Darter	1	3	1	0	1	6
Hybognathus regius	Eastern Silvery Minnow	0	0	0	0	5	5
Ictalurus furcatus	Blue Catfish	9	8	1	0	1	19
Ictalurus punctatus	Channel Catfish	0	0	1	0	0	1
Lepomis gibbosus	Pumpkinseed	18	6	2	0	4	30
Lepomis macrochirus	Bluegill	3	1	3	1	2	10
Lepomis sp.	unk. sunfish	5	1	0	1	0	7
Morone americana	White Perch	846	2129	484	165	135	3759
Morone saxatilis	Striped Bass	0	0	0	0	2	2
Notropis hudsonius	Spottail Shiner	35	59	73	50	39	256
Total		**920**	**2218**	**573**	**224**	**192**	**4127**

The dominant migratory species, White Perch, was ubiquitous occurring at all stations on every sampling date (Tables 6 and 7). A peak in abundance for White Perch was late July (Table 6). Spottail Shiner was ubiquitous throughout the (short) sampling season as well; with numbers increasing until early August after which they decreased again until the end of sampling in mid-September.

In total numbers and species richness of fish, station 7 dominated the other stations by far with 3947 individuals from 17 species (Table 7, Figure 69a). Stations 9 and 10 had 146 individuals from 7 species and 34 individuals from 5 species respectively (Table 7), which is lower than last year, but there were much fewer sampling events in 2020. The relative abundance clearly shows the dominance of White Perch at all sites (69b). A notable species collected at station 9 is Blue Catfish, which is an invasive piscivorous species. One Blue Catfish was collected in the cove as well (station 7). This is a very small portion of the total catch, but an indication that they don't stick to the mainstem as seemed to have been the case in previous years (2017 year was the first year two were found in station 7). A very high number of White Perch was collected, especially considering the truncated sampling season. While ubiquitous, most by far were collected in the Cove (station 7) in late July (Table 6, Figure 69a and 70a). Spottail Shiner showed a similar pattern and had highest abundance by far with 237 individuals at station 7 (Table 7, Figure 69a). At all stations, White Perch made up the most significant proportion of the total catch. Blue Catfish was only a dominant group in trawl samples at Station 9, and Pumpkinseed at Station 10. Station 7 was by far the most productive site due to the high number of White Perch collected there.

White Perch (*Morone americana*), the most common fish in the open waters of Gunston Cove, continues to be an important commercial and popular game fish. Adults grow to over 30 cm long. Sexual maturity begins the second year at lengths greater than 9 cm. As juveniles, they feed on zooplankton and macrobenthos, but as they get larger they consume fish as well.

Spottail Shiner (*Notropis hudsonius*), a member of the minnow family, is moderately abundant in the open water and along the shore. Spawning occurs throughout the warmer months. It reaches sexual maturity at about 5.5 cm and may attain a length of 10 cm. They feed primarily on benthic invertebrates and occasionally on algae and plants.

Trawling collects fish that are located in the open water near the bottom. Due to the shallowness of Gunston Cove, the volume collected is a substantial part of the water column. However, in the river channel, the near bottom habitat through which the trawl moves is only a small portion of the water column. Fishes tend to concentrate near the bottom or along shorelines rather than in the upper portion of the open water.

Table 7. Adult and Juvenile Fish Collected by Trawling. Gunston Cove Study – 2020.

Scientific Name	**Common Name**	**7**	**9**	**10**
Alosa aestivalis	Blueback Herring	2	0	0
Alosa pseudoharengus	Alewife	14	1	0
Alosa sp.	unk. Alosa species	2	0	0
Ameiurus nebulosus	Brown Bullhead	0	0	1
Anguilla rostrata	American Eel	1	0	0
Carassius auratus	Goldfish	2	0	0
Cyprinus carpio	Carp	1	2	0
Dorosoma cepedianum	Gizzard Shad	5	0	0
Dorosoma petenense	Threadfin Shad	1	0	0
Etheostoma olmstedi	Tessellated Darter	6	0	0
Hybognathus regius	Eastern Silvery Minnow	5	0	0
Ictalurus furcatus	Blue Catfish	1	18	0
Ictalurus punctatus	Channel Catfish	0	1	0
Lepomis gibbosus	Pumpkinseed	22	0	8
Lepomis macrochirus	Bluegill	8	0	2
Lepomis sp.	unk. sunfish	1	0	6
Morone americana	White Perch	3638	104	17
Morone saxatilis	Striped Bass	1	1	0
Notropis hudsonius	Spottail Shiner	237	19	0
Total		**3947**	**146**	**34**

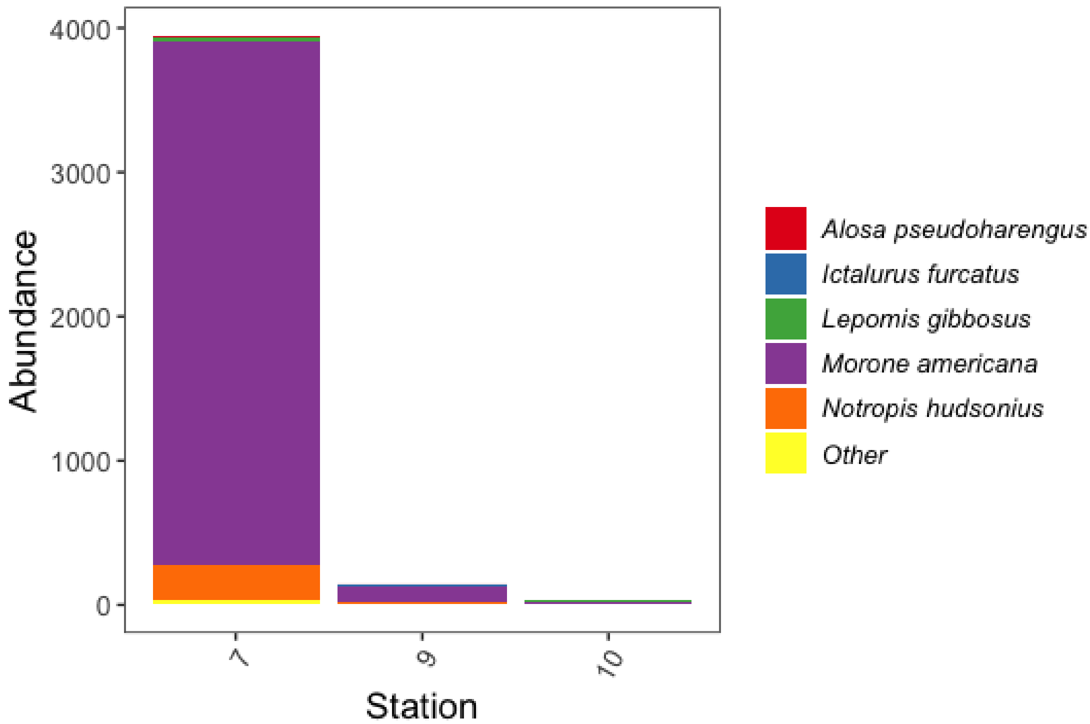

Figure 69a. Adult and Juvenile Fishes Collected by Trawling in 2020. Dominant Species by Station.

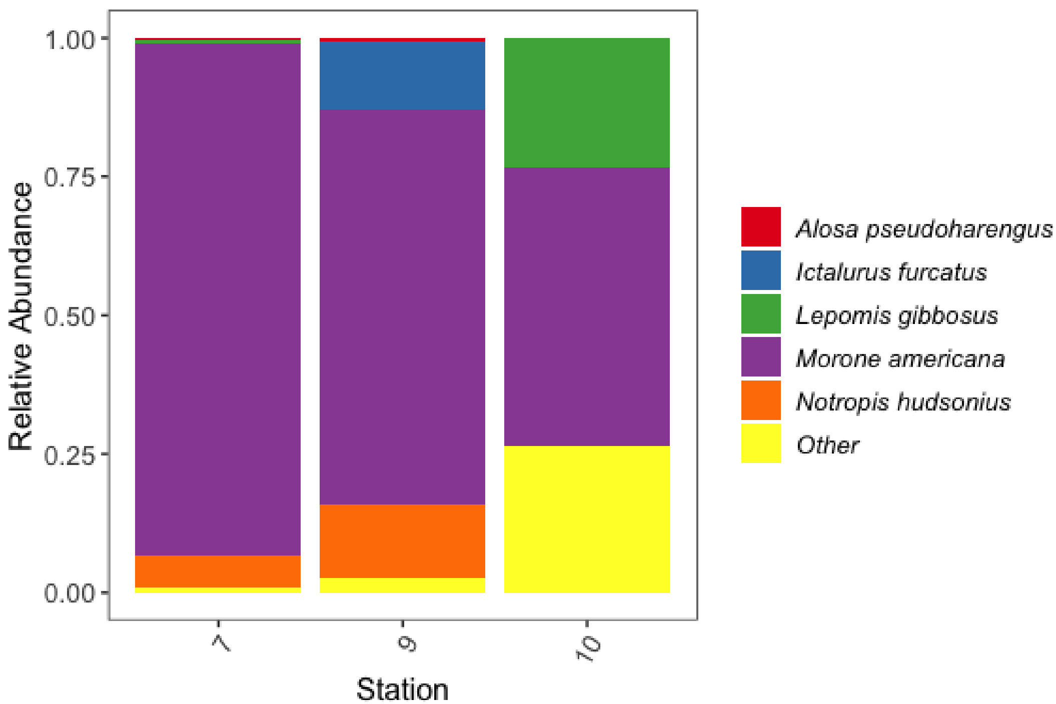

Figure 69b. Relative abundance of Adult and Juvenile Fishes Collected by Trawling in 2020.

When looking at the seasonal trend it is clear that White Perch was the most common species, and dominant in every month (Figure 70a and b). Highest abundance of White Perch was in July. Spottail Shiner were most abundant in August, with high total abundance in June and July as well. White Perch and Spottail Shiner were so dominant each month that other species hardly made the chart (Figure 70a and b). When looking at relative abundance over season can be seen that the composition of the catch is similar between months, and that the main monthly difference is total abundance of the catch with a peak in July (Figure 70a and b). The most productive month was July, which was entirely due to the very large catch of White Perch. Other species in the top five most abundant were Alewife, Blue Catfish and Pumpkinseed.

Blueback Herring (*Alosa aestivalis*) and Alewife (*Alosa pseudoharengus*) were formerly major commercial species, but are now depleted stocks. Adults grow to over 30 cm and are found in the coastal ocean. They are anadromous and return to freshwater creeks to spawn in March, April and May. They feed on zooplankton and may eat fish larvae.

Pumpkinseed (*Lepomis gibbosus)* is a common sunfish found in freshwater with a lot of vegetation. Feeds mostly on insects, mosquito larvae, crustaceans and worms, but also on small fishes, gastropods and small mollusks. They prefer clear water and vegetation to hide.

Blue Catfish (*Ictalurus furcatus*) is an introduced species from the Mississippi River basin. They have been intentionally stocked in the James and Rappahannock rivers for food and sport. They have expanding their range and seem to replace white catfish and perhaps also Channel Catfish and bullheads. As larvae, they feed on zooplankton; juveniles and adults mostly on fishes, and on benthos, and detritus.

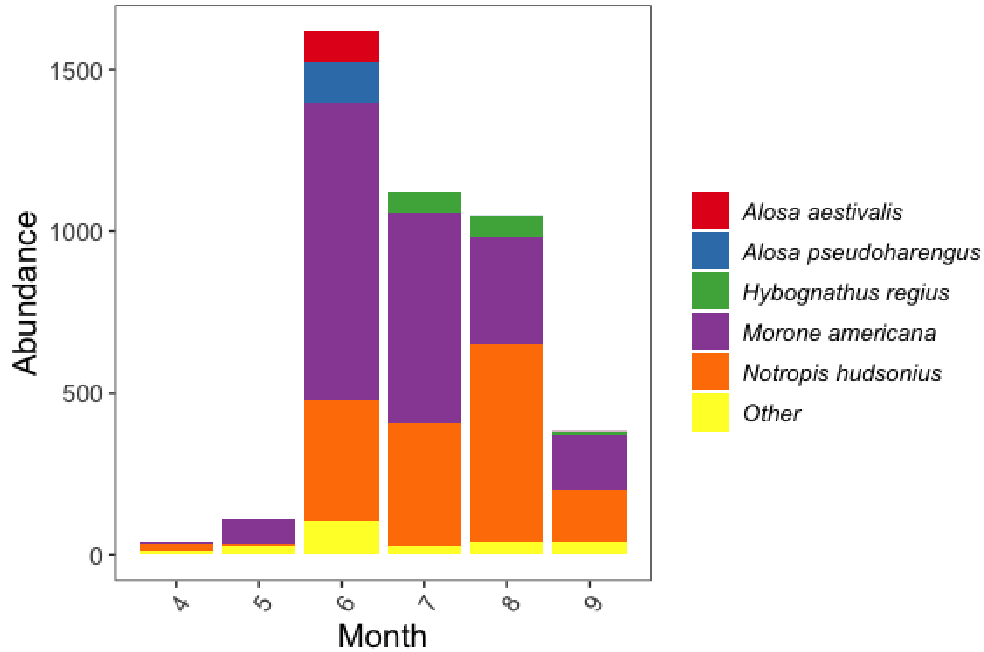

Figure 70a. Adult and Juvenile Fishes Collected by Trawling in 2020. Dominant Species by Month.

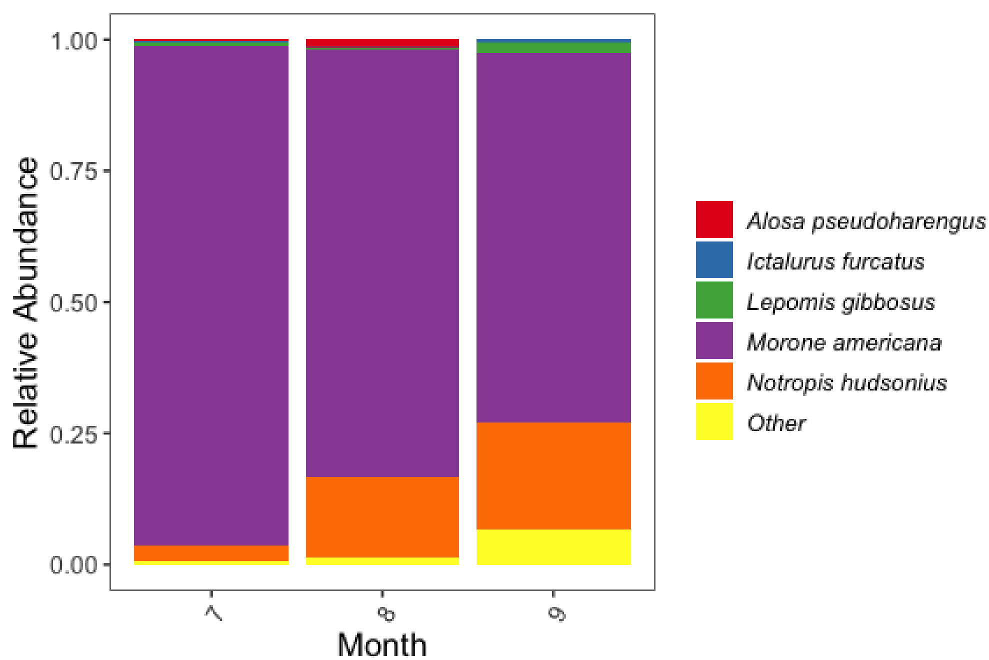

Figure 70b. Relative Abundance for Adult and Juvenile Fishes Collected by Trawling in 2020.

Seines

Seine sampling was conducted approximately semi-monthly at 4 stations between July 10 and September 10. The late start (normally April) was due to a lockdown in response to the COVID-19 pandemic. Stations 4, 6, and 11 have been sampled continuously since 1985. Station 4B was added in 2007 to have a continuous seine record when dense SAV impedes seining in 4. Station 4B is a routine station now, also when seining at 4 is possible. This allows for comparison between 4 and 4B. In 2020, SAV growth was too extensive to seine at Station 4 in September.

A total of 19 seine tows were conducted, comprising 2648 fishes of at least 27 species (Table 8). This is less than previous years, which is simply due to the fact that less samples were taken (19 versus up to 40). Similar to last year, the most dominant species in seine catches was Banded Killifish, with a relative contribution to the catch of 50.38%. The second most common species found were Threadfin Shad who comprised 9.93% of the catch. This is an interesting find as this species has not been seen to come up this far into freshwater in previous years. White Perch was somewhat abundant as well at 6.38% of the catch. Other taxa that contributed at least 1% to total abundance include Alewife (4.15%), Inland Silverside (4.15%), *Alosa sp.* (3.85%), *Lepomis sp.* (3.74%), Goldfish (3.55%), Quillback (2.68%), Eastern Silvery Minnow (2.04%), Mummichog (2.00%), Mosquitofish (1.40%), and Spottail Shiner (1.25%). Other species occurred at low abundances (Table 8).

Banded Killifish was abundant and present at all sampling dates, with highest abundance late July (Table 9, Figure 71). Threadfin Shad appeared in the samples in August and September, with highest catch late August. Total catch was dominated by Banded Killifish every sampling date in 2020. The other most dominant species by month were White Perch and Herring and Shad in July, Threadfin Shad and Inland Silverside in August, and Threadfin Shad in September (Table 9, Figure 71).

Threadfin Shad was a more dominant species than Banded Killifish in station 11, while Banded Killifish was most dominant at all other Stations (Table 10, Figure 72). The highest abundance of White Perch was at Station 11. White Perch as well as Threadfin Shad are pelagic species, and Station 11 is a beach closest to the mainstem. Total abundance was highest at Station 4B with 1073 specimens and lowest at station 4 with 428 specimens (Table 10).

Table 8. Adult and Juvenile Fish Collected by Seining. Gunston Cove Study - 2020.

Scientific Name	**Common Name**	**Abundance**	**Percent**
Fundulus diaphanus	Banded Killifish	1334	50.38
Dorosoma petenense	Threadfin Shad	263	9.93
Morone americana	White Perch	169	6.38
Alosa pseudoharengus	Alewife	110	4.15
Menidia beryllina	Inland Silverside	110	4.15
Alosa sp.	unk. Alosa species	102	3.85
Lepomis sp.	unk. sunfish	99	3.74
Carassius auratus	Goldfish	94	3.55
Carpiodes cyprinus	Quillback	71	2.68
Hybognathus regius	Eastern Silvery Minnow	54	2.04
Fundulus heteroclitus	Mummichog	53	2.00
Gambusia holbrooki	Mosquitofish	37	1.40
Notropis hudsonius	Spottail Shiner	33	1.25
Lepomis macrochirus	Bluegill	27	1.02
Micropterus salmoides	Largemouth Bass	23	0.87
Morone saxatilis	Striped Bass	16	0.60
Lepomis microlophus	Redear Sunfish	12	0.45
Cyprinus carpio	Carp	8	0.30
Lepomis gibbosus	Pumpkinseed	6	0.23
Dorosoma cepedianum	Gizzard Shad	4	0.15
Etheostoma olmstedi	Tessellated Darter	4	0.15
Lepisosteus osseus	Longnose Gar	4	0.15
Lepomis auritus	Redbreast Sunfish	3	0.11
Semotilus atromaculatus	Creek Chub	3	0.11
Enneacanthus gloriosus	Bluespotted Sunfish	2	0.08
Notemigonus crysoleucas	Golden Shiner	2	0.08
Pomoxis nigromaculatus	Black Crappie	2	0.08
Strongylura marina	Atlantic Needlefish	2	0.08
Channa argus	Northern Snakehead	1	0.04
Total		**2648**	**100.00**

Table 9. Adult and Juvenile Fish Collected by Seining. Gunston Cove Study - 2020.

Scientific Name	**Common Name**	**07-10**	**07-24**	**08-07**	**08-21**	**09-10**	**Total**
Alosa pseudoharengus	Alewife	47	0	36	27	0	110
Alosa sp.	unk. Alosa species	18	60	0	2	22	102
Carassius auratus	Goldfish	4	84	3	2	1	94
Carpiodes cyprinus	Quillback	68	2	1	0	0	71
Channa argus	Northern Snakehead	0	1	0	0	0	1
Cyprinus carpio	Carp	0	0	4	4	0	8
Dorosoma cepedianum	Gizzard Shad	0	0	1	3	0	4
Dorosoma petenense	Threadfin Shad	0	0	59	169	35	263
Enneacanthus gloriosus	Bluespotted Sunfish	0	0	0	0	2	2
Etheostoma olmstedi	Tessellated Darter	0	1	2	1	0	4
Fundulus diaphanus	Banded Killifish	247	414	386	240	47	1334
Fundulus heteroclitus	Mummichog	8	14	11	3	17	53
Gambusia holbrooki	Mosquitofish	2	7	13	13	2	37
Hybognathus regius	Eastern Silvery Minnow	23	0	0	9	22	54
Lepisosteus osseus	Longnose Gar	2	0	1	1	0	4
Lepomis auritus	Redbreast Sunfish	0	2	0	1	0	3
Lepomis gibbosus	Pumpkinseed	1	3	1	0	1	6
Lepomis macrochirus	Bluegill	0	16	8	3	0	27
Lepomis microlophus	Redear Sunfish	0	3	0	9	0	12
Lepomis sp.	unk. sunfish	3	92	4	0	0	99
Menidia beryllina	Inland Silverside	2	14	87	5	2	110
Micropterus salmoides	Largemouth Bass	3	10	3	6	1	23
Morone americana	White Perch	33	77	15	33	11	169
Morone saxatilis	Striped Bass	0	8	4	4	0	16
Notemigonus crysoleucas	Golden Shiner	0	0	0	2	0	2
Notropis hudsonius	Spottail Shiner	2	4	10	14	3	33
Pomoxis nigromaculatus	Black Crappie	0	2	0	0	0	2
Semotilus atromaculatus	Creek Chub	0	0	2	1	0	3
Strongylura marina	Atlantic Needlefish	0	0	2	0	0	2
Total		**463**	**814**	**653**	**552**	**166**	**2648**

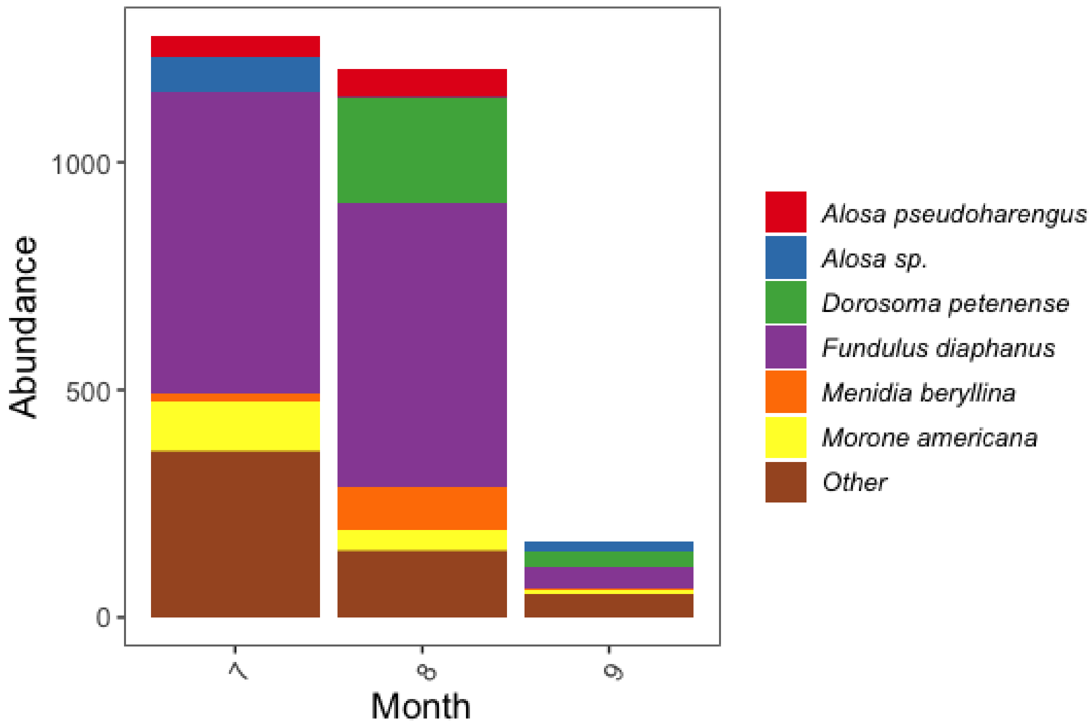

Figure 71. Adult and Juvenile Fish Collected by Seining in 2020. Dominant Species by Month.

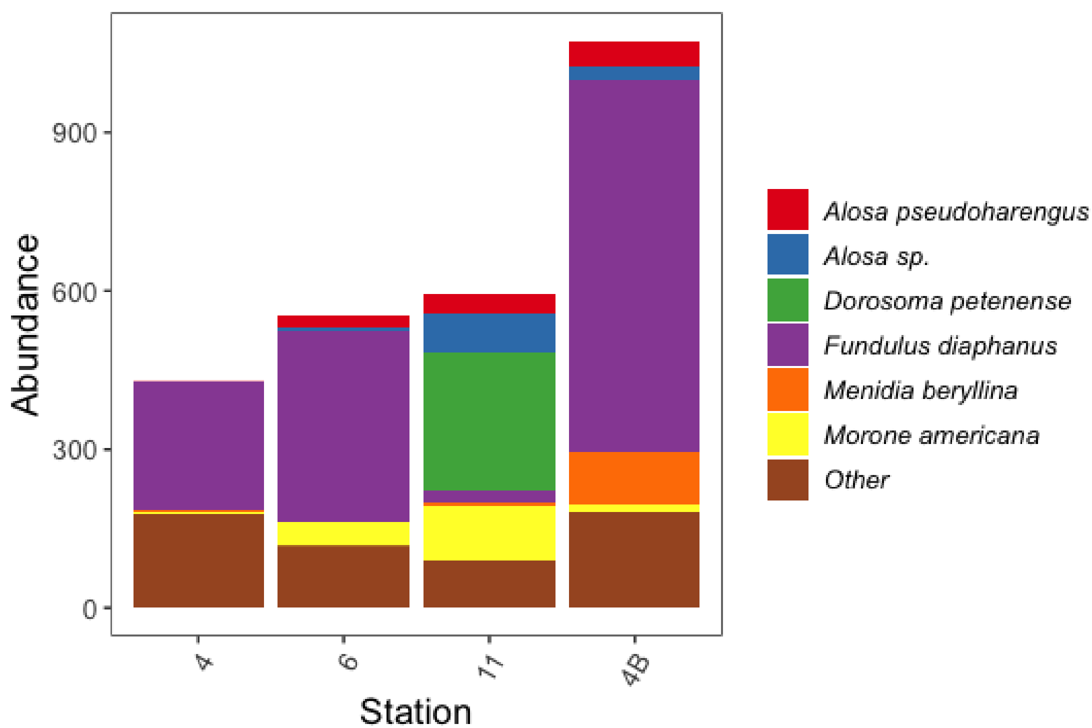

Figure 72. Adult and Juvenile Fishes Collected by Seining in 2020. Dominant Species by Station.

Table 10. Adult and Juvenile Fish Collected by Seining in 2020 per station in Gunston Cove.

Scientific Name	**Common Name**	**4**	**6**	**11**	**4B**
Alosa pseudoharengus	Alewife	1	23	37	49
Alosa sp.	unk. Alosa species	0	6	71	25
Carassius auratus	Goldfish	80	13	0	1
Carpiodes cyprinus	Quillback	0	0	30	41
Channa argus	Northern Snakehead	1	0	0	0
Cyprinus carpio	Carp	8	0	0	0
Dorosoma cepedianum	Gizzard Shad	0	0	4	0
Dorosoma petenense	Threadfin Shad	0	0	263	0
Enneacanthus gloriosus	Bluespotted Sunfish	0	2	0	0
Etheostoma olmstedi	Tessellated Darter	0	1	0	3
Fundulus diaphanus	Banded Killifish	244	364	24	702
Fundulus heteroclitus	Mummichog	0	3	6	44
Gambusia holbrooki	Mosquitofish	2	9	1	25
Hybognathus regius	Eastern Silvery Minnow	0	2	26	26
Lepisosteus osseus	Longnose Gar	0	3	0	1
Lepomis auritus	Redbreast Sunfish	0	2	0	1
Lepomis gibbosus	Pumpkinseed	1	3	0	2
Lepomis macrochirus	Bluegill	6	17	4	0
Lepomis microlophus	Redear Sunfish	10	2	0	0
Lepomis sp.	unk. sunfish	60	39	0	0
Menidia beryllina	Inland Silverside	3	0	6	101
Micropterus salmoides	Largemouth Bass	5	16	0	2
Morone americana	White Perch	4	45	104	16
Morone saxatilis	Striped Bass	0	0	9	7
Notemigonus crysoleucas	Golden Shiner	1	0	0	1
Notropis hudsonius	Spottail Shiner	1	0	7	25
Pomoxis nigromaculatus	Black Crappie	1	1	0	0
Semotilus atromaculatus	Creek Chub	0	3	0	0
Strongylura marina	Atlantic Needlefish	0	0	1	1
Total		428	554	593	1073

H. Benthic Macroinvertebrates - 2020

Triplicate petite ponar samples were collected from Gunston Cove proper (Station GC7) and in the Potomac River mainstem (Station GC9) monthly from July through September.

Taxonomic Groups: A total of 11 taxa of benthic macroinvertebrates, belonging to 6 orders and 11 families, were recorded during the survey. Two species were non-native (i.e., the Asian clam, *Corbicula fluminea* and the Japanese mystery snail, *Cipangopaludina japonica*). Annelid worms, specifically Oligochaetes, were found in high numbers at both sites over all dates (Figure 73). Overall, they accounted for 64% of all benthic organisms found. Insects were the second highest group in abundance across sites and dates, accounting for 26% of all individuals accounted for. Chironomids were by far the most numerous and omnipresent insect taxon. The only two other insect taxa were the families Leptoceridae and Chaoboridae, both from the order Trichoptera. Leptoceridae were found at both stations in June and July, while Chaoboridae were only found at GC7 during August. Crustaceans (including amphipods and isopods) were the third highest group in abundance across sites and dates, accounting for 7% of all individuals. Gammarid amphipods (scuds) dominated this group with the isopod *Cyathura polita* being the second most common crustacean (Figure 73). The remainder of the taxonomic groups accounted for minor components of the overall abundance. These included Bivalvia (1.8% of total abundance), Turbellaria (i.e., flatworms) (0.2%), and Gastropoda (0.1%). The bivalve group was composed only of the invasive Asian clam, *Corbicula fluminea*, (found at both sites) while there were two species of gastropods found - the Japanese mystery snail, *C. japonica*, and the native spiral snail *Pleurocera virginica* – both at GC9 during August.

Table 11. Taxa Identified in Gunston Cove Tidal Benthic Samples. 2020.

		Average # / ponar	
Taxon	Common Name	GC7	GC9
Platyhelminthes	Flatworms	0	1
Annelida-Oligochaeta*	Oligochaete worms	25	40.1
Annelida-Hirudinea	Leech	1	0
Bivalva-Corbicula*	Asiatic clams	1	2.7
Crustacea-Isopoda-Cyathura*	Isopods	0	2
Crustacea-Amphipoda-Gammarus*	Amphipods	2.2	5.55
Insecta-Diptera-Chironomidae*	Midges	24.1	3.7
Insecta-Diptera-Chaoboridae	Phantom Midges	1	0
Insecta-Trichoptera-Leptoceridae	Caddisflies	1	1
Gastropoda-Viviparidae	Mystery snails	0	1
Gastropoda-Pleuroceridae	Spiral snail	0	1
	TOTAL	55.3	58.0

Taxa identified with an asterisk were found on 3 or more station-dates and were included in the multivariate analysis.

Spatial trends: The average abundance of organisms per ponar sample was higher at GC9 in the Potomac mainstem as compared to the site within Gunston Cove (GC7), but this was entirely attributable to the large number of oligochaetes at that station. GC7, in comparison, had almost equal average numbers of both Chironomidae insect larvae and oligochaetes (Figure 73A). GC9 had a higher diversity of taxa (N=9) than GC7 (N73), likely due to differences in sediment and flow characteristics between the sites. Due to the high abundance of Annelida across all sites, additional analyses were conducted with non-Annelida taxa. Flatworms, isopod crustaceans, and gastropods were present only at GC9. However, phantom midges and leeches were only found at GC7. Chironomid insect larvae were more numerous at GC7 than GC9. When examining all non-Annelida taxa, Insects were the dominant group in percent contribution at GC7 (86%), while Crustaceans dominated at GC9 (34%) (Figure 73C). Other taxa varied in their percent contribution by site.

Temporal trends: Annelida, composed of only oligochaetes, were the dominant taxa recorded during all months (Figure 73B). Crustaceans, driven by Gammarid amphipods, peaked during August and September most likely due to recruitment. Average bivalvia abundances differed monthly across the sampling period (average of 1-4 individuals/ponar) but these trends were driven by GC9 as there was only 1 clam collected at GC7. Only a single individual of Turbellaria was found during only May and July and only at GC9. Comparing percent contributions of all non-Annelida taxa across all of the sites, months were dominated by Insecta (May – 64%, June – 52%, July – 79%, August – 51%, September – 57%) (Figure 73D). Overall, larger increases in abundances and relative percent contributions over the sampling period for many of the taxa described above are in direct relation to seasonal changes and recruitment.

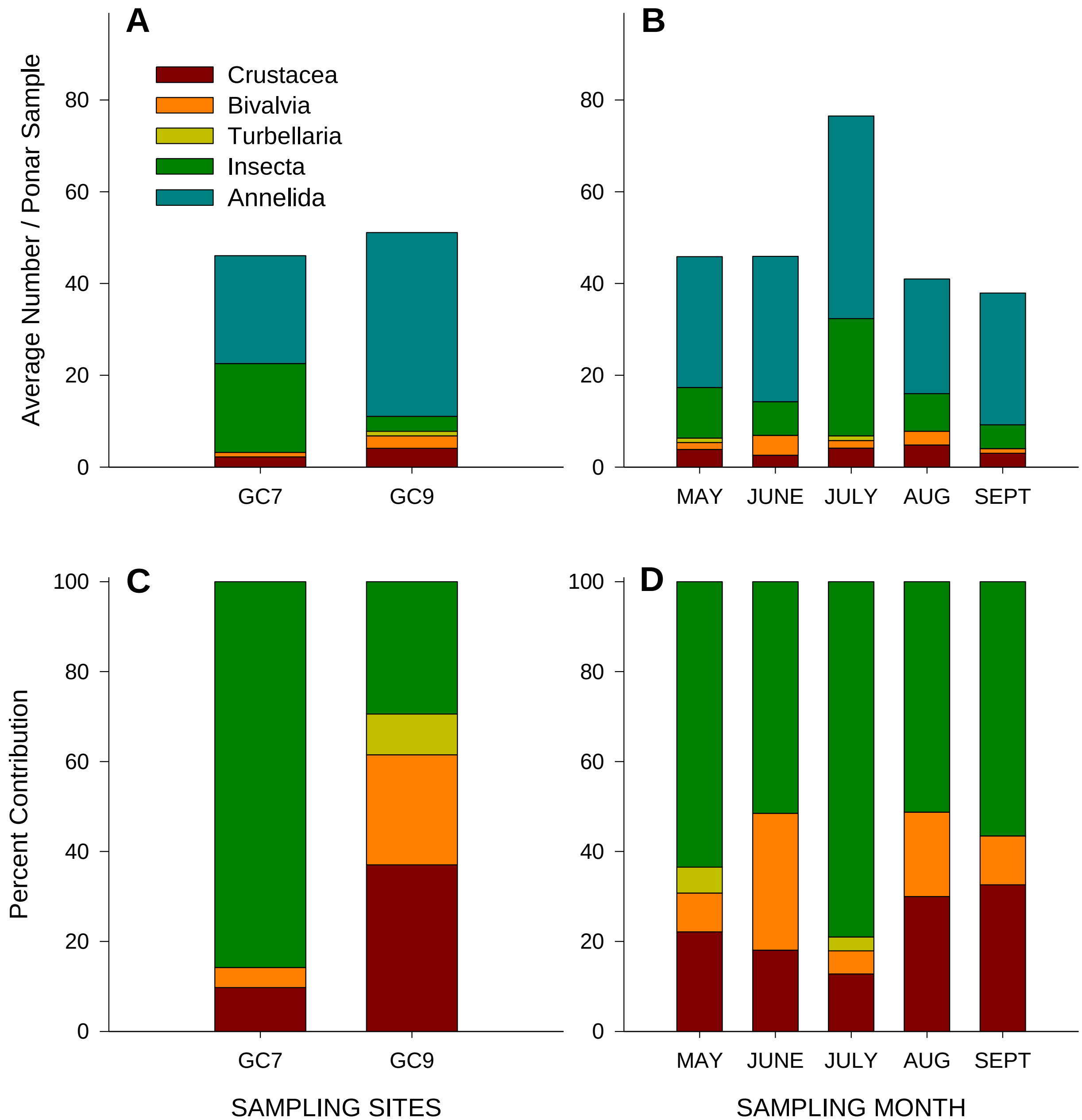

Figure 73. Average number per ponar sample of all benthic macroinvertebrate taxa (A, B) and percent contribution of all non-Annelida benthic macroinvertebrate (C, D) in petite ponar samples collected in 2020 separated by site and month.

Multivariate analyses: Due to the multispecies aspect of benthic communities, it is often useful to use multivariate analyses or ordination to examine relationships among samples. This allows multiple taxa to be considered simultaneously when assessing these relationships. In order to get the most meaningful relationships, the full macroinvertebrate sample/taxa matrix was condensed. Taxa that were present in less than three of the original replicate sample matrix were excluded. Then, the remaining, more consistently found taxa were used in the analysis (indicated by asterisks in Table 11) were averaged over the replicates for each date and station combination. This resulted in one set of taxa values for each station on each date. This reduced matrix (12

samples x 5 taxa) was then subjected to an ordination using a technique called Non-metric Multidimensional Scaling (nMDS). This allows relationships among samples based on their full complement of taxa to be visualized. If successful, relationships among samples can be shown on a two-dimensional plot. The taxa differences responsible for the observed relationships can also be examined. The program PRIMER v.6 was used to conduct the ordinations.
The results of an nMDS ordination using presence-absence data is shown in Figure xx. Nearly all of the GC7 samples separate from the GC9 samples, as noted by the two circles of data points. The June and July GC7 and September GC9 samples are almost on top of one another in the bottom left corner; these samples had the exact same taxa in them. The September GC7 samples (purple circle icon in the top center) were different from the other months because this was the only month in which Gammarid crustaceans were found in the samples. The GC7 samples had either 2 or 3 taxa as compared to either 5 taxa apparent in GC9 samples (except for September, which only had 3 taxa). The higher richness at GC9 is probably due to better habitat conditions especially large and more heterogeneous sediment particle size.

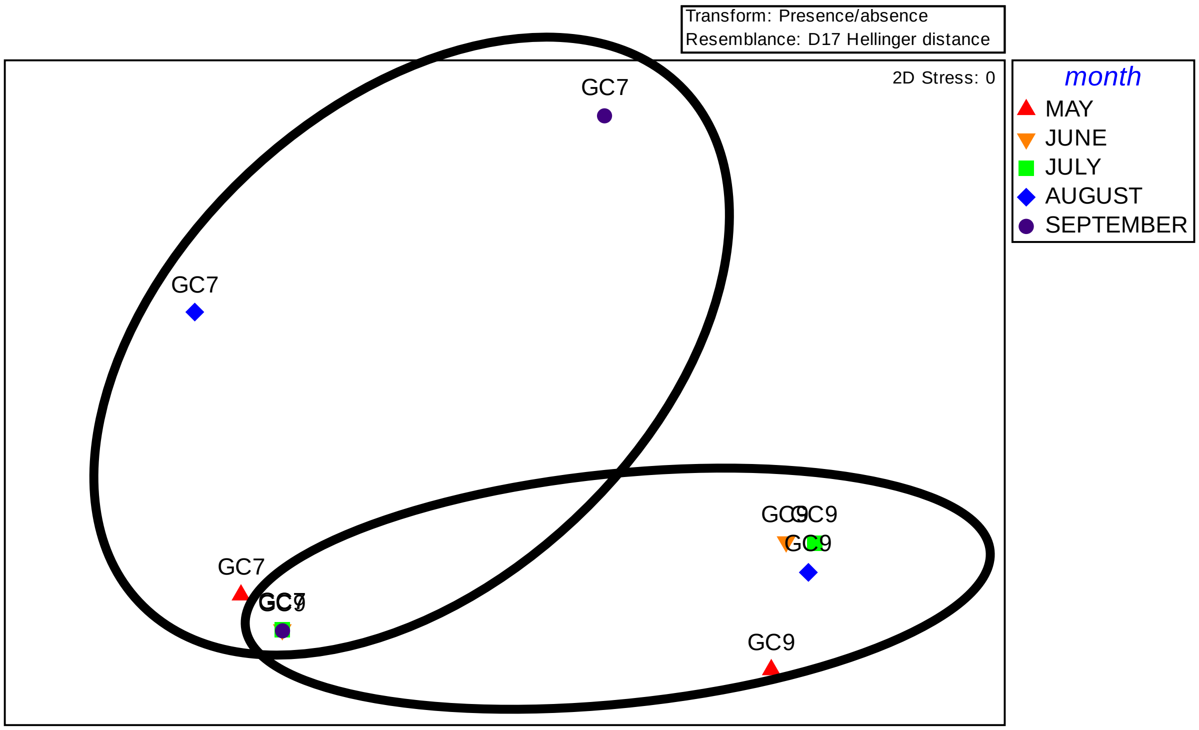

Figure 74. nMDS ordination of benthic samples from tidal stations. The station names are placed above each symbol. Colors represent month. Triplicates were averaged to get a single value for each month-station combination. Data was presence/absence and distance measure was D17 Hellinger similarity.

Influence of Habitat on Community Composition: For this analysis, only communities collected in July and August were used. We assigned all materials greater than 5 mm in the petite ponar sample to one of three categories: leaves/woody debris, mollusc shells, or submerged aquatic vegetation and calculated the percent contribution of each category to the overall habitat (Table 12). At GC7 the macroinvertebrate abundance was correlated with the type of large particles available; as the percent leaves/wood increased and the percent organic matter increased, the abundance increased (Table 12). At GC9 there was no relationship between large particle type and total abundance or richness, but this station had variable amounts of large particles present (range of 8 – 98.5% shell and 1.5 – 91.8% leaves or woody debris). There was only one sampling date in which SAV was recovered – August at both sites.

Table 12. Large substrate composition vs. total abundance and taxa richness of benthic macroinvertebrates in individual replicate samples.

Site	Replicate	Month	% Leaves/Wood	% Shell	% SAV	Total Abundance	Total Richness
GC7	A	July	59.8	40.2	0.0	109	3
	B		87.5	12.5	0.0	154	3
	C		14.4	85.6	0.0	50	3
	A	August	54.0	41.4	4.6	8	2
	B		16.6	83.4	0.0	60	3
	C		3.8	96.0	0.2	45	2
GC9	A	July	3.3	96.7	0.0	55	7
	B		2.6	97.4	0.0	82	4
	C		1.5	98.5	0.0	85	6
	A	August	91.8	8.0	0.1	56	4
	B		43.5	56.5	0.0	35	4
	C		6.7	93.3	0.0	19	5

Summary: Similar to previous years, the macroinvertebrate community was dominated by Oligochaetes (Annelids) across sites. Outside of the Annelids, Crustaceans (dominated by gammarid amphipods) were the most abundant group in the Potomac River mainstem (Station GC9), while Gunston Cove proper (Station GC7) was dominated by Insect larvae from the Chironomidae family (midges). GC9 had the highest number of unique taxa (N=4; Platyhelminthes, Crustacea-Isopoda-*Cyathura polita*, and the two Gastropods - *C. japonica* and *P. virginica*). Comparing percent contributions of all non-Annelida taxa across both sites, months were dominated by Insecta (Figure 73). Ordination analyses of the community indicated a clear separation between communities sampled at the two sites for all months except June and July GC7 and September GC9 samples, which had exactly the same community composition. The macroinvertebrate abundance at GC7 was positively correlated with the percent leaves/wood, but there was no relationship between large particle type and total abundance or richness at GC9. There was also a change of the community composition throughout the months, as common for aquatic communities experiencing changes in abiotic conditions and recruitment during the summer months.

H. Submersed Aquatic Vegetation – 2020

The Virginia Institute of Marine Science annual aerial SAV survey indicate a return to aerial coverage over most of the inner Cove area similar to that observed in most years since 2005 (Figure 76). For 2020, the total SAV coverage in the cove was 178 hectares.

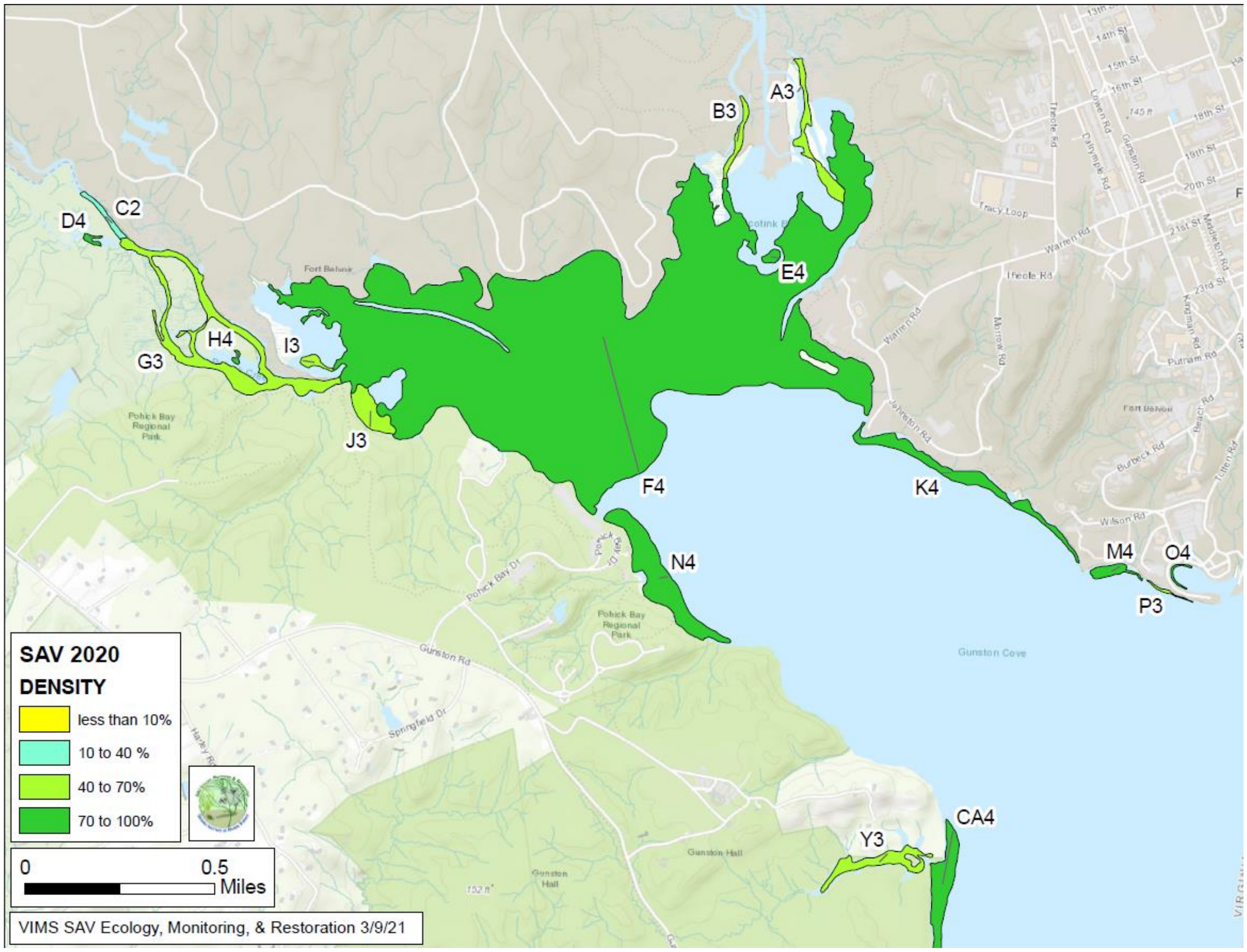

Figure 76. Coverage of Submersed Aquatic Vegetation in Gunston Cove.
VIMS SAV program. Interactive SAV map for 2020. Courtesy: David Wilcox, VIMS, March 9, 2021.

During the data mapping cruise, the distribution of dominant SAV taxa was determined at 15 points in the inner portion of Gunston Cove during the datamapping cruise by inserting a garden rake to the bottom, twisting it to collect plants and pulling it on board. The results are summarized in Table 15. *Hydrilla verticillata* was found at most of the sites, but its coverage intensity was generally only moderate. *Certatophyllum demersum* and *Najas minor* and *Zosterella dubia* were present at about ½ of the sampled points at low to moderate density. *Vallisneria america* and *Zosterella dubia* were left in the table because they were observed during the transects, but did not show up in the rake samples. These results demonstrate that SAV continued to make a partial recovery in 2020 from the very low coverage and density observed in 2018. Note that some of the datamapping cruise occurred outside of the area of SAV coverage (Figure 6).

Table 13. Relative abundance of dominant SAV species determined during data mapping cruise.

Scientific Name	Common Name	Freq (#)	Freq (%)	Avg. Density
Hydrilla verticillata	hydrilla	13	86.7	2.27
Ceratophyllum demersum	coontail	8	53.3	1.00
Najas minor	minor/spiny naiad	8	53.3	0.73
Vallisneria americana	water celery	0	0	0
Zosterella dubia	water stargrass	0	0	0

A total of 15 points were sampled for SAV with a water depth of 2.1 m or less. Frequency (#) is the number of points that contained a particular species of SAV. Frequency (%) is the proportion of points that contained that species. Average density is the average coverage value at those points that contained a particular species. Coverage values ranged from 0.5 (present) to 4 (very abundant).

DISCUSSION

A. 2020 Data

In 2020 air temperature was below normal in April and May, but well above normal from June through August (Table 2). Precipitation was well above normal in April, July, August, and September but below normal in May. Rainfall and runoff patterns relative to sampling dates are shown in Figure 77. The only water quality sample date that was preceeded by substantial rainfall was May 5. River flows which could impact the study area in May and August/September (see Figure 2).

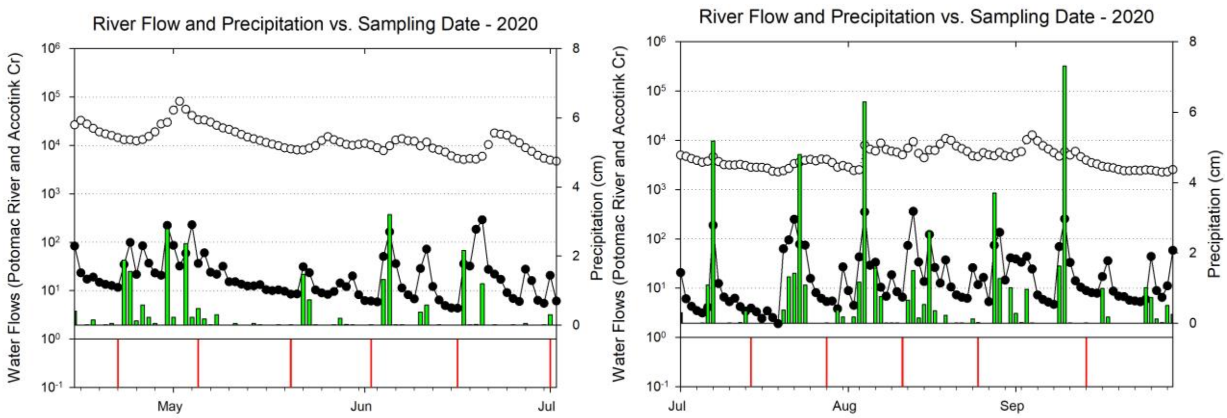

Figure 77. Precipitation (green bars), Accotink Creek flows (solid circles), Potomac River flows (open circles) and water quality/plankton sampling events (red lines at bottom).

Mean water temperature was similar at the two stations with a pronounced dip in late May and a peak of about 30° in late. Specific conductance showed a strong decline in the aftermath of the high early May flows, but recovered by late May and varied over a relatively narrow range for the rest of the year. Dissolved oxygen saturation and concentration (DO) were consistently higher in the cove and there was little seasonal pattern at either site. Field pH patterns mirrored those in DO. Total alkalinity was generally higher in the river than in the cove. Values were similar at the two sites early in the year, but then the cove station steadily decreased. Water clarity as measured by Secchi disk transparency and light attenuation coefficient both exhibited a strong decline in the aftermath of the early May high flows, but recovered and remained stready for the rest of the year. Values indicated only moderately good water clarity.

Ammonia nitrogen never exceeded the rather high detection limit of 0.1 mg/L values making analysis of any temporal or spatial trends impossible. After a slight bump upwards in the cove in May, nitrate values declined steadily through July at both stations with river values consistently about 0.5 mg/L than those in the cove. Nitrite was much lower overall. Organic nitrogen showed marked decline in late May, then increased through July before dropping back in the fall. It was generally about 0.1 mg/L higher in the cove than in the river. Total phosphorus showed a little seasonal or spatial trend hovering at about 0.05 mg/L. Soluble reactive phosphorus was generally somewhat higher in the river, but showed little consistent seasonal trend. N to P ratio declined at both stations through July and then increased slightly in August and September with most values between 15 and 25, a range which is still indicative of P limitation of phytoplankton and SAV. BOD was generally higher in the cove than in the river. TSS was consistently between 10 and 20 except for one high value in the river in September. VSS did not show strong spatial and temporal patterns.

In the cove algal populations as measured by chlorophyll *a* were consistently higher in the cove than in the river except in August. High values in the cove in April were strongly decreased in early May, a possible flow impact. There were two peaks in the cove, late May and late June, reaching 30-40 ug/L. In the river there was a steady increase through the year reaching about 30 ug/L in late July.

Rotifers continued to be the most numerous microzooplankton in 2020. Rotifer densities were unusually high (over 10,000/L) in early June in the cove due to a *Filinia* bloom. *Keratella* and *Brachionus* dominated for the remainder of the year. Rotifer densities were consistently lower in the river than in the cove with *Brachionus a*s the dominant. *Bosmina*, a small cladoceran was low at both stations except for a peak in early June in the cove. *Diaphanosoma*, a larger cladoceran, was very abundant in the cove in mid-June exceeding 4000/m^3. It had two peaks of about 2000/m^3 in the river. *Daphnia* was only found at low values in 2020. *Sida* was present in the river at the same times as *Diaphanosoma*. *Leptodora* exhibited peaks in mid-June in the cove and June and mid-July in the river at 400-600/m^3. Copepod nauplii had a distinct seasonal pattern in the cove reaching 250/L in mid-June. In the river the peak was somewhat lower. The calanoid copepod *Eurytemora* was very abundant in the cove in late May and June attaining 6500/m^3, but was much lower for the rest of the year. It reached almost 5000/m^3 in the river is mid-June. A second calanoid *Diaptomus* was found at much lower levels. Cyclopoid copepods had a strong maximum in the river of 10,000/m^3 in late July, but otherwise were at low levels in 2020.

Several water quality and plankton variables exhibited a strong decline in early May including specific conductance, turbidity, light attenuation, secchi depth, and chlorophyll *a*. These declines were probably due to the impact of runoff from significant rainfall amounts in the three days preceding this sampling. Since samples for analysis by the Noman Cole lab were not collected on this date, we do not have any information on how this event might have affected these variables.

In 2020 ichthyoplankton was dominated by clupeids, most of which were Gizzard Shad (30%), Alewife (15%), and Blueback Herring (12%), and to a much lesser extent Hickory Shad and American Shad. White Perch was found in relatively high densities (18%), mostly found in the Potomac mainstem, confirming its affinity for open water. Inland Silverside was also relatively abundant (6.4%) and found more in the mainstem. Other taxa were found in very low densities. The highest density of fish larvae occurred late May, which was driven by a high density of Clupeid larvae. The non-clupeid larval density was highest in May, driven by White Perch larvae.

Submerged aquatic vegetation returned in 2019 and 2020 after 2018's very low cover, which resulted in fish abundances and gear efficiency that was similar to the years before 2018. Due to COVID restrictions trawl and seine sampling did not start until July. In trawls White Perch dominated at 91%, followed by Spottail Shiner at 6%. No other species exceeded 1%.

White Perch was by far the most abundant species and was found in all months at all stations. We collected a lot less Blue Catfish than in 2018, but still found 18 in the mainstem and 1 in the cove. With the smaller catch in 2019 and 2020, we still found a disparity between catches of Blue Catfish in the mainstem versus the cove, which supports the theory that Blue Catfish has an affinity for the mainstem, potentially leaving embayments like Gunston Cove to serve as a refuge for native catfishes. We collected one native catfish in the cove and one in the mainstem.

In seines, the most abundant species was Banded Killifish comprising 50% of the catch. Banded Killifish was far more abundant in seines than in trawls, which emphasizes the preference of Banded Killifish for the shallow littoral zone (which is the area sampled with a seine, while trawls sample the open water. Other taxa with high abundances were Herring and Shad, as well as White Perch. Abundances remained high throughout the sampling season. Other relatively abundant species collected with the seines were Inland Silverside, Goldfish, Quillback, Mummichog, and Eastern Silvery Minnow.

Due to the short sampling season, fyke nets were not deployed in 2020.

As in most previous years, oligochaetes were the most common invertebrates collected in ponar samples in 2020. Chironomids (midge larvae) were second most dominant in the cove. And third most dominant in the river behind amphipods. Multivariate analysis showed a clear and consistent difference between cove benthic communities and those in the river. Shells were the most dominant large substrate in river benthic samples. In the cove both shells and plant detritus were abundant.

Coverage of submersed aquatic vegetation (SAV) in 2020 was down from 2019 levels, but much higher than in 2018. *Hydrilla,* coontail, and minor naiad were the most abundant SAV taxa..

B. Water Quality Trends: 1983-2020

To assess long-term trends in water quality, data from 1983 to 2020 were pooled into two data files: one for Mason data and one for Noman Cole laboratory data. Then, subgroups were selected based on season and station. For water quality parameters, we focused on summer (June-September) data as this period is the most stable and often presents the greatest water quality challenges and the highest biological activity and abundances. We examined the cove and river separately with the cove represented by Station 7 and the river by Station 9. We tried several methods for tracking long-term trends, settling on a scatterplot with LOWESS trend line. Each observation in a particular year is plotted as an open circle on the scatterplot. The LOWESS (locally weighted sum of squares) line is drawn by a series of linear regressions moving through the years. We also calculated the Pearson correlation coefficient and performed linear regressions to test for statistical significance of a linear relationship over the entire period of record (Tables 16 and 17). This was similar to the analysis performed in previous reports.

Table 14
Correlation and Linear Regression Coefficients
Water Quality Parameter vs. Year for 1984-2020
GMU Water Quality Data
June-September

	Station 7			Station 9		
Parameter	Corr. Coeff.	Reg. Coeff.	Signif.	Corr. Coeff.	Reg. Coeff.	Signif.
Temperature	0.200	0.052	<0.001	0.121	0.028	0.040
Conductivity, standardized to 25°C	0.105	-----	NS	0.009	-----	NS
Dissolved oxygen, mg/L	0.082	-----	NS	0.181	0.020	0.002
Dissolved oxygen, percent saturation	0.002	-----	NS	0.213	0.296	<0.001
Secchi disk depth	0.700	1.66	<0.001	0.323	0.473	<0.001
Light attenuation coefficient	0.684	0.083	<0.001	0.098	-----	NS
pH, Field	0.193	-0.011	0.001	0.179	0.007	0.005
Chlorophyll, depth-integrated	0.637	-3.59	<0.001	0.330	-0.778	<0.001
Chlorophyll, surface	0.622	-3.61	<0.001	0.311	-0.856	<0.001

For Station 7, n=320-339 except pH, Field where n=273 and Light attenuation coefficient where n=257.
For Station 9, n=278-292 except pH, Field where n=240 and Light attenuation coefficient where n=226.

Significance column indicates the probability that a correlation coefficient this large could be due to chance alone. If this probability is greater than 0.05, then NS (not significant) is indicated. Both near surface and near bottom samples included.

Table 15
Correlation and Linear Regression Coefficients
Water Quality Parameter vs. Year for 1983-2020
Fairfax County Environmental Laboratory Data
June-September

	Station 7			Station 9		
Parameter	Corr. Coeff.	Reg. Coeff.	Signif.	Corr. Coeff.	Reg. Coeff.	Signif.
Chloride	0.018	-----	NS	0.063	-----	NS
Lab pH	0.541	-0.035	<0.001	0.362	-0.017	<0.001
Alkalinity	0.099	0.115	0.025	0.384	0.483	<0.001
BOD	0.646	-0.149	<0.001	0.405	-0.041	<0.001
Total Suspended Solids	0.377	-0.871	<0.001	0.199	-0.106	0.002
Volatile Suspended Solids	0.413	-0.548	<0.001	0.390	-0.119	<0.001
Total Phosphorus	0.585	-0.003	<0.001	0.352	-0.001	<0.001
Soluble Reactive Phosphorus	0.118	-0.0001	0.008	0.063	-----	NS
Ammonia Nitrogen	0.320	-0.015	<0.001	0.279	-0.002	<0.001
Nitrite Nitrogen	0.449	-0.003	<0.001	0.160	-0.001	0.0157
Nitrate Nitrogen	0.594	-0.031	<0.001	0.626	-0.031	<0.001
Organic Nitrogen	0.603	-0.044	<0.001	0.405	-0.012	<0.001
N to P Ratio	0.240	-0.260	<0.001	0.338	-0.346	<0.001

For Station 7, both surface and bottom samples used, n=487-530 except Nitrite Nitrogen where n=452
For Station 9, only surface samples used, n=242-266 except Nitrite Nitrogen where n =227.

Significance column indicates the probability that a correlation coefficient this large could be due to chance alone. If this probability is greater than 0.05, then NS (not significant) is indicated.

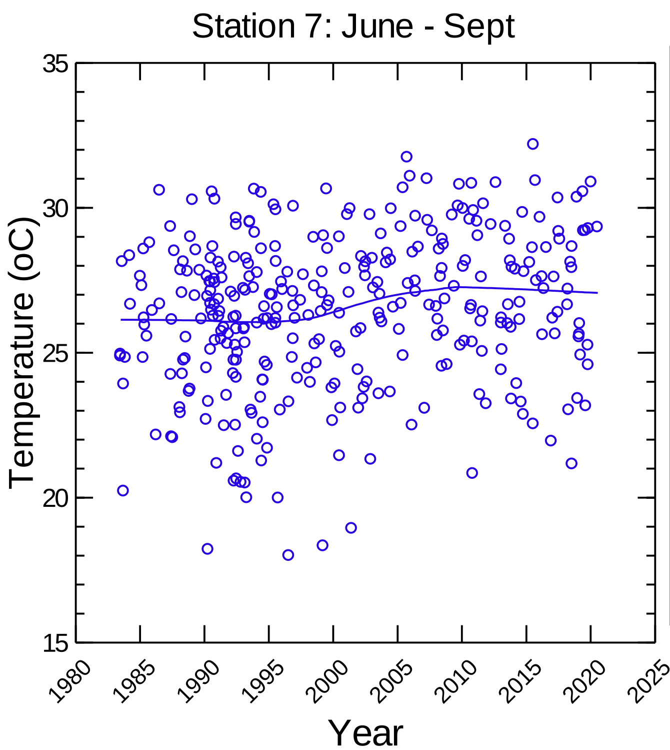

Water temperatures during the summer months generally varied between 20ºC and 30ºC over the study period (Figure 78). The LOWESS curve indicated an average of about 26°C during the period 1984-2000 with a slight upward trend in the last few years to about 27ºC. Linear regression analysis indicated a significant linear trend in water temperature in the cove when the entire period of record is considered (Table 14). The slope of this relationship is 0.05°C/year.

Figure 78. Long term trend in Water Temperature (GMU Field Data). Station 7. Gunston Cove.

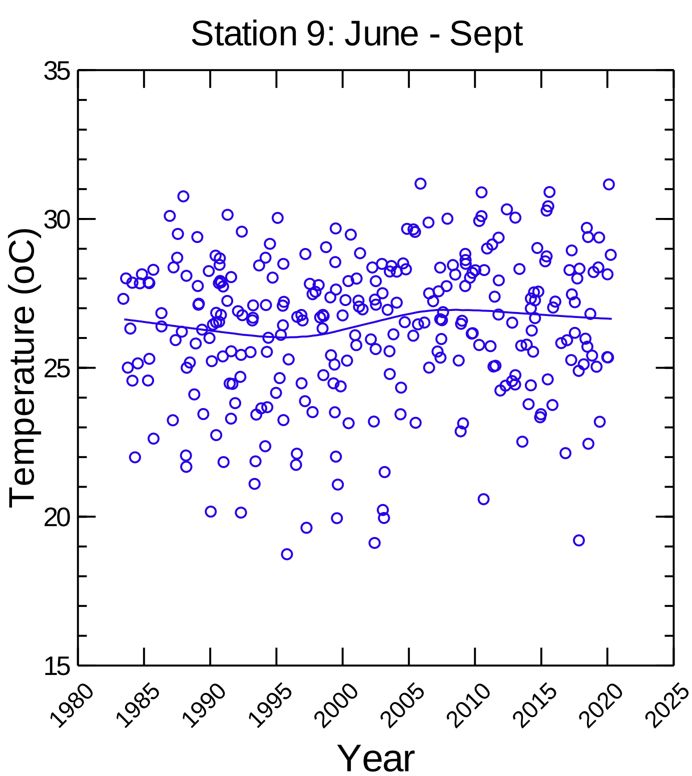

In the river summer temperatures have been similar to those in the cove with fewer readings above 30°C in the river (Figure 79). The long term trend became significant for the first time in 2020 with a slope of about 0.03° per year (Table 14).

Figure 79. Long term trend in Water Temperature (GMU Field Data). Station 9. Gunston Cove.

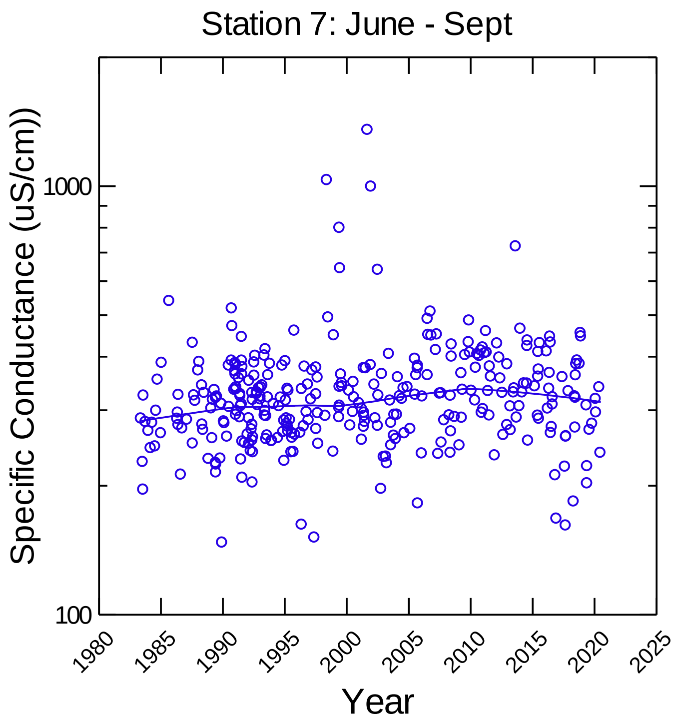

Specific conductance was generally in the range 200-500 µS/cm over the study period (Figure 80). Some significantly higher readings have been observed sporadically. A slight increase in specific conductance was suggested by the LOWESS line over the study period. This was not, however, found to be statistically significant (Table 14).

Figure 80. Long term trend in Specific Conductance (GMU Field Data). Station 7. Gunston Cove.

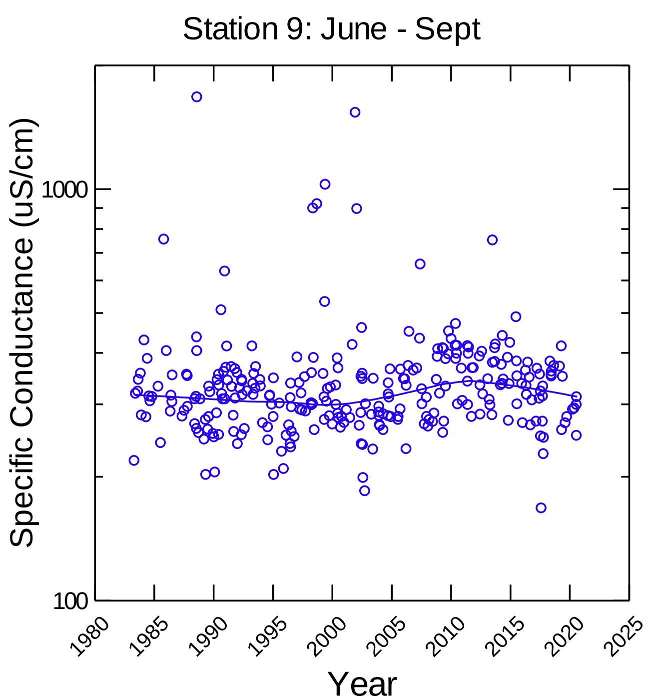

Conductivity values in the river were in the same general range as in the cove (Figure 81). Most values were between 200 and 500 µS/cm with a few much higher values. These higher values are probably attributable to intrusions of brackish water from downstream during years of low river flow. Linear regression did not reveal a significant trend in river conductivity (Table 14).

Figure 81. Long term trend in Specific Conductance (GMU Field Data). Station 9. River mainstem.

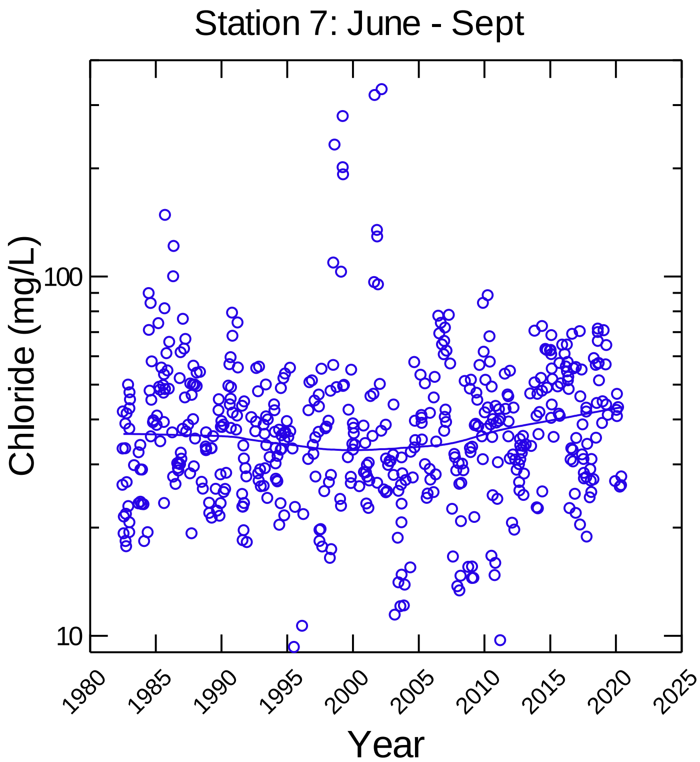

Chloride levels were clustered in a relatively narrow range of 20-70 mg/L for the entire study period (Figure 82). Higher values observed in some years were probably due to the estuarine water intrusions that occur in dry years. The trend line is nearly flat and a linear regression was not statistically significant (Table 15).

Figure 82. Long term trend in Chloride (Fairfax County Lab Data). Station 7. Gunston Cove.

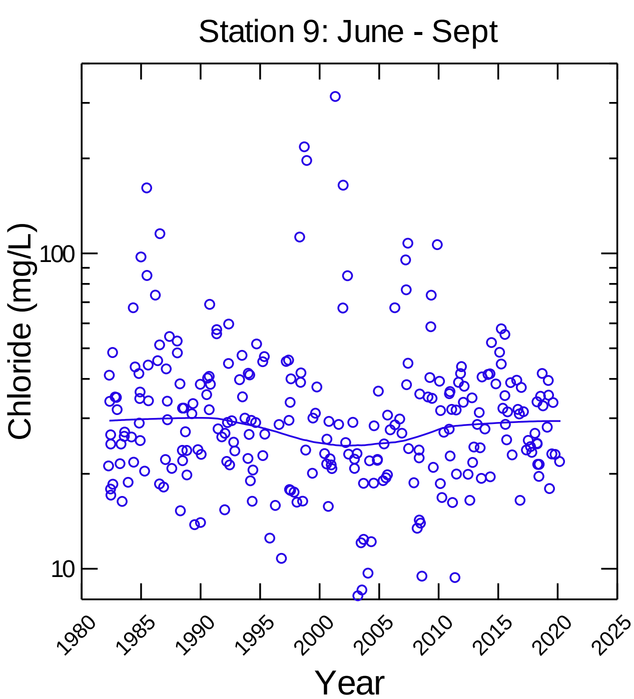

Chloride in the river has been slightly more variable than that in the cove, but in the same general range (Figure 83). The higher readings are again due to brackish water intrusions in dry years. A slight trend of increasing values in the 1980's followed by decreases in the 1990's and increases since 2005 was suggested by the LOWESS trend line. However, temporal linear regression analysis was not statistically significant (Table 15).

Figure 83. Long term trend in Chloride (Fairfax County Lab Data). Station 9. River mainstem.

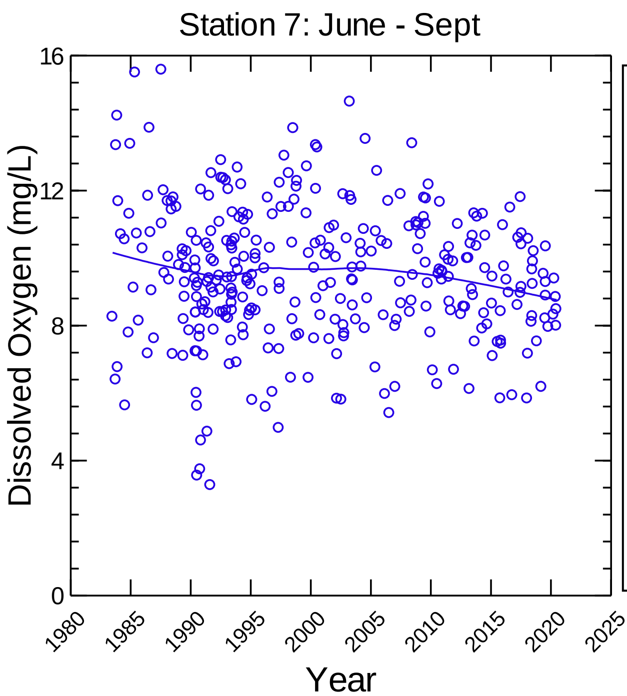

Dissolved oxygen in the cove has generally been in the range 7-13 mg/L during the summer months (Figure 84). A slight downward trend was observed through 1990, but since then the trend line has flattened, suggesting little consistent change and a mean of about 9 mg/L. In the cove dissolved oxygen (mg/L) did not exhibit a significant linear trend over the long term study period (Table 14).

Figure 84. Long term trend in Dissolved Oxygen, mg/L (GMU Data). Station 7. Gunston Cove.

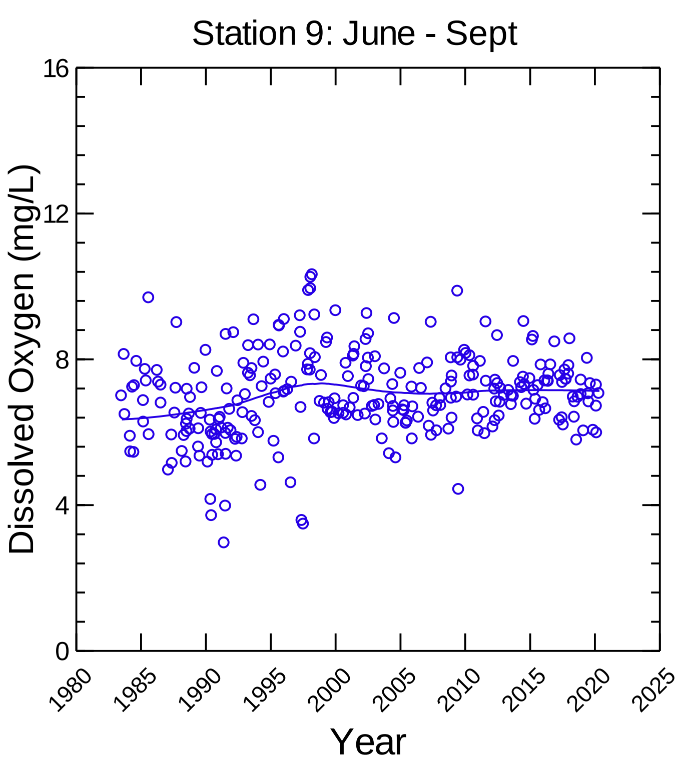

In the river dissolved oxygen values generally were in the range 5-9 mg/L over the long term study period (Figure 85). The LOWESS trend line some subtle changes from year to year, but little consistent pattern. The linear regression analysis over the entire period indicated a significant positive trend with slope of 0.02 mg/L per year or 0.72 mg/L over the period of record (Table 14).

Figure 85. Long term trend in Dissolved Oxygen, mg/L (GMU Data). Station 9. River mainstem.

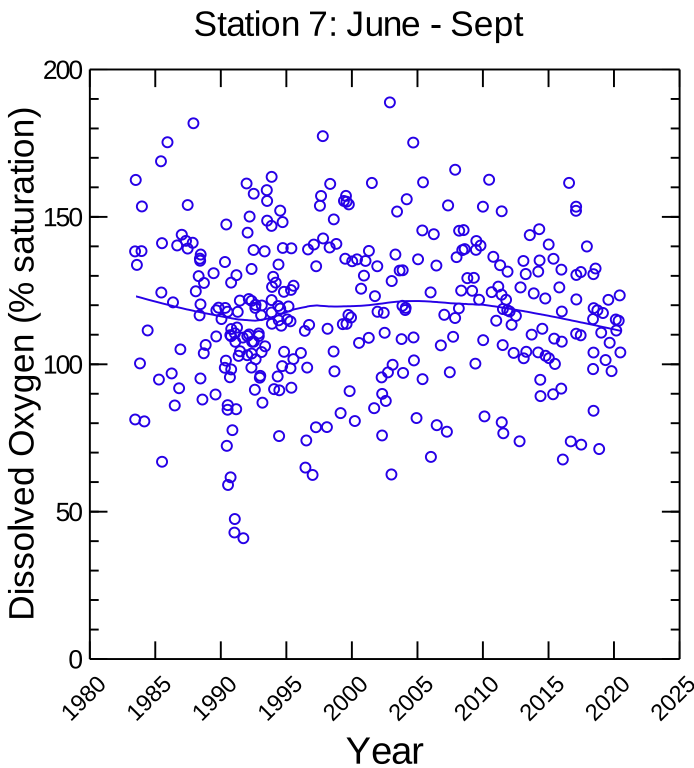

Dissolved oxygen was generally in the range 100-150% saturation in the cove over the long-term study period indicating the importance of photosynthesis in the cove (Figure 86). A decline was indicated by the trend line through 1990 followed by a slight recovery in subsequent years. Percent saturation DO did not exhibit a significant linear trend over the long-term study period (Table 14). 2020 values fell around the trend line at about 110% saturation.

Figure 86. Long term trend in Dissolved Oxygen, % saturation (GMU Data). Station 7. Gunston Cove.

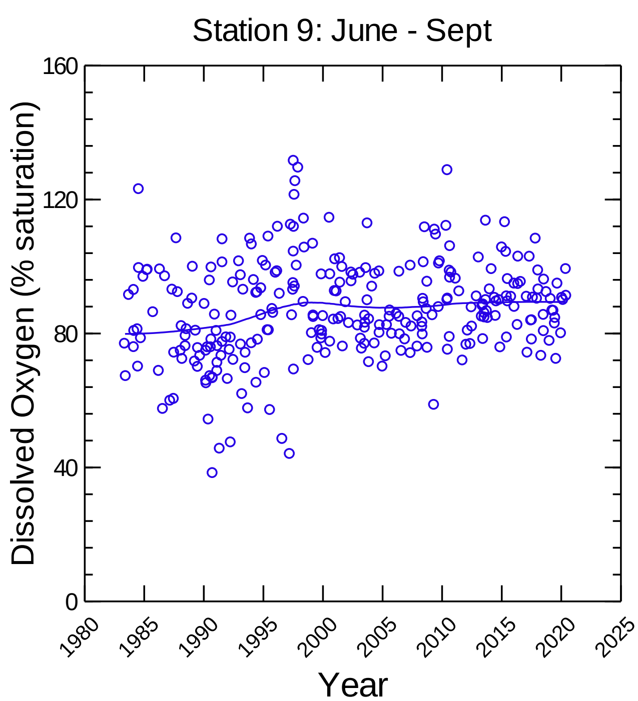

In the river dissolved oxygen was generally less than 100% indicating that photosynthesis was much less important in the river than in the cove and that respiration dominated (Figure 87). The trend line showed a very gradual increase which was statistically significant as indicated by regression analysis with a slope of 0.30% per year or about 11% over the course of the study (Table 14). 2020 readings were near the long-term trend line. Despite this increase river DO was still below cove DO in general.

Figure 87. Long term trend in Dissolved Oxygen, % saturation (GMU Data). Station 9. River Mainstem.

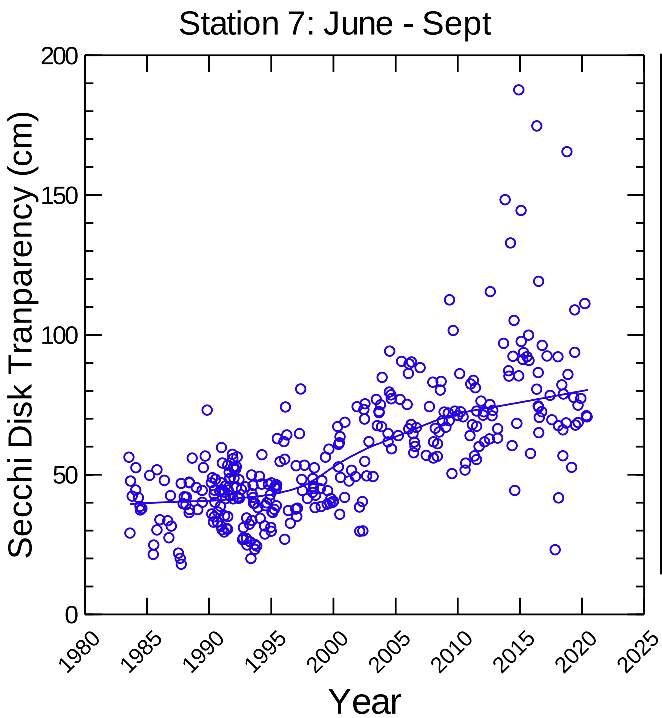

Secchi disk transparency is a measure of water clarity. Secchi disk was fairly constant from 1984 through 1995 with the trend line at about 40 cm (Figure 88). Since 1995 there has been a steady increase in the trend line from 40 cm to 80 cm in 2020. Linear regression was highly significant with a predicted increase of 1.7 cm per year or a total of nearly 60 cm over the study period (Table 14).

Figure 88. Long term trend in Secchi Disk Transparency (GMU Data). Station 7. Gunston Cove.

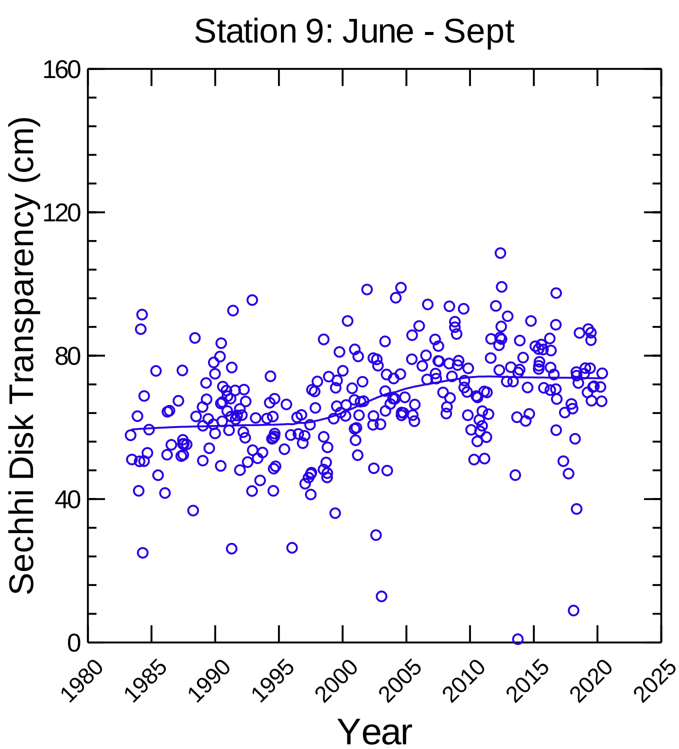

In the river Secchi depth was somewhat greater than in the cove in the 1980’s (Figure 89). The trend line was fairly constant at about 60 cm until about 2000. A rise to about 75 cm was observed by 2005 where it has remained. Linear regression revealed a significant increase of 0.47 cm per year with total increase of 16 cm predicted over of the study period (Table 14). Observations in 2020 were near the trend line.

Figure 89. Long term trend in Secchi Disk Transparency (GMU Data). Station 9. River mainstem.

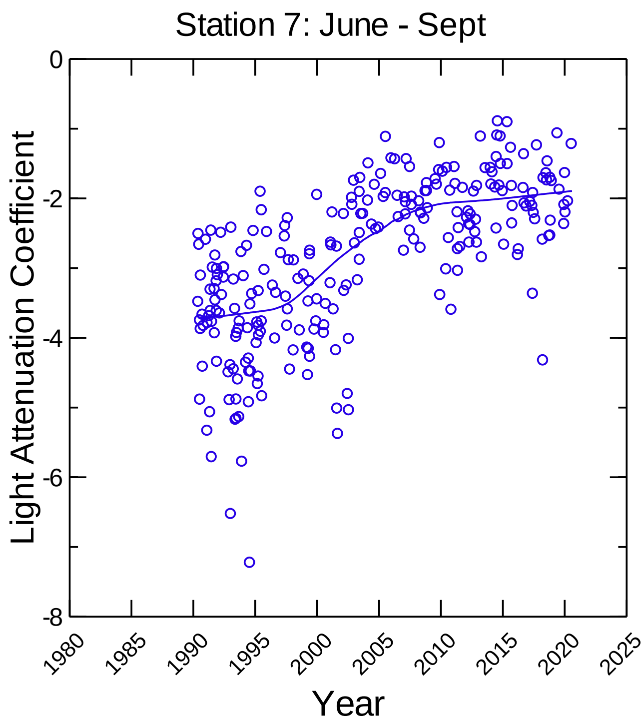

Light attenuation coefficient, another measure of water clarity, reinforces the conclusion that water clarity has been improving in the cove since 1995 (Figure 90). Trend line for the coefficient rose from about -4 to -2 m^{-1} during this time. Values in 2020 were near the trend line. Regression analysis revealed a significant linear increase in light attenuation coefficient over the period 1991-2020 with a slope of 0.083 per year yielding a prediction that light attenuation improved by about 2.4 units over this period (Table 14).

Figure 90. Long term trend in Light Attenuation Coefficient (GMU Data). Station 7. Gunston Cove.

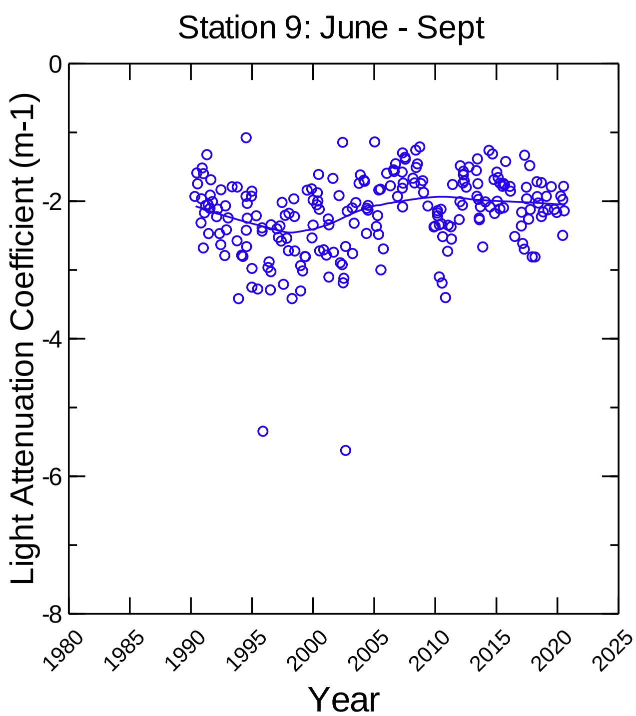

In the river light attenuation coefficient suggested a decline in light transparency between 1991 and 1997 followed by an increase through about 2008 (Figure 91). Between 2008 and 2016 the trend line indicates that light transparency has held fairly constant. Regression did not produce a significant slope over the period (Table 14).

Figure 91. Long term trend in Light Attenuation Coefficient (GMU Data). Station 9. River mainstem.

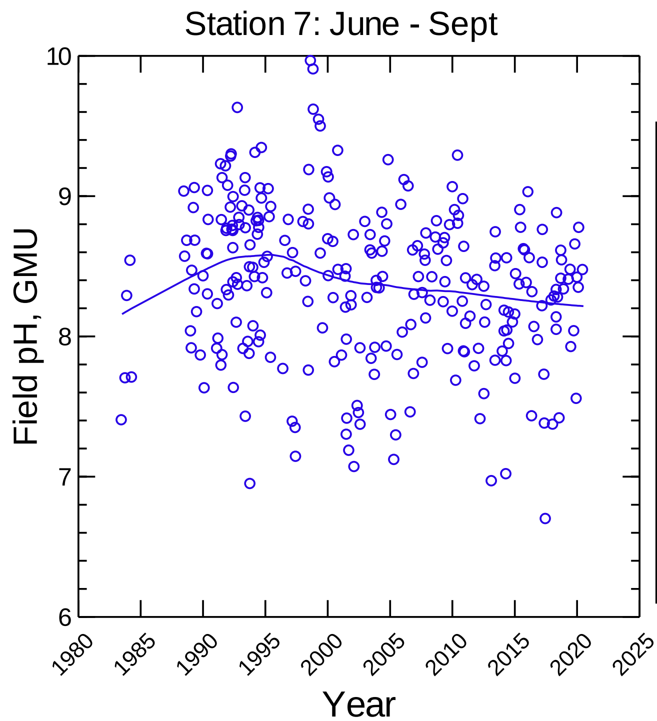

Field pH has not been measured as consistently over the entire study period as other parameters. Cove values have generally been in the 8-9 range. There is a clear trend of decreasing values since 1995 (Figure 92). Linear regression analysis now gives some evidence of a declining linear trend with a slope of -0.011 units per year when the entire study period was considered (Table 14).

Figure 92. Long term trend in Field pH (GMU Data). Station 7. Gunston Cove.

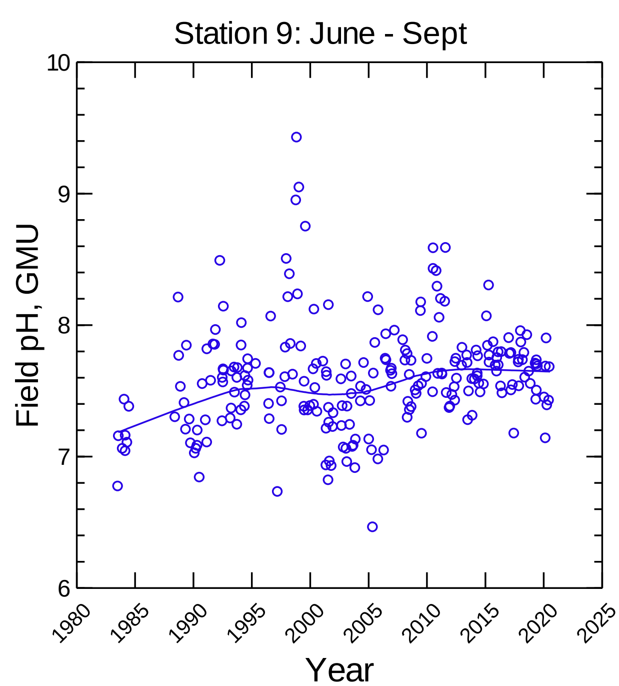

In the river a different pattern has been observed over this period (Figure 93). pH in the river has been consistently lower by about 1 pH unit than in the cove. If anything, the trend line has shown a tendency to increase. When all years were considered, field pH in the river shows a significant increase at a rate of 0.007 units per year (Table 14).

Figure 93. Long term trend in Field pH (GMU Data). Station 9. River mainstem.

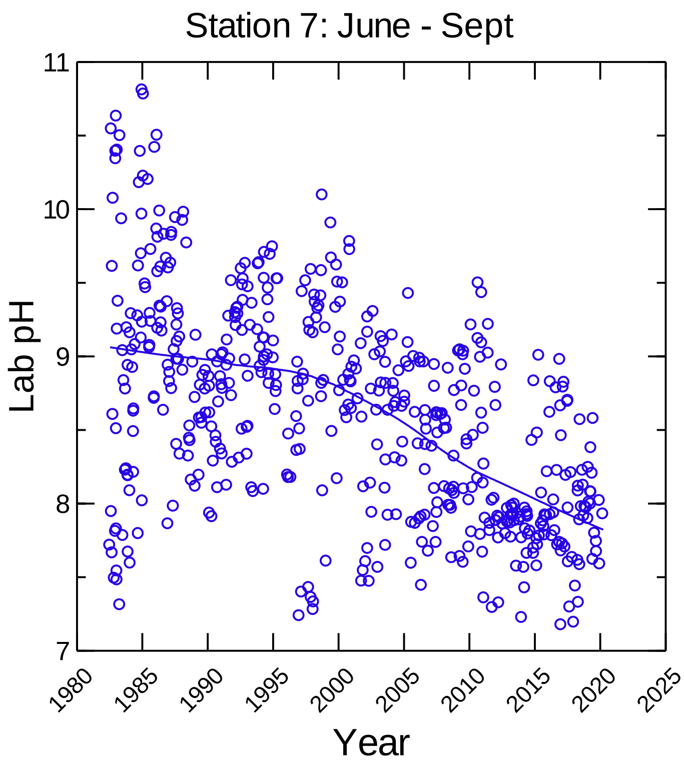

Lab pH as measured by Fairfax County personnel has shown a clear decline, especially since 2000 (Figure 94) with the trend line decreasing from about 9.0 to about 7.8. Linear regression indicates a significant decline in lab pH over the study period at a rate of about 0.035 pH units per year or a total of 1.2 units over the study period (Table 15). 2020 data were generally near the trend line.

Figure 94. Long term trend in Lab pH (Fairfax County Lab Data). Station 7. Gunston Cove.

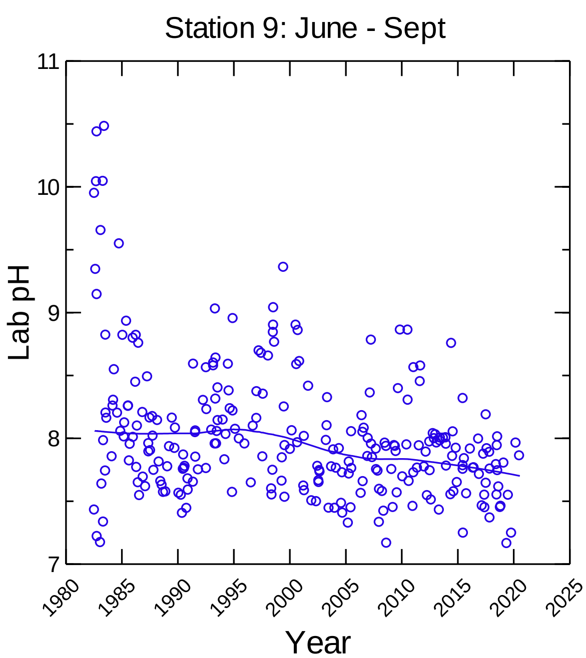

In the river, long term pH trends as measured by Fairfax County lab personnel indicate that most values fell between 7.2 and 8.2 (Figure 95). The trend line has increased and decreased slightly over the years. pH in the river showed a significant linear decline with a rate of 0.017 per year yielding a total decline of 0.60 units over the long-term study period (Table 15).

Figure 95. Long term trend in Lab pH (Fairfax County Lab Data). Station 9. Potomac mainstem.

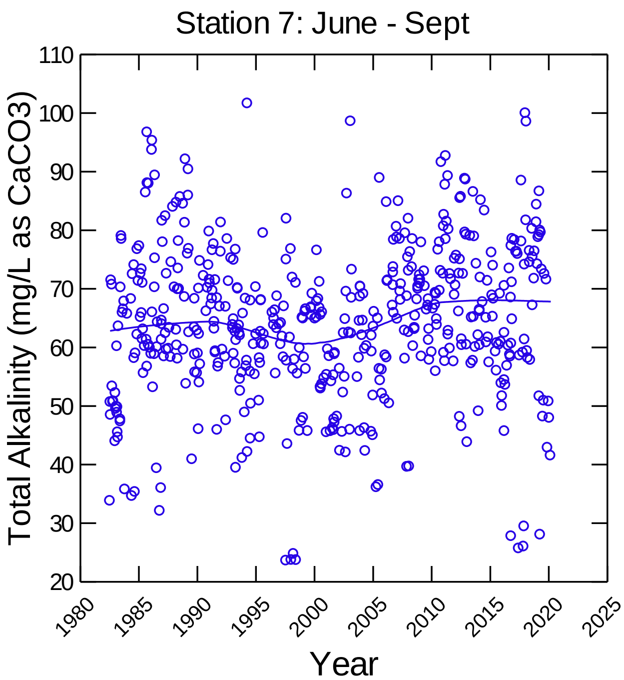

Total alkalinity as measured by Fairfax County personnel exhibited little variation early on and a slow increase since 2000 (Figure 96). The trend line at 2020 was slightly higher than it was in 1983. Overall, a very weak statistically significant linear trend has developed in total alkalinity in the cove over this period with a slope of 0.12 mg/L per year yielding a projected increase of about 4.3 mg/L over the entire study period (Table 15).

Figure 96. Long term trend in Total Alkalinity (Fairfax County Lab Data). Station 7. Gunston Cove.

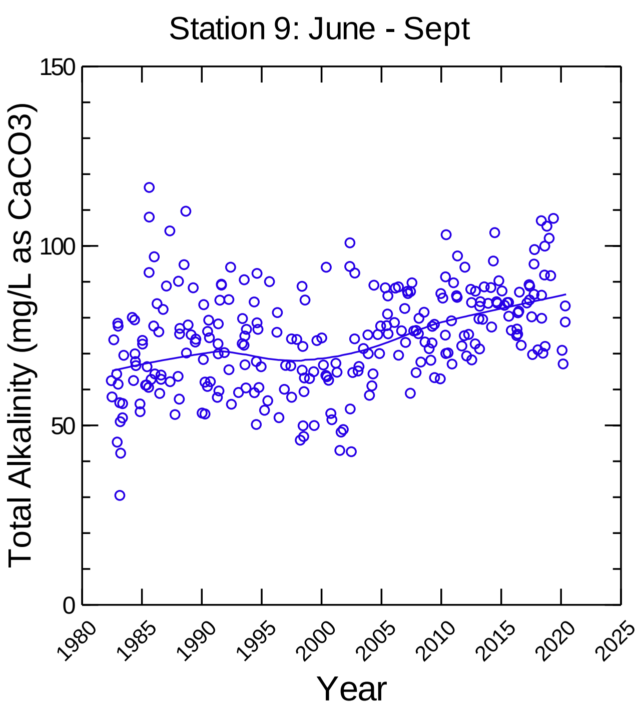

In the river a similar pattern has been observed over the three decades with an even clearer recent increase (Figure 97). There is a significant linear trend over the period with a slope of 0.48 mg/L suggesting a modest increase of about 17 mg/L over the entire study period (Table 15).

Figure 97. Long term trend in Total Alkalinity (Fairfax County Lab Data). Station 9. Potomac mainstem.

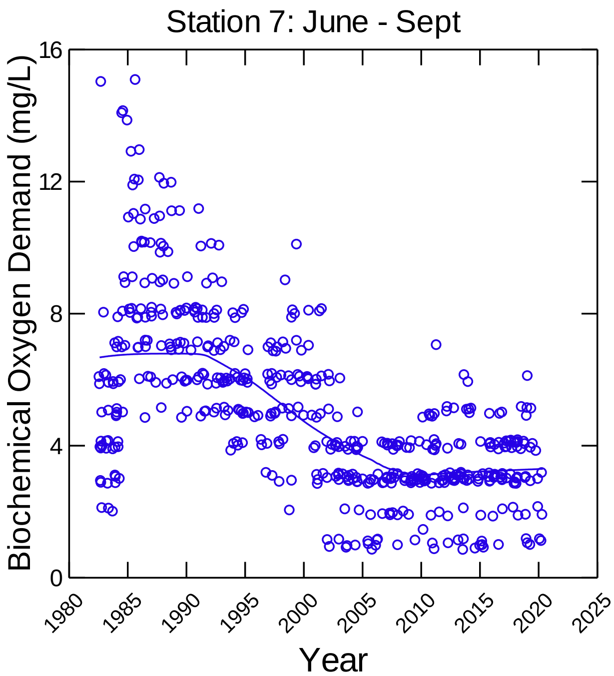

Biochemical oxygen demand has shown a distinct pattern over the long-term study period in Gunston Cove (Figure 98). In the 1980's the trend line rose from about 6 mg/L to 7 mg/L by 1989. Since then there has been a steady decline such that the trend line has dropped back to about 3 mg/L. BOD has shown a significant linear decline over the entire study period at a rate of 0.15 mg/L per year yielding a net decline of about 5.2 mg/L over the entire period of record (Table 15). It is difficult to tell if the decline is continuing as many readings are now below the detection limit.

Figure 98. Long term trend in Biochemical Oxygen Demand (Fairfax County Lab Data). Station 7. Gunston Cove.

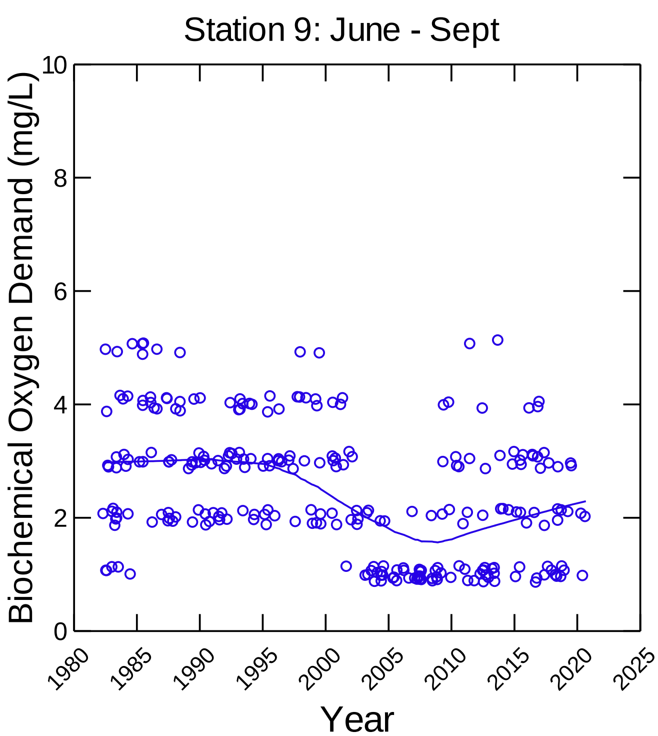

In the river biochemical oxygen demand exhibited a less distinct pattern through the mid 1990's (Figure 99). However, since that time it has decreased somewhat to a trend line value of about 1.0 mg/L. BOD in the river has exhibited a significant linear decrease at a rate of 0.04 units when the entire period of record was considered (Table 15). This would project to an overall decrease of 1.4 units. Many values now are non-detects of less than 2 mg/L making trends difficulty to examine.

Figure 99. Long term trend in Biochemical Oxygen Demand (Fairfax County Lab Data). Station 9. Potomac mainstem.

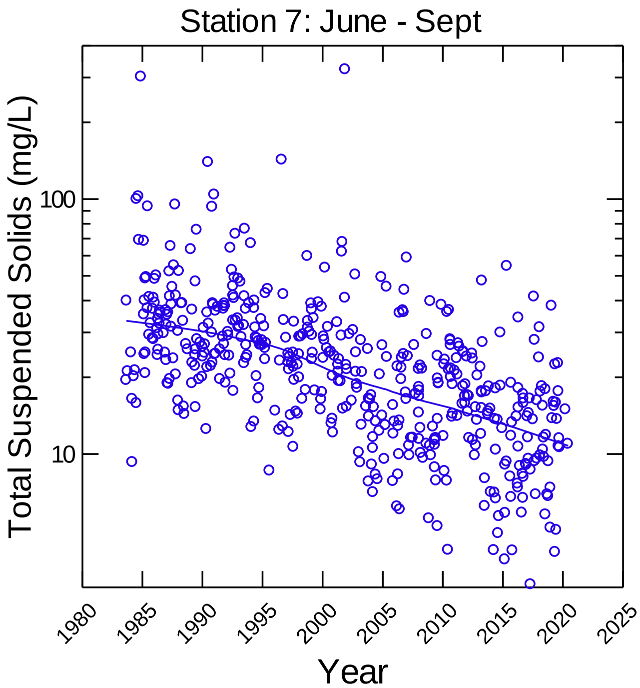

Total suspended solids (TSS) has shown a great deal of variability over the long-term study period. Nonetheless, a decreasing trend in TSS is clear in the cove with the trend line decreasing from about 32 mg/L in 1983 to about 10 mg/L in 2020 (Figure 100). Linear regression was significant indicating a decline of 0.87 mg/L per year yielding a total decline of 31 mg/L since 1984 (Table 15). Most readings in 2020 were near the trend line.

Figure 100. Long term trend in Total Suspended Solids (Fairfax County Lab Data). Station 7. Gunston Cove.

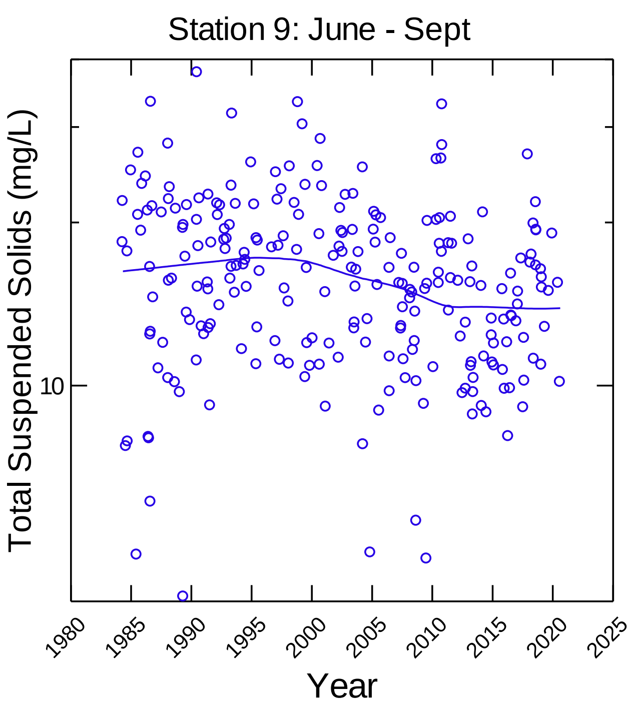

In the river TSS trends have not been as apparent (Figure 101). While much higher values have been observed sporadically, the LOWESS line remained steady at about 18-20 mg/L through most of the period with a slight decrease to about 15 mg/L suggested recently. In the river TSS exhibited a significant linear decline over the period of record at a rate of about 0.11 units per year yielding a total decline of about 3.8 mg/L over the entire study period (Table 15).

Figure 101. Long term trend in Total Suspended Solids (Fairfax County Lab Data). Station 9. Potomac mainstem.

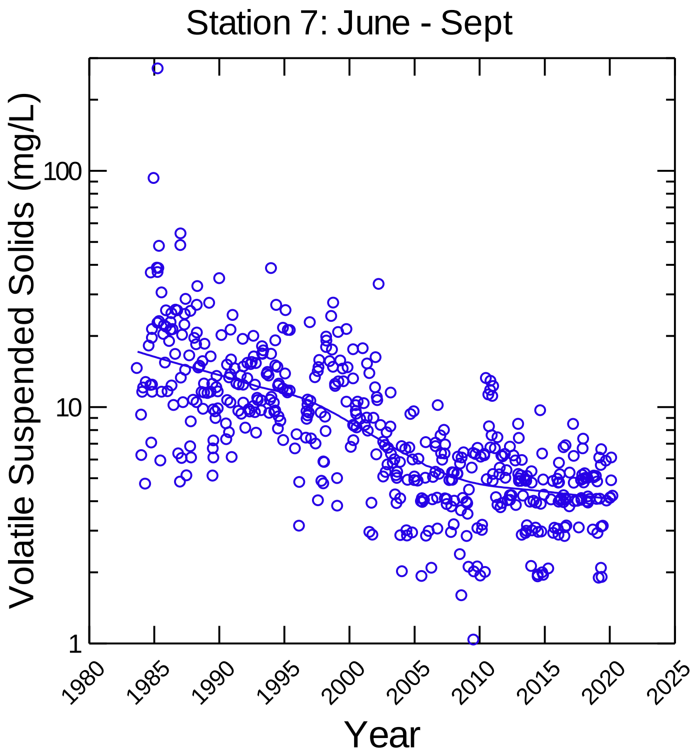

Volatile suspended solids have consistently declined over the study period in the cove (Figure 102). The LOWESS trend line has declined from 20 mg/L in 1984 to about 4 mg/L in 2020. VSS has demonstrated a significant linear decline at a rate of 0.55 mg/L per year or a total of 20 mg/L over the study period (Table 15).

Figure 102. Long term trend in Volatile Suspended Solids (Fairfax County Lab Data). Station 7. Gunston Cove.

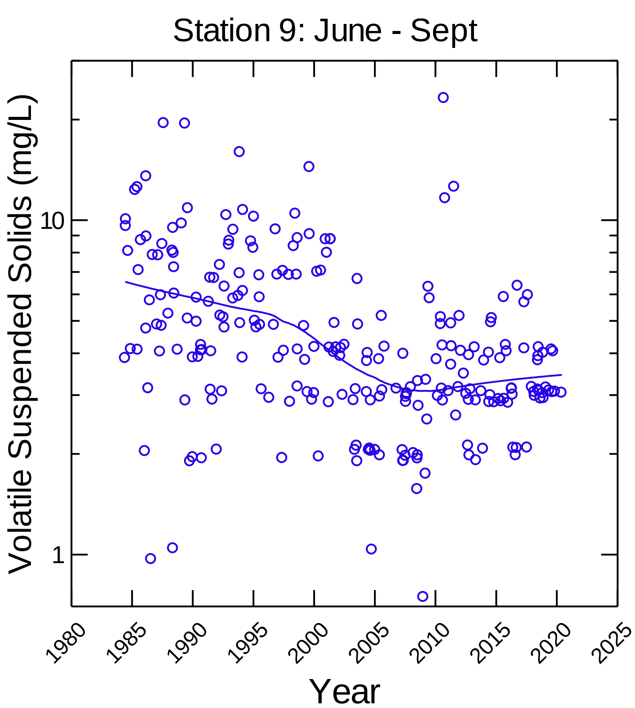

In the river the trend line for volatile suspended solids (VSS) was steady from 1984 through the mid 1990's, but decreased from 1995 to 2005. Trend line values of about 7 mg/L in 1984 dropped to about 3.5 mg/L by 2020 (Figure 103). VSS in the river demonstrated a significant linear decline at a rate of 0.12 mg/L per year or 4.2 mg/L since 1984 (Table 15).

Figure 103. Long term trend in Volatile Suspended Solids (Fairfax County Lab Data). Station 9. Potomac mainstem.

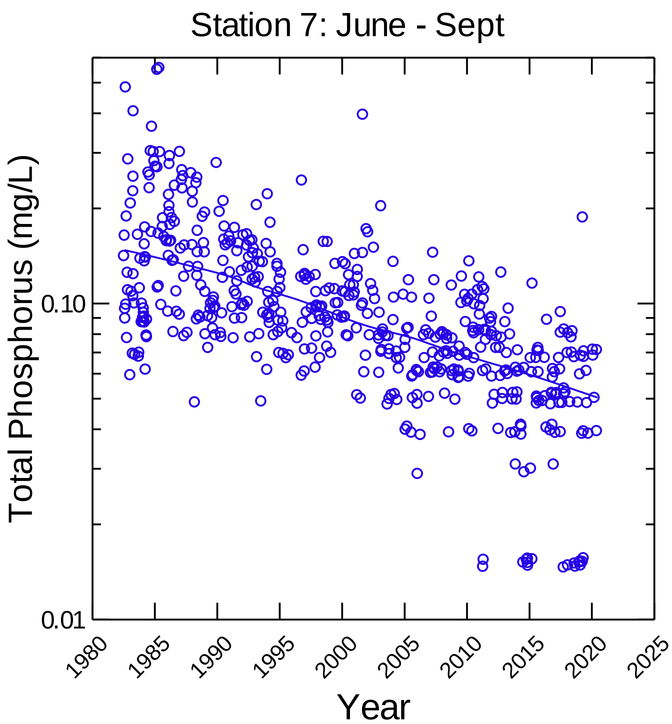

In the cove, total phosphorus (TP) has undergone a consistent steady decline since the late 1980's (Figure 104). By 2020 the trend line had dropped to 0.05 mg/L, less than half of the starting level. Linear regression over the entire period of record indicated a significant linear decline of -0.003 mg/L per year or 0.11 mg/L over the entire study period (Table 15).

Figure 104. Long term trend in Total Phosphorus (Fairfax County Lab Data). Station 7. Gunston Cove.

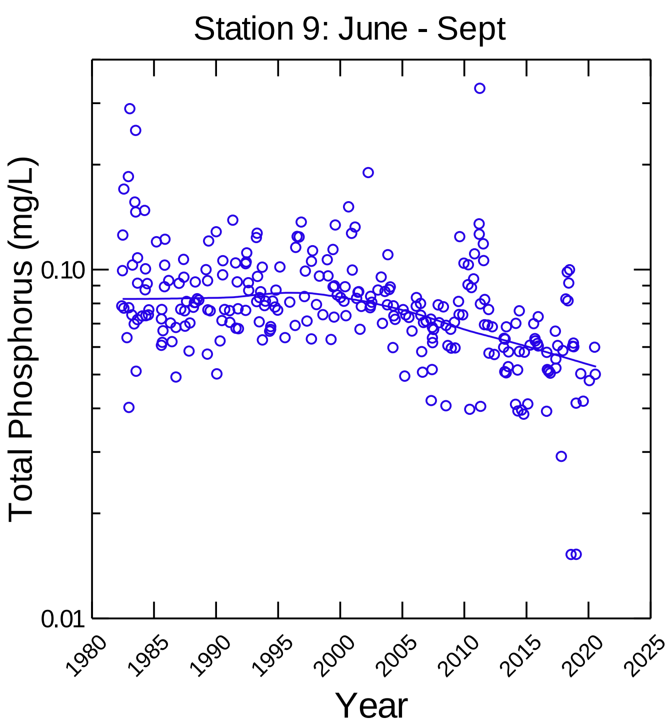

Total phosphorus (TP) values in the river have shown less of a trend over time (Figure 105). Values were steady through about 2000, then declined somewhat. TP exhibited a slight, but significant linear decrease in the river over the long-term study period with a very modest slope of -0.001 mg/L per year (Table 15).

Figure 105. Long term trend in Total Phosphorus (Fairfax County Lab Data). Station 9. Potomac mainstem.

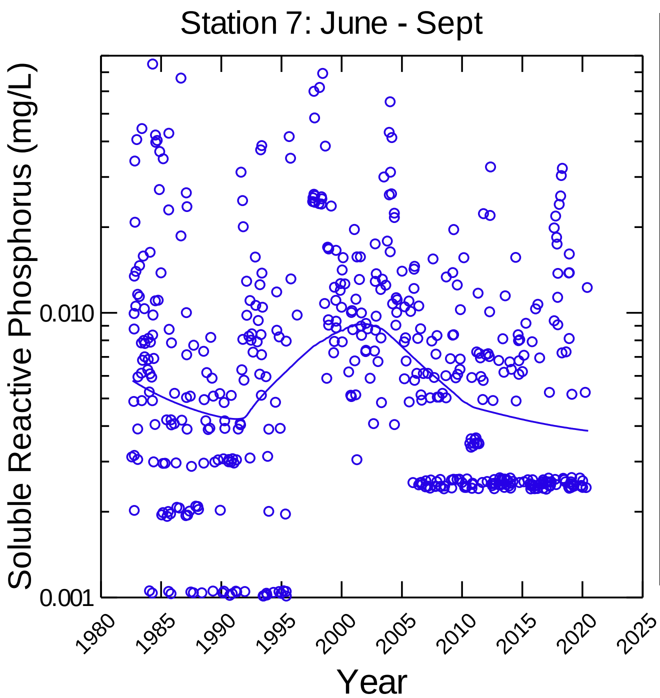

Soluble reactive phosphorus (SRP) declined in the cove during the first few years of the long-term data set, but demonstrated an increase to near its initial level by 2000 (Figure 106). Since then a decline has ensued. (Table 15). One possibility is that less SRP is entering the cove water; another is that increased SAV is taking more up. Note also that the detection limit has changed and that many readings are at the detection limit making trend analysis difficult and uncertain.

Figure 106. Long term trend in Soluble Reactive Phosphorus (Fairfax County Lab Data). Station 7. Gunston Cove.

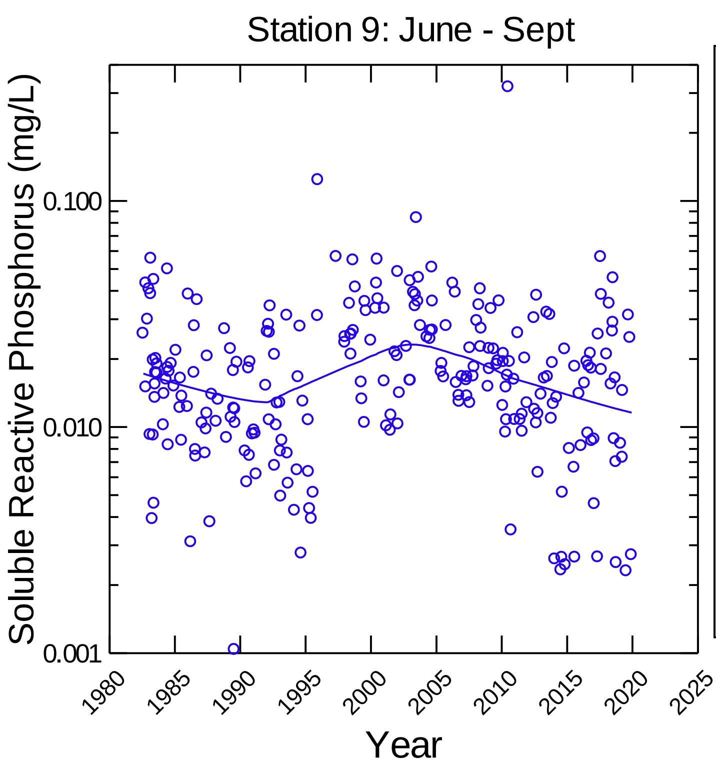

Soluble reactive phosphorus (SRP) in the river has generally been present at higher levels than in the cove, but has undergone a similar decline-resurgence-decline (Figure 107). Linear regression was not significant (Table 15). There were a significant number of non-detect values, but fewer than in the cove.

Figure 107. Long term trend in Soluble Reactive Phosphorus (Fairfax County Lab Data). Station 9. Potomac mainstem.

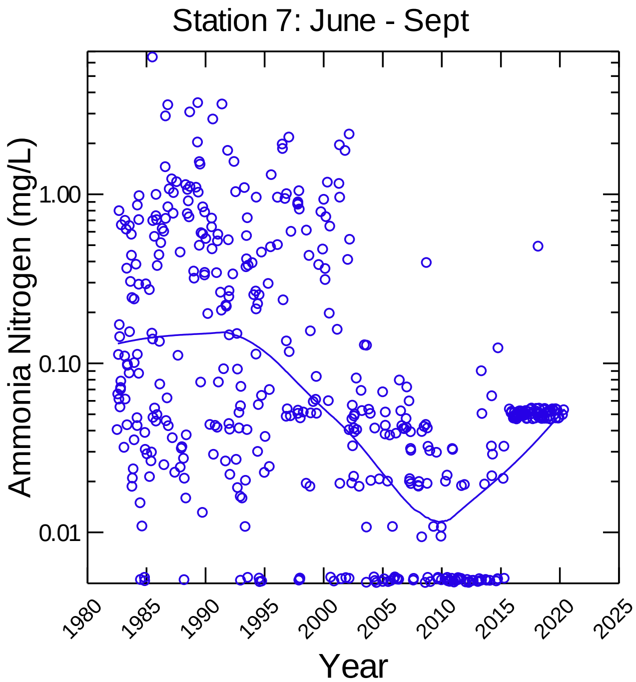

Ammonia nitrogen levels were very variable over the long term study period in the cove, but a trend of decreasing values is evident from the LOWESS trend line (Figure 108). Since 1989 the trend line has decreased from about 0.2 mg/L to about 0.02 mg/L. Linear regression has revealed a significant decline over the entire period of record with a rate of 0.015 mg/L per year yielding a total decline of 0.58 mg/L (Table 15). Note the increase in values below the detection limit over time (clustered at bottom of graph) and then, more recently, an increase in the detection limit to such a level that it is no longer possible to track trends.

Figure 108. Long term trend in Ammonia Nitrogen (Fairfax County Lab Data). Station 7. Gunston Cove.

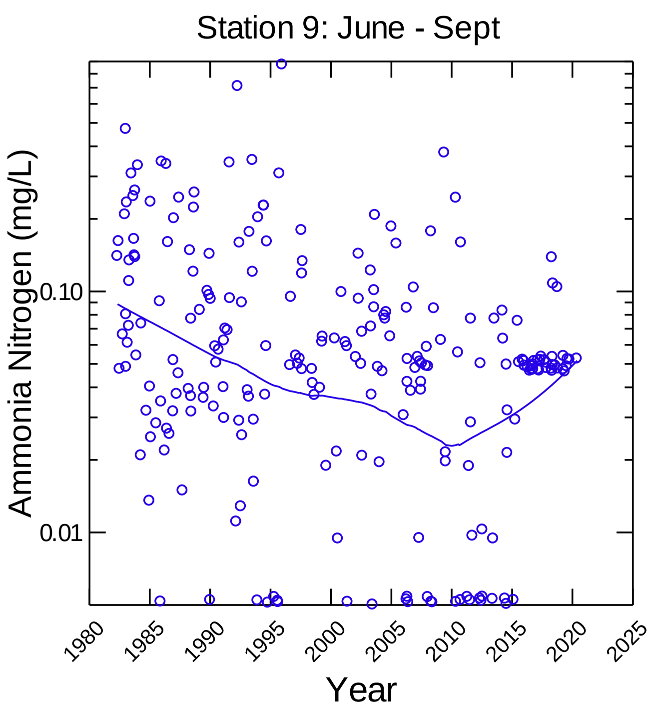

In the river a decreasing trend in ammonia nitrogen has also been observed over most of the study period (Figure 109). Between 1983 and 1999 the trend line dropped from 0.1 mg/L to 0.04 mg/L. Since 1999 it has continued to decline and is now at about 0.02 mg/L. Overall, in the river ammonia nitrogen has demonstrated a significant decline over the study period at a rate of 0.002 mg/L per year or a total of 0.07 over the study period (Table 15). Again, the number of non-detects is increasing and making it impossible to track future trends.

Figure 109. Long term trend in Ammonia Nitrogen (Fairfax County Lab Data). Station 9. Potomac mainstem.

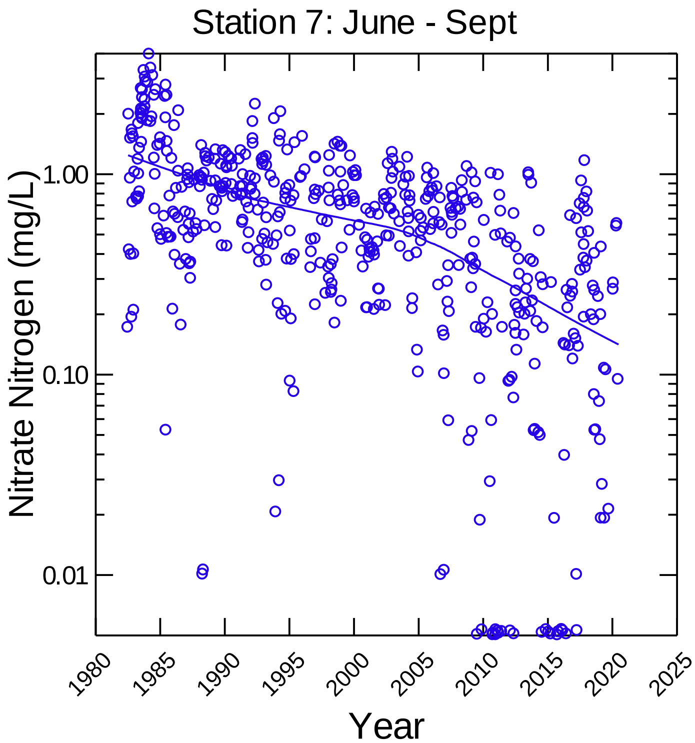

Nitrate nitrogen has demonstrated a steady decline in the cove over the entire period of record (Figure 110). The trend line was at about 1 mg/L in 1983 and by 2020 was below 0.15 mg/L. Linear regression suggested a decline rate of 0.031 mg/L per year yielding a total decline of 1.1 mg/L over the long-term study period (Table 15).

Figure 110. Long term trend in Nitrate Nitrogen (Fairfax County Lab Data). Station 7. Gunston Cove.

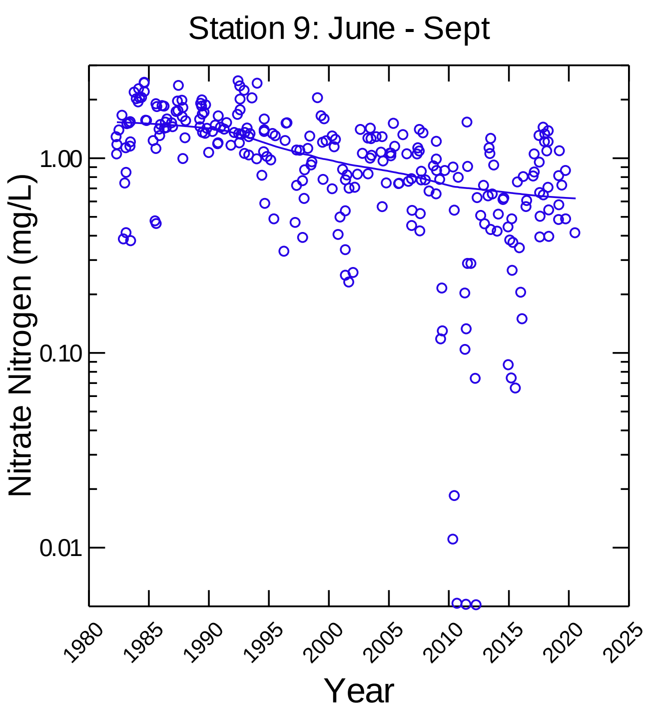

In the river nitrate nitrogen has declined steadily since about 1985 (Figure 111). The trend line dropped from 1.5 mg/L in the mid 1980's to 0.6 mg/L in 2020. Linear regression indicated a rate of decline of 0.031 mg/L per yr which would yielded a 1.1 mg/L decrease in nitrate nitrogen over the study period (Table 15).

Figure 111. Long term trend in Nitrate Nitrogen (Fairfax County Lab Data). Station 9. River mainstem.

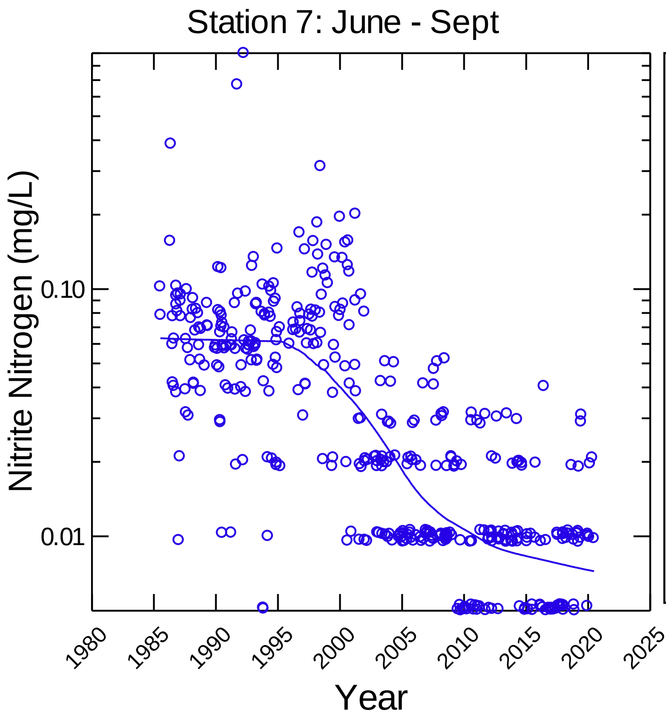

The trend line for nitrite nitrogen indicated steady values at about 0.06-0.07 mg/L through 1999 (Figure 112). Since then there is clear evidence for a decline with the LOWESS line dropping below 0.01 in 2013. Linear regression revealed a significant decline with a slope of 0.003 mg/L per year when the entire period of record was considered (Table 15). Most values in recent years have been at or below the detection limits.

Figure 112. Long term trend in Nitrite Nitrogen (Fairfax County Lab Data). Station 7. Gunston Cove.

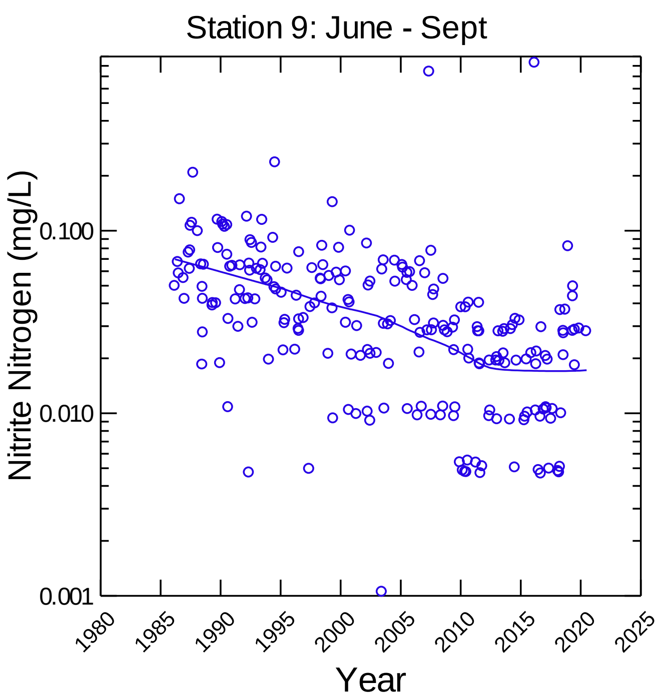

Nitrite nitrogen in the river demonstrated a pattern of decrease during the long term study period (Figure 113). The LOWESS line dropped from 0.07 mg/L in 1986 to less than 0.01 mg/L in 2018. Linear regression indicated a significant linear decline at a rate of 0.001 mg/L per year or 0.03 mg/L over the study period (Table 15).

Figure 113. Long term trend in Nitrite Nitrogen (Fairfax County Lab Data). Station 9. Potomac mainstem.

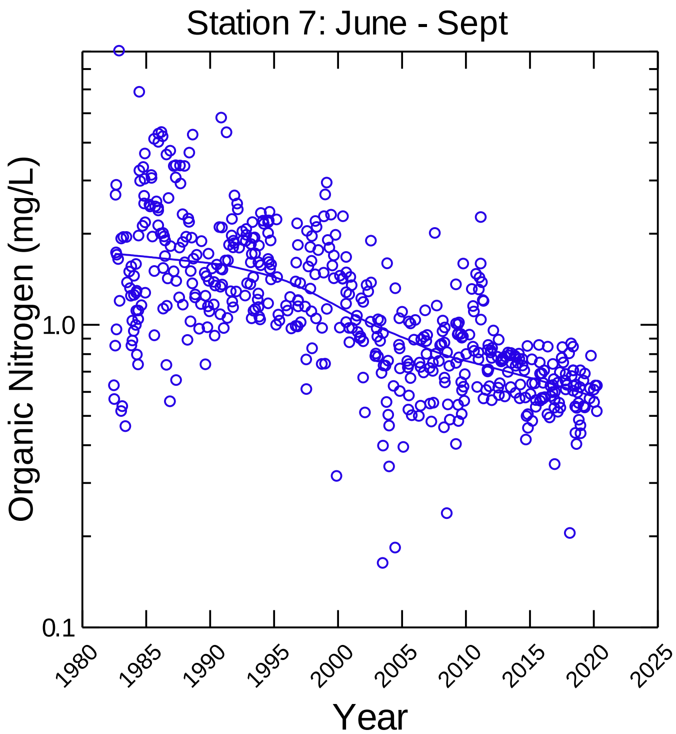

Organic nitrogen in the cove was fairly high in the 1980's and has since undergone a consistent decline through 2020 (Figure 114). In 1983 the trend line was at 1.5 mg/L and dropped below 0.6 mg/L by 2020. Regression analysis indicated a significant decline over the study period at a rate of about 0.044 mg/L per year or a total of 1.6 mg/L over the whole study period (Table 15).

Figure 114. Long term trend in Organic Nitrogen (Fairfax County Lab Data). Station 7. Gunston Cove.

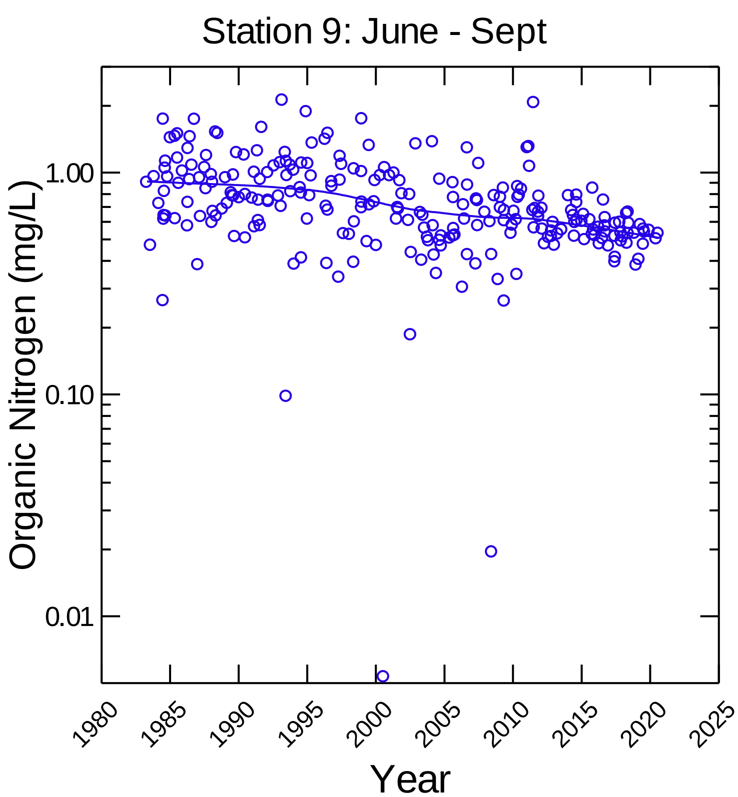

In the river organic nitrogen was steady from 1984 through 1995 and since then has shown perhaps a modest decline (Figure 115). The LOWESS line peaked at about 0.9 mg/L and has dropped to about 0.6 mg/L. Regression analysis indicated a significant linear decline at a rate of 0.01 mg/L when the entire period of record was considered for a total decline of 0.3 mg/L (Table 15).

Figure 115. Long term trend in Organic Nitrogen (Fairfax County Lab Data). Station 9. River mainstem.

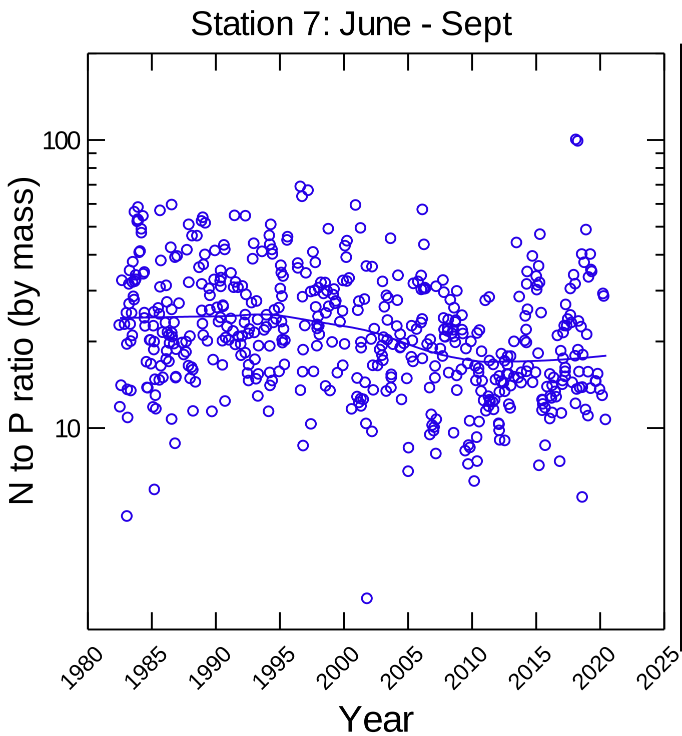

Nitrogen to phosphorus ratio (N/P ratio) in the cove exhibited large variability, but the trend line was flat until about 1995. Since then, there has been a clear decline with the LOWESS line approaching 18 by 2020 (Figure 116). Regression analysis over the period of record indicates a statistically significant decline at a rate of 0.26 per year or about 9 units over the entire period (Table 15). This ratio is calculated using nitrate, TKN, and TP values and is less accurate when any of those are below detection limits.

Figure 116. Long term trend in N to P Ratio (Fairfax County Lab Data). Station 7. Gunston Cove.

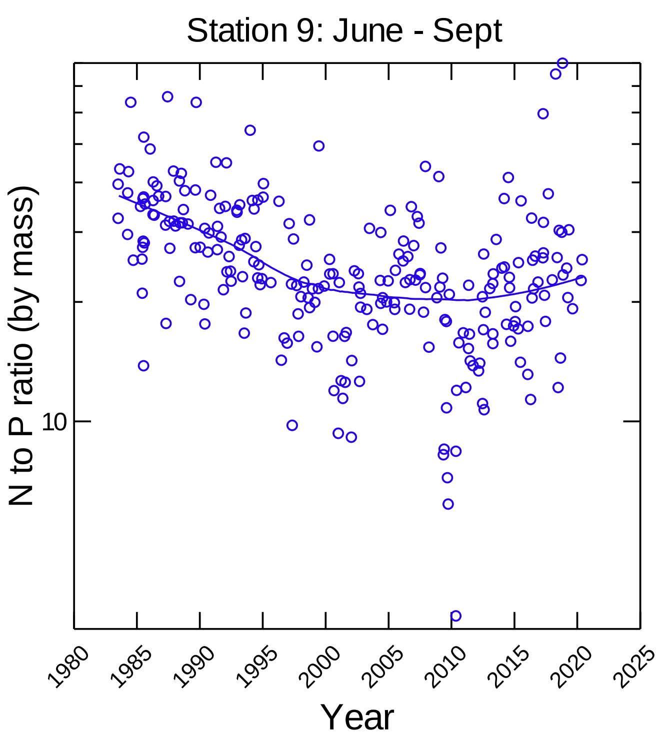

Nitrogen to phosphorus ratio in the river exhibited a strong continuous decline through about 2000 and has declined more slowly since then (Figure 117). The LOWESS trend line declined from about 35 in 1984 to 20 in 2010 before rising in the last decade. Linear regression analysis confirmed this decline and suggested a rate of 0.35 units per year or a total of 12 units over the long term study period (Table 15).

Figure 117. Long term trend in N to P Ratio (Fairfax County Lab Data). Station 9. River mainstem.

C. Phytoplankton Trends: 1984-2020

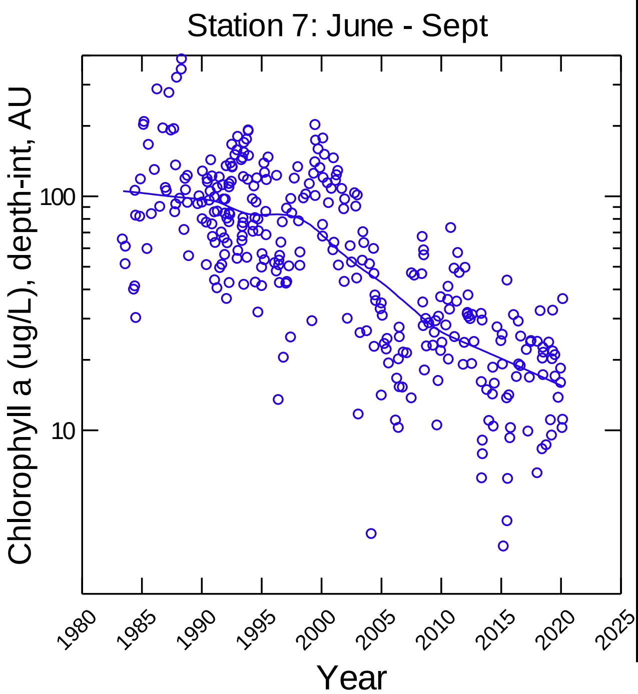

After increasing through much of the 1980's, depth-integrated chlorophyll *a* in the cove demonstrated a gradual decline from 1988 to 2000 and a much stronger decrease since then (Figure 118). The LOWESS line has declined from about 100 µg/L to about 15 µg/L in 2020. The observed decrease has resulted in chlorophyll values within the range of water clarity criteria allowing SAV growth to 0.5 m and 1.0 m (43 µg/L and 11 µg/L, respectively) (CBP 2006). This would imply adequate light to support SAV growth over much of Gunston Cove. Regression analysis has revealed a clear linear trend of decreasing values at the rate of 3.6 µg/L per year or 130 µg/L over the 35-year long term data set (Table 14).

Figure 118. Long term trend in Depth-integrated Chlorophyll *a* (GMU Lab Data). Station 7. Gunston Cove.

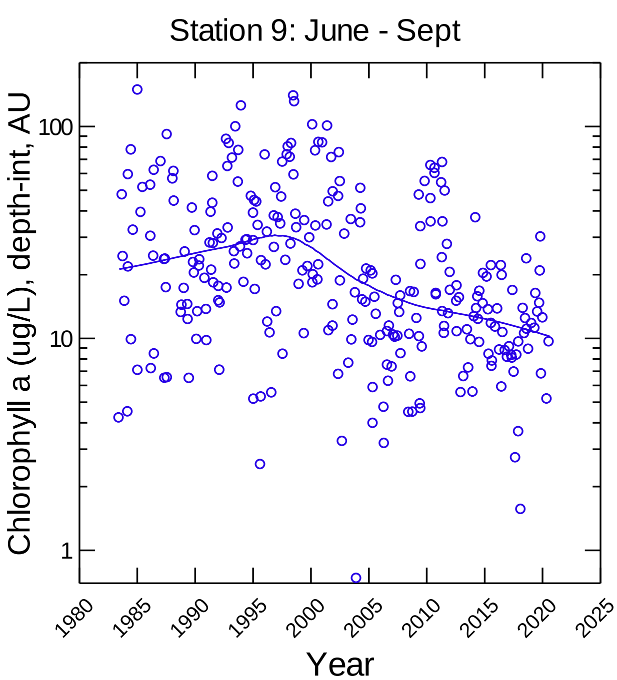

In the river depth-integrated chlorophyll *a* increased gradually through 2000 with the trend line rising from 20 to 30 µg/L (Figure 119). This was followed by a strong decline reaching about 10 µg/L by 2020. Regression analysis revealed a significant linear decline at a rate of 0.78 µg/L/yr when the entire period is considered (Table 14) yielding a total decline of about 28 ug/L.

Figure 119. Long term trend in Depth-integrated Chlorophyll *a* (GMU Lab Data). Station 9. River mainstem.

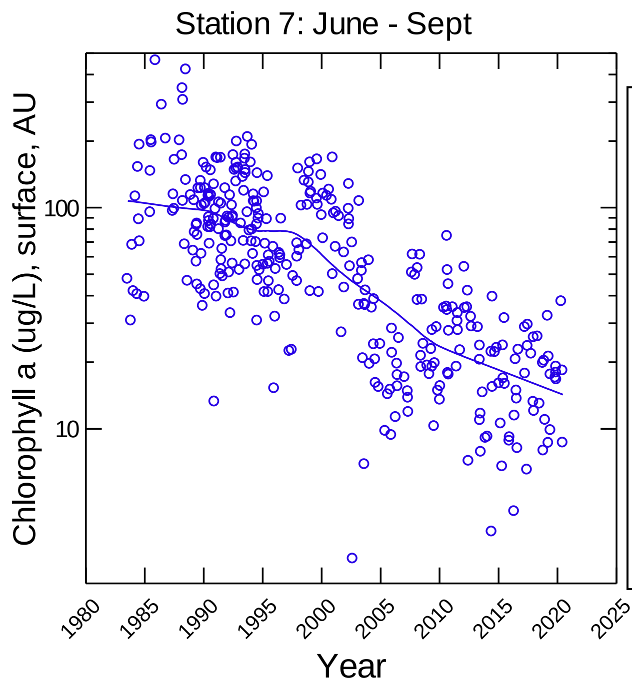

Surface chlorophyll *a* in the cove also exhibited a clear decline over the long-term study period, especially since 2000 (Figure 120). Trend line values of about 100 µg/L in 1988 dropped to less than 15 µg/L in 2020. Linear regression confirmed the linear decline and suggested a rate of 3.6 µg/L per year or 130 µg/L over the entire study (Table 16).

Figure 120. Long term trend in Surface Chlorophyll *a* (GMU Data). Station 7. Gunston Cove.

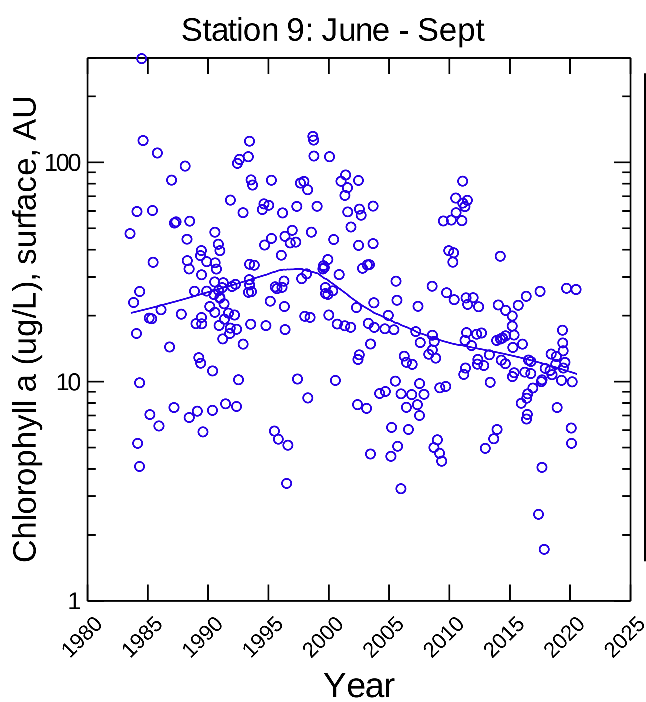

In the river the LOWESS line for surface chlorophyll *a* increased slowly from 1983 to 2000 and then declined markedly through 2020 (Figure 121). Values have stabilized since then at about 12 µg/L. Linear regression revealed a significant decline in surface chlorophyll across this period with a rate of 0.86 µg/L/yr or about 30 µg/L over the whole period (Table 16).

Figure 121. Long term trend in Surface Chlorophyll *a* (GMU Data). Station 9. River mainstem.

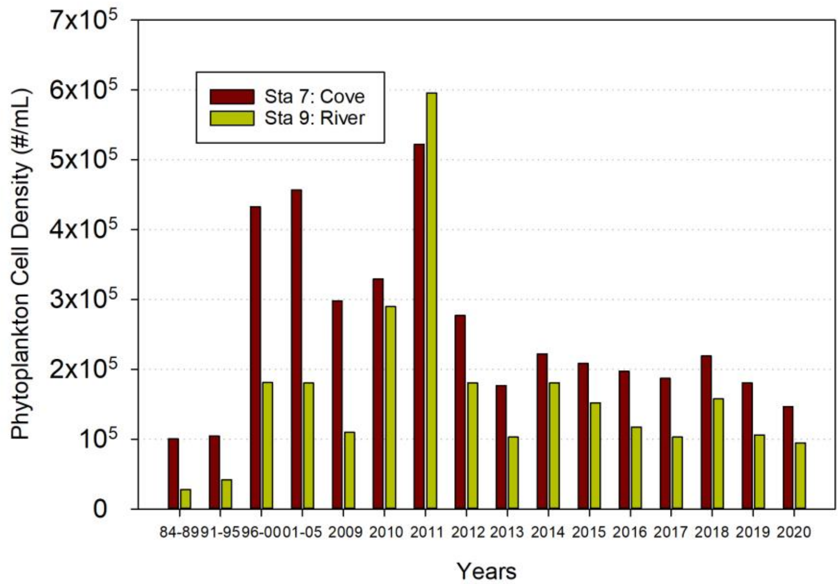

Phytoplankton cell density in both the cove and the river in 2020 was similar to values observed since 2012 (Figure 122). While cell density does not incorporate cell size, it does provide some measure of the abundance of phytoplankton and reflects the continuing decrease in phytoplankton in the study area which is expected with lower nutrient loading and should help improve water clarity.

Figure 122. Interannual Comparison of Phytoplankton Density by Region.

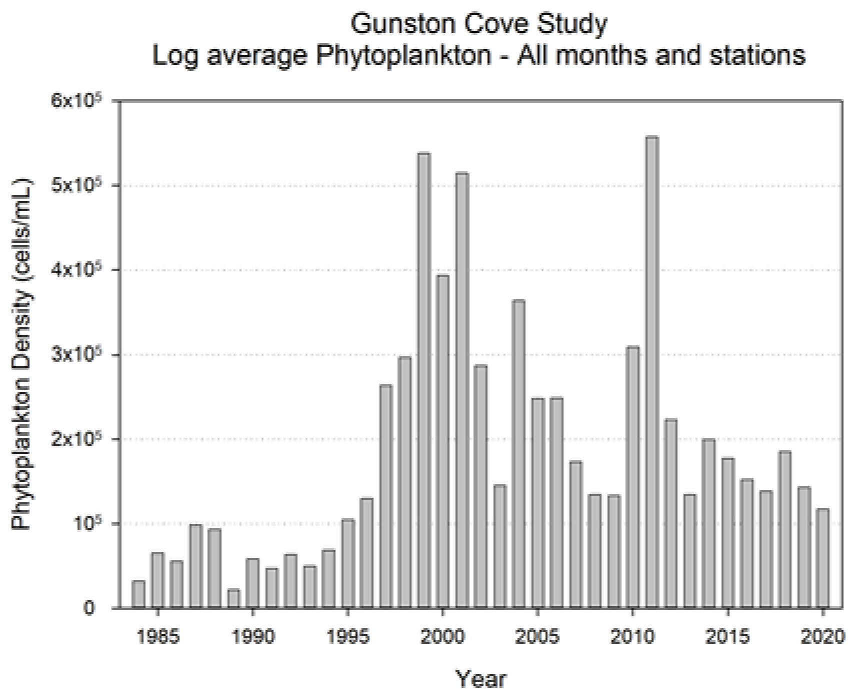

By looking at individual years (Figure 123), we see that phytoplankton densities in 2020 remained lower than the high levels observed during the 1995 to 2005 period and were among the lowest observed in any year since 1997.

Figure 123. Interannual Trend in Average Phytoplankton Density.

D. Zooplankton Trends: 1990-2020

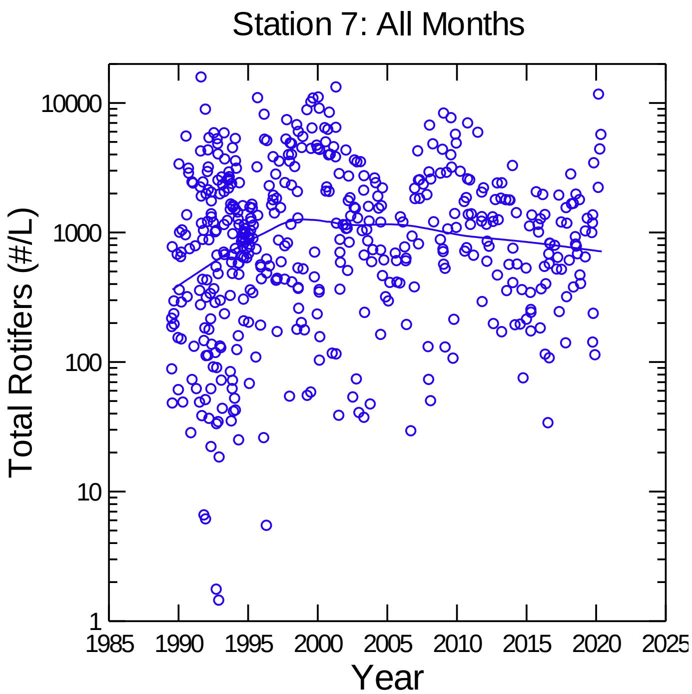

In the Cove total rotifers continued to exhibit a slow decline after an initial decade (1990-2000) of steady increase (Figure 124). The LOWESS fit line indicated about 600/L in 2020, up from about 400/L in 1990. Linear regression analysis continued to indicate a statistically significant linear increase in total rotifers over the period since 1990 (Table 16), but it is becoming more tenuous.

Figure 124. Long term trend in Total Rotifers. Station 7. Gunston Cove.

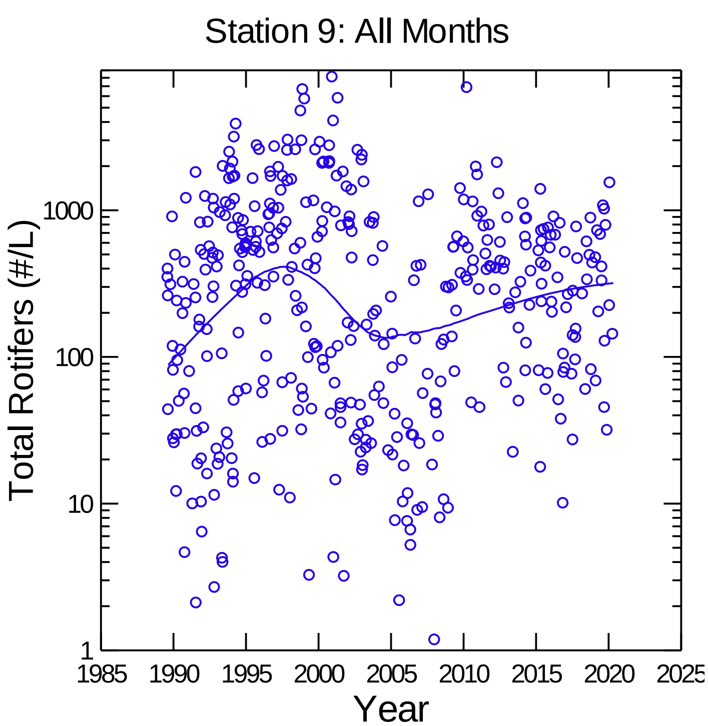

In the Potomac mainstem, rotifers exhibited an initial increase from 1990 to 1998, followed by a decline from 1999 to 2005 and more recently another increase (Figure 125). Trend line values in 1990 were about 80/L and as of 2020 are about 300/L approaching 1998 values. However, when the entire 1990-2018 period was considered, total rotifers did not exhibit a significant linear trend in the river (Table 16).

Figure 125. Long term trend in Total Rotifers. Station 9. River mainstem.

Table 16
Correlation and Linear Regression Coefficients
Zooplankton Parameters vs. Year for 1990-2020
All Nonzero Values Used, All Values Logged to Base 10

	Station 7			Station 9		
Parameter	Corr. Coeff.	Reg. Coeff.	Signif.	Corr. Coeff.	Reg. Coeff.	Signif.
Asplanchna (m)	0.057 (341)	---	---	0.022 (205)	---	---
Brachionus (m)	0.085 (470)	---	---	0.069 (393)	---	---
Conochilidae (m)	0.062 (408)	---	---	0.104 (328)	---	---
Filinia (m)	0.102 (412)	0.010	0.039	0.156 (292)	-0.012	0.008
Keratella (m)	0.264 (480)	0.022	<0.001	0.112 (405)	0.010	0.024
Polyarthra (m)	0.098 (462)	0.008	0.036	0.006 (374)	---	---
Total Rotifers (m)	0.114 (498)	0.008	0.011	0.037 (418)	---	---
Bosmina (m)	0.099 (293)	---	---	0.093 (339)	---	---
Diaphanosoma (M)	0.254 (395)	-0.036	<0.001	0.260 (302)	-0.030	<0.001
Daphnia (M)	0.150 (311)	-0.017	0.008	0.158 (211)	-0.014	0.021
Chydorid cladocera (M)	0.027 (279)	---	---	0.018 (202)	---	---
Leptodora (M)	0.316 (235)	-0.034	<0.001	0.368 (174)	-0.035	<0.001
Copepod nauplii (m)	0.392 (477)	0.024	<0.001	0.184 (414)	0.014	<0.001
Calanoid copepods (M)	0.216 (563)	-0.023	<0.001	0.085 (437)	---	---
Cyclopoid copepods (M)	0.098 (524)	-0.011	0.025	0.087 (423)	---	---
Adult and copepodid copepods (M)	0.141 (593)	-0.014	<0.001	0.078 (458)	---	---

n values (# of non-zero data points) are shown in Corr. Coeff. column in parentheses. Number of total samples indicated in headings.
Significance column indicates the probability that a correlation coefficient this large could be due to chance alone. If this probability is greater than 0.05, then NS (not significant) is indicated. * = marginally significant. M indicates species was quantified from macrozooplankton samples; m indicates quantification from microzooplankton samples.

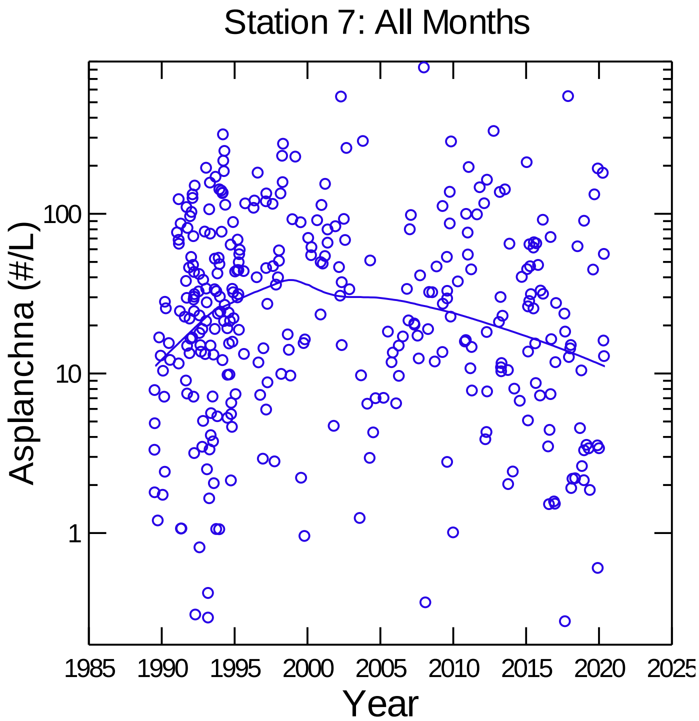

Asplanchna has shown a similar trend as total rotifers at a much lower abundance level (Figure 126). The LOWESS line increased in the 1990's, but has sinced decreased to near initial levels of about 10/L in 2020. No linear trend was found over the study period (Table 16).

Photo credit: Laura Birsa

Figure 126. Long term trend in *Asplanchna*. Station 7. Gunston Cove.

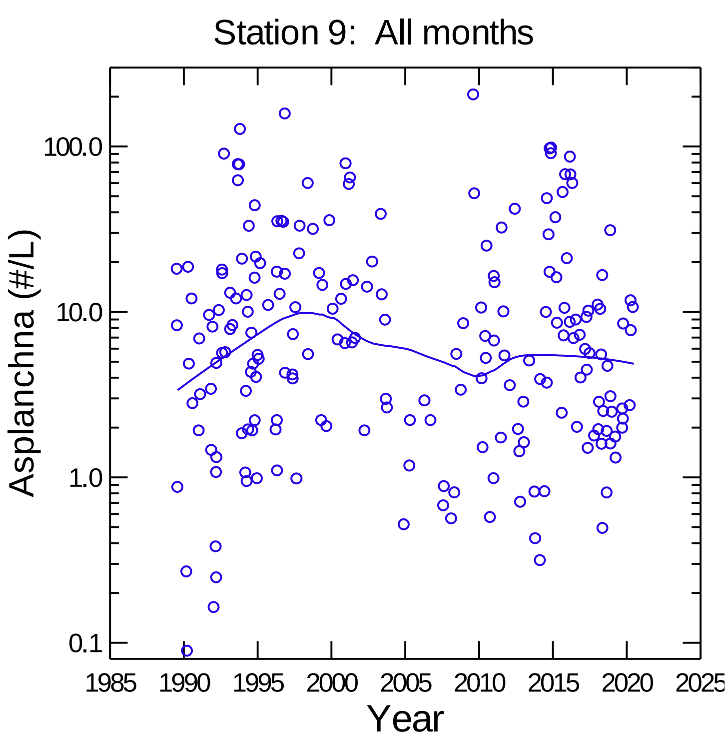

Asplanchna was found at lower densities in the river and the trend line was at about 5/L in 2020 (Figure 127). No linear trend was indicated when the entire study period was considered (Table 16).

Figure 127. Long term trend in *Asplanchna*. Station 9. River mainstem.

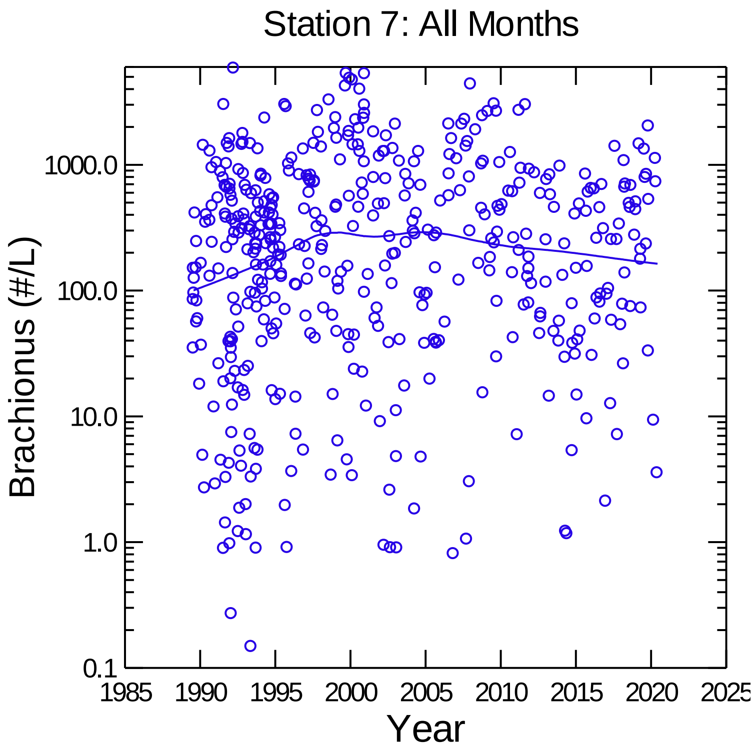

Figure 128. Long term trend in *Brachionus*. Station 7. Gunston Cove.

Brachionus is the dominant rotifer in Gunston Cove and the trends in total rotifers are generally mirrored in those in *Brachionus* (Figure 128). The LOWESS line for *Brachionus* suggested about 200/L in 2020, about twice what was found in 1990. No linear trend was found over the study period (Table 16).

Photo credit: Laura Birsa

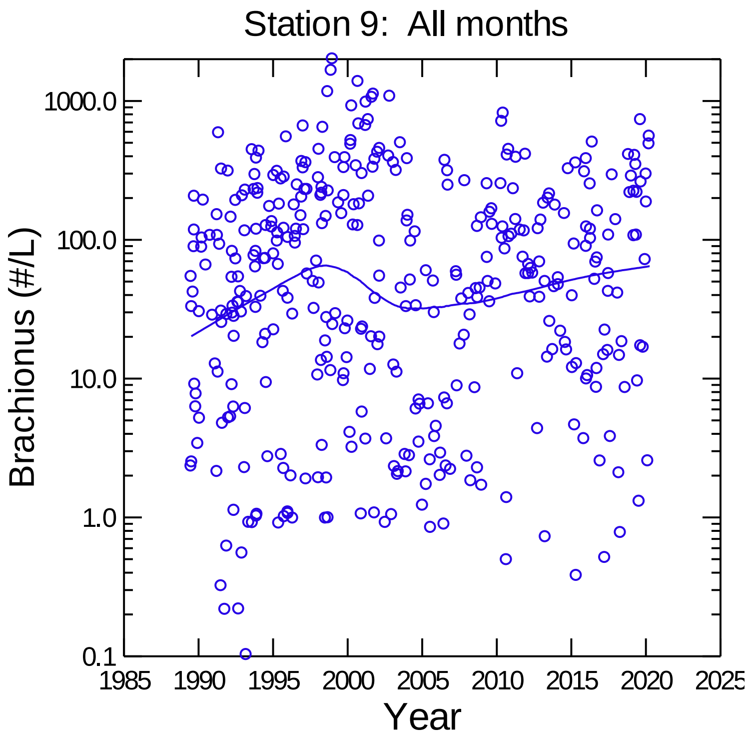

Figure 129. Long term trend in *Brachionus*. Station 9. River mainstem.

Brachionus was found at lower densities in the river. In the river the LOWESS line for *Brachionus* increased through 2000, but dropped markedly from 2000-2005. Since 2005 a steady increase has been noted with the trend line reaching about 60/L in 2020 (Figure 129). No linear trend was indicated when the entire study period was considered (Table 16).

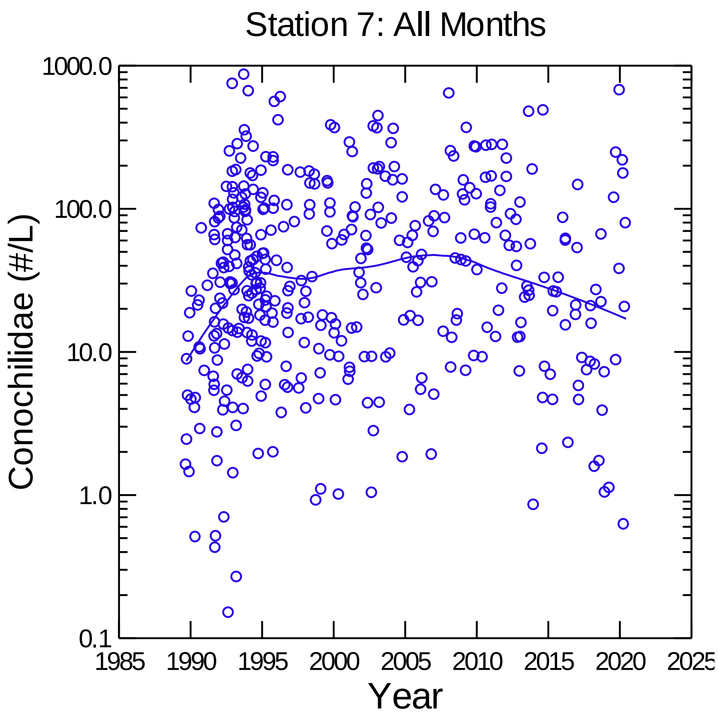

Conochilidae increased strongly from 1990-1995 and since then has leveled off. In 2020 the LOWESS trend line stood at about 18/L (Figure 130). This was well above levels of about 9/L in 1990. Over the entire period of record, there was not a significant linear increase (Table 16).

Photo credit: Laura Birsa

Figure 130. Long term trend in Conochilidae. Station 7. Gunston Cove.

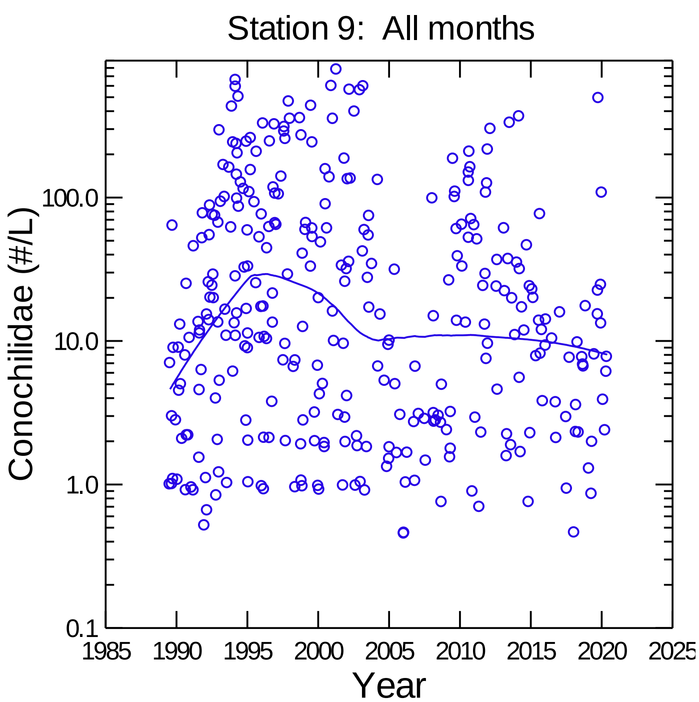

In the river, Conochilidae exhibited a strong increase in the early 1990's similar to that observed in the cove (Figure 131). This was followed by a period of decline and recently a constant value. The trend line has gone from 3/L in 1990 to 30/L in 1995 to about 9/L in 2020. When the entire period of record was examined, no linear trend was found (Table 16).

Figure 131. Long term trend in Conochilidae. Station 9. River mainstem.

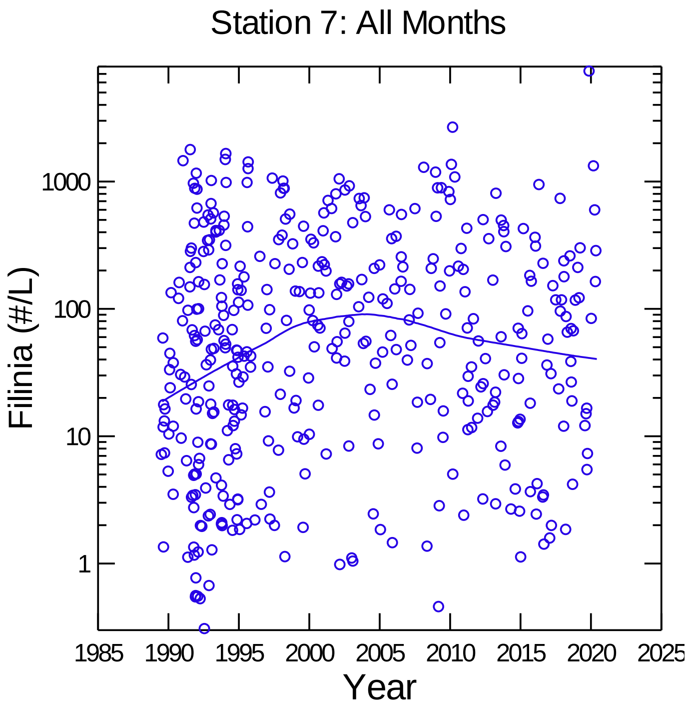

In the cove *Filinia* exhibited a steady increase from 1990 through 2000 rising from about 20/L to nearly 100/L (Figure 132). It has shown a gradual decline in recent years to about 40/L in 2020. When the entire period of record was considered, there is evidence for a linear increase in the cove and in fact one very high reading 7000/L was observed in 2020 (Table 16).

Photo credit: Laura Birsa

Figure 132. Long term trend in *Filinia*. Station 7. Gunston Cove.

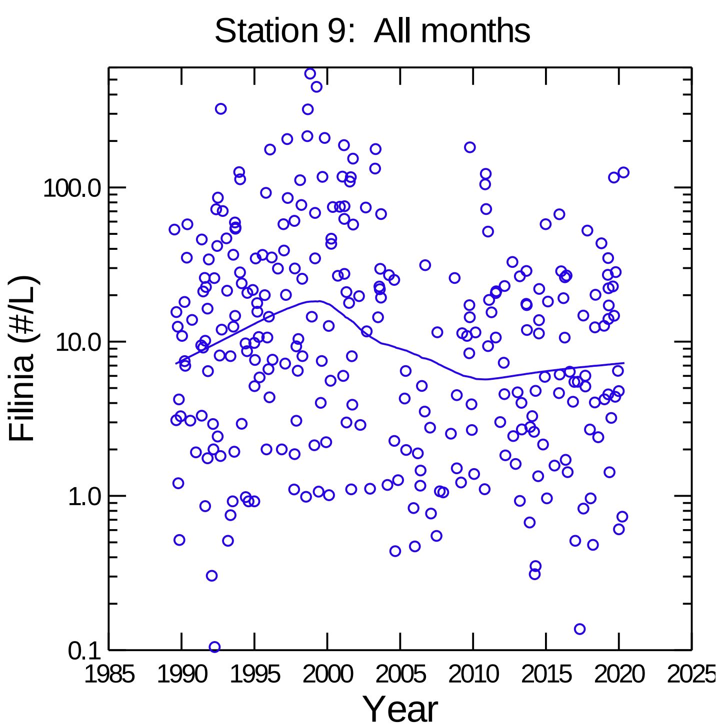

In the river *Filinia* demonstrated an increase through about 2001, declined from 2001-2010 and remained steady since. The trend line indicates about 7/L in 2020, about equal to the 7/L in 1990, but well below the peak of 20/L in 2000 (Figure 133). When the entire period of record was examined, there was a significant negative linear trend (Table 16).

Figure 133. Long term trend in *Filinia*. Station 9. River mainstem.

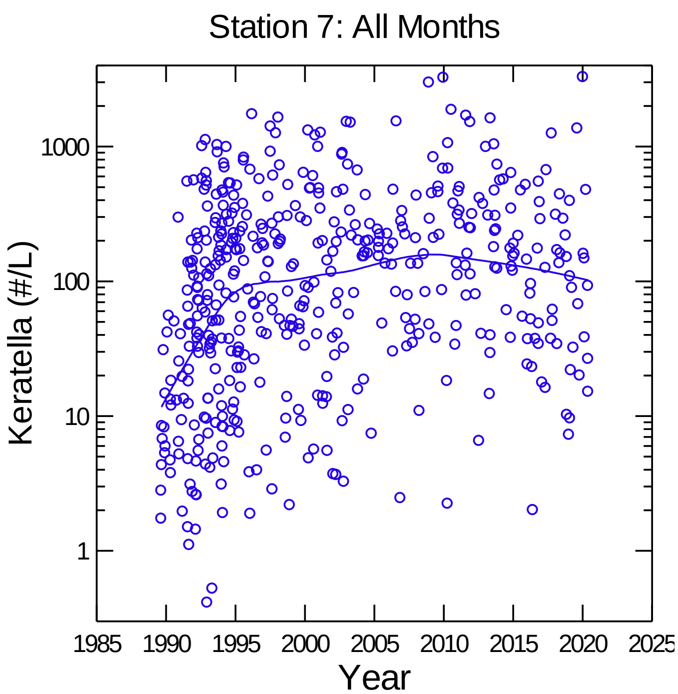

Keratella increased strongly from 1990 to 1995 and has shown a milder increase since then and most recently a slight decline with the trend line approaching 100/L in 2020 (Figure 134). When the entire period of record was examined, there was a significant linear increase (Table 16).

Figure 134. Long term trend in *Keratella*. Station 7. Gunston Cove.

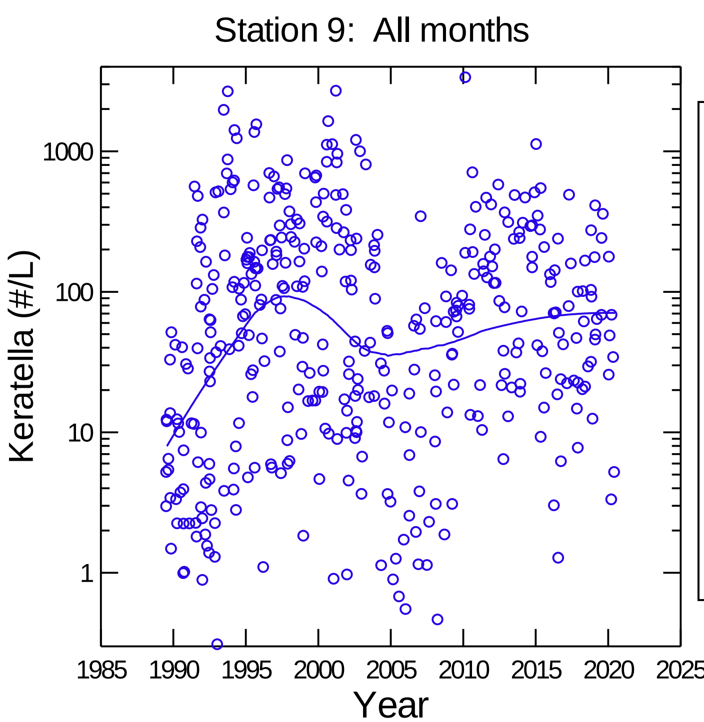

In the river *Keratella* increased from less than 10/L in 1990 to peak values of about 100/L in the mid to late 1990's (Figure 135). The trend line then declined to about 25/L, but since 2005 it has increased reaching about 80/L in 2020. Linear regression showed evidence of a linear increase when the entire study period was considered (Table 16).

Figure 135. Long term trend in *Keratella*. Station 9. River mainstem.

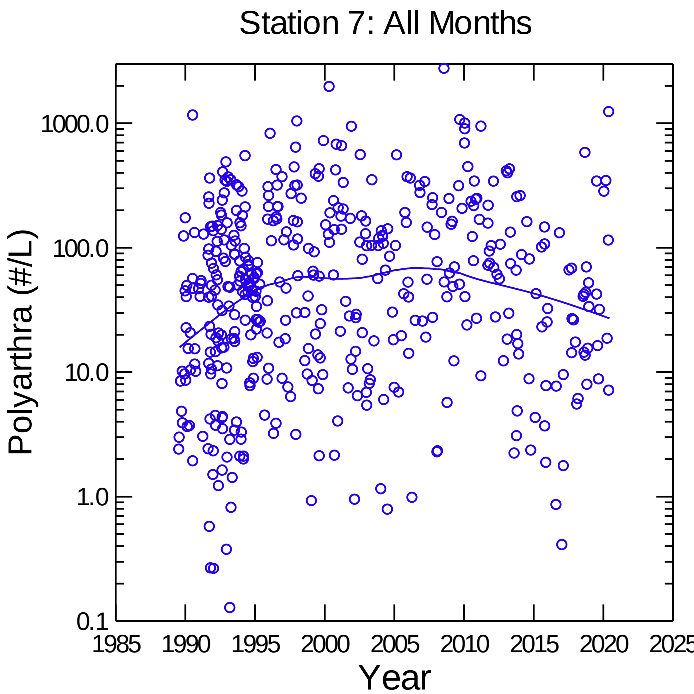

The trend line for *Polyarthra* in the cove increased steadily from 1990 to about 2000 rising from 15/L to about 60/L (Figure 136). Since 2000 densities have increased more slowly and now are dropping again reaching 25/L by 2020. Regression analysis indicated a significant linear increase when the entire period of record was examined (Table 16).

Figure 136. Long term trend in *Polyarthra*. Station 7. Gunston Cove.

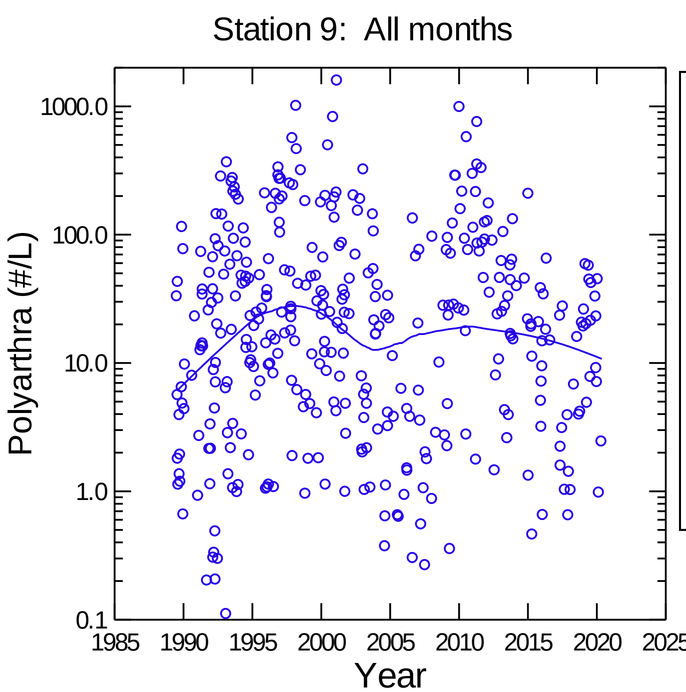

In the river *Polyarthra* showed a marked increase from 1990 to 2000 and then a decline to 2005. By 2020 the trend line approached 10/L (Figure 137). Linear regression analysis indicated a marginally significant positive trend over the period of record (Table 16).

Figure 137. Long term trend in *Polyarthra*. Station 9. River mainstem.

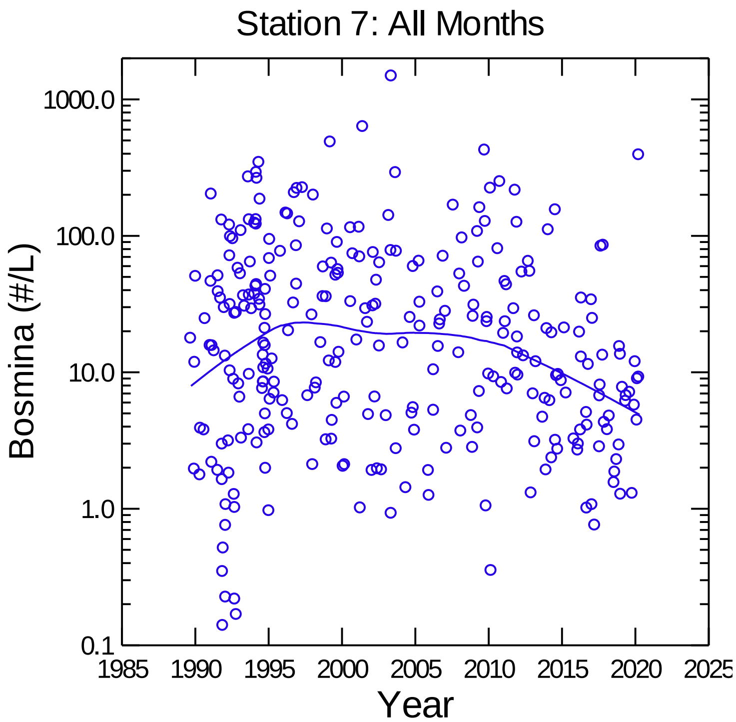

The trend line for *Bosmina* in the cove showed an increase from 8/L in 1990 to about 20/L in 2000 (Figure 138). Since 2000 densities have declined reaching about 5/L in 2020. Linear regression did not indicate a significant trend in the cove over the entire period of record (Table 16).

Figure 138. Long term trend in *Bosmina*. Station 7. Gunston Cove.

Photo credit: Laura Birsa

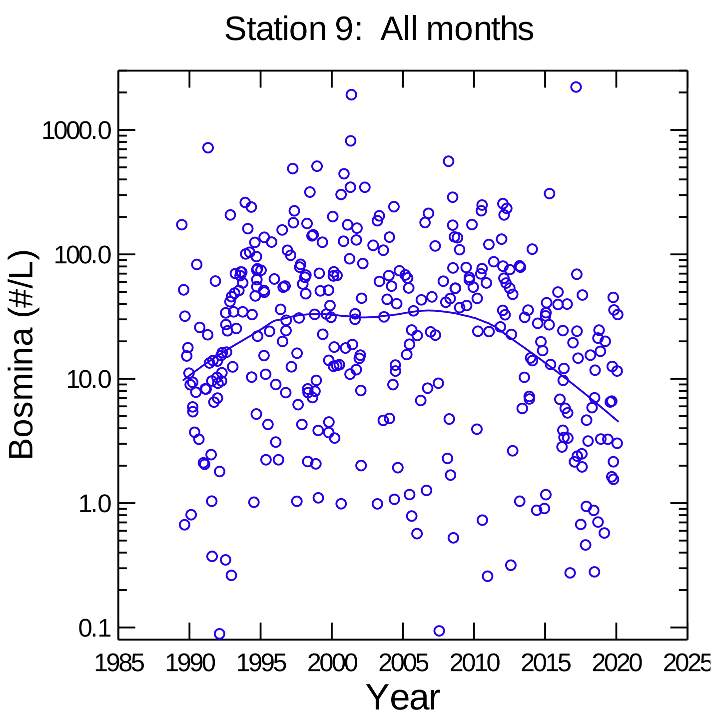

In the river mainstem the LOWESS curve for *Bosmina* increased from 1990 to 1995, and remained rather constant from 1995 to 2010 at about 30/L (Figure 139). Recently, it has declined markedly to about 4/L in 2020. Regression analysis did not indicate a significant linear trend over the entire period of record (Table 16).

Figure 139. Long term trend in *Bosmina*. Station 9. River mainstem.

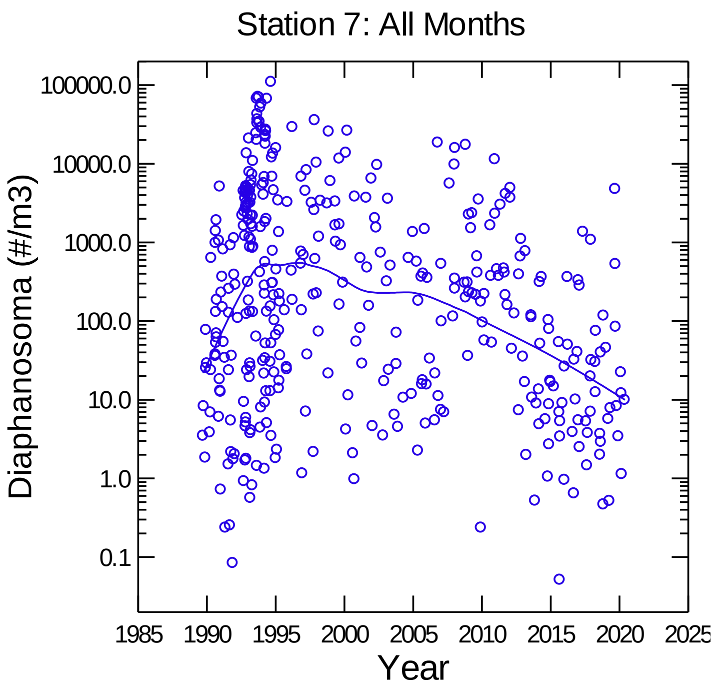

Diaphanosoma increased strongly in the early 1990s from about 12/m^3 nearly 1000/m^3. It gradually declined and by 2020 the trend line was nearing 10/m^3 (Figure 140). Linear regression analysis of the entire period of record indicated a significant decline (Table 16).

Photo credit: Laura Birsa

Figure 140. Long term trend in *Diaphanosoma*. Station 7. Gunston Cove.

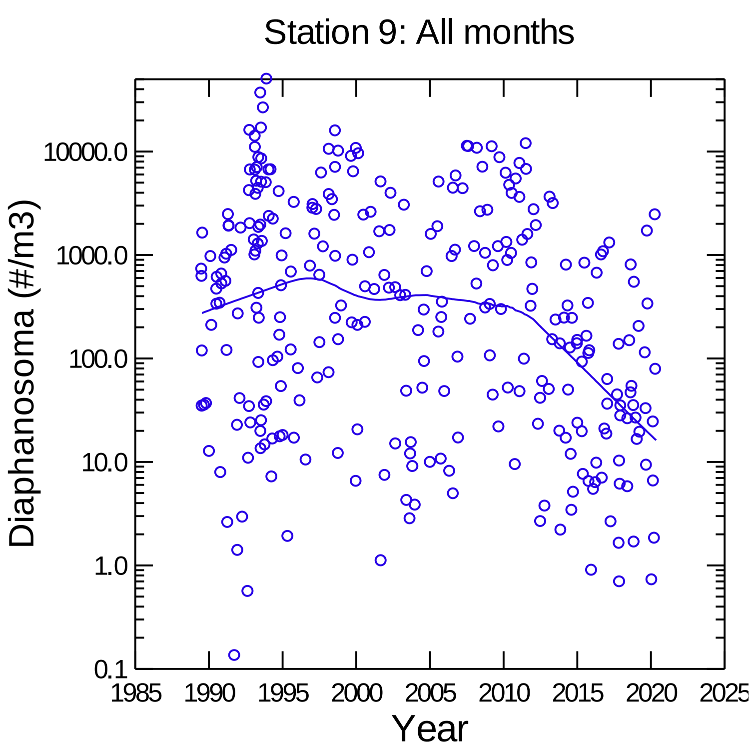

In the river the LOWESS line suggested a generally stable pattern in *Diaphanosoma* until 2010 until a decline set in (Figure 141). The trend line value of 20/m^3 found in 2020 compared with values as high as 600/m^3 in 1999. Regression analysis indicated significant declining trend over the period of record (Table 16).

Figure 141. Long term trend in *Diaphanosoma*. Station 9. River mainstem.

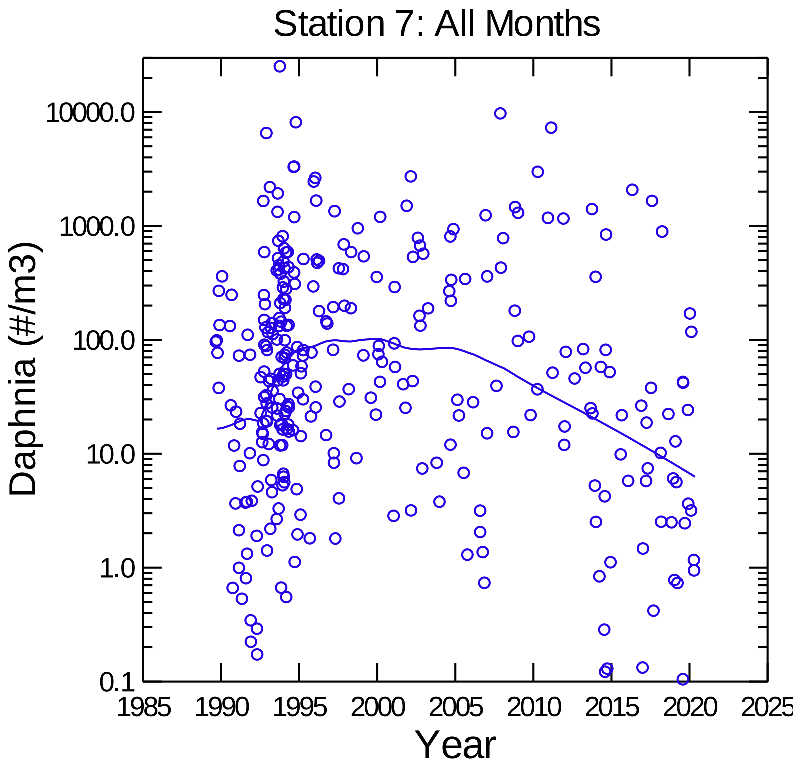

Figure 142. Long term trend in *Daphnia*. Station 7. Gunston Cove.

Daphnia in the cove has declined slowly since 1995 from about 100/m^3 to 5/m^3 in 2020 (Figure 142). Regression analysis examining the entire period of record showed a significant decline (Table 16).

Photo credit: Laura Birsa

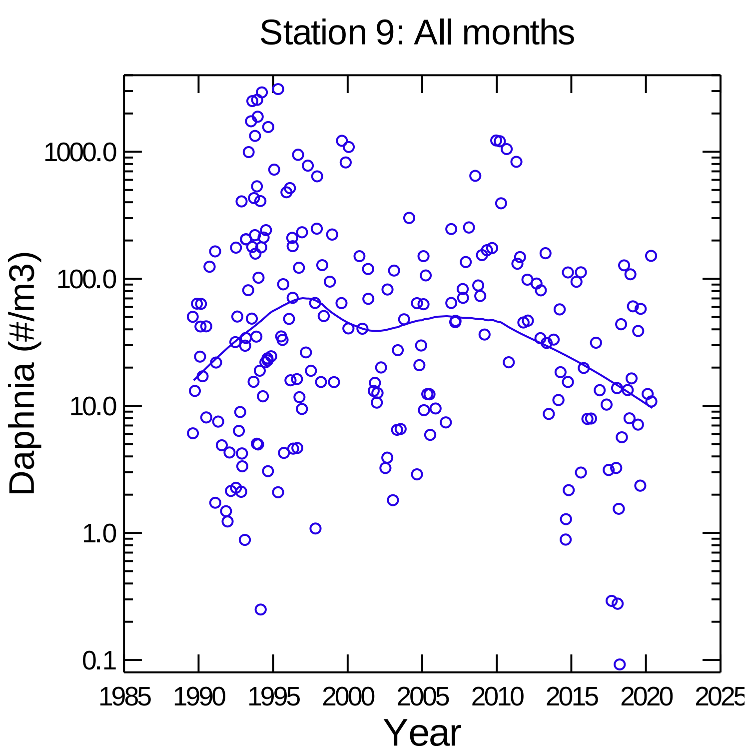

Figure 143. Long term trend in *Daphnia*. Station 9. River mainstem.

Daphnia in the river increased early on, but has since declined slightly (Figure 143). The trend line in 2020 dropped to 10/m^3, even lower than the level observed at the beginning of the record in 1990. Regression analysis indicated a significant negative trend over the study period (Table 16).

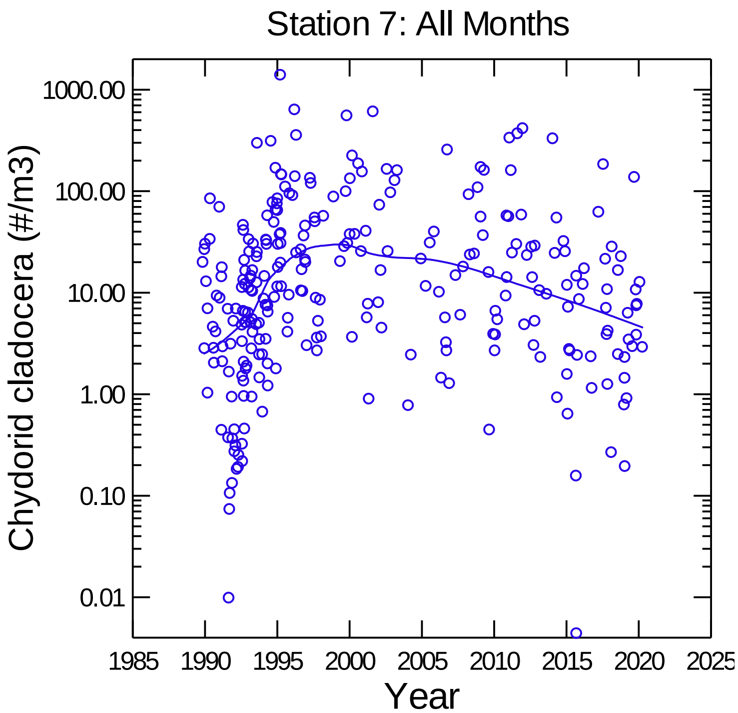

Chydorid cladocera in the cove have increased in the 1990's, but have undergone a slow and consistent decline since that time and 2020 values are near those of 1990 (Figure 144). Regression analysis did not show a significant linear temporal trend (Table 16).

Photo credit: Laura Birsa

Figure 144. Long term trend in Chydorid Cladocera. Station 7. Gunston Cove.

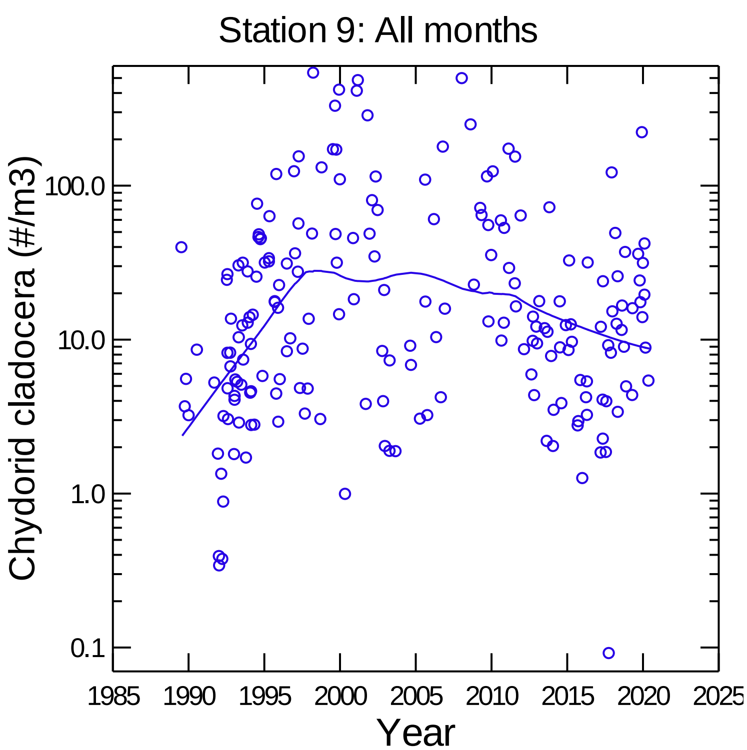

In the river chydorids continued a decrease to about 9/m^3 in 2020, slightly above the low of about 2/m^3 in the early 1990's (Figure 145). There was no evidence for a significant linear trend (Table 16).

Figure 145. Long term trend in Chydorid Cladocera. Station 9. River mainstem.

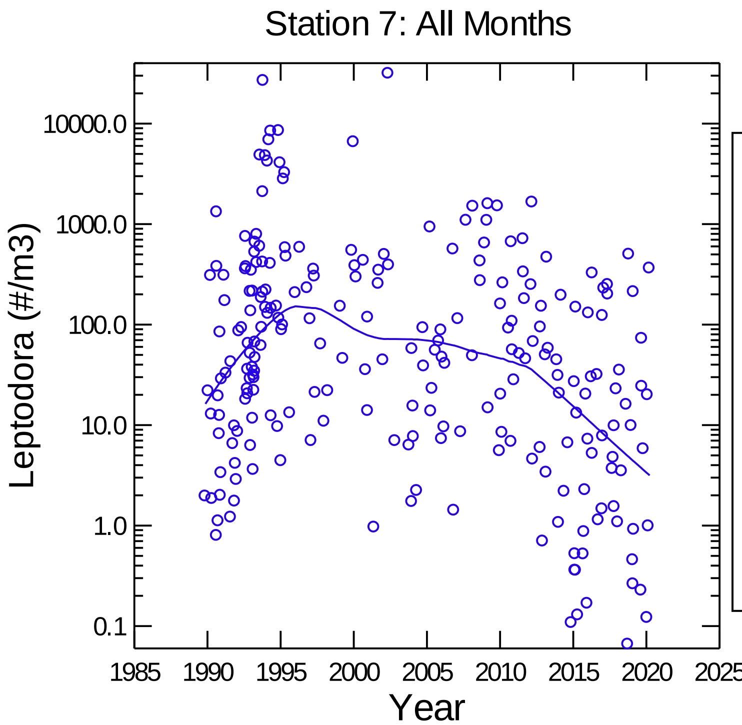

In the cove the trend line for *Leptodora*, the large predaceous cladoceran, has gradually decreased since 1995 and in 2020 reached about 3/m^3, down from its high of about 150/m^3 in 1994 (Figure 146). There was evidence for a significant negative linear trend in *Leptodora* over the entire study period (Table 16).

Figure 146. Long term trend in *Leptodora*. Station 7. Gunston Cove.

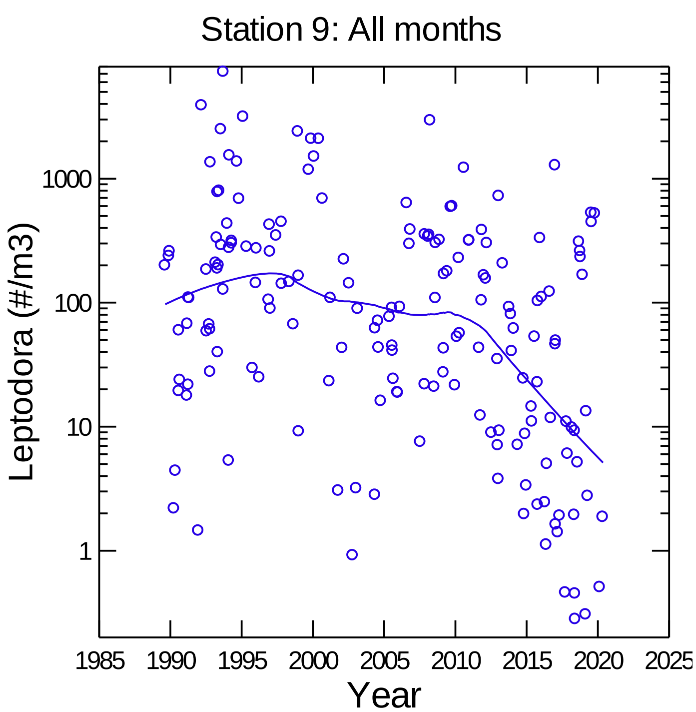

In the river, *Leptodora* densities continued a general decline which began in 1995 resulting in trend line values of about 5/m^3 for 2020 (Figure 147). These values are well below the peak of 200/m^3 in 1994. Interestingly, four data points in 2020 were well above the trend line. Linear regression analysis detected a significant negative linear trend when the whole study period was considered (Table 16).

Figure 147. Long term trend in *Leptodora*. Station 9. River mainstem.

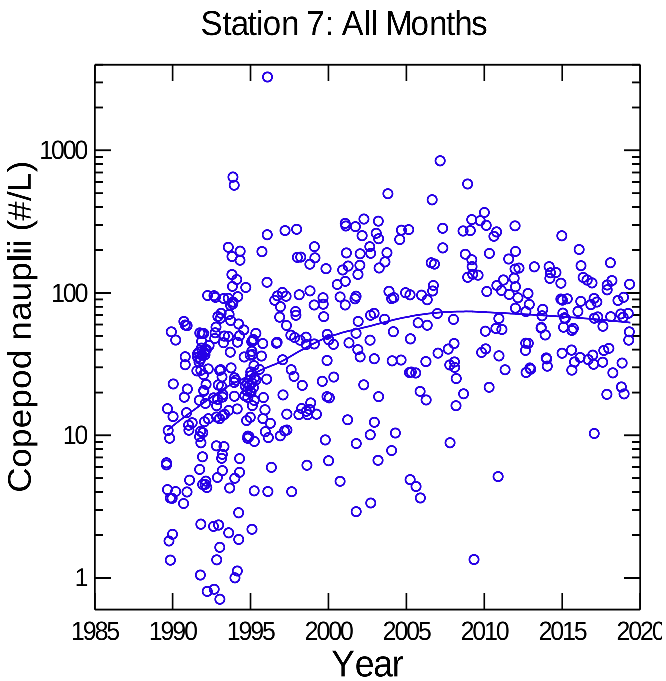

Copepod nauplii, the immature stages of copepods, have shown a positive trend since inception, but it is now leveling at about 70/L as of 2020 (Figure 148). These values are well above the initial values of about 10/L in 1990. A strong linear increase was observed over the study period (Table 16).

Photo credit: Laura Birsa

Figure 148. Long term trend in Copepod Nauplii. Station 7. Gunston Cove.

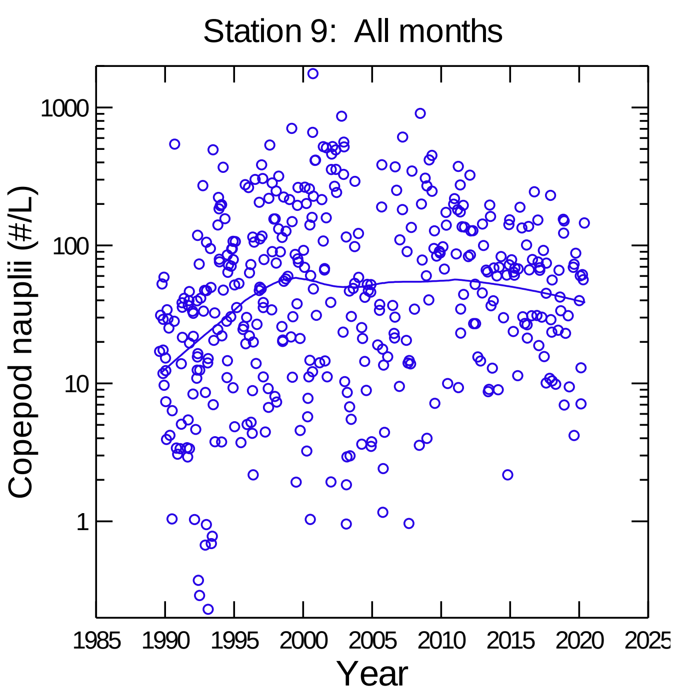

In the river, copepod nauplii showed a a similar leveling of an upward trend (Figure 149). The 2020 LOWESS trend line value was about 40/L, up from an initial value of 10/L in 1990, similar to the previous peak. A significant linear increase was found for nauplii in the river over the study period (Table 16).

Figure 149. Long term trend in Copepod Nauplii. Station 9. River mainstem.

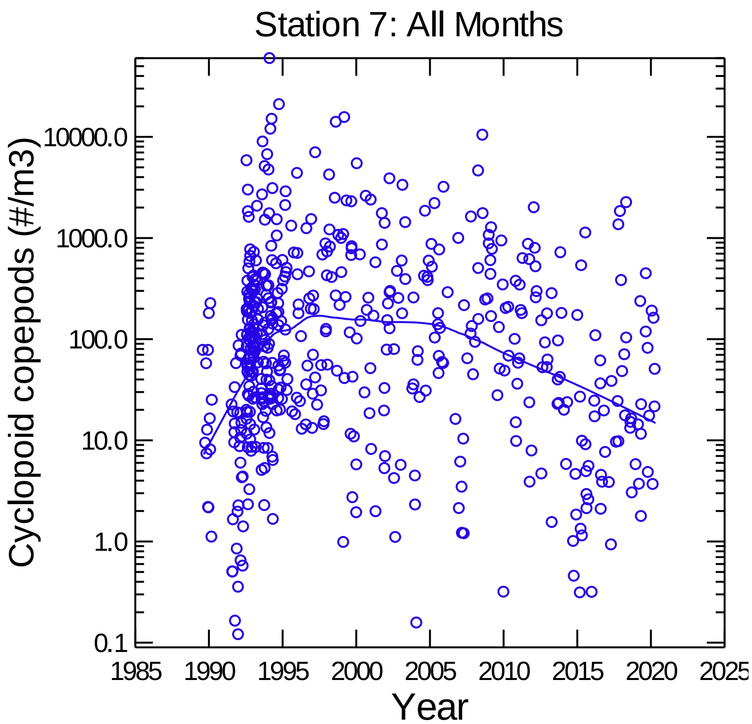

In the cove, cyclopoid copepods increased strongly in the early 1990’s, were steady from 1995 to 2005 at about 200/m^3, and since have decreased slowly to about 13/m^3 in 2020 (Figure 150). Cyclopoid copepods exhibited a significant negative linear trend in the cove over the study period (Table 16).

Photo credit: Laura Birsa

Figure 150. Long term trend in Cyclopoid Copepods. Station 7. Gunston Cove

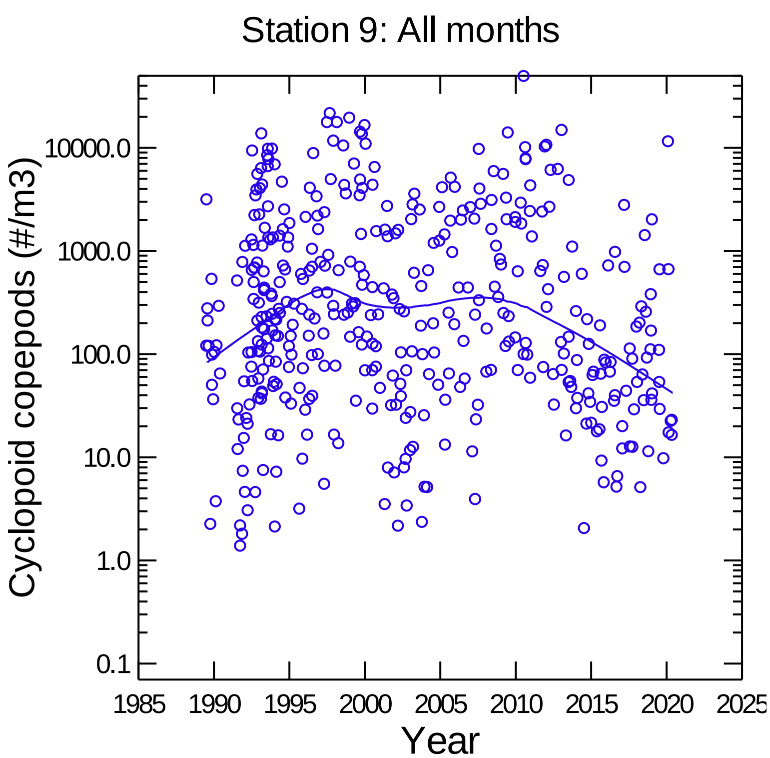

Cyclopoid copepods have shown several cycles over the period (Figure 151). The trend line has varied from 90/m^3 to about 400/m^3. In 2020 cyclopoids were at a low point of about 40/m^3. No linear increase was found when the entire study period was considered (Table 16).

Figure 151. Long term trend in Cyclopoid Copepods. Station 9. River mainstem

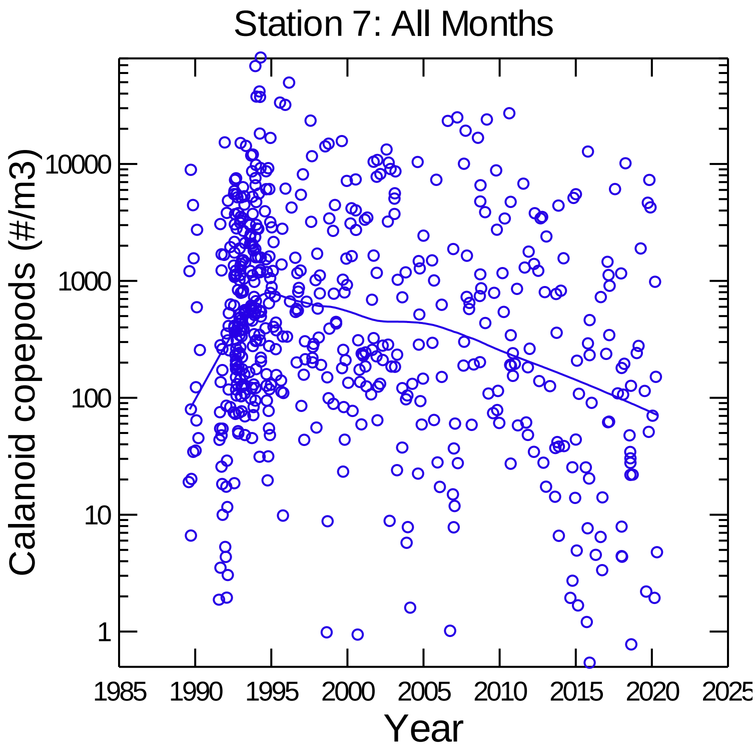

Calanoid copepods (Figure 152) in the cove increased greatly in the early 1990's to near 1000/m^3 and then have gradually declined to about 70/m^3 in 2020. A significant negative trend was revealed by regression analysis (Table 16).

Photo credit: Laura Birsa

Figure 152. Long term trend in Calanoid Copepods. Station 7. Gunston Cove

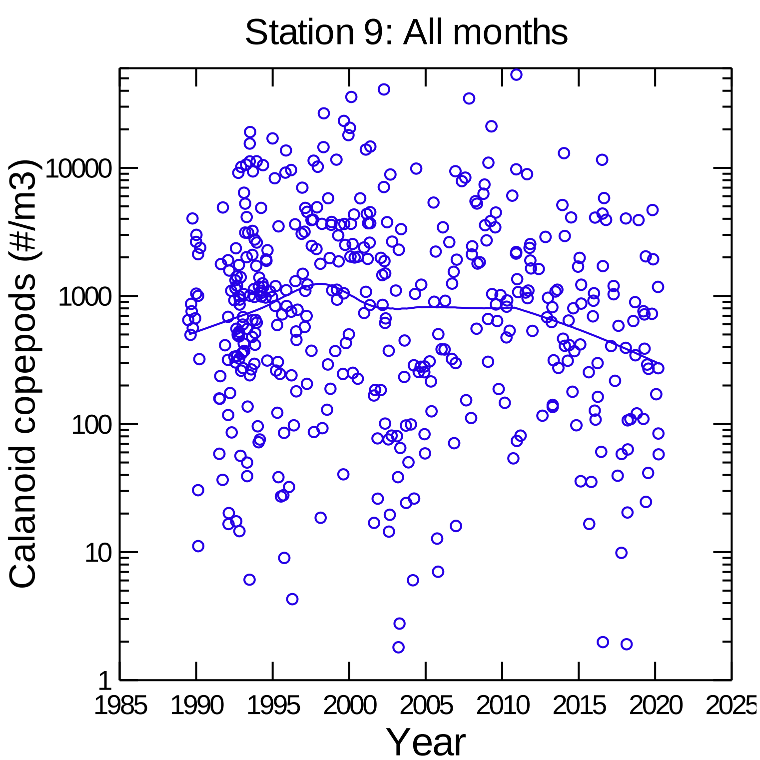

In the river calanoid copepods have varied a lot over the years, but the trend line has changed only gradually and was at 300/m^3 in 2020 (Figure 153). There was not a statistically significant linear trend (Table 16).

Figure 153. Long term trend in Calanoid Copepods. Station 9. River mainstem

E. Ichthyoplankton Trends: 1993-2020

Ichthyoplankton monitoring provides a crucial link between nutrients, phytoplankton, zooplankton and juvenile fishes in seines and trawls. The ability of larvae to find food after yolk is consumed may represent a critical period when survival determines the abundance of a year-class. The timing of peak density of feeding stage fish larvae is a complex function of reproductive output as well as the temperature and flow regimes. These peaks may coincide with an abundance or scarcity of zooplankton prey. When the timing of fish larva predators overlaps with their zooplankton prey, the result is often a high abundance of juveniles that can be observed in high density in seines and trawl samples from throughout the cove. In addition, high densities of larvae but low juvenile abundance may indicate that other factors (e.g., lack of significant refuge for settling juveniles) are modifying the abundance of a year-class.

The dominant species in the ichthyoplankton samples, namely Clupeids (which are primarily river herring and Gizzard Shad), *Morone* sp. (mostly White Perch), and Atherinids (Inland Silversides), all exhibited a spike in density in 1996 followed by a decline in numbers until about 2008. Yellow Perch showed a similar peak in 1996 and has not been a dominant species since. The declines in Clupeid larvae were followed by increases starting in 2010 (Figure 154; Table 17). Especially 2010-2012 showed very high density of these larvae, while numbers decreased again from 2013-2016. There may be an increasing trend again with a small increase in 2017 and a slightly larger increase in 2019. It is possible that this is natural variation, and that these populations rely on a few highly successful yearclasses. A moratorium on river herring since 2012 may be allowing the numbers to increase over time.

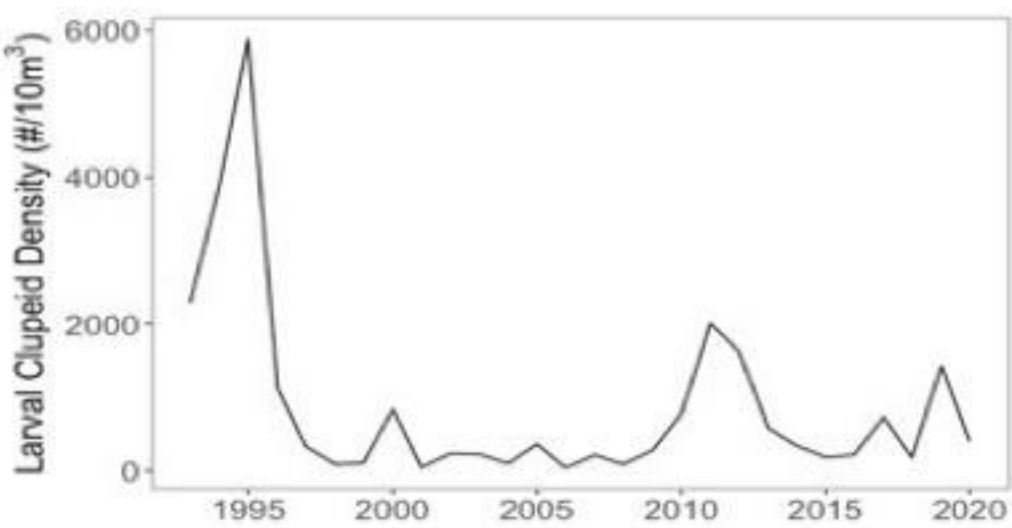

Figure 154. Long-term trend in Clupeid Larvae (*Alosa sp.* and *Dorosoma sp.*; abundance 10 m^{-3}).

Table 17. Density of larval fishes Collected in Gunston Cove and the Potomac mainstem (abundance 10 m^{-3}).

Year	*Alosa sp.*	*Dorosoma sp.*	*Lepomis sp.*	*Morone sp.*	*Perca flavescens*	*Menidia beryllina*
2020	176	155	1	95	0	44
2019	975	365	1	39	0	1
2018	72	38	4	4	0	3
2017	312	148	41	62	1	5
2016	105	87	2	87	0	7
2015	41	29	0	2	0	21
2014	102	115	0	61	0	0
2013	133	220	3	112	1	1
2012	476	1395	0	330	0	0
2011	149	2007	0	62	0	0
2010	247	1032	0	88	15	10
2009	38	276	0	58	0	2
2008	4	85	0	61	1	1
2007	17	209	0	40	12	5
2006	9	37	0	8	20	8
2005	88	280	0	35	0	3
2004	245	94	0	42	0	5
2003	110	170	0	30	6	4
2002	998	30	0	28	1	1
2001	95	5	0	3	0	1
2000	8	97	0	128	2	102
1999	435	94	3	63	0	13
1998	674	84	1	115	3	0
1997	1305	265	31	146	6	8
1996	834	1118	0	571	91	0
1995	721	810	10	333	8	9
1994	640	202	38	176	0	57
1993	33	298	1	112	1	15

The peaks in abundance over the season reflect characteristic spawning times of each species (Figures 155, 157, 159, and 161). Clupeid larval density shows a distinct peak mid-May (Figure 155). Clupeid larvae are dominated by Gizzard Shad, which spawns later in the season than river herring (Alewife and Blueback Herring). However, river herring larvae are part of this peak as well; although their spawning season is from mid-March to mid-May, spawning occurs higher upstream, and larvae subsequently drift down to Gunston Cove. An early peak is seen for *Morone sp*., which is mostly White Perch (Figure 157). White Perch begin spawning early and larval densities slowly taper off. Consequently, White Perch larvae are found throughout most of the sampling season. Silversides have a small peak in late May/early June, with low densities continuing to be present throughout the season (Figure 159). The earliest peak is from Yellow Perch (Figure 161), which may even be at its highest before our sampling starts.

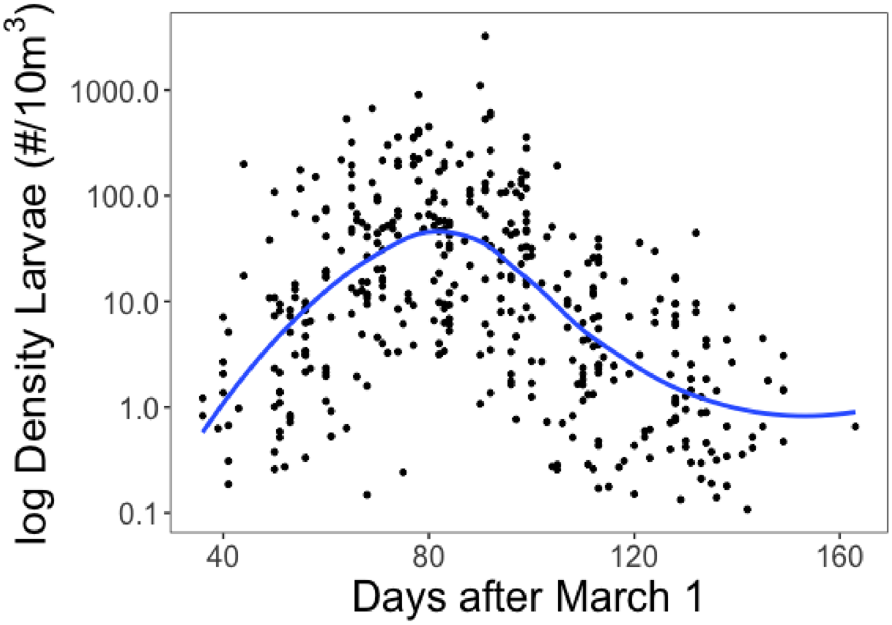

The seasonal pattern in clupeid larvae for 1993-2020 (Figure 141) shows that a peak in density occurs about 80 days after March 1, or mid-May.

Figure 155. Seasonal pattern in Clupeid larvae (*Alosa sp.* and *Dorosoma sp.*; abundance 10 m^{-3}). The x-axis represents the number of days after March 1.

The long-term trend in annual average density of *Morone* larvae shows a high similarity with that of Clupeid larvae (Figure 154). While densities are lower, the same pattern of high peaks in 1995 and 2012, and low densities in other years is seen. Looking at the seasonal pattern (Figure 155), we may miss high densities of larvae occurring in spring, as our sampling of larvae in Gunston Cove starts mid-April (and July in 2020). With the high abundance of juveniles and adults each year, our *Morone* larval sample is likely not representative of the total larval production. White perch is also a migratory species, and juveniles may come in the system from elsewhere.

The long-term in annual average density of Inland Silverside larvae also shows the highest peaks early in the timeseries, with highest peaks occurring in 1994 and 2000. However, after some small peaks in 2006, 2010, and 2015, 2020 showed the third highest peak in the period of record. While we do not produce any information on causation in this survey, this peak occurred during the COVID-19 pandemic, where perhaps some reduced intensity of activities have allowed for a successful Inland Silverside year-class.

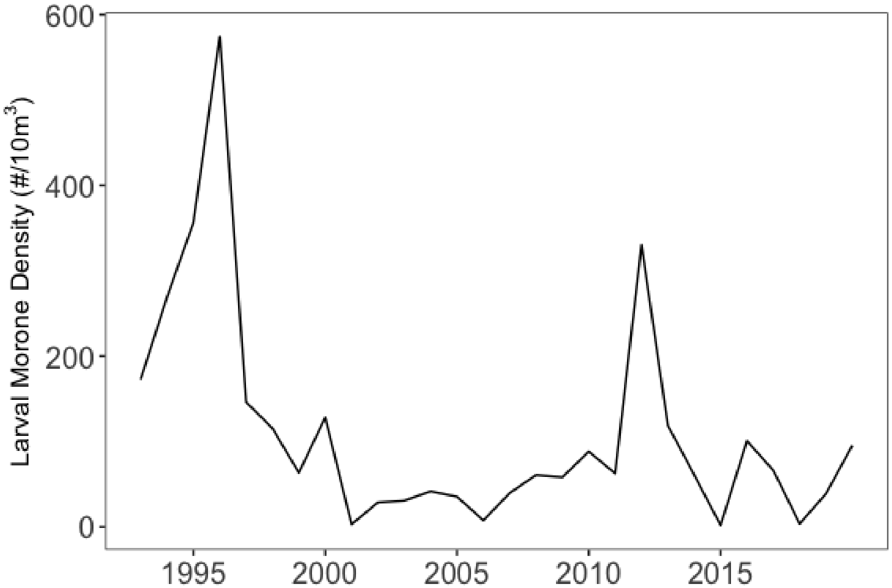

The trend in number of White Perch and Striped Bass larvae per 10 m^3 since 1993 is depicted in the graph in Figure 142. Two peaks are observed in 1995 and 2012 with low densities in other years.

Figure 156. Long term trend in *Morone sp.* larvae (abundance 10 m^{-3}).

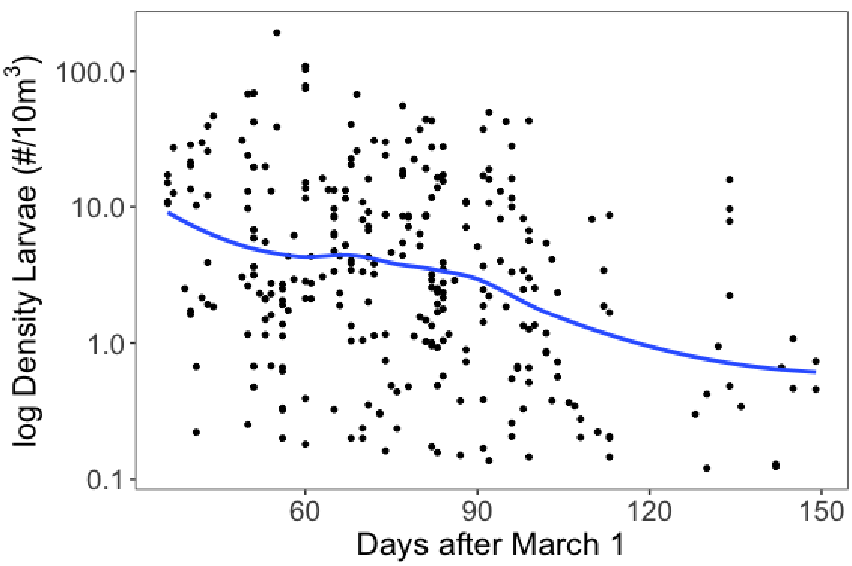

The seasonal density of *Morone* sp. larvae per 10 m^3 is shown in Figure 143. Highest densities are at the start of the sampling season.

Figure 157. Seasonal pattern in *Morone sp.* larvae (abundance 10 m^{-3}). X-axis represents days after March 1st.

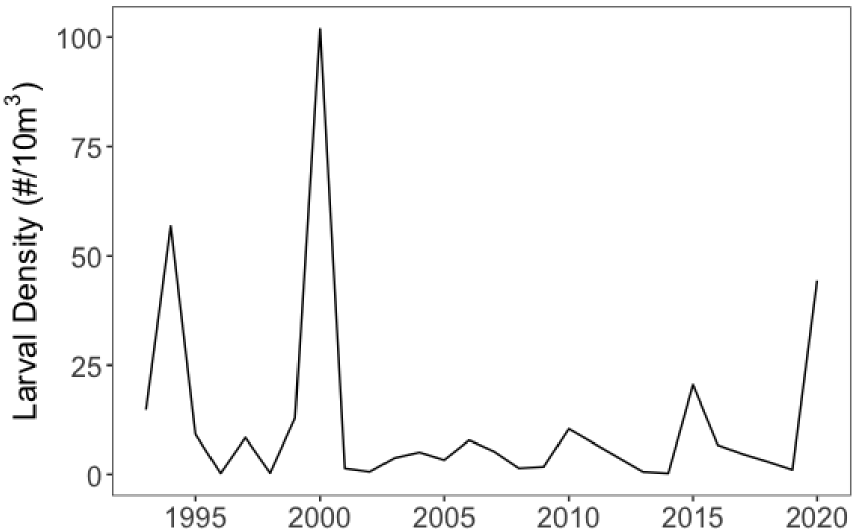

The long-term trend in density of Inland Silverside is presented in Figure 144. After high peaks in 1994 and 2000, densities have been moderate to low with some small peaks in 2006, 2010, and 2015. 2020 adds the third highest peak in the period of record.

Figure 158. Long-term trend in *Menidia beryllina* larvae (abundance 10 m^{-3}).

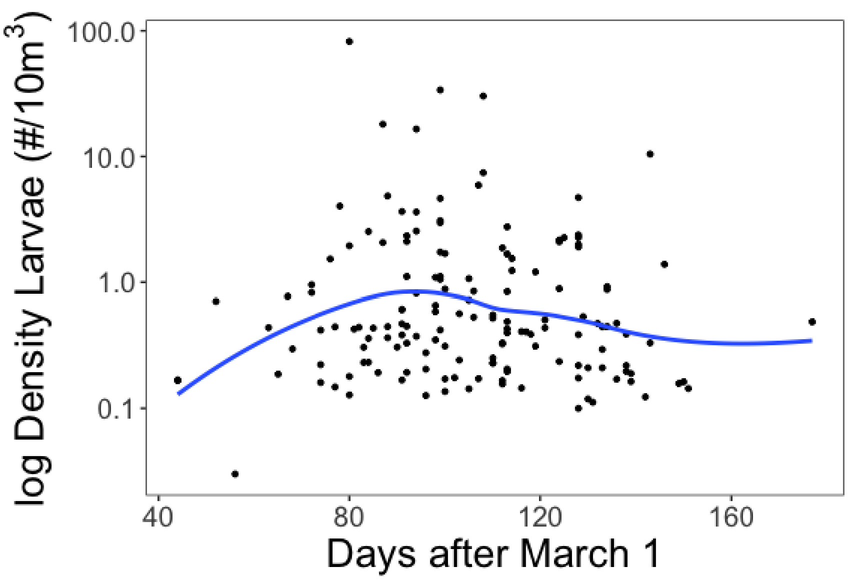

The seasonal occurrence of Inland Silverside per 10m^3 is shown in a LOWESS graph in Figure 145. The pattern shows maximum density around 90 days after March 1, or around the first week of June.

Figure 159. Seasonal pattern in *Menidia beryllina* larvae (abundance 10 m^{-3}). The x-axis represents the number of days after March 1.

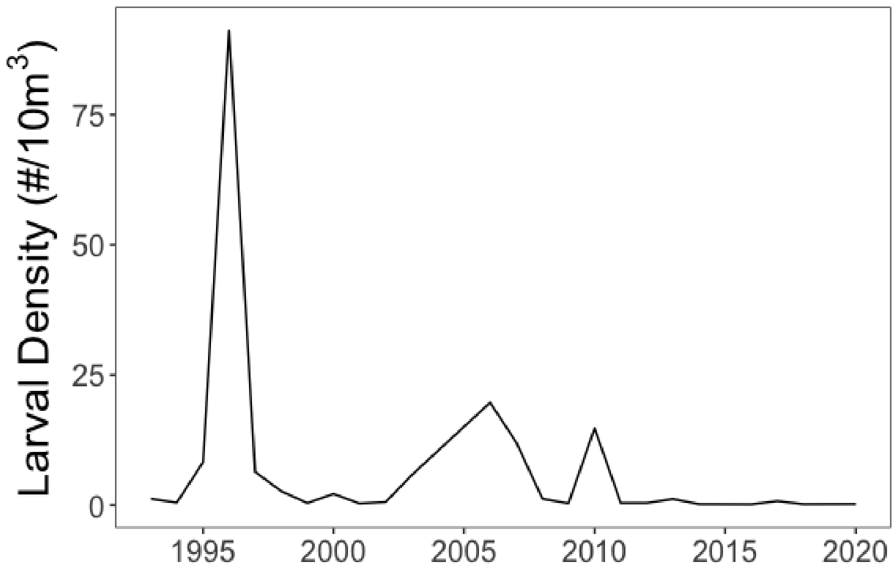

The long-term trend in density of Yellow Perch larvae since 1993. Following unusually high densities in 1996, abundances decreased to low values, especially since 2011.

Figure 160. Long-term trend in *Perca flavescens* larvae (abundance 10 m^{-3}).

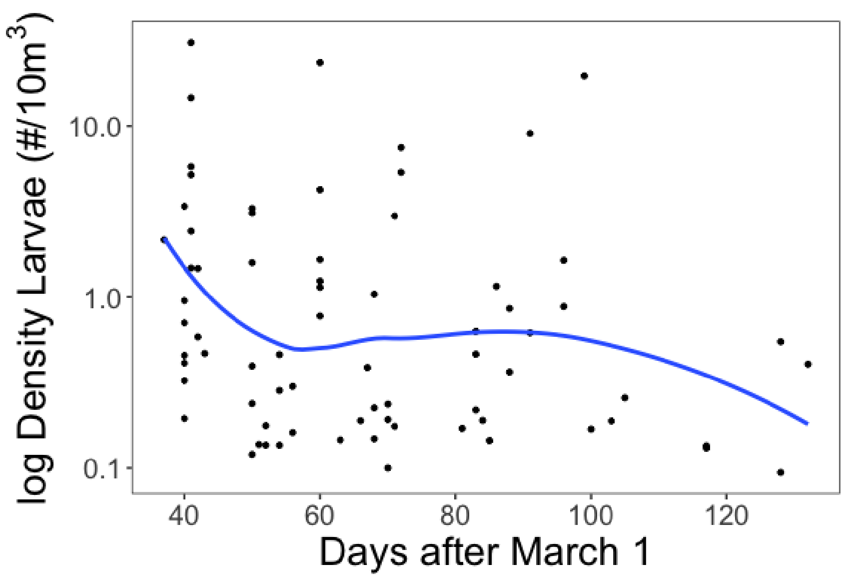

The long-term pattern of seasonal occurrence of Yellow Perch larval density is presented in Figure 147. The greatest densities occur in early to mid-April, while spawning continues producing low densities throughout the season. Total density is low, which is likely the main reason for this unpronounced spawning pattern.

Figure 161. Seasonal pattern in *Perca flavescens* larvae (abundance 10 m^{-3}). The x-axis represents the number of days after March 1.

F. Adult and Juvenile Fish Trends: 1984-2020

Trawls

Overall patterns

Annual abundance of juvenile fishes inside Gunston Cove is indexed by mean catch per trawl in the inner cove (stations 7 and 10 combined; Table 18, Figure 162). Since 1984, this index has fluctuated by over an order of magnitude, and the pattern was predominately due to changes in the catch rate of White Perch (Figure 162). The one high peak in 2004 that was not caused by high White Perch abundance was caused by a large catch of Blueback Herring (Figure 163). The few trawls performed in 2020 had an unprecedented number of White Perch per trawl. With this large peak in catch per trawl, at the end of a times series with higher peaks and shallower troughs since 2006, there seems to be an increasing trend in CPUE driving by White Perch abundances (Figure 162). The high numbers of White Perch were predominantly very small juveniles. Trawl catches in station 7 and 10 were highly dominated by White Perch. Spottail Shiner was represented in the catches with high abundance as well.

Before 2020, strong cohorts punctuated White Perch catch rates in 1993, 2007, 2010, 2012, 2015 and 2019. The peak in 2020 was unprecedented; this after a higher frequency of strong year-classes after 2006 results in an overall increase in trend starting that time.

The remaining component of the total catch (species other than White Perch) made up a moderate to large proportion of the catch until 1990; a relative small part of the catch between 1991 and 2000; and moderate to large proportion of the catch from 2001 to 2019. There was a high peak in catches other than White Perch in 2004, which was primarily due to exceptionally high catches of Blueback Herring (Figure 162; Figure 163). The high peak in Blueback Herring catches in 2004 stands out in otherwise low catches (Figure 163). Generally, both herring species have been found in higher abundances since 2000 than in the decade before that. We included *Alosa sp*. (unidentified herring or shad) in Figure 163 in 2016 (for all years), so that abundances of herring or shad are not missed simply because they could not be identified to the species level. This revealed the second highest peak in Alosines in 2010.

Table 18. Mean catch per trawl of adult and juvenile fishes at Stations 7 and 10 combined. 1984-2020.

Year	All Species	White Perch	All Alosa Sp.	Blueback Herring	Alewife	Gizzard Shad	Bay Anchovy	Spottail Shiner	Brown Bullhead	Pumpkinseed
2020	568.7	522.1	2.6	0.3	2.0	0.7	0.0	33.9	0.1	4.3
2019	269.1	141.9	5.0	0.1	0.9	0.0	0.9	104.4	0.1	2.3
2018	147.1	79.1	2.7	0.0	0.4	0.2	0.0	30.5	0.8	4.8
2017	151.7	106.5	1.2	0.0	0.5	0.0	0.0	11.7	0.1	6.2
2016	170.4	121.7	12.7	0.0	0.1	0.1	0.3	13.7	0.3	1.2
2015	284.2	172.3	34.4	26.1	4.2	0.2	0.1	64.4	0.1	1.1
2014	92.3	46.2	10.4	2.1	1.3	0.2	1.4	15.6	0.3	0.5
2013	158.8	97.9	13.1	6.8	2.9	0.1	1.4	31.0	0.6	1.8
2012	164.5	128.7	1.7	0.1	0.2	3.3	0.4	11.8	0.6	2.1
2011	96.8	43.5	3.3	0.1	1.2	0.1	0.0	19.9	0.1	2.0
2010	372.9	248.1	109.1	0.2	52.9	2.2	0.4	6.0	0.5	1.4
2009	93.7	18.3	46.6	1.0	45.2	0.6	6.2	2.7	0.1	3.1
2008	69.8	16.1	0.1	0.0	0.0	4.0	0.2	2.5	0.6	7.0
2007	227.2	141.4	37.2	23.6	8.8	0.1	15.8	20.1	0.2	2.6
2006	26.1	9.6	2.7	1.6	0.6	0.2	2.3	3.0	0.4	1.8
2005	68.4	21.0	33.1	11.8	16.4	1.1	0.0	6.6	0.4	1.4
2004	408.4	23.4	373.2	337.5	33.1	0.9	0.6	8.0	0.0	0.5
2003	54.2	13.2	23.9	18.8	3.5	0.0	7.4	2.8	0.1	0.4
2002	80.1	15.1	39.5	9.8	28.5	0.1	15.8	0.6	0.0	1.7
2001	143.5	47.0	50.6	40.5	9.9	0.3	35.1	2.8	3.3	1.4
2000	68.0	53.3	5.4	3.6	1.9	2.3	1.7	1.3	1.9	0.6
1999	86.9	63.2	4.7	4.2	0.5	1.0	5.4	4.8	2.4	1.8
1998	83.2	63.8	3.0	2.2	0.8	0.5	3.7	6.4	0.9	1.6
1997	81.4	61.6	2.9	1.9	1.0	5.0	2.6	2.9	1.5	1.4
1996	54.1	37.1	8.5	4.0	4.4	0.5	0.2	2.6	0.5	2.0
1995	90.4	71.1	6.2	4.1	2.1	0.4	3.0	2.9	2.1	1.9

1994	102.8	77.7	6.5	6.5	0.0	0.4	1.1	6.3	2.4	2.6
1993	246.6	216.0	2.0	1.4	0.6	1.4	0.6	7.3	4.5	3.4
1992	112.8	81.6	0.2	0.2	0.0	0.9	0.8	2.4	11.5	5.1
1991	123.1	91.5	1.4	0.9	0.5	7.6	2.5	2.7	11.6	1.7
1990	68.8	31.6	24.1	21.1	3.1	0.1	1.1	1.1	9.0	0.5
1989	78.2	14.9	16.4	16.1	0.2	42.1	0.2	0.5	3.0	0.6
1988	126.6	74.5	20.3	10.5	7.0	13.5	8.3	1.9	5.2	0.7
1987	109.2	54.6	19.6	16.4	3.2	5.6	8.8	0.7	17.2	1.4
1986	130.9	69.9	24.6	1.8	22.7	4.2	4.0	1.2	18.1	0.6
1985	135.9	43.9	25.8	8.6	10.7	2.9	48.2	1.1	9.8	0.1
1984	213.2	127.4	11.9	6.0	0.6	13.3	22.0	1.5	32.9	0.2

Table 19. Mean catch per trawl of selected adult and juvenile fishes for all months at Station 9. 1988-2020

Year	All Species	All Alosa Sp.	Alewife	Blueback Herring	White Perch	Bay Anchovy	Spottail Shiner	Brown Bullhead	Blue Catfish	Channel Catfish	Tesselated Darter
2020	29.2	0.2	0.2	0.0	20.8	0.0	3.8	0.0	3.6	0.2	0.0
2019	54.7	24.5	11.3	9.6	16.1	0.0	8.9	0.0	1.3	0.0	0.5
2018	41.8	0.0	0.0	0.0	27.6	0.0	1.6	0.7	8.5	0.0	1.8
2017	9.0	0.1	0.0	0.0	8.5	0.0	0.0	0.0	0.2	0.0	0.0
2016	10.1	2.0	0.0	0.0	2.0	4.9	0.0	0.0	1.2	0.0	0.0
2015	15.8	10.3	7.8	0.2	1.5	0.5	0.2	0.2	2.8	0.2	0.0
2014	16.9	6.8	3.7	1.0	3.0	3.3	0.1	0.1	3.1	0.0	0.4
2013	12.2	3.9	2.1	0.6	1.5	1.6	0.0	0.0	4.5	0.0	0.2
2012	62.1	0.0	0.0	0.0	21.6	31.7	0.8	0.0	7.3	0.3	0.0
2011	33.9	0.4	0.2	0.0	21.2	0.0	0.2	0.1	5.1	6.4	0.3
2010	38.7	0.1	0.0	0.0	10.8	7.9	0.0	0.1	19.5	0.0	0.0
2009	34.6	2.3	0.5	0.4	13.7	7.6	0.5	0.2	8.7	0.6	0.1
2008	118.7	0.1	0.0	0.0	13.9	99.9	0.6	0.1	3.7	0.0	0.0
2007	253.8	52.7	17.2	2.5	195.7	0.7	1.1	0.0	1.8	0.0	0.9

2006	68.1	0.2	0.0	0.2	31.0	3.0	0.2	8.0	19.9	4.6	0.0
2005	95.0	15.4	14.3	1.1	36.5	12.1	1.8	2.1	18.3	4.7	0.1
2004	41.9	3.8	3.4	0.3	20.4	0.0	1.1	0.0	5.2	6.6	0.3
2003	65.8	0.3	0.1	0.1	32.6	0.0	0.6	0.0	7.4	14.4	1.2
2002	55.2	1.2	0.7	0.4	28.2	0.5	0.1	0.0	6.8	10.8	1.0
2001	77.1	0.1	0.1	0.1	40.1	22.2	0.1	0.9	2.7	5.5	0.8
2000	52.1	0.1	0.1	0.0	43.4	0.0	0.1	2.1	0.0	3.9	0.0
1999	23.1	0.0	0.0	0.0	18.9	0.2	0.0	0.2	0.0	2.4	0.0
1998	22.3	0.1	0.1	0.0	12.9	0.4	0.1	0.2	0.0	6.2	2.0
1997	50.1	0.0	0.0	0.0	37.8	0.0	1.1	0.4	0.0	9.1	0.4
1996	13.8	0.0	0.0	0.0	7.0	0.0	0.1	0.1	0.0	5.7	0.8
1995	30.5	0.3	0.3	0.0	16.8	0.2	0.2	4.2	0.0	8.0	0.1
1994	32.0	0.0	0.0	0.0	13.4	0.1	0.0	2.4	0.0	6.4	3.5
1993	31.2	0.1	0.0	0.1	6.4	0.0	6.2	1.4	0.0	6.8	7.5
1992	29.0	0.1	0.0	0.1	13.4	0.0	0.2	1.1	0.0	1.8	3.3
1991	70.9	0.1	0.1	0.0	43.7	2.0	0.1	1.1	0.0	15.9	0.2
1990	102.8	0.1	0.1	0.0	50.8	0.0	0.1	5.1	0.0	40.9	0.1
1989	14.2	1.0	0.2	0.8	7.8	0.4	0.0	1.5	0.0	1.9	0.3
1988	19.2	0.2	0.2	0.0	5.2	11.5	0.0	0.0	0.0	0.8	0.0
1986	1.0	0.0	0.0	0.0	0.0	0.0	0.0	0.0	0.0	0.0	0.0

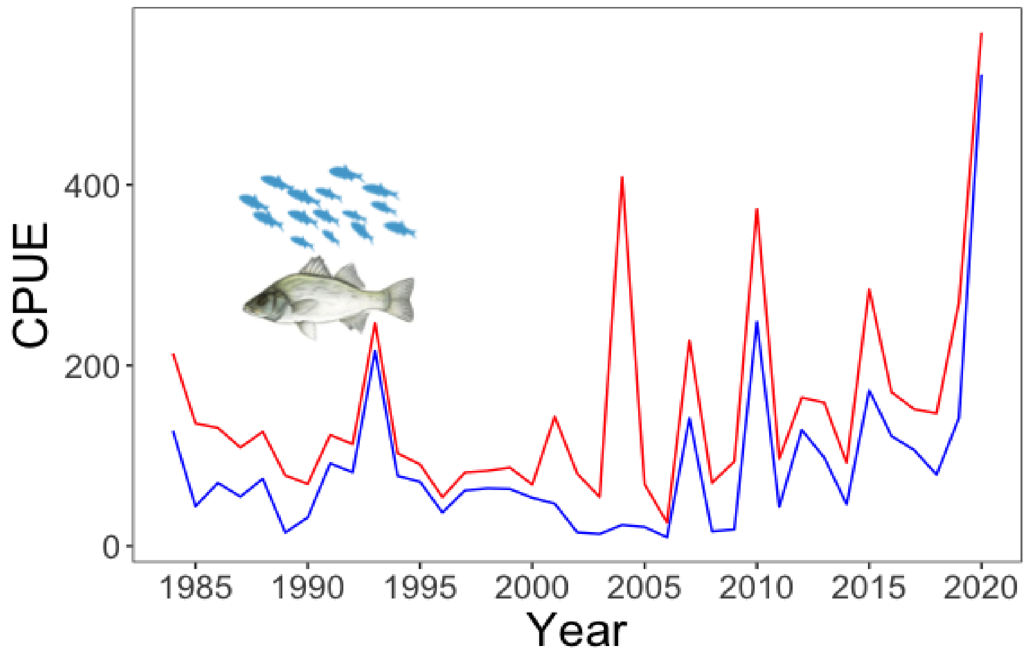

Figure 162. Trawls. Annual Averages. All Species (red) and *Morone americana* (blue). Cove Stations 7 and 10. 1984-2020.

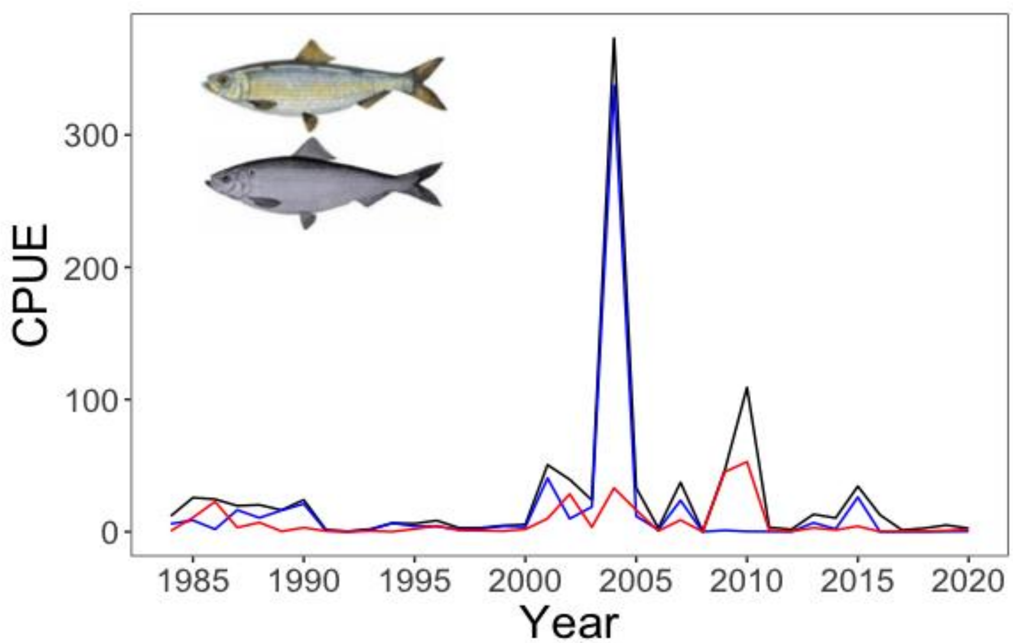

Figure 163. Trawls. Annual Averages. *Alosa aestivalis* (blue), *Alosa pseudoharengus* (red), and all combined *Alosa sp.* (black). Cove Stations 7 and 10.

Gizzard Shad (*Dorosoma cepedianum*) catch rates in trawls in 2020 were low which contributes to a pattern of low abundance after a high peak in 1989 (Figure 164). Smaller peaks later occurred in 1991, 1997, 2008, and 2012, that were all an order of magnitude lower than the 1989 peak. Bay Anchovy (*Anchoa mitchilli*) catch rates in 2020 were low like they were in the last five years at inner cove stations, and trends in the data suggests decreasing trend over the length of the survey. They are primarily resident in more saline portions of the estuary, and display sporadic occurrence in tidal freshwater. Any decreases in Gunston Cove therefore do not indicate a declining trend in the abundance of this species overall.

Spottail Shiner and sunfishes have been consistently collected in the majority of all trawl and seine samples (Figure 165). An increasing trend has been observed for Spottail Shiner since the beginning of the survey. In recent years (since 2000), a more sharply increasing pattern is seen in the midst of high variability, with high numbers in 2007, 2011, 2013, 2015, and 2018 (Figure 165). We collected an unprecedented high number of Spottail Shiner specimens in 2019. These individuals were mostly juveniles, indicating relatively high reproductive success as measured by this survey. In 2020 the numbers were lower again, but still high on average, contributing to the increasing trend. The trends for sunfishes showed a similar pattern of higher abundance since 2005 than before. Other sunfish species than Bluegill and Pumpkinseed have been included in the trend, which better reveals the increases in sunfishes that also include Green Sunfish, Redbreast Sunfish, and hybrids. Peaks occurred in 2008, 2011, and 2017. Sunfishes are associated with SAV, so their trend seems closely aligned with the expansion of SAV in 2005.

One Brown Bullhead specimen was captured in cove trawls in 2020, fitting the trend of continuing decline that has proceeded continuously since the start of the survey (Figure 166). Tessellated Darter (*Etheostoma olmstedi*) was collected in low numbers in trawl samples. The highest peak in abundance since the start of collections was seen in 2018. The second highest peak in the period of record was observed in 1992. The lower abundance in 2020 results in a flat trend with abundances of Tessellated Darter usually low.

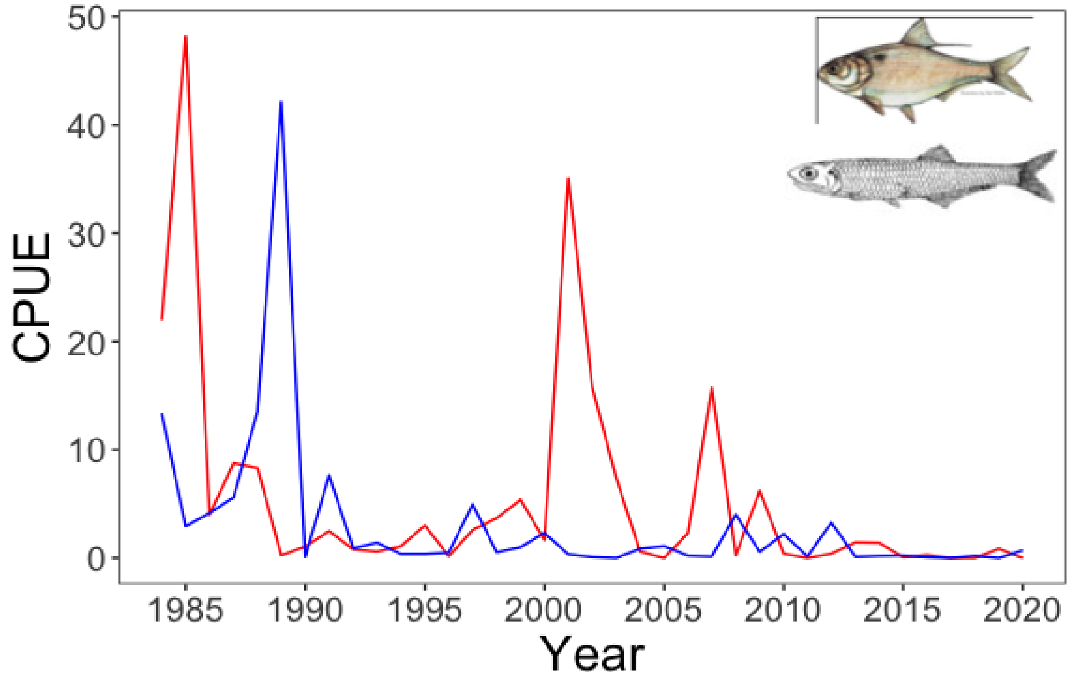

Figure 164. Trawls. Annual Averages. Cove Stations 7 and 10. *Dorosoma cepedianum* (blue) and *Anchoa mitchilli* (red).

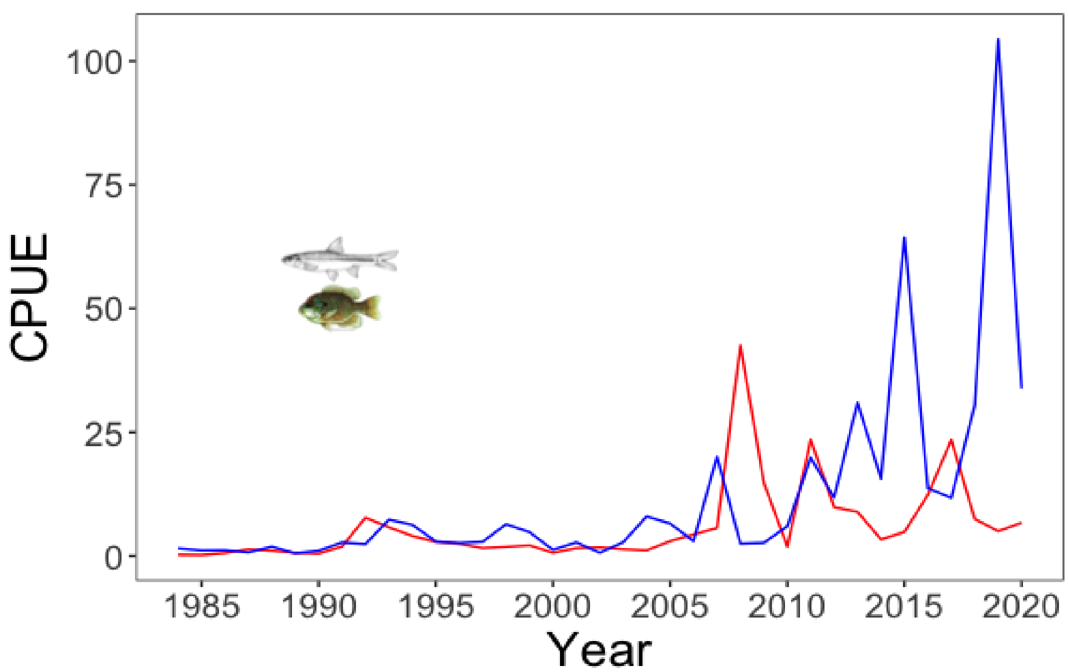

Figure 165. Trawls. Annual Averages. *Notropis hudsonius* (blue) and all *Lepomis sp.* (red). Cove Stations 7 and 10.

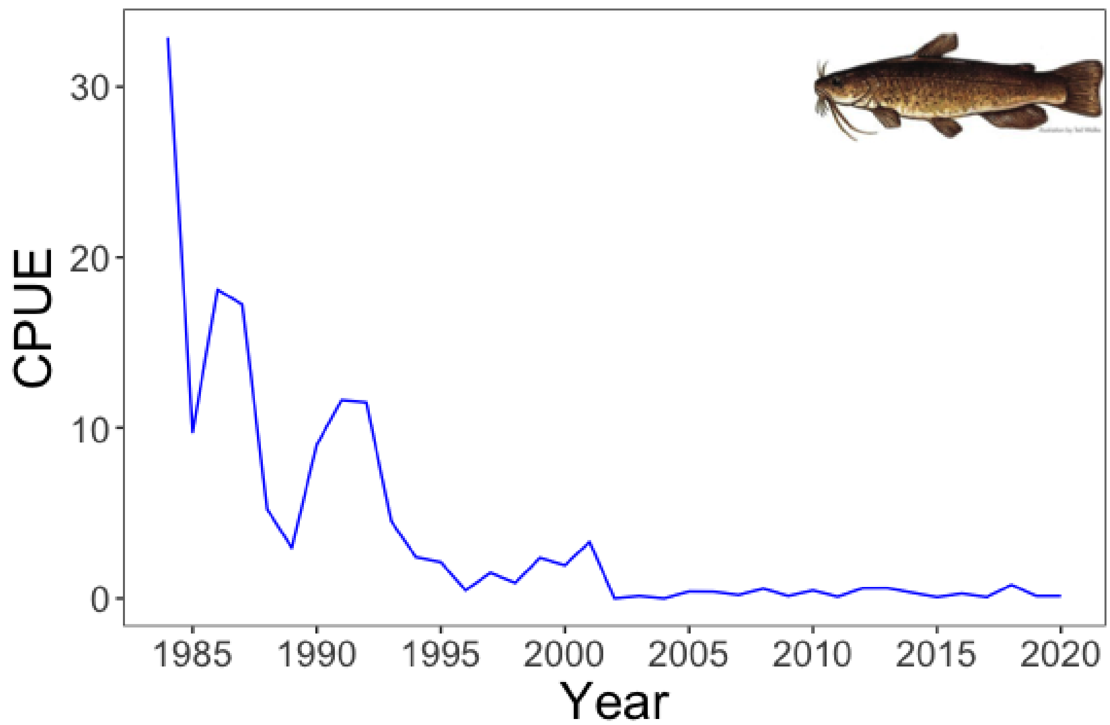

Figure 166. Annual Averages. *Ameiurus nebulosus*. Cove Stations 7 and 10.

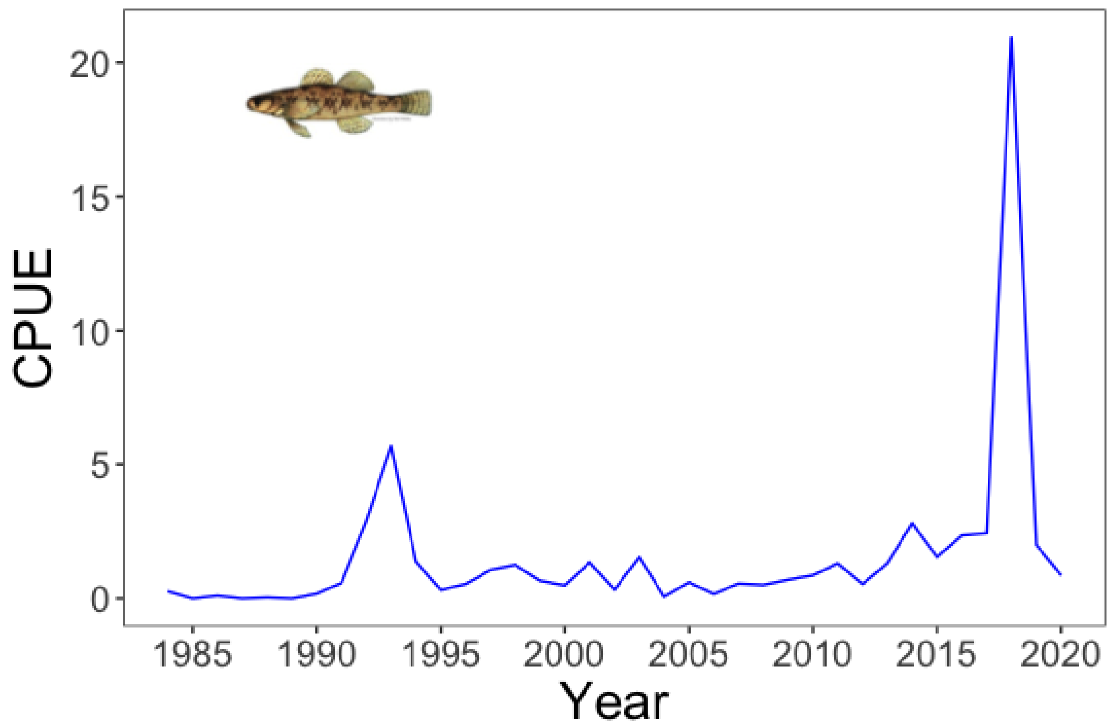

Figure 167. Trawls. Annual Averages of *Etheostoma olmstedi*. Cove stations 7 and 10.

Mean total catch at station 9 in 2020 was moderately high (Table 19, Figure 168). Total catch was mainly comprised of White Perch, as total catch went down from 2019 and White Perch catch went up. The high total abundance in 2019 was due to catches of Spottail Shiner and Alosines. In 2018 an increase in catch was due to an increase in Blue Catfish catch. Blue Catfish was spotted in Station 9 again in 2019 and 2020. Blue Catfish is regularly collected at station 9 the last 15 years, and hardly ever at the inner cove stations. Before 2017, Blue Catfish was never collected at the inner cove station, but a few were collected there too in 2017, 2018, 2019 and 2020.

At the river channel station (station 9), catches in 2020 were comparable to what has been collected in the last decade (Figure 168). As in the inner cove, much of the variation at station 9 is directly attributable to the catch of White Perch. In 2020, total catch in Station 9 was highly dominated by White Perch catches (Table 19, Figure 168). Two other species with relatively high abundance were Spottail Shiner and Blue Catfish (Table 19).

Since 1988 when station 9 was incorporated as part of the survey, Bay Anchovy, Spottail Shiner, and American Eel have occurred sporadically at station 9 (Figure 169). We find high abundance of Bay Anchovy once every 5 years or so, with one very distinct peak in 2008. Spottail Shiner is found in low numbers every year at station 9, which saw an uptick in 2019, and remained relatively high in 2020. American Eel has remained rare since 1994.

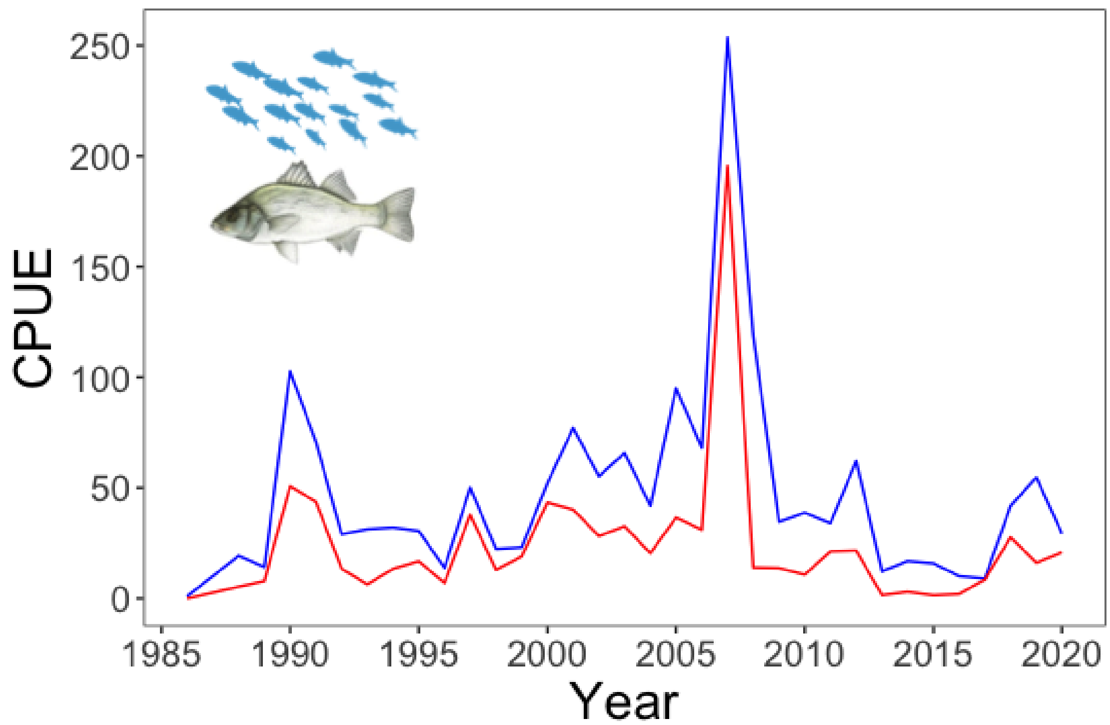

Figure 168. Trawls. Annual averages. River Station (9). Total catch (blue) and *Morone americana* (red).

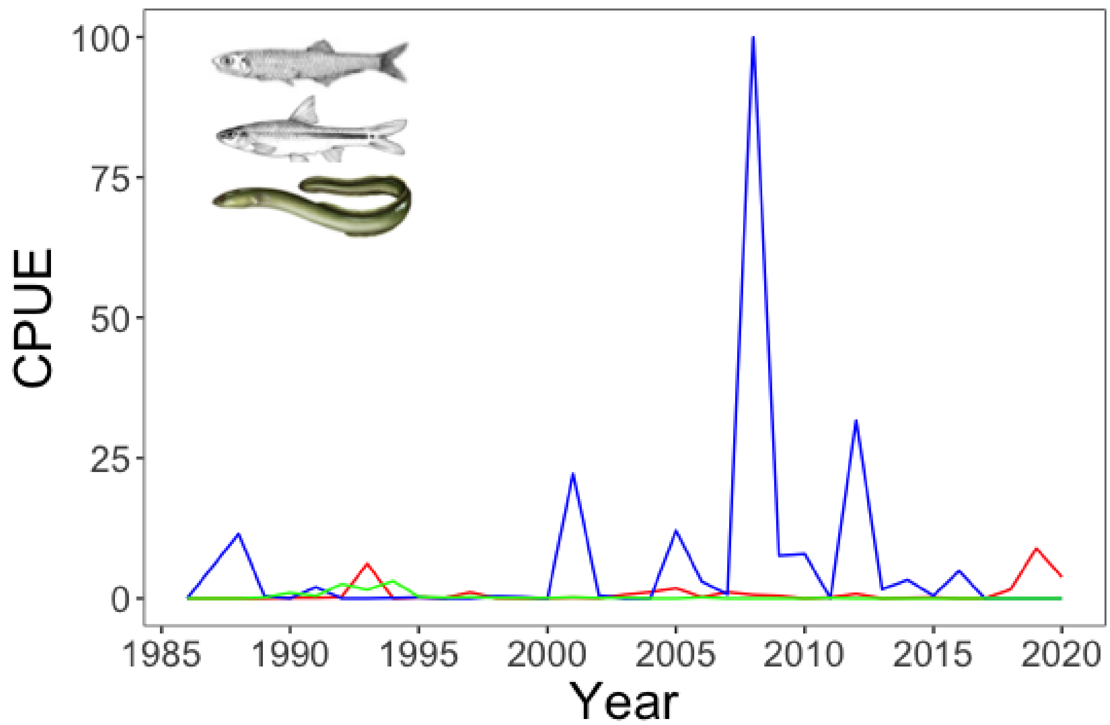

Figure 169. Trawls. Annual Averages. River Station (9). *Anchoa mitchilli* (Blue), *Notropis hudsonius* (red), and *Anguilla rostrata* (green).

Catch rates for native catfish species have been variable and low at station 9 since 2007 (Figure 170), with only a small peak from Channel Catfish in 2011. While no Channel Catfish was observed in 2018, ten White Bullhead and eight Brown Bullhead were collected in station 9 in 2018. While it is good to see that especially White Bullhead, a species that has not been collected at station 9 anymore for years, has not been completely extirpated, these numbers do not reverse the long-term mean trends identifying a decline in native catfishes. One Channel Catfish and no other native bullheads were collected at Station 9 in 2020, while 18 Blue Catfishes were collected. The invasive Blue Catfish was positively identified on the survey in 2001 and has been captured in high numbers relative to White Bullhead, Channel Catfish and Brown Bullhead ever since (Figure 170). Since Blue Catfish occupy the same niche, but can grow to larger sizes, it generally outcompetes the native catfish population (Schloesser et al., 2011). Blue Catfish established itself in 2001 with relatively high numbers, but the trend has remained flat since then (Figure 170). The system may have reached a new stable state that includes Blue Catfish in high numbers, and other catfishes in low numbers. Continued monitoring in the growth of this population is warranted. Of note is that we are not capturing very large specimens with the otter trawl, and very large Blue Catfishes have been reported in this area.

Station 9 generally represents low catch rates for the demersal species Tessellated Darter and Hogchoker (Figure 171). In 2018 however, while not unprecedented as in the cove, the mainstem saw a peak in Tessellated Darter abundance. Less were collected in 2019, but abundances were still above average for recent years. No Tesselated Darters or Hogchokers were collected in 2020, which is same as the last year two years for Hogchoker.

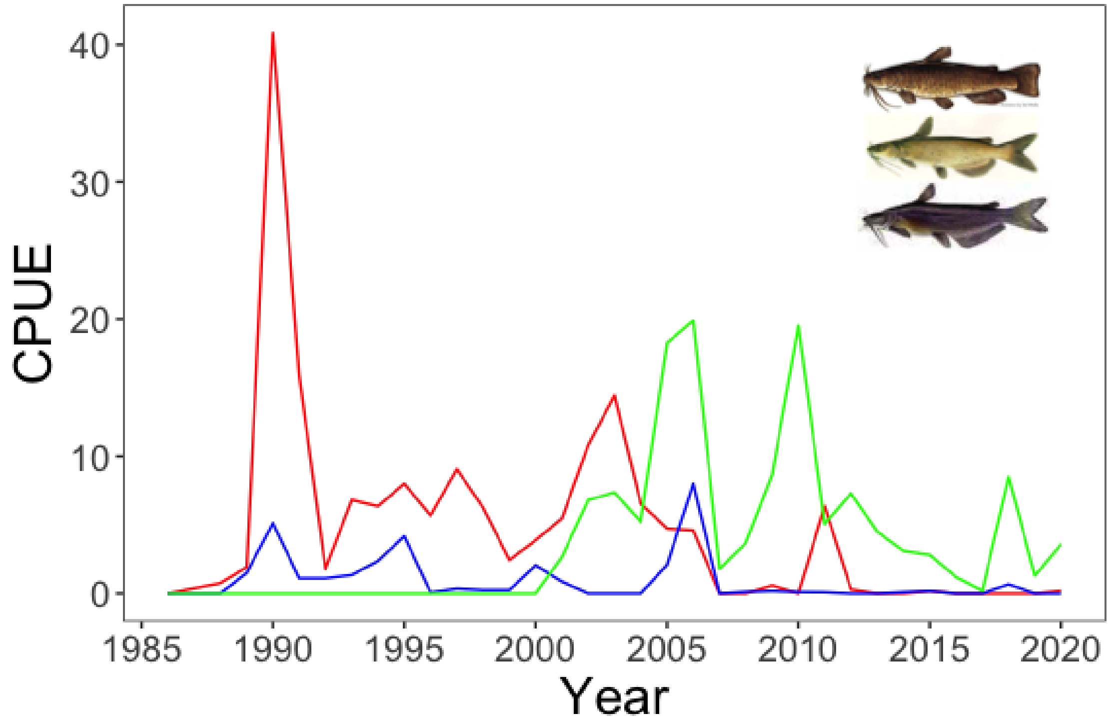

Figure 170. Trawls. Annual Averages. River Station (9). *Ameiurus nebulosus* (blue), *Ictalurus punctatus* (red), and *Ictalurus furcatus* (green).

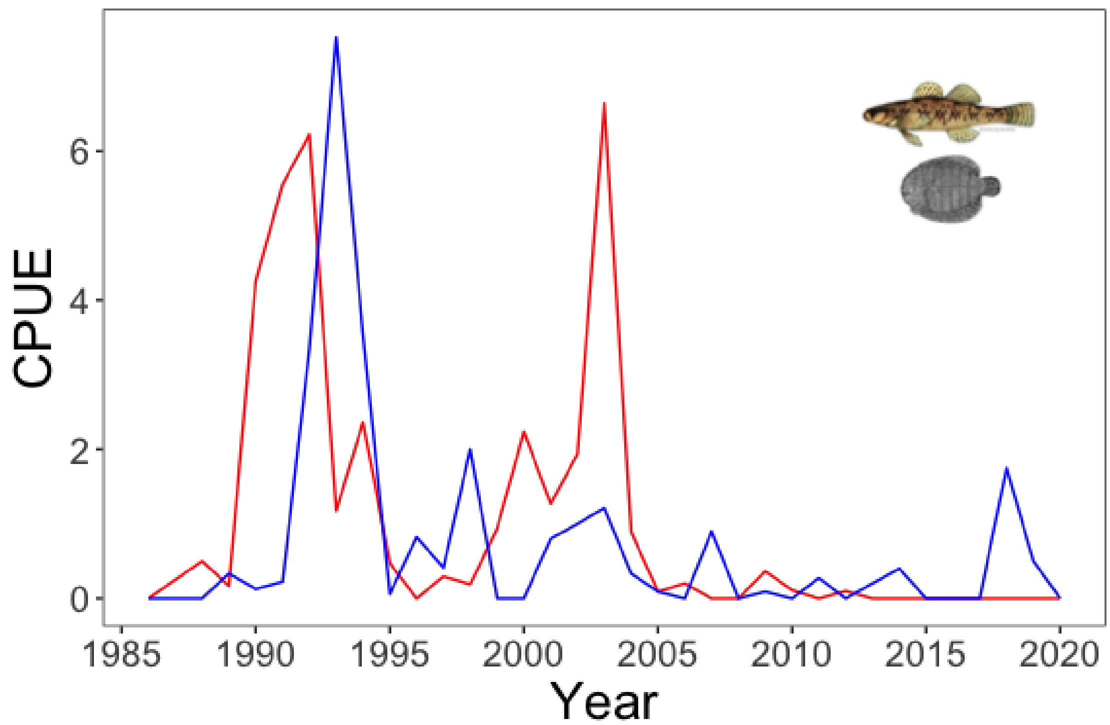

Figure 171. Trawls. Annual Averages. *Etheostoma olmstedi* (blue) and *Trinectes maculatus* (red). River Station (9).

The mean catch of all trawl stations combined in 2020 was up again from last year and not only higher than the long-term mean of 103, but the highest of the period of record (Table 20). This is due to the unprecedented catch per trawl in 2020 of White Perch in station 7 (Table 20, 21). While using catch per unit effort allows for between year comparisons, the low number of trawls performed in 2020 could have resulted in a higher chance of higher variability (either very high or very low CPUE; Table 22). When all trawls are performed in all months, the catch needs to be consistently high to achieve the highest catch on record. However, when only a few trawls are performed, the catch has a higher chance of unprecedent high numbers, when a school of fishes is encountered that is not balanced out by other trawls where a school of fishes is not encountered. Collections in 2021 will provide us with a more balanced view of what the current trend is, and if the high numbers of 2020 are a chance high catch or a sign of increased abundance.

Table 20. Mean catch per trawl of selected adult and juvenile fishes for all months at Stations 7, 9, and 10 combined. 1984-2020.

Year	All Species	White Perch	All Alosa Sp.	Blueback Herring	Alewife	Gizzard Shad	Bay Anchovy	Spottail Shiner	Brown Bullhead	Blue Catfish	Channel Catfish
2020	343.9	313.2	1.6	0.2	1.2	0.4	0.0	21.3	0.1	1.6	0.1
2019	179.8	89.5	13.1	4.1	5.2	0.0	0.5	64.6	0.1	0.6	0.0
2018	106.3	59.2	1.6	0.0	0.2	0.1	0.0	19.3	0.7	3.4	0.0
2017	89.6	63.9	0.7	0.0	0.3	0.0	0.0	6.6	0.0	0.2	0.0
2016	103.6	71.8	8.2	0.0	0.0	0.0	2.2	8.0	0.2	0.5	0.0
2015	161.2	94.0	23.3	14.2	5.8	0.1	0.2	35.0	0.1	1.3	0.1
2014	62.1	28.9	8.9	1.7	2.3	0.1	2.2	9.4	0.2	1.3	0.0
2013	102.4	60.8	9.6	4.4	2.6	0.2	1.5	19.1	0.4	2.3	0.0
2012	123.5	85.8	1.0	0.0	0.1	2.0	12.9	7.4	0.4	2.9	0.2
2011	74.5	35.6	2.3	0.1	0.9	0.1	0.0	12.9	0.1	2.0	2.3
2010	247.6	159.1	68.2	0.1	33.0	1.4	3.2	3.8	0.3	7.9	0.0
2009	73.4	16.7	31.4	0.8	29.9	0.4	6.7	1.9	0.2	3.0	0.3
2008	83.8	15.5	0.1	0.0	0.0	2.9	28.7	2.0	0.4	1.2	0.0
2007	236.1	159.5	42.4	16.6	11.6	0.1	10.7	13.8	0.1	0.7	0.0
2006	41.1	17.2	1.8	1.1	0.4	0.1	2.5	2.0	3.1	7.1	1.6
2005	77.8	26.5	26.8	8.0	15.6	0.7	4.3	4.9	1.0	7.0	1.8
2004	271.0	22.3	234.7	211.1	22.0	0.5	0.4	5.4	0.0	2.0	2.5
2003	58.1	19.7	16.0	12.6	2.3	0.0	4.9	2.1	0.1	2.5	5.4
2002	71.7	19.6	26.5	6.6	19.0	0.1	10.6	0.4	0.0	4.1	4.6
2001	122.3	44.8	34.5	27.6	6.8	0.3	31.0	1.9	2.5	0.9	1.8
2000	65.3	48.8	4.2	2.3	1.9	1.5	1.1	2.1	1.9	0.0	1.3
1999	65.6	48.4	3.1	2.8	0.3	0.7	3.7	3.2	1.7	0.0	0.8
1998	62.9	46.8	2.0	1.4	0.6	0.4	2.6	4.3	0.7	0.0	2.1
1997	71.0	53.6	2.0	1.3	0.7	3.3	1.7	2.3	1.1	0.0	3.1
1996	36.0	23.7	4.5	2.1	2.3	0.3	0.1	1.5	0.3	0.0	2.4
1995	78.8	58.4	3.7	2.4	1.3	1.2	2.9	2.2	1.9	0.0	4.7

1994	90.5	68.1	2.4	2.3	0.1	0.3	0.8	6.5	1.4	0.0	2.1
1993	162.4	131.7	2.3	2.0	0.3	1.0	2.2	7.6	1.9	0.0	2.1
1992	119.8	88.2	1.3	0.6	0.7	0.4	1.0	2.3	4.5	0.0	1.5
1991	148.9	82.4	17.5	12.5	5.0	5.3	26.2	2.8	4.5	0.0	2.8
1990	67.5	31.2	19.1	16.1	3.0	0.1	0.8	2.5	4.0	0.0	6.9
1989	62.4	9.1	26.4	25.8	0.6	20.8	0.6	0.4	1.4	0.0	0.6
1988	79.5	32.9	18.8	14.4	3.3	6.9	13.7	1.2	2.4	0.0	0.3
1987	104.1	49.7	15.3	14.1	1.2	6.5	20.5	1.2	7.2	0.0	0.1
1986	84.1	49.3	13.2	2.5	10.7	2.3	4.9	0.8	7.2	0.0	0.1
1985	93.1	33.0	18.7	7.7	5.6	1.4	29.4	1.4	4.6	0.0	0.3
1984	149.3	95.4	7.9	4.8	0.4	6.4	17.7	1.9	14.1	0.0	0.4

Table 21. Mean catch per trawl of adult and juvenile fishes in all months at each station.

Year	**7**	**9**	**10**
2020	789.4	29.2	17.0
2019	356.2	54.7	112.4
2018	199.7	41.8	88.6
2017	187.9	9.0	30.7
2016	224.3	10.1	35.8
2015	360.0	15.8	31.7
2014	103.2	16.9	70.4
2013	236.0	12.2	30.3
2012	225.4	62.1	42.6
2011	113.5	33.9	76.4
2010	616.7	38.7	7.3
2009	142.8	34.6	49.1
2008	49.8	118.7	89.9
2007	390.1	253.8	64.4
2006	40.7	68.1	7.8
2005	106.4	95.0	22.0
2004	740.5	41.9	28.9
2003	68.9	65.8	39.5
2002	88.8	55.2	70.9
2001	167.8	77.1	119.1
2000	95.1	52.1	42.5
1999	117.1	23.1	56.8
1998	88.2	22.3	78.2
1997	111.2	50.1	51.6
1996	73.9	13.8	31.5
1995	109.3	30.5	71.4
1994	144.9	32.0	60.7
1993	377.1	31.2	116.1
1992	155.5	29.0	70.2
1991	185.9	70.9	66.5
1990	76.5	102.8	62.0
1989	52.6	14.2	103.8
1988	154.8	19.2	98.5
1987	84.6	NA	136.9
1986	101.8	1.0	157.1
1985	123.0	NA	148.8
1984	220.6	NA	205.8

Table 22. The number of trawls per station in each month at Stations 7, 9, and 10 in each year.

Year	Station	2	3	4	5	6	7	8	9	10	11	12
2020	10	0	0	0	0	0	2	0	0	0	0	0
2020	7	0	0	0	0	0	2	2	1	0	0	0
2020	9	0	0	0	0	0	2	2	1	0	0	0
2019	10	0	0	1	2	2	0	0	0	0	0	0
2019	7	0	0	1	1	2	2	2	1	0	0	0
2019	9	0	0	1	2	2	2	2	1	0	0	0
2018	10	0	0	1	2	2	2	1	1	0	0	0
2018	7	0	0	1	2	2	2	2	1	0	0	0
2018	9	0	0	1	2	4	2	2	1	0	0	0
2017	10	0	0	1	2	0	0	0	0	0	0	0
2017	7	0	0	1	2	2	2	2	1	0	0	0
2017	9	0	0	1	2	2	2	2	1	0	0	0
2016	10	0	0	1	2	1	0	0	0	0	0	0
2016	7	0	0	1	2	2	2	2	1	0	0	0
2016	9	0	0	1	2	2	2	2	1	0	0	0
2015	10	0	0	1	2	0	0	0	0	0	0	0
2015	7	0	0	1	2	2	2	2	1	0	0	0
2015	9	0	0	1	2	2	2	2	2	0	0	0
2014	10	0	0	1	2	2	0	0	0	0	0	0
2014	7	0	0	1	2	2	2	2	1	0	0	0
2014	9	0	0	1	2	2	2	2	1	0	0	0
2013	10	0	0	1	2	2	1	0	0	0	0	0
2013	7	0	0	1	2	2	2	2	1	0	0	0
2013	9	0	0	1	2	2	2	2	1	0	0	0
2012	10	0	0	1	2	2	0	0	0	0	0	0
2012	7	0	0	1	2	2	2	2	1	0	0	0
2012	9	0	0	1	2	2	2	2	1	0	0	0
2011	10	0	0	1	2	3	2	0	1	0	0	0
2011	7	0	0	1	2	3	2	2	1	0	0	0
2011	9	0	0	1	2	3	2	2	1	0	0	0
2010	10	0	0	1	1	2	2	0	0	0	0	0
2010	7	0	0	1	1	2	2	2	1	0	0	0
2010	9	0	0	1	1	2	2	2	1	0	0	0
2009	10	0	0	1	2	2	2	3	1	0	0	0
2009	7	0	0	1	2	2	2	2	1	0	0	0
2009	9	0	0	1	3	2	2	2	1	0	0	0
2008	10	0	0	1	2	2	2	2	1	0	0	0

2008	7	0	0	1	2	2	2	2	1	0	0	0
2008	9	0	0	1	1	2	1	2	1	0	0	0
2007	10	0	0	1	2	2	2	2	1	0	0	0
2007	7	0	0	1	2	2	2	2	1	0	0	0
2007	9	0	0	1	2	2	2	2	1	0	0	0
2006	10	0	0	1	2	2	1	2	0	0	0	0
2006	7	0	0	1	2	2	2	2	1	0	0	0
2006	9	0	0	1	2	2	2	2	1	0	0	0
2005	10	0	0	1	2	2	2	2	0	0	0	0
2005	7	0	0	1	2	2	2	2	1	1	0	0
2005	9	0	0	1	2	2	2	2	1	1	0	0
2004	10	0	0	0	1	2	2	1	1	0	0	0
2004	7	0	0	0	1	2	2	2	1	0	0	0
2004	9	0	0	1	1	2	2	2	1	0	0	0
2003	10	0	1	2	2	2	2	1	1	1	1	1
2003	7	0	1	2	2	2	2	1	1	1	1	1
2003	9	0	1	2	2	2	2	1	1	1	1	1
2002	10	0	0	2	2	2	2	2	2	1	1	1
2002	7	0	1	2	2	2	2	2	2	1	1	1
2002	9	0	1	2	2	2	2	2	2	1	1	1
2001	10	0	1	2	2	1	2	3	2	1	1	1
2001	7	0	1	2	2	1	2	3	2	1	1	1
2001	9	0	1	2	1	1	2	3	2	1	1	1
2000	10	0	1	2	2	3	2	3	2	1	1	1
2000	7	0	1	2	2	3	2	2	2	1	1	1
2000	9	0	1	2	2	3	2	2	2	1	1	1
1999	10	0	1	2	2	2	2	2	2	1	1	1
1999	7	0	1	2	2	2	2	2	2	1	1	1
1999	9	0	1	2	2	2	2	2	2	1	1	1
1998	10	0	1	2	2	2	2	2	2	1	1	1
1998	7	0	1	2	2	2	2	2	2	1	1	1
1998	9	0	1	2	2	2	2	2	2	1	1	1
1997	10	0	1	2	2	2	2	2	2	2	1	1
1997	7	0	1	2	2	2	2	2	2	2	1	1
1997	9	0	1	2	2	2	2	2	2	2	1	1
1996	10	0	1	2	1	2	2	1	2	1	1	1
1996	7	0	2	2	2	2	2	1	2	1	1	1
1996	9	0	1	2	2	1	2	1	2	1	1	1
1995	10	0	1	2	2	2	2	2	2	2	1	0
1995	7	0	1	2	2	2	2	2	2	2	1	0
1995	9	0	1	2	2	2	2	2	2	3	1	0
1994	10	0	1	1	1	2	2	0	2	2	1	0

1994	7	0	1	1	1	2	2	0	2	2	1	0
1994	9	0	0	1	1	2	2	0	2	2	1	0
1993	10	0	0	1	2	2	3	2	2	2	1	1
1993	7	0	0	1	2	2	3	2	2	2	1	1
1993	9	0	1	1	2	2	3	2	2	2	1	1
1992	10	0	1	1	1	1	1	1	1	1	1	1
1992	7	0	1	1	1	1	1	1	1	1	1	1
1992	9	0	1	1	0	1	1	1	1	1	1	1
1991	10	0	1	2	1	1	1	1	1	1	1	0
1991	7	0	1	1	1	1	1	1	1	1	1	0
1991	9	0	1	1	1	1	1	1	1	1	1	0
1990	10	0	1	1	2	1	1	1	1	1	0	0
1990	7	0	1	1	1	1	1	1	1	1	0	0
1990	9	0	1	1	1	1	1	1	1	1	0	0
1989	10	1	1	1	1	1	1	2	2	1	1	0
1989	7	1	1	1	1	1	1	2	2	1	1	0
1989	9	1	1	1	1	1	1	2	2	1	1	0
1988	10	0	1	1	1	2	2	2	2	1	1	0
1988	7	0	1	1	1	2	2	2	2	1	1	0
1988	9	0	0	0	0	0	0	0	2	1	1	0
1987	10	0	1	1	1	1	1	1	1	1	0	0
1987	7	0	1	1	1	1	1	1	1	1	1	0
1986	10	0	2	1	1	1	1	1	1	1	1	0
1986	7	0	1	1	1	1	1	1	1	1	1	0
1986	9	1	0	0	0	0	0	0	0	0	0	0
1985	10	0	0	1	1	1	0	1	1	2	1	0
1985	7	0	0	1	1	1	0	1	1	2	1	0
1984	10	0	1	2	4	3	4	2	4	5	2	1
1984	7	0	1	2	4	2	4	2	5	5	2	1

Seines

Overall Patterns

The long-term trend of seine catches shows a stable pattern of catches amidst inter-annual variability (Table 23, Figure 172). Of the three most abundant years high catches were due to a high abundance of Alosines those years: 1994 and 2004 were driven primarily by large catches of Alewife, whereas high catch rates in 1991 were a result of high catch rates of Blueback Herring (Table 23). The most abundant species in seine catches overall and in 2020 is Banded

Killifish. The number of seine tows over the period of record is shown in Table 24.

Table 23. Mean Catch per Seine of Selected Adult and Juvenile Fishes at all Stations and all Months. 1985-2020.

Year	All Species	White Perch	Banded Killifish	Blueback Herring	Alewife	All Alosa Sp	Spottail Shiner	Inland Silverside
2020	139.4	8.9	70.2	0.0	5.8	11.2	1.7	5.8
2019	112.6	15.4	42.6	0.0	0.6	28.3	1.3	4.9
2018	118.5	4.5	50.5	0.0	0.0	46.4	2.3	1.8
2017	100.9	9.2	57.9	0.0	0.3	0.9	2.0	14.9
2016	114.3	11.6	64.5	0.0	0.0	6.9	1.2	8.1
2015	171.2	33.1	76.1	0.5	0.4	17.1	5.2	4.7
2014	169.5	11.9	121.4	3.5	0.1	8.3	4.1	4.1
2013	117.4	8.3	92.6	0.1	0.2	2.1	0.4	0.7
2012	186.0	5.4	131.7	0.0	2.1	4.5	6.1	12.4
2011	140.8	31.0	76.3	0.0	1.3	2.0	2.4	1.5
2010	249.4	15.8	175.6	0.1	1.6	4.6	1.6	1.3
2009	186.5	18.7	67.4	0.3	0.1	1.4	3.6	6.9
2008	196.5	15.4	51.8	0.3	0.1	2.5	3.0	14.9
2007	130.4	15.0	40.6	6.7	2.2	17.6	3.4	2.3
2006	165.3	7.6	113.7	3.2	0.4	6.2	3.6	16.2
2005	202.0	32.0	125.2	1.0	5.4	7.2	9.7	5.6
2004	304.5	45.3	99.1	11.1	73.8	85.2	38.1	9.5
2003	100.6	7.5	42.9	2.3	2.8	7.5	7.3	4.8
2002	164.4	23.1	89.7	0.0	2.2	3.2	12.5	14.4
2001	134.0	30.2	54.6	0.0	4.9	5.6	14.3	7.6
2000	152.2	28.9	26.2	1.7	6.0	7.7	23.5	50.1
1999	108.1	18.3	19.0	14.4	0.4	14.8	12.3	25.0
1998	111.6	22.2	31.6	2.1	1.0	3.1	25.9	8.7
1997	96.8	12.8	34.0	17.6	1.5	19.0	4.5	13.8
1996	103.6	29.1	18.2	15.4	5.4	22.2	11.8	4.7
1995	88.8	26.1	16.3	2.1	2.8	5.0	5.8	12.5
1994	294.9	15.6	13.9	0.0	250.2	250.2	7.2	0.1
1993	73.6	13.4	26.1	3.2	1.3	4.5	8.5	9.1
1992	154.5	43.6	35.8	39.2	0.0	39.2	9.0	5.8
1991	204.9	30.2	45.1	66.2	0.2	66.4	17.5	6.0
1990	118.7	41.2	27.8	7.4	1.1	8.5	9.0	4.0
1989	130.8	39.9	25.8	1.8	0.5	2.2	8.1	1.9
1988	146.5	42.1	48.6	2.2	0.3	2.6	9.3	6.2
1987	108.9	36.7	31.9	0.0	0.0	0.0	8.0	11.6
1986	130.5	55.1	15.3	0.2	0.8	1.3	6.4	20.0

1985	120.2	36.8	11.7	0.0	0.1	0.2	13.2	29.3

Table 24. The number of seines in each month at Station 4, 4B, 6, and 11 in each year. 1985-2020.

Year	Station	1	2	3	4	5	6	7	8	9	10	11	12
2020	4	0	0	0	0	0	0	2	2	0	0	0	0
2020	6	0	0	0	0	0	0	2	2	1	0	0	0
2020	11	0	0	0	0	0	0	2	2	1	0	0	0
2020	4B	0	0	0	0	0	0	2	2	1	0	0	0
2019	4	0	0	0	1	2	2	2	0	0	0	0	0
2019	6	0	0	0	1	2	2	2	2	1	0	0	0
2019	11	0	0	0	1	2	2	2	2	1	0	0	0
2019	4B	0	0	0	1	2	2	2	2	1	0	0	0
2018	4	0	0	0	1	2	2	2	2	1	0	0	0
2018	6	0	0	0	1	2	2	2	2	1	0	0	0
2018	11	0	0	0	1	2	2	2	2	1	0	0	0
2018	4B	0	0	0	1	2	2	2	2	1	0	0	0
2017	4	0	0	0	1	2	2	0	0	0	0	0	0
2017	6	0	0	0	1	2	2	2	2	1	0	0	0
2017	11	0	0	0	1	2	2	2	2	1	0	0	0
2017	4B	0	0	0	1	2	2	2	2	1	0	0	0
2016	4	0	0	0	1	2	1	0	0	0	0	0	0
2016	6	0	0	0	1	2	2	2	2	1	0	0	0
2016	11	0	0	0	1	2	2	2	2	1	0	0	0
2016	4B	0	0	0	1	2	2	2	2	1	0	0	0
2015	4	0	0	0	1	2	2	0	0	0	0	0	0
2015	6	0	0	0	1	2	2	2	2	1	0	0	0
2015	11	0	0	0	1	2	2	2	2	1	0	0	0
2015	4B	0	0	0	1	2	2	2	2	1	0	0	0
2014	4	0	0	0	1	2	2	1	1	0	0	0	0
2014	6	0	0	0	1	2	2	2	2	1	0	0	0
2014	11	0	0	0	1	2	2	2	2	1	0	0	0
2014	4B	0	0	0	1	2	2	2	2	1	0	0	0
2013	4	0	0	0	1	2	2	2	1	0	0	0	0
2013	6	0	0	0	1	2	2	2	2	1	0	0	0
2013	11	0	0	0	1	2	2	2	2	1	0	0	0
2013	4B	0	0	0	1	2	2	2	2	1	0	0	0
2012	4	0	0	0	1	2	2	1	0	0	0	0	0
2012	6	0	0	0	1	2	2	2	2	1	0	0	0
2012	11	0	0	0	1	2	2	2	2	1	0	0	0

2012	4B	0	0	0	1	2	2	2	2	1	0	0	0
2011	4	0	0	0	1	3	3	3	2	1	0	0	0
2011	6	0	0	0	1	2	3	2	2	0	1	0	0
2011	11	0	0	0	1	2	3	2	2	1	0	0	0
2011	4B	0	0	0	1	2	3	2	2	1	0	0	0
2010	4	0	0	0	1	1	2	2	2	1	0	0	0
2010	6	0	0	0	1	1	2	2	2	1	0	0	0
2010	11	0	0	0	1	1	2	2	2	1	0	0	0
2010	4B	0	0	0	1	1	2	2	2	1	0	0	0
2009	4	0	0	0	1	2	2	2	2	1	0	0	0
2009	6	0	0	0	1	2	2	2	2	1	0	0	0
2009	11	0	0	0	1	2	2	2	2	1	0	0	0
2009	4B	0	0	0	1	2	2	2	2	1	0	0	0
2008	4	0	0	0	1	2	2	2	2	1	0	0	0
2008	6	0	0	0	1	2	2	2	2	1	0	0	0
2008	11	0	0	0	1	2	2	2	2	1	0	0	0
2008	4B	0	0	0	1	2	2	2	2	1	0	0	0
2007	4	0	0	0	1	2	1	2	2	1	0	0	0
2007	6	0	0	0	1	2	1	2	2	1	0	0	0
2007	11	0	0	0	1	2	1	2	2	1	0	0	0
2007	4B	0	0	0	0	0	0	2	2	1	0	0	0
2006	4	0	0	0	1	2	1	0	0	1	0	0	0
2006	6	0	0	0	1	2	2	2	0	0	0	0	0
2006	11	0	0	0	1	2	2	2	2	1	0	0	0
2005	4	0	0	0	1	2	2	2	1	0	0	0	0
2005	6	0	0	0	1	2	2	2	1	0	0	0	0
2005	11	0	0	0	1	2	2	2	2	1	1	0	0
2004	4	0	0	0	1	1	2	1	0	0	0	0	0
2004	6	0	0	0	1	1	2	0	0	0	0	0	0
2004	11	0	0	0	1	1	2	2	2	1	0	0	0
2003	4	0	0	1	2	2	2	2	2	1	1	1	1
2003	6	0	0	1	2	2	2	2	2	1	1	1	1
2003	11	0	0	1	2	2	2	2	2	1	1	1	1
2002	4	0	0	1	2	2	2	2	2	2	1	1	1
2002	6	0	0	1	2	2	2	2	2	2	1	1	1
2002	11	0	0	1	2	2	2	2	2	2	1	1	1
2001	4	0	0	1	2	2	1	2	3	2	1	1	1
2001	6	0	0	1	2	2	1	2	3	2	0	1	1
2001	11	0	0	1	2	2	1	2	3	2	1	1	1
2000	4	0	0	1	2	2	3	2	2	2	1	1	1
2000	6	0	0	1	2	2	3	2	2	2	1	1	1
2000	11	0	0	1	2	2	3	1	2	0	1	1	2

1999	4	0	0	1	2	2	2	2	2	2	0	1	1
1999	6	0	0	1	1	2	1	2	2	2	1	1	1
1999	11	0	0	1	2	2	2	2	2	2	1	1	1
1998	4	0	0	1	2	2	2	2	2	2	1	1	1
1998	6	0	0	1	2	2	2	2	2	2	1	1	1
1998	11	0	0	1	2	2	2	2	2	2	1	1	1
1997	4	0	0	1	2	2	2	2	2	2	2	1	1
1997	6	0	0	1	2	2	2	2	2	2	2	1	1
1997	11	0	0	1	3	4	2	2	2	2	2	1	1
1996	4	0	0	1	2	2	2	2	1	2	1	1	1
1996	6	0	0	1	2	2	2	2	1	2	1	1	1
1996	11	0	0	1	2	2	2	2	1	2	1	1	1
1995	4	0	0	1	1	2	2	2	2	2	2	1	0
1995	6	0	0	1	2	2	2	2	2	2	2	1	0
1995	11	0	0	1	2	2	1	2	2	3	2	1	0
1994	4	0	0	0	0	1	1	0	0	1	1	0	0
1994	6	0	0	3	0	1	1	0	0	1	1	0	0
1994	11	0	0	3	0	1	1	0	0	1	1	0	0
1993	4	0	0	1	2	2	1	3	2	0	1	1	1
1993	6	0	0	1	1	2	1	3	2	0	1	1	1
1993	11	0	0	1	2	2	1	3	2	0	1	1	1
1992	4	0	0	1	1	1	1	1	1	1	1	1	0
1992	6	0	0	1	1	1	1	1	1	1	1	1	0
1992	11	0	0	0	1	1	1	1	1	1	1	1	0
1991	4	0	0	1	1	1	1	1	1	1	1	1	0
1991	6	0	0	1	1	1	1	1	2	1	1	2	0
1991	11	0	0	1	1	1	1	1	1	1	1	1	0
1990	4	0	0	1	1	1	1	1	1	1	0	0	0
1990	6	0	0	1	1	1	1	1	1	1	0	0	0
1990	11	0	0	1	1	1	1	1	1	1	0	0	0
1989	4	0	0	1	1	1	1	1	1	1	1	1	0
1989	6	0	0	1	1	1	1	1	1	1	1	1	0
1989	11	0	0	1	1	1	1	1	1	1	1	1	0
1988	4	0	0	1	1	0	2	2	1	1	1	1	0
1988	6	0	0	1	1	1	2	2	2	1	1	1	0
1988	11	0	0	1	1	1	2	2	2	1	1	1	0
1987	4	0	0	1	1	0	1	1	0	0	1	1	0
1987	6	0	0	1	1	0	1	1	0	0	1	0	0
1987	11	0	0	1	1	0	1	1	0	0	1	1	0
1986	4	0	1	0	1	0	1	0	0	3	4	0	0
1986	6	1	1	0	1	1	1	0	0	5	2	1	0
1986	11	2	1	0	1	1	1	0	2	4	4	1	0

1985	4	0	0	0	1	0	0	0	1	2	3	4	0
1985	6	0	0	0	0	0	0	0	1	3	3	4	0
1985	11	0	0	0	0	0	0	0	2	3	3	4	0

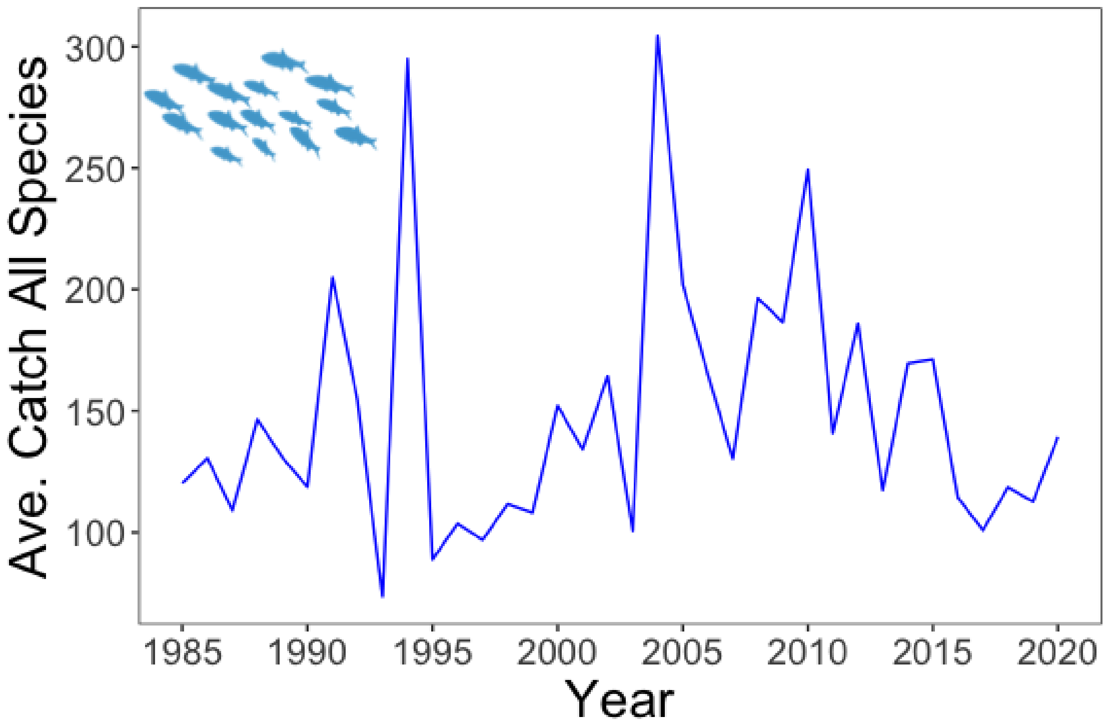

Figure 172. Seines. Annual Average over Stations 4, 4A, 6, and 11. All Species. 1985-2020.

Overall, Banded Killifish and White Perch have been the dominant species in seine samples throughout the survey. In 2020, the general trend of decreasing White Perch catches and increasing Banded Killifish catches over the period of record continued (Figures 173 and 174). The decrease in White Perch seen in seine catches is indication of the shifted ecosystem state to an SAV dominated system, since Banded Killifish prefers SAV habitat, while White Perch prefers open water. The decreasing trend in white Perch, and increasing trend in Banded Killifish, seems to be leveling out, and a new stable state in the relative contribution of these two species may have been reached. Subsequent years will determine whether this is indeed the case.

Over the course of the survey mean annual seine catch rates of White Perch have exhibited a gradual decline (Figures 173). An important factor is the pronounced increase in SAV, creating habitat for other species than White Perch, which is a pelagic species. Long-term trends in mean annual catch rates for the two dominant species in seine hauls have exhibited a negative association (r=-0.427) over the course of the survey. White Perch mean catches have declined steadily since the beginning of the survey, while Banded Killifish numbers have increased since the start of the survey, and experienced a prominent increase since 1999 (Figure

174).

The relative success of Banded Killifish is coincidentally (rather than functionally related) to declines in White Perch as these species show very little overlap in ecological and life history characteristics. Instead, as mentioned above, prominent increases in mean catch rates of Banded Killifish are associated with development of SAV in the cove since 2000. The SAV provides refuge for Banded Killifish adults and juveniles and may enhance feeding opportunities with epifaunal prey items. Essentially, the habitat of White Perch in Gunston Cove has decreased, while the habitat of Banded Killifish has increased. However, White Perch does reside in SAV covered areas as well, just in lower numbers.

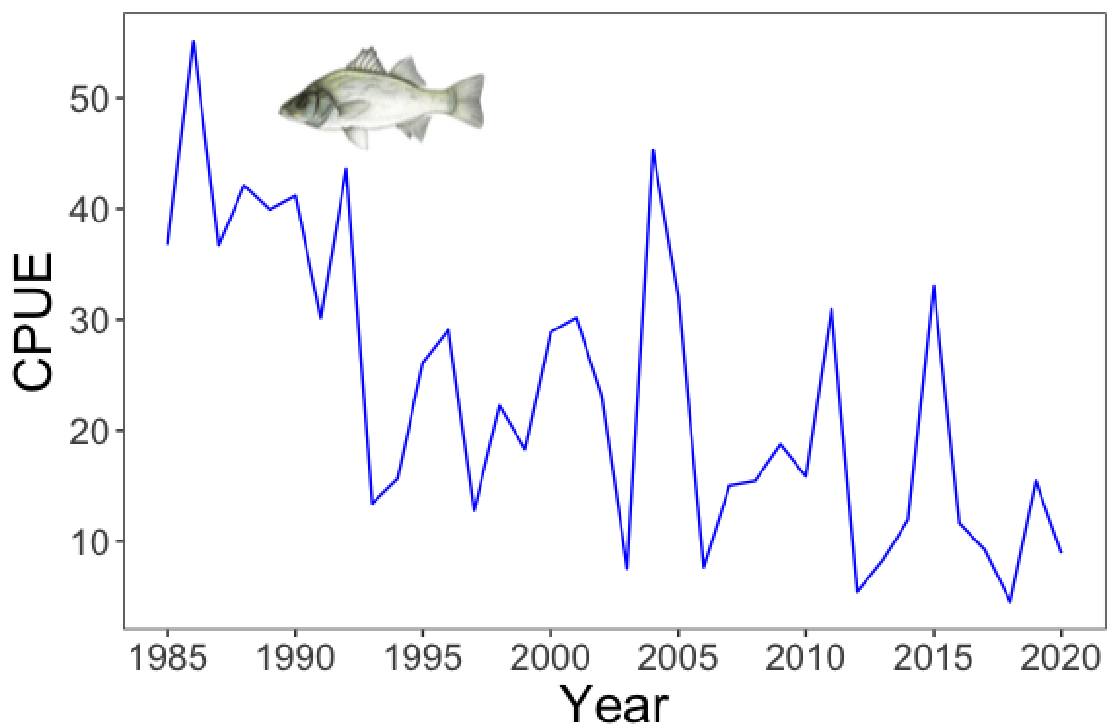

Figure 173. Seines. Annual Average Stations 4, 4A, 6, and 11. *Morone americana*. 1985-2020.

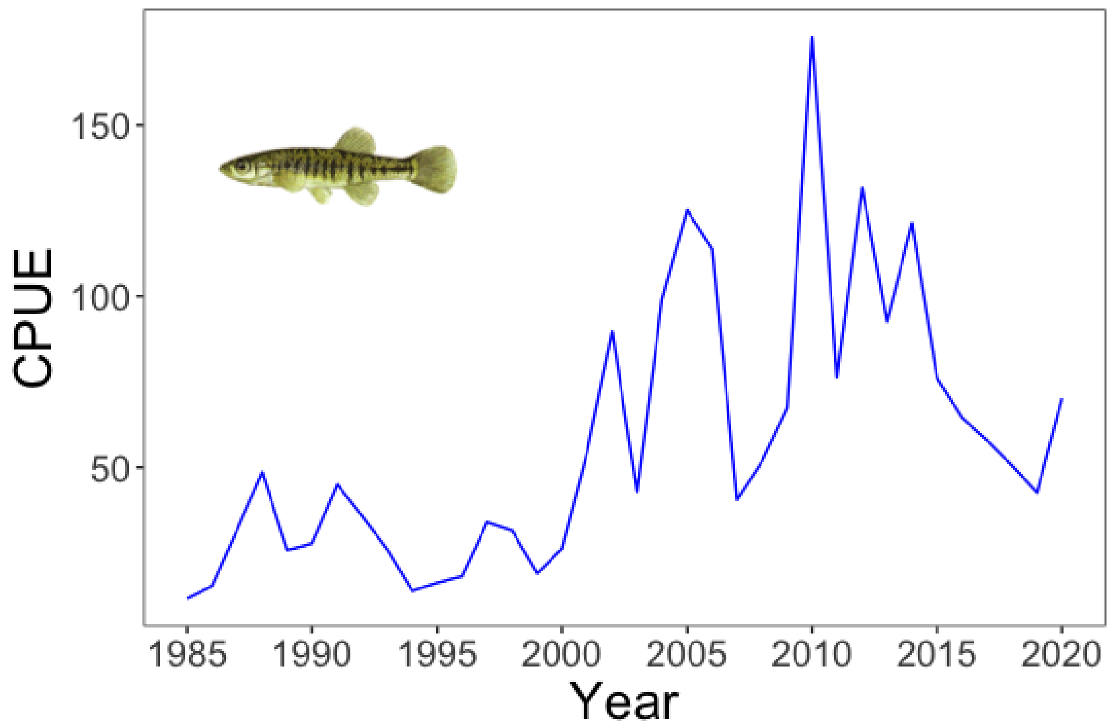

Figure 174. Seines. Annual Average Stations 4, 4A, 6, and 11. *Fundulus diaphanus*. 1985-2020.

Mean annual catch rates for river herring (Alewife and Blueback Herring) have exhibited sporadic peaks related to the capture of a large schools of fish (exceeding 200 for Alewife and approaching 100 individuals for Blueback Herring) in single hauls (Figure 175). Typically, less than 10 of either species were captured in a single sample. Both Alewife and Blueback Herring are listed as species of concern and have experienced declines throughout the Chesapeake Bay watershed. The moratorium on river herring since January 2012 has been put in place as an aid in the recovery. The moratorium (on fishing) may result in an increase in river herring over time. We added the category 'all *Alosa sp*.' to figure 175 in 2016 because a large portion of the Alosines cannot be identified to the species level. That revealed that Alosine abundances have been slightly higher since 2005 then just based on Alewife and Blueback Herring findings. For example, relatively high peaks in Alosines have been found in 2007, 2010, 2015, 2018, 2019 and now in 2020. Abundances are not sufficiently high that the stocks can be considered recovered. Continued monitoring will be key in determining the success of the moratorium. The high numbers of spawning adult river herring in 2015 in Pohick Creek, as described in the 2015 Anadromous Report, could signal the start of the recovery of these species. After lower abundances in 2016 and 2017, 2018 showed another peak for Alewife, indicating the large cohort of 2015 successfully returned to spawn (described in the 2018 Anadromous Report). Moderate levels of spawning adults were collected again in 2019, and 2020 could not be sampled because the spawning season of River herring occurred during the lockdown in response to the COVID-19 pandemic.

Owing to their affinity for marginal and littoral zone habitats, Spottail Shiner and Inland Silverside are consistently captured at moderate abundances throughout the course of the survey (Figure 176). Highest peaks occurred in 1999 and 2004 for Inland Silverside and Spottail Shiner respectively (Figure 176). After these high peaks, Inland Silverside remains relatively abundant with small peaks in 2006, 2008, 2012, and 2017, while Spottail Shiner decreases in seine collections.

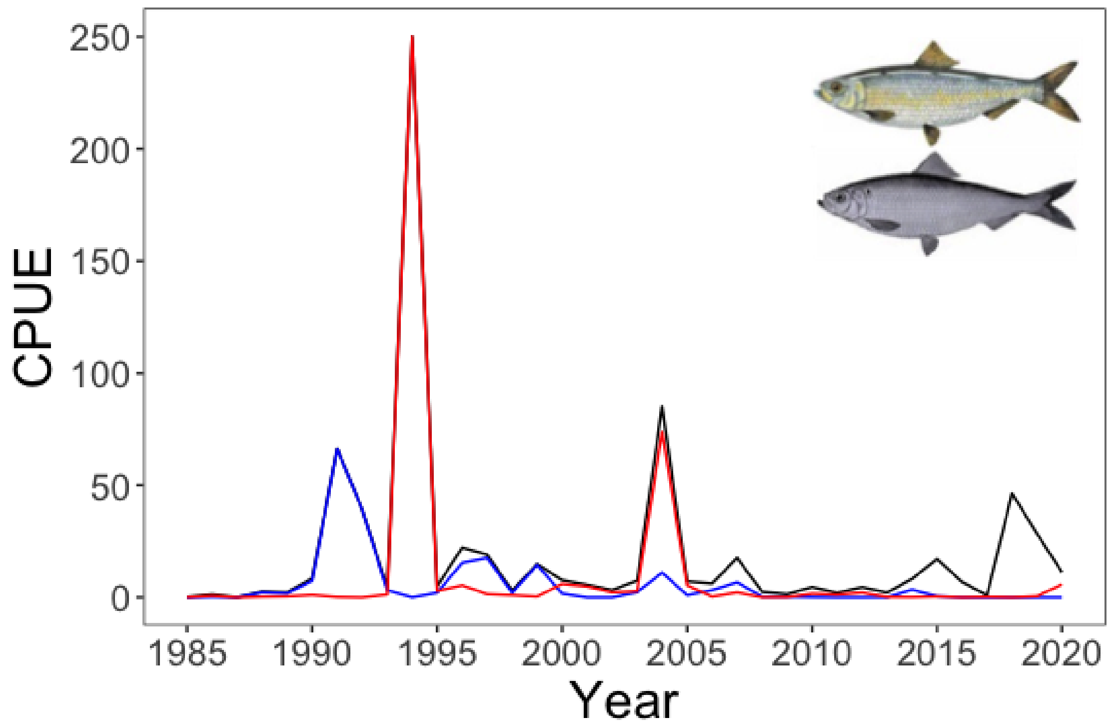

Figure 175. Seines. Annual Average over 4, 4A, 6, and 11 Stations. *Alosa aestivalis* (blue), *A. pseudoharengus* (red), and all *Alosa sp.* (black; *A. aestivalis*, *A. pseudoharengus*, *A. mediocris*, *A. sapidissima*, and unidentified Herring and Shad species). 1985-2020.

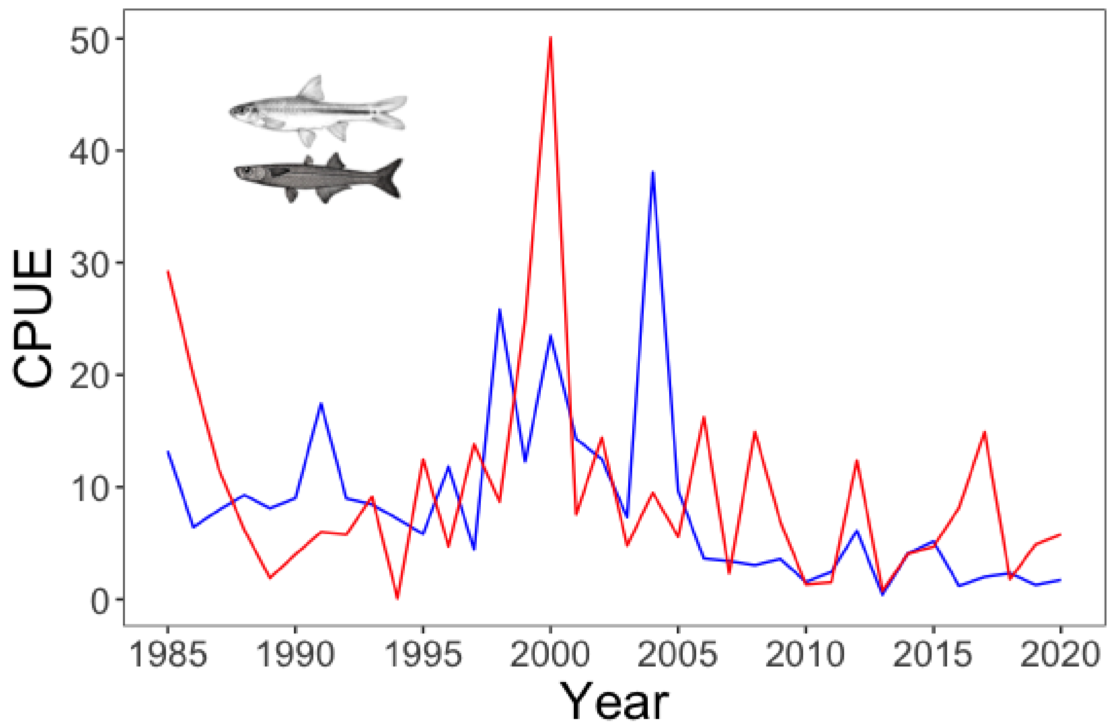

Figure 176. Seines. Annual Average over 4, 4A, 6, and 11 Stations. *Notropis hudsonius* (blue) and *Menidia beryllina* (red). 1985-2020.

Long-term Species Composition Changes

The species composition and community structure are changing throughout the time of the survey as indicated by trawl and seine catches. The expansion of SAV beds in the inner cove seems to be driving some of these changes. The main trend related to increasing SAV beds is a decline in White Perch and an increase in Banded Killifish in collections taking place in the littoral zone (seine hauls), where the SAV grows. A detailed multivariate analysis of the community structure shifts in the Gunston Cove fish community since the start of the Gunston Cove survey based on seine collections has recently been published (De Mutsert et al. 2017). White Perch does not decline in the open water station of the cove (trawls at station 7), and saw unprecedented high abundances per trawl in 2020. Another community shift can be seen in the catfishes. Since the introduction of the invasive Blue Catfish in Gunston Cove in 2001, Blue Catfish has become prevalent in the trawl catches, while the abundances of other catfishes (Brown Bullhead, Channel Catfish, White Catfish) have been declining. The trend in Blue Catfish abundance is currently not increasing, and seems to have reached a plateau. Potentially, a new stable state has been achieved with high Blue Catfish abundances and low abundances of other catfishes. We generally do collect some Brown Bullhead specimens in the fyke nets, but abundances are low there as well. More fyke net collections are needed to determine if there is a spatial shift of Brown Bullhead towards SAV beds, which would not be unusual for this species that prefers vegetated habitat.

With the reported increases and decreases in species abundances it is interesting to evaluate the effect of these community structure changes on the overall diversity of the fish community. This is analyzed by calculating the Simpson's Index of Diversity for each year from 1984 to 2020 (Figure 177). In this index, calculated as 1-($\boldsymbol{\Sigma}$ $(n_i/N)^2$), the communities with higher diversity have higher values (approaching 1). The Simpson's Index of Diversity was 0.620 in 2020. This relatively low value was due to the low number of samples taken in 2020, and the high abundance of White Perch in these samples, resulting in high dominance of one species. Overall, the index shows that the Cove represents a healthy and stable diversity, with fish species that are characteristic of Potomac River tributaries.

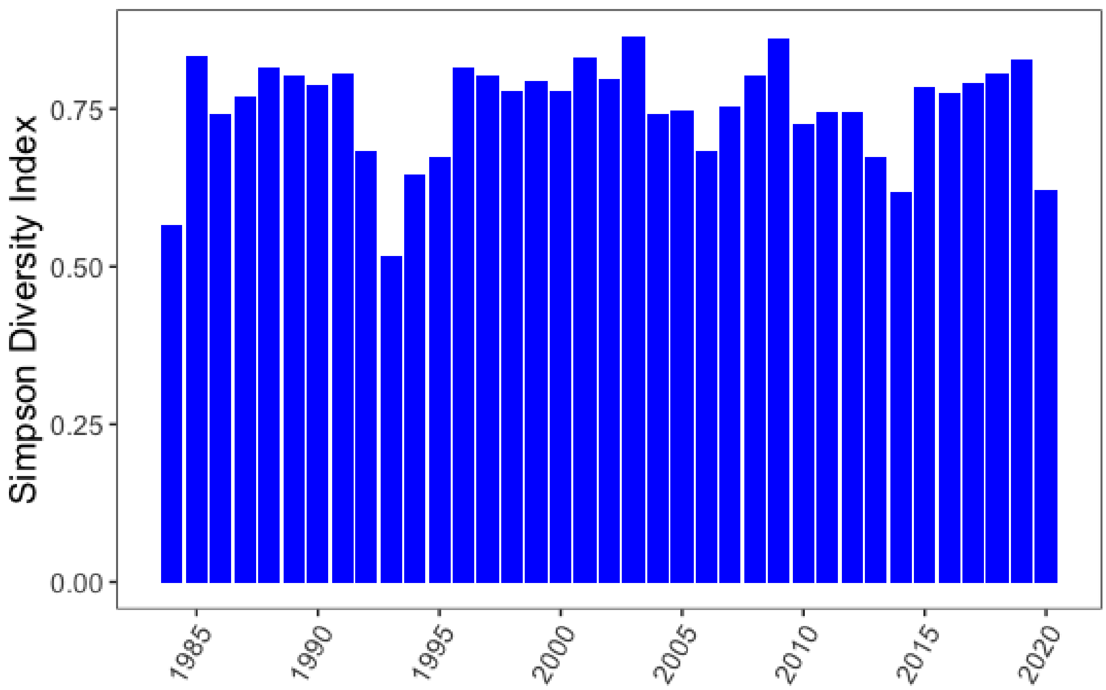

Figure 177. Simpson Diversity Index of fish species collected in Gunston Cove all years.

G. Benthic Macroinvertebrates Trends: 1994-2020

Summary: Similar to previous years, the macroinvertebrate community was dominated by Oligochaetes (Annelids) across sites. Outside of the Annelids, Crustaceans (dominated by gammarid amphipods) were the most abundant group in the Potomac River mainstem (Station GC9), while Gunston Cove proper (Station GC7) was dominated by Insect larvae from the Chironomidae family (midges). GC9 had the highest number of unique taxa (N=4; Platyhelminthes, Crustacea-Isopoda-*Cyathura polita*, and the two Gastropods - *C. japonica* and *P. virginica*). Comparing percent contributions of all non-Annelida taxa across both sites, months were dominated by Insecta. Ordination analyses of the community indicated a clear separation between communities sampled at the two sites for all months except June and July GC7 and September GC9 samples, which had exactly the same community composition. The macroinvertebrate abundance at GC7 was positively correlated with the percent leaves/wood, but there was no relationship between large particle type and total abundance or richness at GC9. There was also a change of the community composition throughout the months, as common for aquatic communities experiencing changes in abiotic conditions and recruitment during the summer months.

Comparison among Years: Benthic invertebrates have been monitored in a consistent fashion since 2009. Data from 2016-2020 are assembled below (Figure 178), and trends are generally consistent among years. The composition of the benthic macroinvertebrate community in the Potomac River mainstem (Station GC9) and Gunston Cove proper (Station GC7) seems to reflect mainly the texture of bottom substrates. In the cove at Station 7, the bottom sediments are fine and organic with anoxia just below the surface. These conditions favor chironomids and oligochaetes and are not very supportive of the other taxa found in the river. Interestingly, as submerged aquatic vegetation has become more established, gastropods are becoming more abundant and chironomids (midge larvae) are declining; however this trend has not been consistent the past two years (2019, 2020). In the river, sediments are coarser and are comprised of a mixture of bivalve shells (mainly the invasive bivalve *Corbicula fluminea*) and sand/silt. This type of substrate supports a wider array of species, as supported by the data from this year showing higher species diversity in the river versus cove.

Oligochaetes are generally the most abundant taxon at both stations across all years (Figure 178). However, if Annelids are removed and we examine the other dominant taxon groups, we see a few different trends in dominant taxa between the two sites across years (Figure 178). In general, Gunston Cove proper (Station GC7) is dominated by the insect larvae of Chironomids (midges), while the Potomac River mainstem (Station GC9) is dominated by Gammarid amphipods. Amphipods have generally occurred sporadically at low levels in Gunston Cove proper (Station GC7). Amphipods are consistently the second most abundant macroinvertebrate at GC9 and the third most abundant macroinvertebrate at GC7. Isopods have been commonly found in the Potomac River mainstem (Station GC9) since 2010 and sporadically in Gunston Cove proper (Station GC7); they reached their highest densities in both sites in 2016. Turbellaria (flatworms) and Hirundinea (leeches) are found in low numbers sporadically at both sites and were present in several river samples since 2014. Bivalves and Gastropods also occur in low numbers at both sites, with approximately the same average number of Gastropods across sites and years. The Potomac River mainstem (Station GC9) has, on average, a higher abundance of Bivalves than GC7, mostly driven by the invasive Asian clam *Corbicula fluminea*. GC9 receives higher water flow and movement, which many species of Bivalvia require, and may help explain why there are higher abundances of Bivalvia located closer to the Potomac River. The consistent finding of even small numbers of taxa other than chironomids and oligochaetes in Gunston Cove proper (Station GC7) is encouraging and could be the result of improved water quality conditions in the cove.

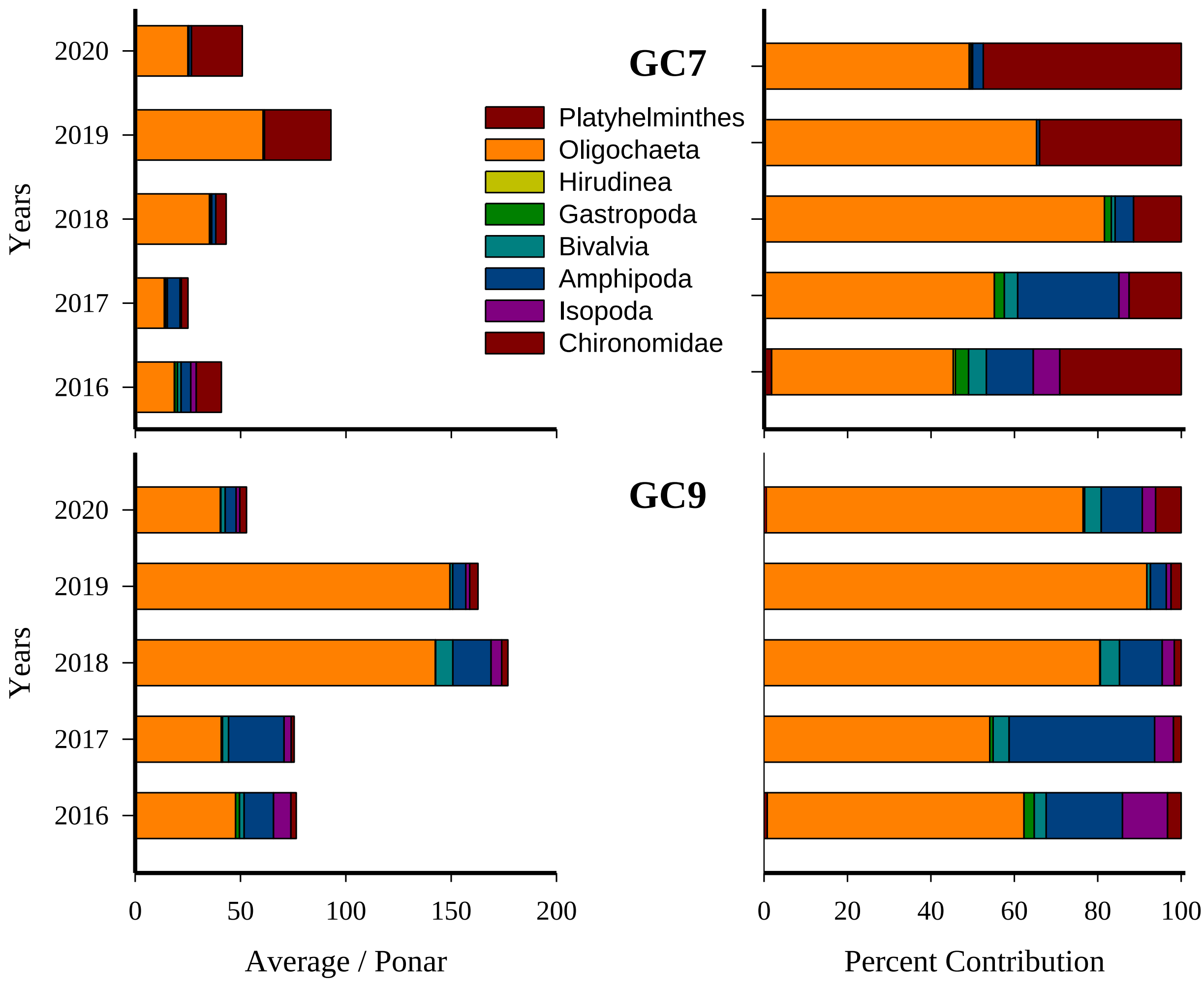

Figure 178. Average number per ponar sample (Left) and percent contribution (Right) of the eight dominant benthic invertebrate taxa in Gunston Cove embayment samples collected between 2016 and 2020 separated by site and year. Note the dominance of the Oligochaeta (worms).

H. Submersed Aquatic Vegetation (SAV) Trends: 1994-2020

A comprehensive set of annual surveys of submersed aquatic vegetation in the Gunston Cove area is available on the web at http://www.vims.edu/bio/sav/. This is part of an ongoing effort to document the status and trends of SAV as a measure of Bay recovery by conducting aerial mapping in early fall of each year. Maps of SAV coverage in the Gunston Cove area are available on the web site for the years 1994-2017 except for 2001, 2011, and 2018. Unfortunately, aerial mapping was not done in 2018 due to severe weather and poor imagery issues. Although the standardized data was not available, it was obvious that SAV was much reduced in 2018. In 2019 and 2020, average Secchi disk transparency increased to pre-2018 levels and SAV rebounded to near record levels (Figure 179).

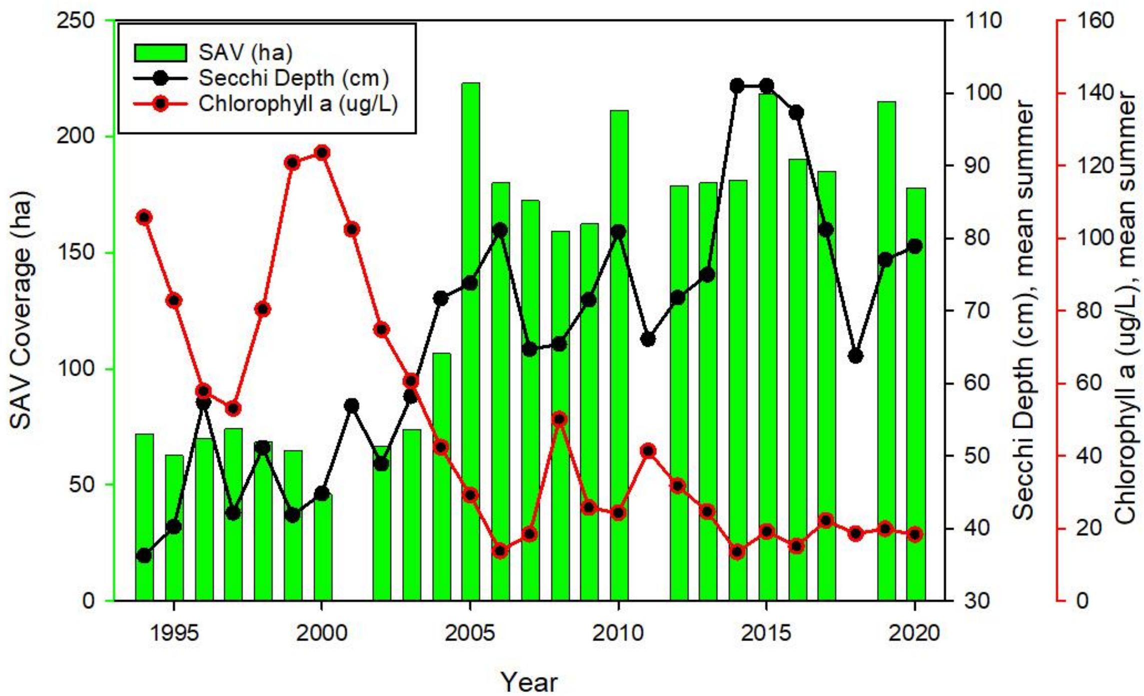

Figure 179. Gunston Cove SAV Coverage. Graphed with average summer (June-September) Depth-integrated Chlorophyll a (µg/L) and Secchi Depth (cm) measured at Station 7 in Gunston Cove.

LITERATURE CITED

Bigelow, H.B. and W.C.Schroeder. 1953. Fishes of the Gulf of Maine. Fishery bulletin No. 74, Vol. 53. U.S. Government Printing Office. Washinton, D.C. 577 pp.

Carter, V., P.T. Gammon, and N.C. Bartow. 1983. Submersed Aquatic Plants of the Tidal Potomac River. Geological Survey Bulletin 1543. U.S. Geological Survey. 63 pp.

Chesapeake Bay Program. 2006 Ambient water quality criteria for dissolved oxygen, water clarity, and chlorophyll *a* for the Chesapeake Bay and its tidal tributaries. 2006 Addendum. Downloaded from Bay Program website 10/13/2006.

Cummings, H.S., W.C. Purdy, and H.P. Ritter. 1916. Investigations of the pollution and sanitary conditions of the Potomac watershed. Treasury Department, U.S. Public Health Service Hygienic Laboratory Bulletin 104. 231 pp.

Dahlberg, M.D. 1975. Guide to coastal fishes of Georgia and nearby states. University of Georgia Press. Athens, GA 187 pp.

De Mutsert, K., Sills, A., Schlick, C.J.C., and R.C. Jones. 2017. Successes of restoration and its effects on the fish community in a freshwater tidal embayment of the Potomac River, USA. Water 9(6), 421; doi:10.3390/w9060421

Douglass, R.R. 1999. A Field Guide to Atlantic Coast Fishes: North America (Peterson Field Guides). Houghton Mifflin Harcourt, Boston. 368 pp.

Eddy, S. and J.C. Underhill. 1978. How to know the freshwater fishes. 3rd Ed. W.C. Brown Co. Dubuque, IA. 215 pp.

Hildebrand and Schroeder. 1928. Fishes of the Chesapeake Bay. U.S. Bureau of Fisheries Bulletin 53, Part 1. Reprinted 1972. T.F.H. Publishing, Inc. Neptune, NJ. 388 pp.

Hogue, J.J, Jr., R.Wallus, and L.K. Kay. 1976. Preliminary guide to the identification of larval fishes in the Tennessee River. Technical Note B19. Tennessee Valley Authority. Knoxville, TN.

Islam, S. 2001. Seasonal dynamics of micro-, nanno-, and picoplankton in the tidal freshwater Potomac River in and around Gunston Cove. Ph.Dissertation. George Mason University. 127 pp.

Jenkins, R.E. and N.M. Burkhead. 1994. The freshwater fishes of Virginia. American Fisheries Society. Washington, DC. 1080 pp.

Jones, P.W., F.D. Martin, and J.D. Hardy, Jr. 1978. Development of fishes of the Mid-Atlantic bight. Volumes I-VI. Fish and Wildlife Service, U.S. Department of the Interior. FWS/OBS-78/12.

Jones, R.C. 2020. Recovery of a Tidal Freshwater Embayment from Eutrophication: a Multidecadal Study. *Estuaries and Coasts*. Forthcoming in print. Available online at: https://link.springer.com/article/10.1007/s12237-020-00730-3

Kelso, D.W., R.C. Jones, and P.L. deFur. 1985. An ecological study of Gunston Cove - 1984-85. 206 pp.

Kraus, R.T. and R.C. Jones. 2011. Fish abundances in shoreline habitats and submerged aquatic vegetation in a tidal freshwater embayment of the Potomac River. Environmental Monitoring and Assessment. Online: DOI 10.1007/s10661-011-2192-6.

Lippson, A.J. and R.L. Moran. 1974. Manual for identification of early development stages of fishes of the Potomac River estuary. Power Plant Siting Program, Maryland Department of Natural Resources. PPSP-MP-13.

Loos, J.J., W.S. Woolcott, and N.R. Foster. 1972. An ecologist’s guide to the minnows of the freshwater drainage systems of the Chesapeake Bay area. Association of Southeastern Biologists Bulletin 19: 126-138.

Lund, J.W.G., C. Kipling, and E.C. LeCren. 1958. The inverted microscope method of estimation algal numbers and the statistical basis of estimations by counting. Hydrobiologia 11: 143-170.

Mansueti, A.J. and J.D. Hardy, Jr. 1967. Development of fishes of the Chesapeake Bay region: an atlas of egg, larvae and juvenile stages: Part 1. Natural Resources Institute. University of Maryland. 202 pp.

Merritt, R.W. and K.W. Cummins. 1984. An introduction to the aquatic insects of North America. 2nd edition. Kendall/Hunt Publishing Co., Dubuque, IA. 722 pp.

Page, L.M., and B.M. Burr. 1998. A Field Guide to Freshwater Fishes: North America North of Mexico (Peterson Field Guides). Houghton Mifflin Harcourt, Boston. 448 pp.

Pennack, R.W. 1978. Fresh-water invertebrates of the United States. 2nd ed. Wiley-Interscience. New York, NY.

Schloesser, R.W., M.C. Fabrizio, R.J. Latour, G.C. Garman, G.C., B. Greenlee, M. Groves and J. Gartland. 2011. Ecological role of blue catfish in Chesapeake Bay communities and implications for management. American Fisheries Society Symposium 77:369-382.

Scott, W.B. and E.J. Crossman. 1973. Freshwater fishes of Canada. Bulletin 184. Fisheries Research Board of Canada. Ottawa, Canada. 966 pp.

Standard Methods for the Examination of Water and Wastewater. 1980. American Public Health Association, American Waterworks Association, Water Pollution Control Federation. 15th ed. 1134 pp.

Thorp, J.H. and A.P. Covich, eds. 1991. Ecology and classification of North American Freshwater Invertebrates. Academic Press. San Diego, CA. 911 pp.

Wetzel, R.G. 1983. Limnology. 2nd ed. Saunders. 767 pp.

Wetzel, R.G. and G.E. Likens. 1991. Limnological analyses. 2nd ed. Springer-Verlag. 391 pp.